eman ta zabal zazu

Universidad   Euskal Herriko
del País Vasco   Unibertsitatea

UNIVERSIDAD DEL PAIS VASCO

EUSKAL HERRIKO UNIBERTSITATEA

ESCUELA DE INGENIERÍA DE BILBAO

BILBOKO INGENIERITZA ESKOLA

PhD thesis

OPTIMIZED CHARGING CONTROL METHOD FOR PLUG-IN ELECTRIC VEHICLES IN LV DISTRIBUTION NETWORKS

PRESENTED BY

Mr. Javier García Villalobos

SUPERVISED BY

Prof. Dr. Ms. Inmaculada Zamora Belver

2016

AKNOWLEDGEMENT

"Daily work— my hands' employment,
To complete is pure enjoyment!
Let, oh, let me never falter!
No! There is no empty dreaming:
Lo! These trees, but bare poles seeming,
Yet will yield both food and shelter"

Goethe

INDEX OF CONTENTS

INDEX OF FIGURES

INDEX OF TABLES

NOMENCLATURE

ACP: Accumulated charging profile
AIS: Artificial immune systems
AT: Arrive time
BEV: Battery electric vehicle
BOL: Beginning of life
BMS: Battery management system
BSS: Battery swapping stations
CC/CV: Constant current/constant voltage
CCS: Combined charging system
CDF: Cumulative distribution function
CHP: Combined heat and power
CNG: Compressed natural gas
CP: Charging point
CT: Connection time
DG: Distributed generator
DM: Decision maker
DoD: Deep of discharge
DSM: Demand side management
DSO: Distribution system operator
DT: Departure time
EDF: Earliest deadline first
EOL: End of life
EV: Electric vehicle
EVSE: Electric vehicle supply equipment
EVSEM: Electric vehicle supply equipment manager
FO: Fleet operator
G2V: Grid to vehicle
GEV: Generalized extreme value
GHG: Greenhouse gas
HEV: Hybrid electric vehicle
ICT: Information and communication technology
ICEV: Internal combustion engine vehicle
LCFS: Low carbon fuel standard
LF: Load demand forecast
LLF: Least laxity first
LNG: Liquefied natural gas
LP: Linear programming
MAPE: Mean absolute percentage error
MAS: Multi-agent system
MG: Microgrid
MGCC: Microgrid central controller

MO: Market operator
MOO: Multi-objective optimization
MOO-NF: Multi-objective optimization no forecast
MOO-WF: Multi-objective optimization with forecast
MPC: Model predictive control
NHTS: National household travel survey
PEV: Plug-in electric vehicle
PEV-PR: Plug-in electric vehicle penetration rate
PHEV: Plug-in hybrid electric vehicle
PM: Permanent magnet
PO: Pareto optimal
PSO: Particle swarm optimization
PV: Photovoltaic
QP: Quadratic programming
RAU: Regional aggregation unit
RCD: Residual current detector
RES: Renewable energy resources
RHC: Receding horizon control
RPC: Reactive power control
SOC: State of charge
SOH: State of health
SOO: Single objective optimization
SRM: Switched reluctance motor
TOU: Time of use
TSO: Transmission system operator
V2G: Vehicle to grid
VC: Vehicle controller
VCP: Vehicle charging profile
VPP: Virtual power plant
VUF: Voltage unbalance factor
VUR: Voltage unbalance reduction
WTP: Willing to pay

CHAPTER 1

INTRODUCTION

1.1 - BACKGROUND

1.2 - AIMS OF THE THESIS

1.3 - STRUCTURE OF THE DOCTORAL THESIS

1. INTRODUCTION

1.1 Background

In the last decade, electric vehicles have become a sustainable alternative to current vehicles based on internal combustion engines. Governments of industrialized countries are taking measures to push the development and marketing of electric vehicles in order to face global warming and air pollution of cities. Between these measures, financial incentives, tax exemptions and tax deductions are the most common. Furthermore, several countries have stablished emission standards, which are designed to limit the pollutant emissions of new light vehicles sold in these countries.

Moreover, better and more affordable batteries have reduced noticeably the overall cost of the electric vehicles. Although, electric vehicles have a small market niche, it is expected that sales will continue to grow due to two main reasons: the economy of scale and new battery developments. Regarding to economy of scale, some companies are building battery factories to reduce their costs. Additionally, it must be pointed out that batteries are widely used in others growing sectors such as distributed energy storage and unmanned vehicles.

Most of the electric vehicles are charged through a wire connection between the vehicle and the LV distribution network. This type of electric vehicle, which has the possibility to be connected to the grid, is known as plug-in electric vehicle (PEV). Nowadays, PEVs are charged immediately after they are plugged into the electrical power supply. This action usually happens when PEV users arrive home and it usually matches with the higher residential power demand. Therefore, the uncontrolled charging of a significant amount of PEVs will result in a greater energy demand, which can lead to several problems such as: increase of energy losses, peak power, voltage deviations, overload issues, reduction of distribution transformer lifetime, etc.

In this aspect, some countries are encouraging the charging of PEVs at night by using time of use (TOU) tariffs. This way, the energy demand of PEVs is delayed in order to avoid an increase of peak power. However, this strategy could not be good enough to deal with the charge of an important number of PEVs. In addition, TOU tariffs can produce avalanche effects, that is, a large number of PEVs starting their charging process at the same time.

Regarding to the mentioned LV distribution network problems, they depend on several factors such as: number of PEVs, their energy demand, charging power, charger efficiency, connection and disconnection time, etc. Some of the mentioned factors depend on driving and charging behavior of PEV users. Thus, it is necessary to develop a model in order to know and compare the impacts produced by the application of different charging strategies at different penetration rates of PEVs.

Also, it is necessary to develop new charging methods or strategies in order to reduce as much as possible the impacts on LV distribution networks. Furthermore, these new charging strategies should be beneficial to all stakeholders (PEV users, utilities and network operators) in order to avoid conflict of interests. This is especially important because PEV users will not allow any control of their PEVs if they are not rewarded. Considering these aspects, research community has proposed a wide range of solutions to improve the integration of PEVs into electric networks. However, most of them are partial solutions or

important aspects have been ignored. Thus, there is still a considerable room for improvement.

1.2   Aims of the thesis

Electromobility could be the new paradigm in the private transport sector. The integration of PEVs into electric networks and the implementation of them with smart grid technologies could bring benefits to all stakeholders. In this context, this thesis has the main objective of developing a new smart charging algorithm, with the following characteristics:

- Reducing the charging cost for the PEV users. In a free electricity market, where electricity prices vary each hour in function of the demand level and the mix of generation, PEVs should be charged at hours with the lowest electricity cost whenever it is possible.
- Improving the load factor of the electric network. That is, reducing the difference between peak and off-peak power demand. This is particularly interesting for electric utilities because it will increase the economic efficiency of electric infrastructure. Furthermore, increasing the load factor will delay or reduce the possible grid reinforcement needs.
- Reducing the expected impacts of massive integration of PEVs into LV distribution networks, allowing a greater PEVs penetration level without compromising the distribution network reliability.

Apart from the mentioned characteristics, the proposed algorithm should be reliable and not dependent of the number of controlled PEVs. In addition, users' privacy should be kept as much as possible.

The proposed methodology has been tested through simulations, using real data of a LV distribution network located in Borup (Denmark). Additionally, a new driving and charging behavior model has been developed, as a necessary previous step to test the viability of the proposed smart charging algorithm.

1.3   Structure of the doctoral thesis

This thesis is structured in 6 chapters. This first chapter contains the background and aims of the thesis as well as the structure of the document.

The second chapter is focused on describing the role of electric vehicles and their current status and perspectives in the transport sector. Also, the main drivetrain topologies and the most important components of this type of vehicles are presented.

In the third chapter, different aspects related to PEVs and electric distribution networks are introduced. These aspects include charging methods, charging strategies, impacts on LV distribution networks due to the charging of PEVs and opportunities to be exploited in the integration of PEVs and electric networks.

Before the new methodology is presented, the fourth chapter includes a state-of-art of the already proposed smart charging algorithms. In addition, theory of mathematical programming is introduced due to its importance as a mathematical tool to solve optimization problems.

After that, the proposed methodology is explained in chapter five. In the first part of this chapter, the simulation setup used in this thesis has been explained. Then, the grid topology and the model of PEVs have been introduced. The distribution network used in this thesis is based on a real one located in Denmark. Additionally, real consumption data of households have been used. Then, a new driving and charging behavior model has been developed based on 2009 NHTS, which database is freely available. After that, several smart charging algorithms, which are part of the proposed methodology, are tested. Following, the new proposed smart charging algorithm is presented and their characteristics analyzed using the driving and charging model proposed in this thesis and the LV distribution network of Borup. Two different versions have been developed, depending on whether load forecasting is used. Additionally, an improvement to reduce voltage unbalances, named as VUR, has been proposed. To end this chapter, a comparative analysis has been carried out and a possible system architecture is proposed.

Finally, the sixth chapter gathers the conclusions drawn from the research work developed in this thesis and proposes future areas that could be explored to continue the research initiated in this thesis.

The thesis is completed with a list of references of previous works as well as four annexes containing additional data and figures from the study cases analyzed in this thesis.

CHAPTER 2

LAND TRANSPORT SECTOR: TOWARDS ELECTRIC MOBILITY

2.1 - INTRODUCTION

2.2 - ELECTRIC VEHICLES IN LAND TRANSPORT SECTOR. CHALLENGES AND OPPORTUNITIES

2.3 - CURRENT STATE OF ELECTRIC VEHICLES AROUND THE WORLD

2.4 - PLUG-IN ELECTRIC VEHICLE DRIVETRAIN TOPOLOGIES

2.5 - MAIN COMPONENTS OF PLUG-IN ELECTRIC VEHICLES

2.6 - CONCLUSIONS

2. LAND TRANSPORT: TOWARDS ELECTRIC MOBILITY

2.1 Introduction

Currently, land transport sector is facing important challenges regarding the energetic model based on oil products such as gasoline and gasoil. The use of these fuels in internal combustion engine vehicles (ICEVs) is the main cause of pollution in cities, which can affects the habitants' health. Indeed, air pollution not only causes respiratory problems to adults and children but also may cause heart attacks, strokes, messes with the metabolic system and has links to diabetes. Therefore, policymakers are giving more importance to this issue and have begun to promote projects of low emission vehicles.

Additionally, the combustion of these types of fuels produces greenhouse gases (GHG) such as CO_2, which is one of the gases responsible of the global warming. The earliest impacts of climate change are starting to be noticed in many parts of the world.

Apart from environmental aspects, economic and politic aspects must be also taken into account. Nowadays, the production capacity of petrol and natural gas has increased because of the use of hydraulic fracturing technique and, as consequence, oil prices have fallen. However, developed countries continue promoting the alternative energies for road transport, in order to reduce as much as possible the oil dependency. Furthermore, the dependence and excessive use of oil entails geopolitical problems because of the instability of some producing countries and the use of oil as economic weapon.

In this context, the society has begun to understand that ICEVs should not be the future of mobility. Thus, alternative vehicles are being developed during last decades. Among them, electric vehicles (EVs) are one of the most outstanding solution.

This chapter presents the challenges, opportunities and current state of electric vehicles in land transport sector. In addition, an overview on main drivetrain topologies and components of electric vehicles is provided.

2.2 Electric vehicles in land transport sector. Challenges and opportunities

Land transport sector depends largely on oil products. In fact, 71% of the petroleum consumed in the world in 2011 was due to the transport sector. In addition, the 93% of the energy consumed by the transport sector depends on petroleum [1]. Several actions have been taken in order to reduce this dependency. On the one hand, public transport has been developed, especially electric trains (high speed trains, trams and subways). On the other hand, efficiency in private transport has been improved, by reducing the weight of vehicles and using more efficient ICEs. However, the improvements made on the ICEs are not enough to drastically reduce oil consumption. In this context, carmakers and researchers have proposed several options to overcome this problem.

The solutions proposed include vehicles powered by biodiesel, ethanol, compressed natural gas (CNG), liquefied natural gas (LNG), hydrogen, compressed air, electric vehicles, etc. In the last decade, it seems that electric vehicles are leading the way in terms of efficiency and sustainability. Compared with conventional vehicles, EVs present various advantages listed as follows:

- Reduces consumption of oil and decreases energy dependency from oil producing countries. Decreasing oil imports will improve the balance of payments of no producing countries.
- Reduces GHG emissions in function of electricity generation mix [2], [3].
- Improves air quality in cities and, as a consequence, public health of citizens.
- Increases transport sector efficiency, while the cost per kilometer is significantly lower than with internal combustion engine vehicles [2].
- Can be charged from a wide range of different primary energy sources, adapting to the locally available energy sources.
- Could bring another set of advantages, due to the interaction between EVs and the electric grid, such as: integration of more intermittent renewable energy sources (RES), improvement of the electric grid efficiency and reliability and decrease of GHG intensity of the grid.

Taking into account these advantages, governments of different countries are encouraging the purchase of electric vehicles by subsidizing or financing them and implementing other actions, such as: tax exemption, tax deductions, transit and parking facilities, etc. Furthermore, some countries have established, or are in the process of establishing, limits on pollutant emissions for light vehicles. These countries are, mainly, Australia, Canada, China, European Union, Japan, South Korea and the United States [4], [5]. To adapt their vehicles to these new regulations, automobile manufacturers have reduced emissions of ICEVs and are developing new electric drive vehicles. Thus, a strong annual sales growth of EVs is expected over the coming years/decades, being possible to reach a million of units sold globally in 2017 [6].

Additionally, in recent years a new technology is being developed, the autonomous car, self-driving car or driverless car. This technology consists in reducing as much as possible the intervention of drivers in the driving process. This way, traffic accidents will be probably reduced and drivers' comfort will be improved. This type of technology is strongly associated with electric vehicles as they are better suited to host this new technology.

2.3   Current state of electric vehicles around the world

Electric vehicles technology is not new. In fact, electric vehicles were very popular at the end of 19th Century and the early 20th because they provided a level of comfort and ease of use not reachable by gasoline cars of the time. During that period, autonomy limit of electric vehicles was not such a problem because road infrastructure was incipient.

However, a set of events contributed to the decline of the electric vehicles of that period. These events were: the discovery of large petroleum reserves, the improvement of road transport infrastructures, the invention of electric starter and muffler for gasoline engines (which increased the comfort level of ICEVs) and, finally, the introduction of mass production of ICE cars by Henry Ford. At the end of this period, an electric car cost almost twice than an ICEV. In addition, EVs had by far less autonomy and speed.

After a period in which EVs technology usage was marginal, the interest on EVs has increased during the last decades. In fact, new carmakers have appeared to satisfy this new market, such as Tesla Motors. Currently, most of carmakers are developing new electric cars. So, it is expected that this trend will continue in the future.

Figure 2.1 shows the evolution of worldwide PEV sales. In spite of the fall of oil prices in the last year, PEV sales are still growing strongly. Currently, the top five markets for PEVs are: the United States, China, UK, Norway and Japan, in that order. The main characteristics are the following:
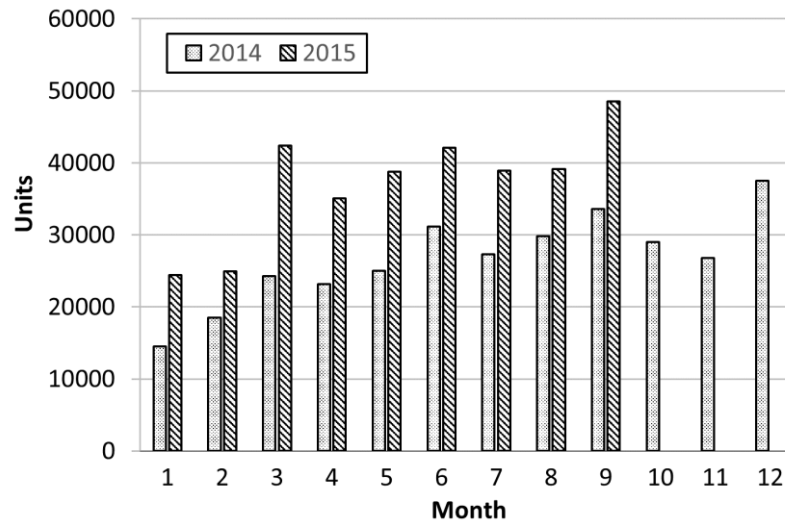
Figure 2.1. Worldwide sales of plug-in electric vehicles

- The United States is currently the biggest market for plug-in electric vehicles, where 55,357 PHEVs and 63,416 BEVs were sold in 2014. The market share for PEVs was 0.72%. In the same year, 451,702 hybrid electric vehicles (HEVs) were sold.

- Regarding to Chinese market, it has the largest increase in PEV sales by far. In fact, the PEV sales in 2014 has tripled compared to 2013. PEVs market share has increased 0.09% in 2013 to 0.25% in 2014. This trend is continuing in 2015, achieving the 0.8% of market share. Thus, above 24,000 PEVs were sold only in October, close to the number of PEVs sold in the United States and Europe in September. Additionally, current PEV sales in China do not depend only on a few PEV models, as in the past years. Currently, there are several car models pulling the market up, in a sustained way, confirming what many analysts have forecasted for years: the EV revolution will start in China.

- In UK, PEV sales have also increased noticeably in the last years. Around 4,000 PEVs were sold in 2013. However, in 2014 PEV sales achieved 14,000 units which is an increase of 350%. This trend continues in 2015, when 13,000 units were sold only in the first half of the year, reaching the 1% of car market share.

- With regard to Norway, this country has implemented multiple incentives to encourage buying electric vehicles. These incentives include: no purchase taxes (25% of value-added tax), no recurring taxes, free public parking, exempt in toll payments and the permission of driving in bus lanes. Incentives have been set to achieve a target of 50,000 electric cars (2% of Norway's vehicle fleet) by 2018, but this target has been surpassed in April of 2015, two years earlier. Currently, the government of Norway has to decide what to do with these incentives.

- In contrast, PEV sales in Japan have stagnated in 2014 and 2015, mainly due to the lack of new models of PEVs made by Japanese carmakers. Toyota and Honda still do not have a battery electric vehicle model, because they have decided to develop the fuel cell vehicle based on hydrogen. Note that Toyota has put up for sale the Toyota Mirai, a fuel cell vehicle which has a Chademo connection. This way, the vehicle can be used to power houses in emergency situations.

Following, the most outstanding drivetrain topologies of electric vehicles and their advantages and drawbacks are presented.

2.4 Plug-in electric vehicle drivetrain topologies

In this thesis, an electric vehicle is defined as a vehicle which uses at least one electric motor for traction purposes. Thus, plug-in electric vehicles can be considered as a subcategory of electric vehicles. There is no an international definition for plug-in electric vehicle but according to the U.S. Department of Energy, a PEV can be defined as a light vehicle which draws electricity from a battery with a capacity of at least 4kWh and is capable of being charged from an external source [7]. Within this definition several types of PEVs can be distinguished, mainly plug-in hybrid electric vehicles (PHEV), battery electric vehicles (BEV) and fuel cell plug-in hybrid electric vehicles (FC-PHEV). In contrast, vehicles such as hybrid electric vehicles (HEV) are not considered as PEVs. The batteries of these types of vehicles are charged with electricity generated internally by using an internal combustion engine and they cannot be charged with electricity drawn from the electric grid.

2.4.1 Plug-in hybrid vehicles (PHEV)

Plug-in hybrid electric vehicles are powered by an electric motor and an internal combustion engine and they can be plugged into the electric grid in order to charge their batteries. An ICE and a battery are used to provide energy to the vehicle. This way, the advantages of both types of technologies are obtained. That is, the ICE provides better autonomy and refueling times while the electric engine reduces pollutant emissions and increases overall efficiency. Additionally, batteries of PHEVs can be partly charged by using a regenerative braking system, so an additional efficiency improvement is achieved compared to conventional cars.

Internal combustion engines have poor efficiency at low or partial load. In fact, urban driving is the most energy demanding condition for ICEVs. With the use of an electric motor, the efficiency at partial load is noticeably improved. Furthermore, electric motors almost do not require energy when they are not used (i.e. when the car is stopped in a traffic light). In this context, there are several developments to shut down ICE when the vehicle is stopped or idle, to save fuel. These developments are known as start/stop systems.

In general, PHEVs have two modes of operation: charge depleting mode and charge sustaining mode. In charge depleting mode, the vehicle is only powered by the on-board battery until a predetermined state of charge (SOC) of the battery is reached. This mode is used at low speed, i.e. in urban areas or in traffic jams. In contrast, in charge sustaining mode, the SOC of the battery is kept within a predetermined range. The objective of this mode is to operate the two power sources as efficiently as possible. This mode is also used when batteries are depleted, after having driven in charge depleting mode.

PHEVs are more complex than ICEVs and BEVs, because of the use of two different engines. Besides, there are three different architectures to integrate an ICE and an electric motor in a vehicle, classified in: series hybrid, parallel hybrid and series-parallel hybrid.

2.4.1.1 Series hybrid powertrain

In the series hybrid topology (S-PHEV), the traction is only electric and the electric energy to feed it can be drawn either from the on-board battery or the ICE through an electric generator, as shown in Figure 2.2. Apart from batteries, super-capacitors can be also used as energy storage. Being the traction electric, there is no need of a multiple-speed transmission or gearbox and, as a consequence, vehicle's weight and simplicity is improved.
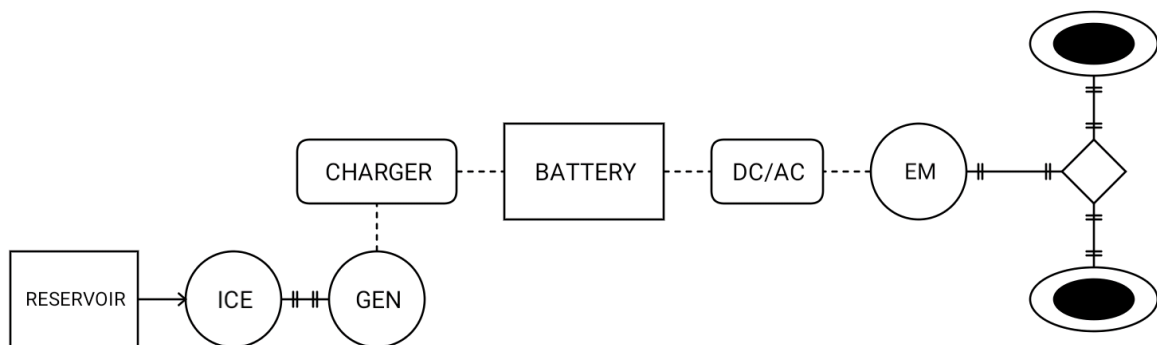
Figure 2.2. Series hybrid power train configuration

Additionally, the ICE power generation is decoupled from the power demanded by the driver. Due to this feature, two advantages are obtained. On the one hand, the ICE can run at its maximum efficiency point, even if the vehicle changes its speed, while the battery provides the rest of the power demand, acting as energy buffer. On the other hand, the PHEV design is easier because the ICE-generator set is not coupled with the wheels.

However, this topology has an important drawback related to the number of energy conversions needed. That is, mechanical power of the ICE must be converted into electric power and then again in mechanical power. So, there is a relevant loss of efficiency, especially at high speeds. For that reason, this topology is more convenient for low speeds. Furthermore, the traction device must be designed to meet the maximum sustained power demand and, as a consequence, electric motor and battery are quite large, raising the cost of this configuration.

Usually, this type of configuration is also called as extended-range electric vehicle (EREV), where a little ICE is included in the electric vehicle, in order to provide backup power in the event that batteries are depleted.

2.4.1.2 Parallel hybrid powertrain

Parallel hybrid topology (P-PHEV) is the most common of hybrid architectures and the least expensive. In this topology (Figure 2.3), the traction can be provided by both engines. So, mechanical transmission is more complex than in the series hybrid one but, in turn, electric generator is removed.

The ICE must be designed to provide the maximum sustained power demand as the electric motor only works if the battery is not depleted. This way, the ICE in parallel hybrid architecture is larger than in the series hybrid one but electric motor and batteries are smaller. As a consequence, this topology is more suited for high speeds. Nevertheless, it is less efficient at low speeds or in traffic jams because of its reduced battery capacity and electric motor power.
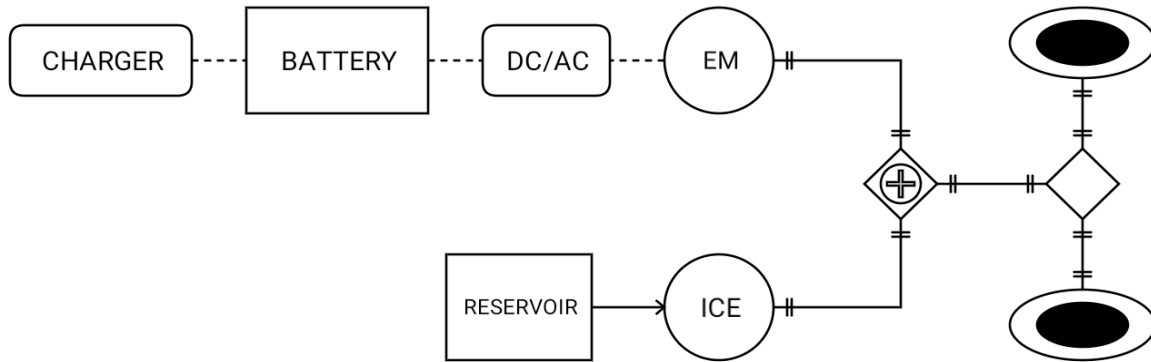
Figure 2.3. Parallel hybrid drivetrain architecture

An alternative parallel hybridization consists of an ICE providing torque to one of the axles of the vehicle, while an electric motor does the same with the other axle. This way, mechanical system is simplified and four-wheel traction can be provided. In this configuration, electric engine not only provides power but also can act as regenerative braking, charging the battery when driver brakes or when battery is depleted. This type of parallel hybridization is called as "through the road" (TTR hybrid). This powertrain configuration is used in the BMW i8 and the Volvo V60 PHEV.

2.4.1.3 Series-parallel hybrid powertrain

In series-parallel configuration (SP-PHEV), the ICE can deliver mechanical torque directly as well as electric power through a generator, as shown in Figure 2.4. In order to do so, it incorporates a so called power-split device, which allows the transmission of the ICE torque either to the wheels or the generator. In this topology, a control system determines the best balance between both traction devices to achieve better efficiency and performance.
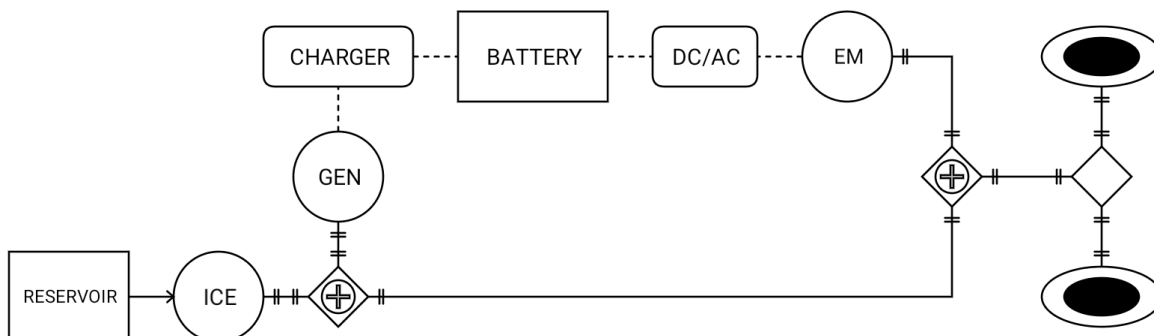
Figure 2.4. Scheme of a series-parallel hybrid powertrain

However, the system is mechanically more complex and it needs a generator such as in the series hybrid configuration. As a consequence, the cost is relatively higher compared to series and parallel drivetrain topologies.

2.4.2 Battery electric vehicles (BEV)

Also named as full electric vehicle or all-electric vehicle, battery electric vehicles are only powered by electricity obtained from a battery and, optionally, from ultracapacitors. These batteries are charged from the electric grid. Also, a regenerative braking system can be used to charge the batteries when the vehicle is decelerating. The architecture of BEVs is less complex than in PHEVs, as shown in Figure 2.5. Their main components are:

- Electric battery, which provides power to all loads of the BEV.
- Battery management system (BMS), which monitors and manages the battery overall status in order to avoid premature battery degradation and safety problems.
- Electric charger, which extracts energy from the electric network to charge the batteries according to BMS.
- Inverter or motor drive, which transforms direct current into alternating current. It provides power to electric traction motor of the vehicle.
- Electric motor, which gives the mechanical torque needed by the vehicle.
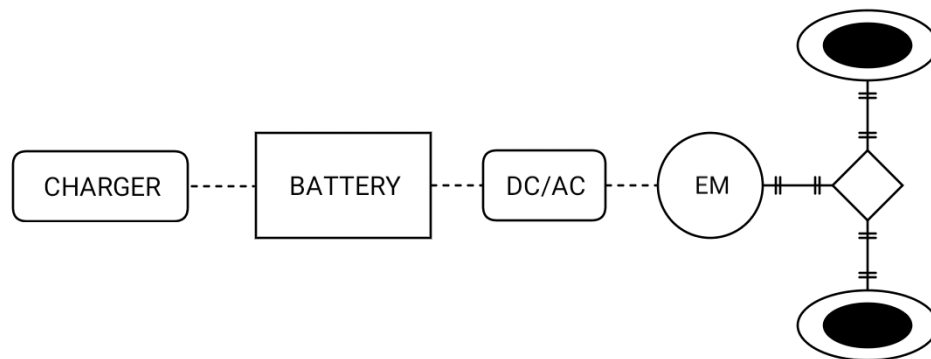
Figure 2.5. Battery electric vehicle basic architecture

However, this type of PEV needs heavy batteries to achieve enough autonomy for daily use. As a consequence, initial cost is higher, although it is expected that the price of kWh of battery will continue falling in the future, making this type of PEV economically competitive. Also, it must be taken into account that the cost per kilometer of a BEV is 3-4 times less than a conventional car. Nevertheless, BEVs have several drawbacks related to battery technology such as: slow charging times and limited autonomy. Due to these two problems a new term known as "range anxiety" has been coined. This term is defined as the fear of being run out of energy when driving an electric vehicle.

2.4.3 Fuel cell plug-in hybrid electric vehicle

A fuel cell device converts hydrogen and oxygen (obtained from the air) in electricity, heat and water, without emitting any pollutants. This type of electric vehicle can be classified as series hybrid EV but, in this case, a fuel cell powered by hydrogen is used instead of an ICE (Figure 2.6). Thus, overall efficiency is improved because fuel cell efficiency can reach 40-50% in comparison with 35% of a diesel ICE [8]. Additionally, unlike in ICEs, fuel cells efficiency remains high at partial loads. The operation of the system is quite similar as in an S-PHEV: the fuel cell is running often at its maximum efficiency point while the battery supplies or absorbs the lack or excess of energy. Furthermore, this type of configuration permits the reduction of the fuel cell size and cost, compared to pure fuel cell electric vehicles [9].
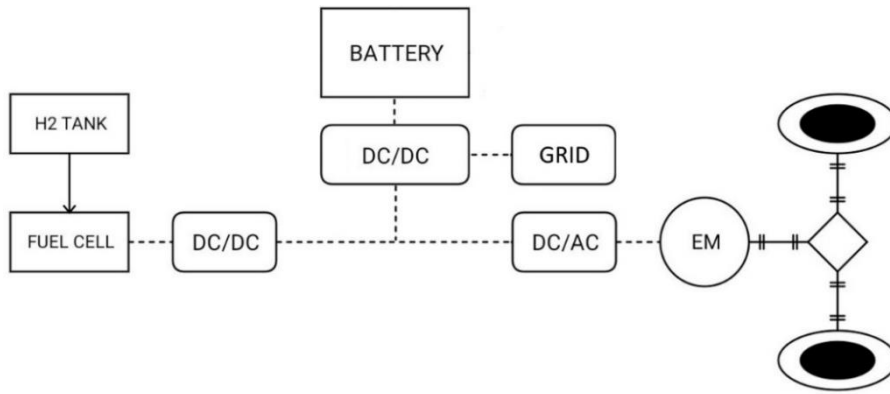
Figure 2.6. Scheme of fuel cell plug-in electric vehicle

Although hydrogen can be produced by the clean process of electrolysis, currently hydrogen is usually generated using steam reforming of methane or natural gas. Then, hydrogen can be stored in compressed tanks inside of the FC-PHEV. Recharging time for this type of PEV is very fast (about 5 minutes) compared to charging a battery from the grid. However, hydrogen stations are expensive (about €3 million) [10].

2.4.4   Comparative between analyzed powertrains

In Table 2.1 a comparison between the different characteristics of powertrains used for plug-in electric vehicles is presented. Currently, most of commercially available PEVs are parallel PHEVs and BEVs.

Table 2.1. Characteristics of different plug-in electric vehicles

	S-PHEV	P-PHEV	SP-PHEV	BEV	FC-PHEV
Traction type	Electric	Electric ICE	Electric ICE	Electric	Electric
Energy Storage	Battery Gasoline/diesel	Battery Gasoline/diesel	Battery Gasoline/diesel	Battery	Battery Hydrogen
Charging infrastructure	Electric grid Gas stations	Electric grid Gas stations	Electric grid Gas stations	Electric grid	Electric grid H2 stations
Autonomy	Regular	Very good	Very good	Bad	Regular
Refueling time	Very fast (gas) Very slow (battery)	Very fast (gas) Very slow (battery)	Very fast (gas) Very slow (battery)	Very slow	Very fast
Initial cost	High	Regular	High	Very high	Very high
Refueling cost	Regular (gas) Very low (battery)	Regular (gas) Very low (battery)	Regular (gas) Very low (battery)	Very low	High
Other characteristics	- Big battery and electric motor - Need a generator - No gearbox	- Limited electric range - Reduced battery and no need of a generator	- Need a generator - Need a power-split device	- Very high efficiency - Zero emissions - Low maintenance	- High efficiency - Zero emissions
Drawbacks	- Less efficient at high speeds	- Less efficient at low speeds	- Complex mechanical architecture	- Battery cost and lifetime	- Fuel cell cost - Lack of infrastructure
Market examples	Chevrolet Volt Fisker Karma Cadillac ELR BMW i3*	Honda Insight Honda Accord plug-in Volvo V60 plug-in BMW i8 Peugeot 3008 Hybrid4 Audi A3 e-tron Mercedes C350 plug-in	Toyota Prius plug-in	Nissan Leaf Tesla Model S Fiat 500e VW e-Up! VW e-Golf Renault Zoe BMW i3*	Toyota Mirai

* BMW i3 has an option to include a little ICE in the vehicle for backup power purposes

2.5   Main components of plug-in electric vehicles

In this subsection, the common components of PEVs are described. These components are the battery, the battery management system, the charger, electric motors and motor drives.

2.5.1   Batteries

Batteries are used for store energy when the EV is plugged into the electrical power supply or when there is an excess of energy in the system, i.e. during regenerative braking. This stored energy is injected to the traction system when it is required by the control unit of the PEV. Also, batteries supply energy to auxiliary elements of the vehicle such as cooling system, lights, etc.

Battery cost is the responsible of 20-40% of the PEV price. However, in the last years, average energy density of batteries has improved from 60Wh/L to 150Wh/L, while cost per kWh has fallen from 800€ to approximately 200€, as can be seen in Figure 2.7. In the short-medium term, it is expected that battery cost will continue falling due to technology improvements and economic scale.
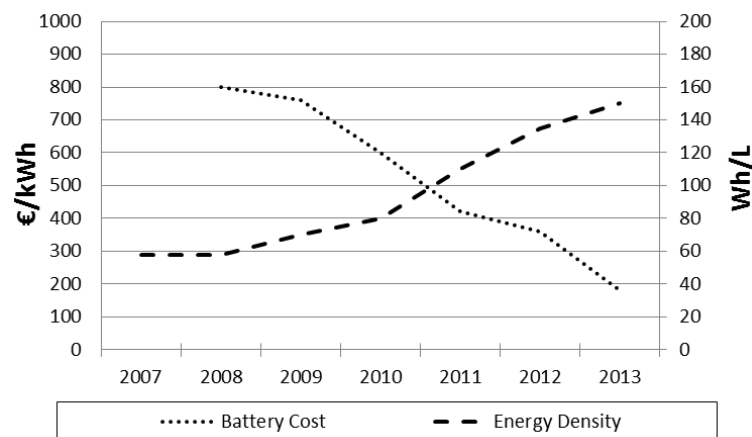
Figure 2.7. Evolution of energy density and battery cost for PEVs [11]

Additionally, battery lifetime is limited. A battery reaches its end of life (EOL) when its capacity is 80% or less of the original capacity at the beginning of life (BOL). In this context, state of health (SOH) of a battery is an indicator of the battery health. A SOH of 100% indicates that the battery is new and it does not suffer any degradation. In contrast, if the battery SOH is 80%, it is said that the battery has reached its EOL. Determining the SOH of a battery is important to know whether a PEV could achieve a determined range or not.

Battery degradation has to be taken into account when it is used not only for travel purposes but also for delivering energy to provide others services. Two types of aging process can be distinguished: aging during cycling and calendar aging. Furthermore, there is a cross-dependency between this two aging mechanism [12]. On the one hand, the calendar life is the loss of capacity due to the pass of time although no use of the battery is made. The calendar life is influenced by temperature and state of charge (SOC) level. On the other hand, the cycle aging refers to the loss of capacity produced by the repetitive process of charging and discharging and depends on the number of cycles, deep of discharge level (DoD), temperature and charging/discharging rate (C-rate).

As can be seen in Figure 2.8, DoD has a great influence in battery degradation. Thus, delivering energy from PEV batteries makes only sense if DoD is limited to small values.
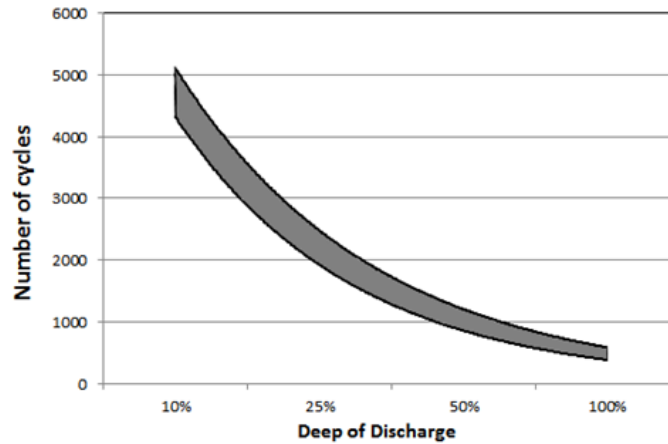
Figure 2.8. Cycle aging in function of DoD for Li-Ion batteries

Four main types of batteries have been used for powering electric cars: lead acid batteries, ZEBRA batteries, nickel–metal hydride batteries (NiMH) and Lithium-Ion batteries.

2.5.1.1 Lead acid batteries

Lead acid battery was invented in 1859 and since then it has been used in multiple applications, even in electric vehicles. This technology is the most mature and the cheapest amongst the different types of batteries. In fact, most of the electric vehicles were powered by these batteries until the development of NiMH and Li-Ion batteries.

However, this type of battery has several drawbacks, which makes it inadequate for mobility applications: the low power and energy density, the limitation of DoD (it is not recommended to discharge the battery below 50% of the SOC), the short lifetime and the relatively high self-discharge.

Currently, lead acid batteries are used in conventional vehicles to start the ICE, for little electric vehicles such as forklifts, golf carts, etc. and static applications such as energy storage for photovoltaic systems.

2.5.1.2 ZEBRA batteries

Zebra batteries were developed by Zeolite Battery Research Africa Project in 1985 and, among other applications, are also used for powering electric vehicles [13]. This type of battery works at high temperature (270-350ºC) and provides a very good energy density (3-4 times higher than lead acid). Additionally, it presents free maintenance, zero self-discharge, unaffected by external temperature and easy estimation of SOC level. Furthermore, it has a good cycle life of more than 1,000 cycles and an excellent calendar life up to 12 years.

However, it uses about 14% of the energy stored per day to maintain its temperature when it is not in use. Otherwise, a preheated cycle, which may last 12 hours, is needed. Zebra batteries are under research in order to reduce its operational temperature.

2.5.1.3 Nickel–metal hydride batteries

NiMH batteries are used in some PHEVs because of its good reliability properties. That is, NiMH batteries can last over 3,000 cycles (10 years) and the operating temperature range has been extended over 100ºC (from -30 to 75ºC). Furthermore, the chemical components used in this battery are more stable than in the Li-Ion batteries and, therefore, they are safer in case of incorrect use.

Although, NiMH batteries are comparable, in cost per kWh, to Li-Ion ones, however they have twice the weight. Additionally, NiMH batteries have several shortcomings such as: self-discharge issues, memory effects problems and they can deteriorate after a long period of storage. So, taken into account the falling prices of Li-Ion batteries [11], it is expected that NiMH technology will become obsolete in the coming years, unless more improvements will be made in this technology.

2.5.1.4 Lithium-Ion batteries

Present and near future battery technology for electric vehicles is based on lithium-ion. Lithium is the lightest and one of the most reactive metals. These characteristics give lithium the ability to achieve very high energy and power densities in applications such as automotive and static storage.

Research about lithium battery began in 1912 but there was not a commercial available battery until 1970s, which was non-rechargeable. The initial use of lithium metal in these batteries avoided the possibility of recharging them because of lithium unstable behavior, especially when they are charged. Furthermore, lithium metal reacts violently when it is exposed to air and water. Under these circumstances, lithium metal can ignite and even explode. In order to overcome these safety and technical concerns, lithium is combined with other elements. This type of rechargeable batteries are called as lithium-ion batteries.

From this point of view, several types of Li-Ion batteries have been developed. Anode is usually made of graphite (carbon) but other components such as lithium titanate can be used. This last option provides a better battery life and operating properties, such as wider temperature operation and faster charging and discharging process, but it has less energy density. For cathodes, there are more chemistry alternatives which provide different characteristics, as can be seen in Table 2.2. Finally, the electrolyte is mostly based on a lithium salt in an organic solution.

Table 2.2. Characteristics of different Li-Ion batteries

	Cell V. (V)	Specific energy (Wh/kg)	Energy density (Wh/L)	Cycle life*	Safety	Cost
Cobalt Oxide (LCO)	3.9	150-200	560	500-1000	Poor	Good
Nickel Cobalt Aluminium Oxide (NCA)	3.8	200-260	600	500	Regular	Regular
Nickel Manganese Cobalt Oxide (NMC)	3.8	150-220	580	1000-2000	Good	Good
Manganese Oxide (LMO)	4.1	100-150	420	300-700	Good	Good
Iron Phosphate (LFP)	3.45	90-120	330	1000-2000	Excellent	Good
Lithium Titanate (LTO)**	2.4	70-80	130	3000-7000	Excellent	Poor

* Depends on DoD and temperature **For anode

Li-Ion battery cell provide a good level of voltage which can allow battery packs with only one cell, as happens in mobile phones. Obviously, for more demanding applications, such

as automotive, more than one battery cell is used. There are three main types of cell depending on the encapsulation, as can be seen in Figure 2.9.

(a)   (b)   (c)
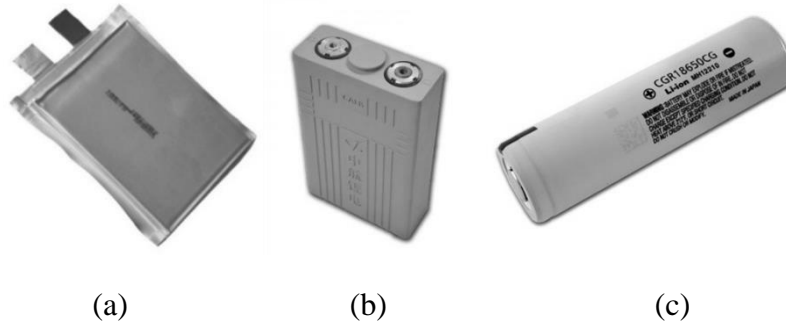
Figure 2.9. Different types of encapsulated cells: (a) pouch (b) prismatic and (c) cylinder

Battery cells are grouped in modules and several modules comprise a battery pack. Each carmaker has used different type of cells and configurations. For example, Nissan Leaf PEV uses 48 modules with 4 pouch cells per module, making a total number of 192 cells. However, Tesla uses smaller cells, specifically the Panasonic 18650 size cylinder cells (also used in common laptops). The 85kWh battery version of Tesla S is composed by 7,104 battery cells divided in 16 modules. Although being more complex, this configuration provides several advantages such as: more space between cells (better cooling and therefore, better lifetime) and improved economic scale. Table 2.3 shows battery cells used in several PEVs.

Table 2.3. Li-Ion battery cells characteristics used in different PEV models

Cell Maker	Chemistry Anode/Cathode	Capacity (Ah)	Encap.	Voltage (V)	Weight (Kg)	Volume (L)	Wh/L	Wh/kg	Used in
AESC	G/LMO-NCA	33	Pouch	3.75	0.80	0.40	309	155	Nissan Leaf
LG Chem	G/NMC-LMO	36	Pouch	3.75	0.86	0.49	275	157	Renault Zoe
Li-Tec	G/NMC	52	Pouch	3.65	1.25	0.60	316	152	Daimler Smart
Li Energy	G/LMO-NMC	50	Prismatic	3.7	1.70	0.85	218	109	M. i-MiEV
Samsung	G/NMC-LMO	64	Prismatic	3.7	1.80	0.97	243	132	Fiat 500
Lishen T.	G/LFP	16	Prismatic	3.25	0.45	0.23	226	116	Coda EV
Toshiba	LTO/NMC	20	Prismatic	2.3	0.52	0.23	200	89	Honda Fit
Panasonic	G/NCA	3.1	Cylindrical	3.6	0.048	0.018	630	233	Tesla Model S

Although different studies have been carried out in order to develop the next generation of batteries, Li-Ion remains the most feasible solution. Furthermore, some aspects of Li-Ion technology are still not well understood such as battery degradation process and safety issues. Therefore, Li-Ion battery has still room to be improved.

2.5.1.5   Future technology in batteries

Different approaches have been proposed as alternative to current Li-Ion batteries in the medium-long term. Lithium Sulphur (Li-S) with a specific energy of about 500Wh/kg is one of them but battery life is still limited. In this context, graphene is proposed to solve this problem [14], [15].

Another promising and cheap technology for the long term is Lithium-air batteries which can achieve 1,500 Wh/L of volumetric energy density, but it is necessary further research in order to address several technical challenges [16].

2.5.2 Battery Management Systems (BMS)

Although Li-ion batteries are designed to be reliable and safe, they still have security concerns, especially when they are over-charged or operated at low or very high temperature. Additionally, battery lifetime could be reduced if battery is over-discharged.

Therefore, batteries of PEVs must be monitored and controlled in order to improve battery lifetime, reduce potential safety risks and provide reliable readings of the SOC, among other functions. In addition, BMS in electric vehicles must be in communication with other parts of the electric vehicle such as the on-board charger, the external charger (in case of fast charging), the cooling system, the system control unit and even the user through a user interface.

Thus, battery management systems have the following functions:

- Acquire data from battery sensors and other devices.
- Manage thermal and overall battery status to ensure a safe operation.
- Determine the SOC and the SOH of the battery.
- Monitor and control the battery charging and discharging.
- Perform cell balancing when it is necessary.
- Improve battery lifetime.
- Establish communication with other elements of the system such as the cooling system, charger, etc.
- Identify and authenticate the battery to prevent non authorized changes on the battery.
- Detect ground faults and current leakages.
- Isolate battery in case of emergency.
- Store historical data to analyze them in case of failure.

Every cell of the battery must be monitored and controlled by the BMS. Thus, three topologies can be distinguished in function of the BMS implementation:

- In the centralized topology, only one BMS unit exists and, therefore, each cell is connected to this control unit through a lot of wires. This solution is the least expensive but the most complex.
- In the distributed BMS, a control unit is attached for each cell and, as a consequence, only a communication wire is used between cells and a central controller. However, this approach is more expensive.
- In the modular BMS, each control unit manages a set of cells. This solution achieves a compromise between cost and complexity.

As mentioned before, PEV batteries are composed by a large number of cells connected both in parallel and series. These cells have to be charged equally but manufacturing deviations can lead that some cells are charged more quickly than other cells. Thus, in the charging process it may occur that some cells are overcharged, deteriorating their lifetime or damaging irreversibly the cells. This problem is even more noticeable when cells are connected in series, because in parallel connection all the cells hold the same voltage.

However, in the parallel connection scheme another problem can appear if one of the cells is short-circuited, because the rest of cell will be discharged through this damaged cell compromising the overall battery safety.

In order to avoid cell overcharging, the BMS has to perform a cell balancing which can be classified in two methods: passive and active cell balancing. On the one hand, passive cell balancing is based on removing the excess of energy on cells with higher SOC. But, this energy is dissipated in internal resistors, so charging efficiency is impacted. On the other hand, active cell balancing searches transfer energy from the most charged cells to the least charged ones, improving overall charging efficiency and reducing charging times. Nevertheless, this last option is more expensive and complex.

In conclusion, the BMS has to cope with current Li-Ion battery problems, such as cell balancing, battery safety, SOC and SOH calculation, etc. These tasks become more and more complex as the number of cells of the battery increases. Thus, the BMS must be designed for each type of battery and plays a key role in the power management and performance of PEVs. In fact, several BMS functions still need to be enhanced.

2.5.3 On-board chargers

On-board chargers convert energy received from the electric grid, the on-board generator (PHEV case) or the regenerative braking system into DC to charge the battery. This device must be communicated with the BMS in order to avoid damaging the battery because of overcharging. Additionally, other security systems can be present such as temperature sensors operating a switching relay. This way, charger can be disconnected when a high temperature is detected somewhere in the battery.

Lithium-Ion batteries are typically charged using constant-current constant-voltage (CC/CV) charging scheme (Figure 2.10). Li-Ion batteries can be damaged if upper voltage limit is surpassed. So, in this scheme, a constant charge current, which is limited by maximum charging current, is injected to the battery.
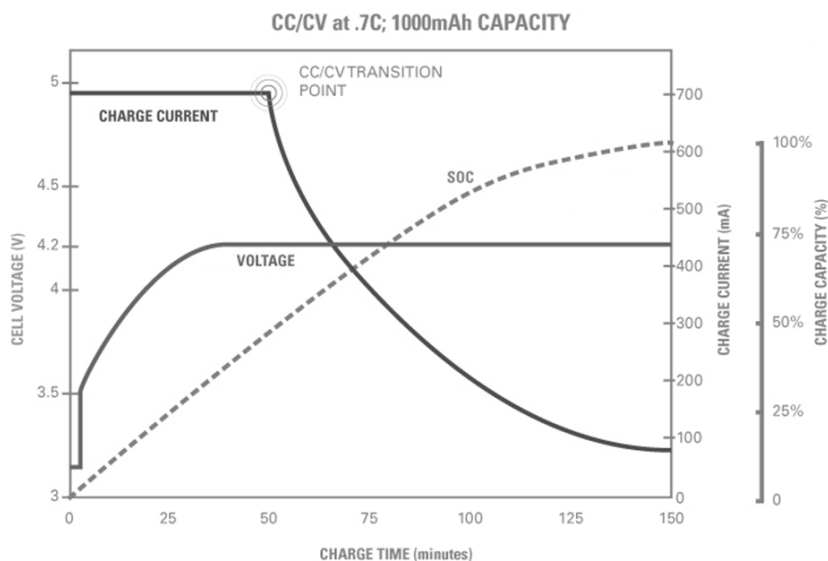
Figure 2.10. Constant current – constant voltage (CC-CV) method for a Li-Ion cell

When upper voltage limit of the battery is reached, charger switches to constant voltage method. This point is named as CC/CV transition point and usually takes place at about 70% of the SOC. During CV period, battery voltage is maintained while charge current decreases, until a predetermined minimum current injection is reached. At this point, it is considered that the battery is fully charged.

2.5.4 Electric motors and drives

Electric vehicle's traction system is composed by one or more electric motors, depending on powertrain and traction configuration selected. Three main types of electric motors have been considered for electric vehicles, induction motor, permanent magnet (PM) motor and switched reluctance motor (SRM):

- Induction motors are a mature technology, which has several advantages such as light weight, robustness, free maintenance, high power density and efficiency and low cost. For automotive applications, squirrel-cage version of induction motors is preferred. Induction motors are typically controlled using constant V/f control but this approach has poor response to fast changes of speed. In order to overcome this issue, field oriented control is used. Even though its good characteristics, induction motor is less efficient than PM motors because of the rotor losses.

- PM motor is considered one of the most attractive solution for automotive applications. Unlike induction motor, there is no current circulation in the rotor, so efficiency is better. Additionally, it has the following advantages: high torque, compactness, low maintenance, very good lifetime, ease of control and silent operation. Nevertheless, PM motors are expensive because rotor is partly made by using rare-earth materials. In addition, they have a limited constant power range which is important to achieve high speeds and they can be demagnetized at high temperatures, so cooling system must be well designed.

- SRM is proven as a very reliable, low cost and simple motor to traction applications. SRM does not use any winding or expensive magnetic material in the rotor. In fact, the rotor is a solid salient-pole with soft magnetic material (laminated steel). The power control is simple, rotor poles tend to align with the nearest stator pole. By switching on/off the successive stator poles, rotation of the rotor is maintained. Due to its robust rotor construction, SRM can achieve very high speeds withstanding better the high centrifugal forces than PM and induction motors. However, two main drawbacks have been found in this type of motor. First, the torque during operation has a high ripple because its discrete nature of operation and, second, operating noise level is also relatively higher.

2.6 Conclusions

Road transport sector is currently in the initial stage to change its energetic model, from using petroleum products to electric mobility. Clearly, current energetic model is not sustainable for long term. Air pollution of some cities is becoming an extremely serious problem. Furthermore, the intensive use of ICEVs is one of the most important factors that contribute to the global warming.

In this context, governments, carmakers and users are beginning to become aware of the abusive use of ICEVs. Thus, electric vehicles have emerged as an eco-friendly alternative

for ICEVs. Within electric vehicles, plug-in electric vehicles are one of the most outstanding technologies. However, as any technology transition, this has to be done smoothly. Under this premise, plug-in hybrid electric vehicles provide an intermediate step until battery or fuel cell technology is fully developed.

In this chapter, different PHEVs powertrains have been analyzed. Series powertrain is relatively easy to implement but it is expensive because it requires a big battery and electric motor. In contrast, parallel powertrain reduces hardware requirements (a generator is not necessary) and purchase cost as well as provides good efficiency at high speed. However, it is mechanically more complex (gearbox is needed). In this regard, TTR configuration reduces mechanical complexity. Finally, series-parallel powertrain stands between both solutions but it also has a complex mechanical system.

Battery electric vehicles remove almost all mechanical devices but their performance is limited by the battery, which also makes them more expensive. Furthermore, charging time of a BEV is very long. Nevertheless, BEV sales are consistently growing in the last years. Finally, plug-in fuel cell electric vehicles could be the perfect combination between efficiency and performance. But currently, the available fuel cell vehicles are being produced in small series.

Regarding to battery technology, currently it is based on Li-Ion batteries. But, even though Li-Ion technology provides a reasonable energy density, it still needs further research to be competitive with conventional ICE technology in terms of cost and performance. Furthermore, there are other issues that have to be solved related to safety and battery lifetime. Thus, a device such as the BMS is needed to closely monitor and control the battery status.

CHAPTER 3

PEVS IN ELECTRIC DISTRIBUTION NETWORKS

3. PEVS IN ELECTRIC DISTRIBUTION NETWORKS

3.1   Introduction

The arrival of plug-in electric vehicles is a great challenge to electric distribution networks. The charge of a large amount of PEVs represents a significant new load demand which should be satisfied. Thus, it is necessary to develop new charging methods, infrastructures and strategies in order to integrate efficiently PEVs into distribution networks.

In this context, there are three different methods for charging PEVs, which are presented in section 3.2. The simplest and most used method is the conductive charging, in which electric energy is delivered from the grid to the PEV battery by using wires. In contrast, inductive charging method does not use wires, in turn, energy is transferred via magnetic fields. Charging time of both methods depends on the charging power used. Thus, two categories are used to define how fast the charging process is. On the one hand, slow charging which is appropriate for charging the PEV at home or workplace. On the other hand, fast charging which is mostly used to charge the battery in the middle of a long trip. Finally, the battery swapping method is based on replacing the depleted battery of a BEV with other battery already charged.

The charging of PEVs can be harmful to electric grids depending on several factors such as PEVs penetration level, the driving and charging behavior of PEV users, etc. On the one hand, impacts of PEVs in electric distribution networks are reviewed in section 3.3. On the other hand, the influence driving and charging behavior of PEV users are analyzed in section 3.4.

Several strategies have been proposed in order to reduce these possible impacts. A classification of the PEV charging strategies is provided in section 3.5. One of the simplest techniques is delaying the charging of PEVs from peak hours to off-peak hours. Incentive prices are used to encourage PEV users to charge their vehicles in low energy demand periods. However, it can be interesting to implement coordinated charging control methods, as PEV market penetration increases, in order to improve the integration of PEVs. Additionally, there are opportunities to be explored such as the integration with renewable energies and the provision of ancillary services, as described in section 3.6. Finally, conclusions of this chapter are summarized in section 3.7.

3.2   Charging methods

Charging methods are being currently developed in order to overcome limited electric range and slow charging rates of PEVs. Among them, conductive charging is the most common but inductive charging could have great potential due to ease of use and improved safety. Finally, battery swapping offers the fastest method in terms of charging time but it can be complex to implement it at large-scale. Following the most relevant characteristics of these charging methods are presented.

3.2.1   Conductive charging

Conductive charging method uses physical direct contact between the PEV connector and the electric vehicle supply equipment (EVSE) or charging point (CP) by using a wire. PEV user must insert a plug into a receptacle on the vehicle in order to charge the battery. Conductive charging technology is efficient, well developed and tested, but users may

prefer not having to plug and unplug their vehicle. Furthermore, conductive charging method can be dangerous if no safety measures are taken, especially in wet conditions. In this context, there are proposals from Volkswagen and Tesla to use robots to connect automatically the vehicle to the charging point without user intervention.

Several standards have been released related to PEV charging equipment. Among them, SAE J1772 and IEC 61851 are the most important.

3.2.1.1 SAE J1772 Standard

Society of Automotive Engineers (SAE) standard J1772 is the reference document for the United States about conductive charging of EVs and PHEVs. This standard establishes the requirements for EVSE and defines four different levels (Table 3.1): AC level 1, AC level 2, DC level 1 and DC level 2.

Table 3.1. Charging levels defined in SAE J1772

	Charger	Location	Power supply	Setting	Connectors
AC Level 1	On-board	Residential Parking lot	120Vac/16A	1.7kW	NEMA 5-15 SAE J1772
AC Level 2	On-board	Residential Commercial	208V-240Vac/16A 208V-240Vac/80A	3.4kW 19.2kW	SAE J1772
DC Level 1	Off-board	Charging stations	208-480Vac (3-phase)	Up to 500Vdc @ 80A	SAE J1772 Combo
DC level 2	Off-board	Charging stations	208-480Vac (3-phase)	Up to 500Vdc @ 200A	SAE J1772 Combo

- AC Level 1 EVSE (often referred as Level 1) provides charging through a 120V AC plug. Most PEVs come with an AC Level 1 EVSE cord set, so that no additional charging equipment is required. On one end of the cord there is a standard NEMA 5-15 connector. On the other end there is a J1772 standard connector, which plugs into the vehicle. This charging method is designed to be used when PEV user does not have a Level 2 EVSE available, e. g. when the user goes to a family member's home. For this reason, it is usually called as occasional charging. Even though Level 1 is the slowest charging method, it can cover driver's needs. For example, 8 hours of charging can replenish more than 40 kilometers of electric range, which is equal or more than the average daily driving distance.

- AC Level 2 EVSE is the most preferred charging method and offers charging through 208V (typical in commercial applications) or 240V (residential applications) electrical supply. It requires installation of home or public charging equipment and a dedicated circuit and measurement device, depending on the EVSE requirements. Additionally, charging power is noticeably higher than in Level 1 case, operating up to 19.2kW. Level 2 EVSE can be located either in homes or public places, such as public parking lots and shopping centers.

- DC level 1 and 2 EVSEs provide a very high charging power, through external DC chargers. These types of EVSEs are usually located along heavy traffic routes and at public stations. This option lets users to charging as fast as possible their PEVs during a long trip. A new version of SAE 1772, for including AC level 3 and DC level 3 is currently under study. In this new version, DC level 3 charge current could reach up to 400A.

3.2.1.2   IEC 61851 Standard

The International Electrotechnical Commission (IEC) promotes the IEC 61851 standard related to electrical connectors and charging modes for electric vehicles. This standard is based partly in the SAE J1772 standard. According to the standard IEC 61851-1 "Electric vehicle conductive charging system" there are four different operation modes for charging, as shown in Figure 3.1.

- Mode 1: the EV is connected to the AC power supply network not exceeding 16A and 250Vac single-phase or 480Vac three-phase, using standardized socket-outlets and the power and protective earth conductors.
- Mode 2: the EV is connected to the AC power supply network, not exceeding 32A and 250Vac single-phase or 480Vac three-phase, using standardized socket-outlets and power and protective earth conductors, together with a control pilot function. Protective devices are usually integrated in the cable, which is provided by the carmaker.
- Mode 3: the EV is connected to the AC power supply network, using dedicated EV supply equipment (EVSE) which has a pilot function (conductor).
- Mode 4: the EV is connected to the AC power supply network through an off-board charger that delivers direct current (DC). This off-board charger is part of an EVSE, which has a pilot function.
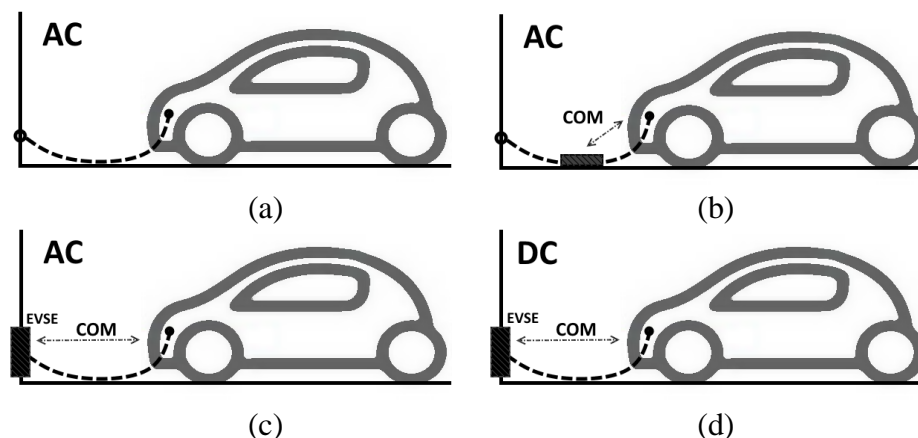
Figure 3.1. Different charging modes according to the IEC 61851-1 standard. (a) Mode 1 (b) Mode 2 (c) Mode 3 and (d) Mode 4

Safety in Mode 1 depends on the external installation of a residual current detector (RCD) and the earth conductor. Without these devices, safety concerns may happen in case of a fault happens. Some countries allow Mode 1, leaving the responsibility of installing the required safety devices to the user. However, other countries do not allow Mode 1, such as the United States, where there are still many installations without RCD devices.

In this context, the inclusion of control and proximity pilot conductor improves overall security of the system. These conductors have to provide the following functions:

- The system should be able to determine that the connector is properly inserted in the vehicle inlet and properly connected to the charging station.
- Vehicle movement by its own propulsion system shall be impossible as long as the vehicle is physically connected.

- Continuous protective earth conductor continuity checking. Earth continuity between the charging station and the vehicle should be continuously verified.
- Energization of the system should not be performed until the pilot function between the charging station and the electric vehicle has been established correctly.
- If the pilot function is interrupted, the power supply to the cable assembly should be interrupted but the control circuit may remain energized.

Additionally, control conductors should also provide other functions:

- Selection of charging rate: an automatism should be provided to ensure that the charging rate does not exceed the rated capacity of the AC power supply network (mains), vehicle or battery capabilities.
- Determination of cooling requirements of the charging area: if additional cooling is required during charging process, it should only be allowed if such cooling is provided.
- Detection/adjustment in real time of available load current of the supply equipment: a control circuit must be provided to ensure that the charging rate shall not exceed the real time available load current of the charging station and its power supply.
- Retaining/releasing of the coupling: a mechanical automatism shall be provided to retain/release the coupler.
- Control of bi-directional power flow if it is available.

3.2.1.3   Charging connectors types

Several dedicated charging systems and plugs have been proposed until now. The standard IEC 62196-2 reflects the following plugs types:

- Type 1: single phase vehicle coupler. Also known as "Yazaki", this type almost corresponds to the SAE J1772-2009, which is the North American standard. The plug is composed by five pins: line 1, line 2, ground, pilot and proximity.
- Type 2: single and three phase vehicle coupler. Also known as "Mennekes", this type reflects the VDE-AR-E 2623-2-2 standard, which is considered to be the European standard. The plug is composed by seven pins: line 1, line 2, line 3, neutral, ground, pilot and proximity.
- Type 3: single and three phase vehicle coupler with shutters. This type of connector has been pushed by the EV Plug Alliance to include shutters to protect electrical pins, as an additional safety measure. However, this solution has lost relevance in favor of Type 2 solution. Furthermore, Mennekes also offers a plug with shutters.

Direct current fast charging plug (Mode 4) is not considered in the IEC 62196-2. CHAdeMO Japanese standard is the most extended DC charging system but is not compatible with Type 1 and Type 2 connectors. IEC 62196-3 and SAE J1772 promote Combined Charging Systems (CCS), which consists in adding DC pins to Type 1 and Type 2 connectors (Figure 3.2). This way, only one receptacle is necessary in the PEV.

There are other standard plugs, such as GB standard for China. Also, Tesla carmaker has developed his own charging system and plugs, within the supercharger network that Tesla is currently building. Only Tesla vehicles can be charged in this network but Tesla vehicles can be also charged in other EVSEs by using adapters. Table 3.2 shows the charging options available for four different PEVs.

Figure 3.2. CCS Type 1 and CCS Type 2 combo receptacles

Table 3.2. Charging options of several PEVs

	Battery (kWh)	Vehicle receptacle	Max. Power (kW)	Mode
Chevrolet Volt	16	SAE J1772 (Type 1)	1.4	2
			3.3	3
BMW i3	22	CCS (Type 2)	2.4	2
			7.4	3
			50	4
Nissan Leaf	24	SAE J1772 (Type 1) CHAdeMO	1.4	2
			3.3/6.6	3
			60	4
Tesla Model S	60/85	Proprietary	10	2
			10/20	3
			120	4

3.2.2 Inductive charging

Inductive charging eliminates the necessity of plugging any wire into the vehicle. This way, safety is considerable improved as no active part of the system is physically accessible. In this system, energy is transmitted electromagnetically through the coupling of two coils, one in the ground (transmitter pad) and the other one inside the vehicle (receiver pad). It works similar to the transformer principle.

Inductive charging presents several disadvantages such as its relatively low efficiency, limited charging power, high complexity and cost. Magnetic coupling is done through an air gap between transmitter pad and vehicle pad. Furthermore, in order to achieve good efficiency and power transfer, both pads must be aligned. In fact, charging process does not start until this misalignment is less than a predetermined distance (100 to 250mm).

Currently, a SAE standard for wireless charging is being developed (SAE J2954) by carmakers, suppliers, industry experts and government representatives. Although this standard is still not published, there is a commercially available product on the market, named Plugless Power [17]. This level 2 EVSE provides 3.3kW of charging power. The system includes an automatic alignment guidance in order to help the driver to align easily the charging pads. System efficiency depends on the air gap, the offset alignment and the charging power but can reach 90% [18]. As a drawback, no PEVs have charging pads pre-installed.

Finally, Korea Advanced Institute of Science and Technology (KAIST) has developed the Online Electric Vehicle (OLEV) technology [19]. This option consists in providing energy to electric vehicles wirelessly, while the vehicle is moving. Power is transmitted electromagnetically from electric cables, which are buried under the surface of the road, to the receiver pad installed on the underbody of the vehicle. Only 5 to 15% of the length of the road has to be modified to integrate this technology. Additionally, battery capacity of

the vehicle can be cut down to the third to fifth part, reducing initial cost of the electric vehicle. This technology is especially suited for electric buses, which routes are fixed.

3.2.3 Battery swapping

Battery swapping method is considered as an alternative to quickly replenish energy of BEVs. It consists in replacing physically a depleted battery for another already charged battery. This process saves time as it may last less than five minutes. In fact, this method is extensively and successfully used in electric forklifts.

Battery swapping is carried out in battery swapping stations (BSS) where replaced batteries are also charged. This way, batteries are charged in a centralized way and the supply network of this type of infrastructure can be specifically designed. However, battery swapping process could not be as easy as it seems because BEV batteries are heavyweight (200kg or more). Furthermore, batteries are usually protected with metal shields to improve safety against underbody impacts which makes the swapping process more difficult.

In addition, a large deployment of BSSs may require the use of standard batteries and almost two or three of them per vehicle (one in the vehicle, one charged and one in charging process). This will increase the cost of BSSs.

3.3 Impact of PEVs in electric distribution networks

PEVs represent a new load that must be satisfied at any moment. Many researchers have analyzed the possible impacts that a large deployment of PEVs can have on electric grids. The most mentioned issues are:

- Changes in load demand curve.
- Changes of generation portfolio.
- Increase of voltage deviations and unbalances.
- Congestion of lines and distribution transformers.
- Increase of energy losses.
- Increase of GHG emissions per kWh of electricity generated.
- Decrease of distribution transformer lifetime.
- Increase of energy cost.
- Increase of harmonic distortion.

Impacts on electricity demand profile depend on charging and driving behavior. Zahra Darabi et al. have developed a stochastic model based on 2001 U.S. NHTS, in order to estimate the impacts on electricity load curve [20]. Results show that peak power demand of PHEVs is produced between 20:30 and 22:00, depending on PHEV battery capacity. Higher charging levels lead to short charging times and therefore, peak power will be higher and earlier than in low charging level approaches.

Long term impacts in residential distribution networks were analyzed in [21]. Researchers use The 2009 U.S. NHTS to model driving and charging behavior while the IEEE 34 Node Test feeder was used as the reference distribution network. They select three years (2020, 2023 and 2026) to analyze the impact of charging PHEVs taking into account the growth of house loads in load curve. In addition, summer and winter scenarios were analyzed. According to the authors, the main problems of uncontrolled charging of PHEVs are: the increase of peak power to average ratio (load factor) and energy losses, in addition to

congestion problems. Voltage deviations were also analyzed but there is no mention about voltage unbalances.

It is expected that with the massive introduction of PEVs, generation portfolio will change. Regarding to this problem, A. Foley et al. have analyzed the possible consequences in electricity market operations, specifically in the Ireland case [22]. Two scenarios have been analyzed, peak and off-peak charging. Both will increase system marginal price which is determined by the most expensive power plant needed to meet the demand during a period of time. Off-peak scenario leads to better system efficiency as it increases the base-load power demand and improves wind energy integration. GHG emissions of electric system will be increased in both scenarios but taking into account GHG emissions avoided by clean operation of PEVs, net emissions will be smaller.

Clement-Nyns et al. have carried out a study about PHEV impacts on residential distribution networks in [23]. A downscaled version of the IEEE 34 Node test feeder was used as network reference, while maximum charging power was set to 4kW (standard outlet maximum power). According to the authors, uncoordinated charging will increase voltage deviations and power losses. Additionally, higher power losses lead to higher electricity cost.

Also, charging of electric vehicles in LV distribution networks will impact on distribution transformer lifetime [24], [25]. One of the main common failures of transformers is the degradation of the insulation, which depends on temperature operation. Charging PEVs will increase the average power demand at transformer level and, therefore, temperature operation of the transformer will be higher. Additionally, gas formation may happen due to loss of insulation. However, load-levelling carried out by coordinated charging of PEVs could reduce the daily expansion/contraction of the transformer. This way, wear of transformer bushing will be reduced. Because of bushing is the main entry point of oxygen, water and other pollutants, load-levelling could improve transformer life expectancy.

Additionally, PEVs are charged through power electronics converters, which produce harmonic distortion in the distribution systems. Harmonic distortion can increase energy losses at transformer level because of the induced eddy or Foucault currents and increased skin effect. This can lead to a loss of life of the transformer [26]. In addition, if a large amount of PEVs are charged at the same time (i.e. night charging), the overall harmonic distortion could be very high. In contrast, reduced ambient temperature registered at nights could help to cooling down the distribution transformer.

3.4 Influence of driving and charging behavior

Driving and charging behavior are key factors to evaluate the impacts on the electric grids. Questions such as how many kilometers per day are done, how many times per day the PEVs are plugged and where and when users plug or unplug their PEVs have to be analyzed. Furthermore, the answer to these questions depend on the type of area (rural or urban), region or country, type of day (weekday or weekend day) and other random factors such as weather, sport events, etc. As a consequence, it is difficult to obtain an accurate model of driving and charging behavior. However, an approximate model can be very useful for utilities to determine where and when users are willing to charge their PEVs. Thus, utilities may properly schedule their electricity generation and address any local problems of stability and reliability. Additionally, parking time has special importance for

V2G concept. Ideally, V2G requires that PEVs are parked and connected as long as possible.

Fortunately, several studies have been carried out in order to know the driving and charging behavior of PEV users. Among them, Green eMotion, which has been carried out in Europe, and the EV Project carried out in the United States are the most important ones.

Green eMotion project has been carried out during four years in different cities of Europe, finishing the project activities at the beginning of 2015. One of the objectives of the project has been to analyze the driving and charging behavior. Within this project, 503 PEVs and 1,501 EVSEs were monitored during three years. More than 94,000 trips and 77,000 charging events were recorded. 37% of PEVs were owned by public entities, 39% by companies and the rest (24%) were owned by private users. Results obtained in this project can be found in [27].

The EV Project was initiated in 2010 to demonstrate the feasibility of EV technology. This project was funded by the DOE (U.S. Department of Energy) and has collected data of PEVs running in 18 American cities. Data obtained in this project has been classified in two parts: BEVs and PHEVs. On the one hand, 2,903 Nissan Leaf were monitored during one year. The total number of trips and charging events were 1,454,220 and 347,222 respectively [28]. On the other hand, data about 923 Chevrolet Volt were collected, making a total of 579,828 trips and 170,311 charging events [29]. All vehicles in this project were privately owned and operated for personal use.

Additionally, a large number of travel surveys have been done in several countries. These travel surveys present the advantage of giving more accurate data about driving patterns because the very high number of participants. Although these travel surveys have not been specifically developed to analyze the usage of electric vehicles, it is expected that the introduction of PEVs will not affect significantly the travel patterns of users. Among them, The 2009 U.S. National Household Travel Survey is the most important travel survey developed [30]. A total amount of 537,022 car trips were recorded. An advantage of this survey is the free access of raw data, allowing researchers to obtain their own travel behavior models. In fact, this survey has been widely used by researchers [21], [31]–[34].

Other similar researches have been carried out with smaller samples, obtained from EV pilot projects. A.P. Robinson et al. have analyzed the charging behavior and evaluated the impact on that charging behavior if a TOU tariffs is implemented [35]. The study comprised 31,765 PEV trips and 7,704 charging events from SwitchEV trial in England.

3.4.1.1   Driving behavior

Driving habits refers to the use given to the PEV, how many kilometers are made daily, how many trips per day and, finally, the energy consumed per kilometer.

A.   Average distance travelled per day and trip

Distance travelled per day and fuel economy will define the energy consumed by a PEV per day. This energy must be produced and transmitted through the electric network to the PEV. Moreover, distance travelled per day will define the minimum autonomy that a PEV must have to satisfy the user needs.

According to 2009 NHTS, people who live in urban areas drive approximately 37.2 km. In contrast, people who live in rural areas travel 55 km on average. Green eMotion has concluded that, on average, private PEV users drive 34.3 km per day [36]. The EV project stated that BEVs users drive 48.7 km per day [28] while PHEVs users drive 65.5 km per day [29].

Nowadays, PEVs can cover most of travel needs of the drivers. As an example, almost 98% of Irish drivers travel less than 100 km, which is achievable by the average autonomy of PEVs (Figure 3.3).
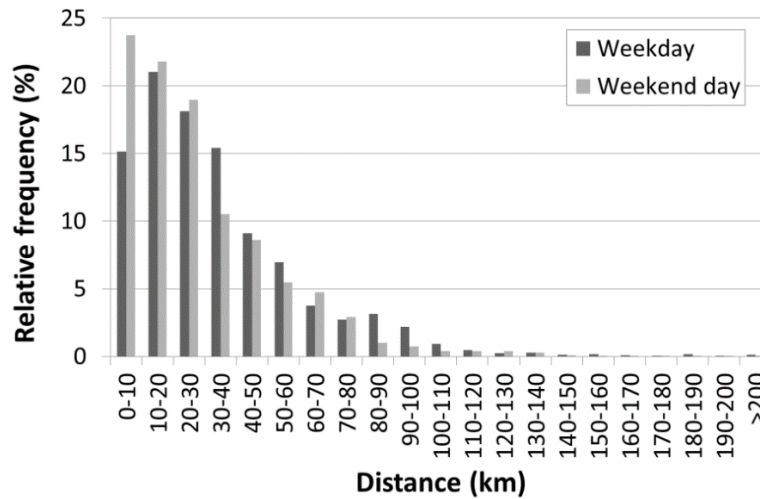
Figure 3.3. Daily distance travelled for the Ireland demo region of Green eMotion [37]

With regard to trip distance, most of the trips were less than 10 km in the Ireland demo region and only 5% of them were more than 25 km, as can be seen in Figure 3.4. Data obtained from "The EV Project" shows an average displacement of 11.1km [28].
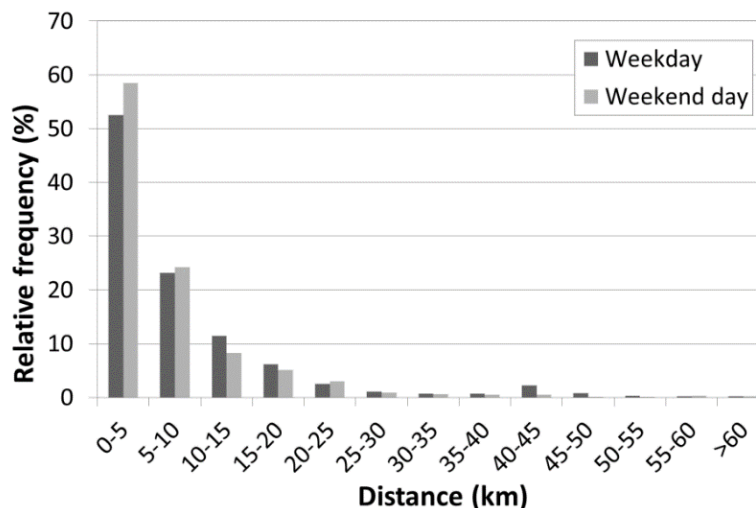
Figure 3.4. Trip distance distribution for the Ireland demo region of Green eMotion [37]

B.   Energy consumption per km

The energy consumed per kilometer depends on multiple factors, such as: battery type, vehicle model, trip length, climatic condition, type of road, etc. Climatic conditions have

special impact in energy consumption per kilometer not only because battery efficiency is affected but also due to the intensive use of comfort and auxiliary systems such as lights, heater or air conditioning. This fact is more noticeably in cold climates where energy consumption in winter can be the double of spring season [36]. Figure 3.5 shows the average energy consumption in Northern demo region (Copenhagen, Malmö and Bornholm).
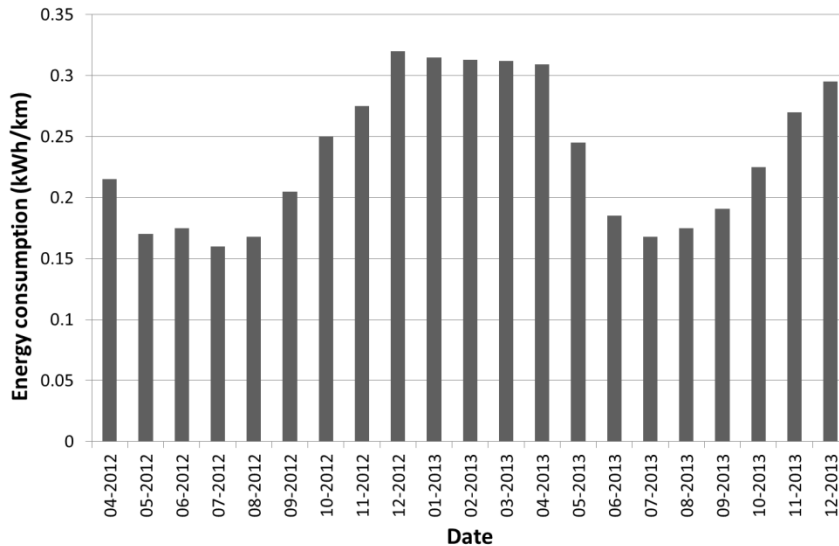
Figure 3.5. Energy consumption per km in Northern demo region [36]

In general, short trips are more energy demanding than long trips. Green eMotion project pointed out that for trips up to 5 km, the energy consumption was 0.22 kWh/km on average while for long trips (40 km or more) the energy consumption was 0.17 kWh/km on average. Furthermore, zebra batteries use more energy in short trips (0.29 kWh/km) than Li-ion batteries (0.22 kWh/km) but for long distances, both have similar energy consumption.

Road type has also an important impact on energy consumption. Dynamometer Drive Schedules or Drive Cycles are standardized test to calculate the energy consumption per kilometer of a vehicle. These drive cycles vary depending on the type of route to be simulated. In the United States, the regulator of these drive cycles is the Environmental Protection Agency (EPA), being the most representative:

- Urban Dynamometer Driving Schedule (UDDS): Represents city driving conditions.
- Highway Fuel Economy Driving Schedule (HFEDS): Represents highway driving conditions under 96 km/h.
- US06: Represent a high acceleration aggressive driving schedule.

Standard SAE J1634 defines procedures to test BEV in order to estimate the energy consumption and range for light-duty vehicles (LDV). As an example, the Nissan Leaf BEV has an energy consumption of 0.194, 0.228 and 0.334 kWh/km for UDDS, HFEDS and US06 respectively (charging efficiency is excluded) [38]. Drive cycles are effective tools to compare which vehicles are the most efficient but may fail to determine the overall energy consumption in real conditions.

3.4.1.2 Charging behavior

Charging behavior term refers to the interaction between the user of a PEV and the EVSE. Location, charging frequency, initial time, charging duration, connection time and initial and final SOC are the most important parameters which comprise charging behavior.

A. Charging location

In contrast to ICEV, PEV users have the opportunity to charge their vehicles in their own homes, because the installation of a charging point requires a small space. PEV users usually prefer home charging, in fact 82% of "The EV Project" charging events were made at home and the rest outside [28]. However, there is an increase of charging events outside home as the charging points increase in other locations [39].

B. Charging frequency

The charging frequency has also influence in economic, social and environmental development of PEVs. A higher charging frequency may allow a reduction of PEV battery size and weight. But such high charging frequency is only possible with a larger number of charging points and bigger investments in infrastructure.

The daily average charge events recorded in The EV project was 1.05. Figure 3.6 shows the distribution of the charging events per day, where a wide variation between 0.15 and 3.2 charging events per day can be seen. This is due to the different users' behaviors: from users that only charge their BEVs when it is absolutely necessary, through users who charge their BEVs every night, to users that charge their BEVs whenever they can, motivated by the thought of charging their BEVs "just in case". Finally, there is another group of users who charge their BEVs more than once a day due to travel requirements, as they cover more kilometers than the autonomy provided by the Nissan Leaf.
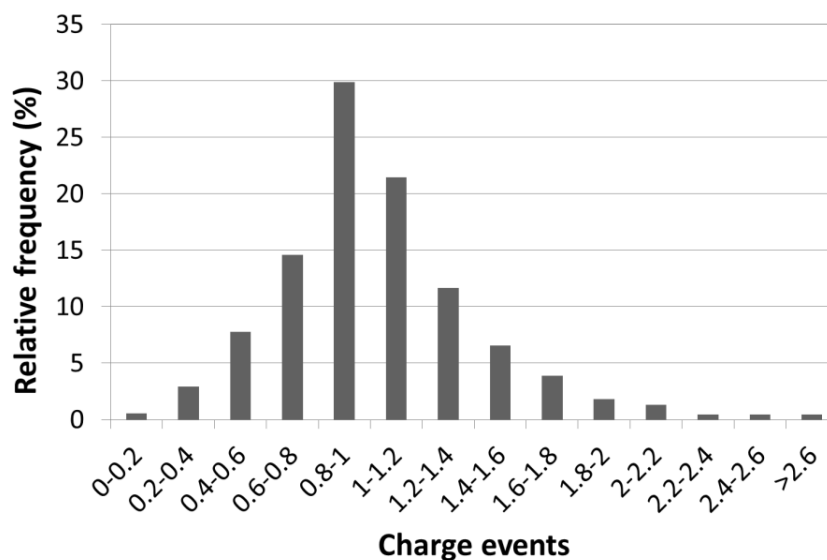
Figure 3.6. Distribution of number of charge events per day for BEVs [28]

In the case of the Chevrolet Volt PHEV [29], charging events are distributed according to Figure 3.7. The daily charging events range from 0 to 2.5, taking an average charge frequency of 1.5 for weekdays and 0.7 for weekends. A decrease in the charging frequency

during weekends can be observed compared to weekdays, mainly because users change their routine. During weekends, PHEVs are generally parked more time away from home and in places where there are no charging points. Undoubtedly, these values could be higher depending on the charging opportunities outside home.
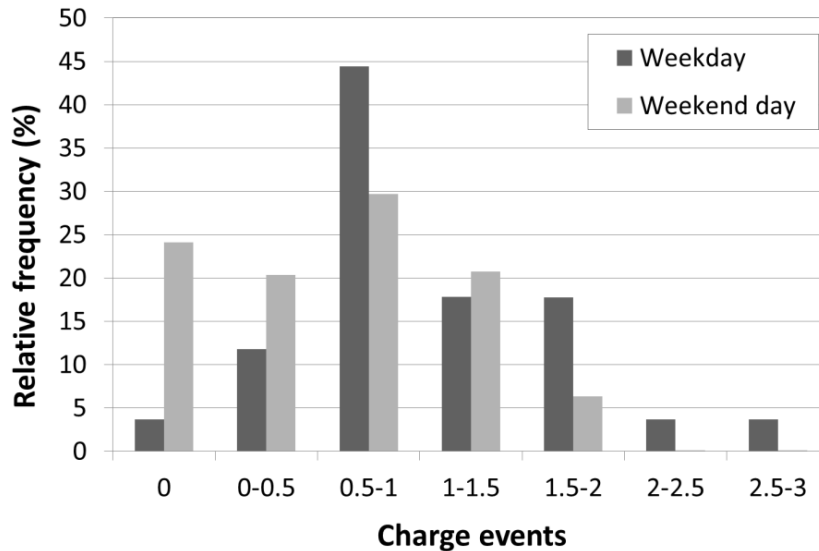
Figure 3.7. Average daily charging frequency for PHEVs [15]

During weekdays, users who regularly connect more than once usually have charging points in their workplaces or they charge at home several times, depending on their employment status. It is important to point out that most of the users, who charge PHEVs less than once a day, often are unaware of the PHEVs operation and the importance of charging them for increasing the efficiency of operation.

With regard to Green eMotion project, it has recorded approximately 0.64 charge events per day. This value increases to 1.56 if days with at least one charge event are taken into account. This project has also stated that charge events are less frequent at weekends. Most of them (around 76%) were carried out during weekdays.

C. Energy consumption per charge event

Location of the EVSE and type of day (weekday or weekend day) have a great influence in PEVs energy demand profile. In this context, Green eMotion project has analyzed energy demand per charge event, for different EVSE or CP locations. Four locations were analyzed: household, office, public parking and street.

Figure 3.8 shows the average energy demand per charge event for different locations. The highest demand of energy for household charging is between 18:00 to 20:00h, while the lowest demand happens between 3:00 to 7:00h. With regard to charging at office, users charge their vehicles more frequency between 21:00 to 22:00h. In contrast, no night charging is produced in this location. Public access parking chargers has the peak power demand from 18:00 to 21:00h. Energy demand in this type of location is more distributed compared to previous locations. Finally, street located EVSEs have more energy demand during mornings (peak at 8:00h) and steadily decrease during the day.

Except for public access parking case, almost no night charging is used and, as a consequence, grid impacts can be higher. Furthermore, household charging, which is the preferred option by users, can produce an important increase of energy demand at peak hours.
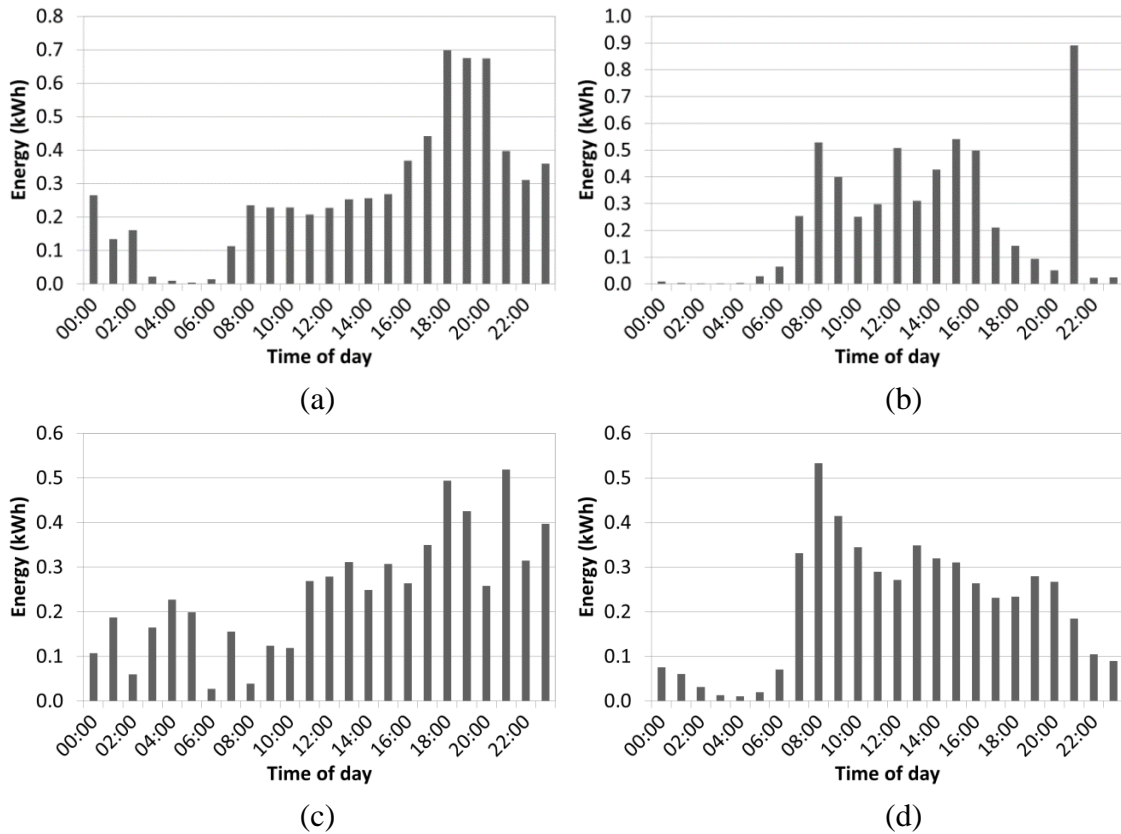
Figure 3.8. Energy per charge event for different EVSE locations: (a) household (b) office (c) public parking and (d) street

Related to home charging, Figure 3.9 shows the PEVs energy demand difference between weekdays and weekend days. Both load curves present similar shape but during weekdays, peak power demand is relatively higher.

Similar behavior has been detected in Nashville, which is part of the demo cities of The EV Project. Peak demand happens around 21:00h, as can be seen in Figure 3.10. In this city, users do not schedule their PEVs to begin charging process at any specific time. Instead, users charge their PEVs as they arrive home and connect them to the grid. This way, the charging demand curve increases gradually.

Additionally, The EV Project has also analyzed the influence of establishing a two-period TOU tariff, in this case in the city of San Francisco. Peak demand is delayed around 4 hours respect to no TOU tariff case of Nashville. Users in San Francisco program their PEVs to begin the charging process between 00:00 and 1:00 hours, which causes a sharp increase in charging demand. This rise triples the charging demand in less than an hour, as can be seen in Figure 3.11. Furthermore, the peak power demand in San Francisco is relatively higher than the Nashville one. At weekdays, the off-peak period is set between midnight and 7:00 hours while at weekends this period begins at 21:00 hours.
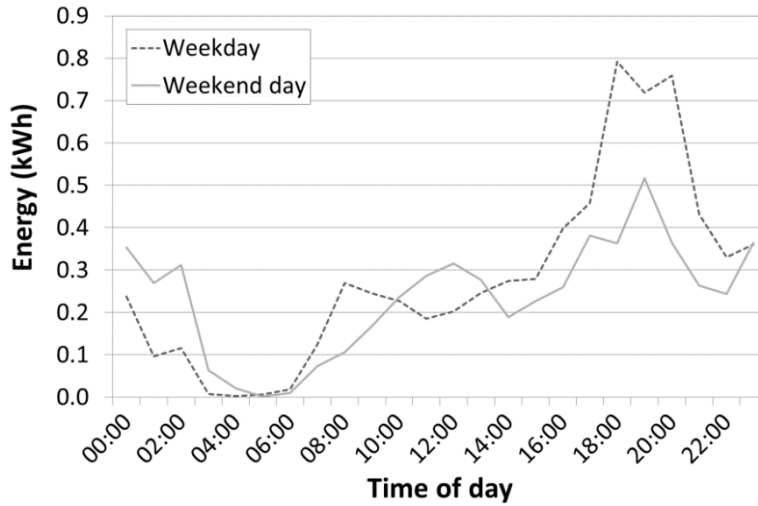
Figure 3.9. Energy demand per charge event at household location (Green eMotion)
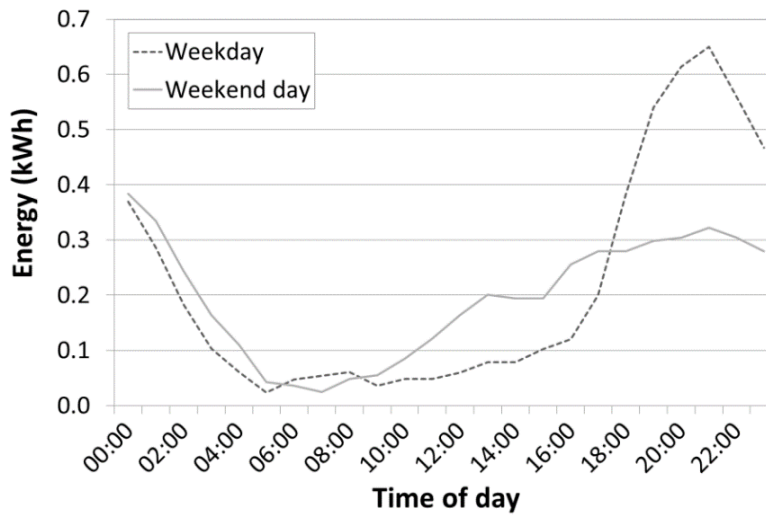
Figure 3.10. Energy demand per charge event in Nashville (The EV project)
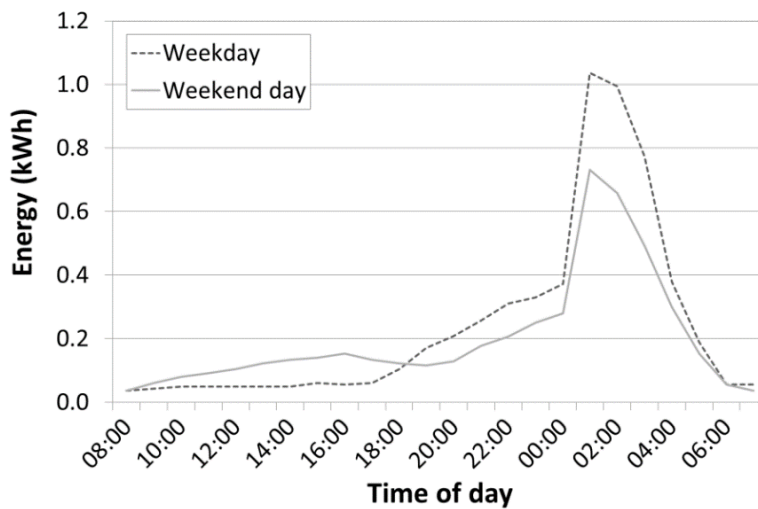
Figure 3.11. Energy demand per charge event in San Francisco (The EV project)

D.   Initial and final SOC of charge events

It is interesting to know the battery initial and final SOC, in order to understand the behavior of the charging process. The initial SOC of the PEV is an indicator of how far users are unloading their PEVs. Furthermore, the final SOC of a charging event indicates when a user interrupts the charging process of the PEV. It is also useful to know that type of behavior, depending on whether the charge is done at home, or during weekdays or weekends.

According to "The EV Project", most of BEVs begin the charge process with a SOC level between 20 and 80% (Figure 3.12). BEV users tend to be more conservative when they charge their vehicles away from home.
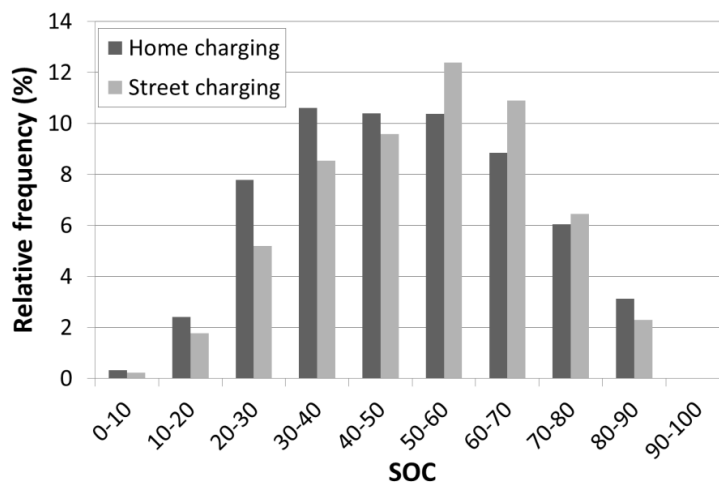
Figure 3.12. Distribution of initial SOC in The EV Project

Furthermore, most charges end with a SOC close to 100% (Figure 3.13). It can be observed the existing peak in the 70-80% SOC range, possibly because the Nissan Leaf offers the possibility of ending the charge process at 80% of SOC, in order to increase the battery life. However, charges made at home usually end up with a higher SOC. Thus, 60% of the charges made at home were full charges while only 40% of charging events done away reached 100% of SOC.
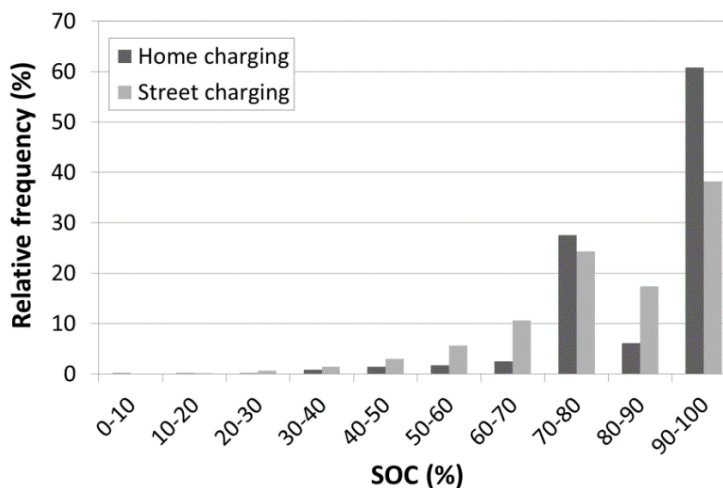
Figure 3.13. Distribution of final SOC in The EV Project

3.4.1.3   The role of smart meters in the integration of PEVs

Currently, smart grid concept is limited to some areas of electric grids, such as high and medium voltage distribution network, large electricity generating plants and some consumers. However, the fast growth of world population is increasing the electricity demand. At the same time, environmental regulation and social aspects are limiting the expansion of transmission networks and generation plants. In this context, where electric grids are near of its maximum capacity, severe energy shortages can happen more frequently. So, it is necessary to take actions in favor of electric grids reliability.

One way to address this problem is improving measurement devices in order to predict more accurately consumers' behavior. Smart meter technology is the key element in this new scenario. Smart meters provide information on real time about electric energy consumption not only to utilities but also to customers. This way, they can become aware of how much electricity they are consuming, how much it cost and what the emissions produced are. In the near future, smart meters will also be able to provide data about gas and water consumption.

In this context, several pilot projects for smart metering have been developed and regulatory effort and investment are currently underway around the world, to implement smart meters as well as increase network communications, remote and automated management of network elements. This way, distributed generation and electric vehicles will be fully integrated and supported. As a first step, combining data obtained from smart meters and PEVs pilot projects can predict distribution network impacts [40].

The predictable large deployment of PEVs can bring technical and economical revenues, if the electric system is properly equipped with communicating devices and the ability to perform some centralized or decentralized levels of control. Smart meters are well-positioned to provide the necessary communication path between PEVs and high-level control devices, as well as perform local management [41], [42].

3.5   Classification of PEVs charging strategies

Most of the times, PEVs are charged in residential EVSEs while fast charging EVSEs are reserved for sporadic charging. Furthermore, electric supply of fast chargers is designed specifically to cope with high power densities. However, current LV distribution networks are not suited to charge a large number of PEVs. In order to overcome this problem several charging approaches have been proposed, which can be classified according to Figure 3.14. These approaches present the following characteristics:

A.   By energy flow: There are two modes of operation between the PEV and the grid regarding energy flow direction. In charging mode, this direction is from the grid to vehicle (G2V) also known as unidirectional. Bi-directional is possible when power flow can also go from vehicle to grid (V2G), also referred as discharging mode. Three elements are required for V2G operation: a bi-directional charger which allows energy flow from and to the battery, a bi-directional smart meter to measure accurately energy and services exchanges and a control system able to exploit the possibilities of the V2G concept, both technically and economically.
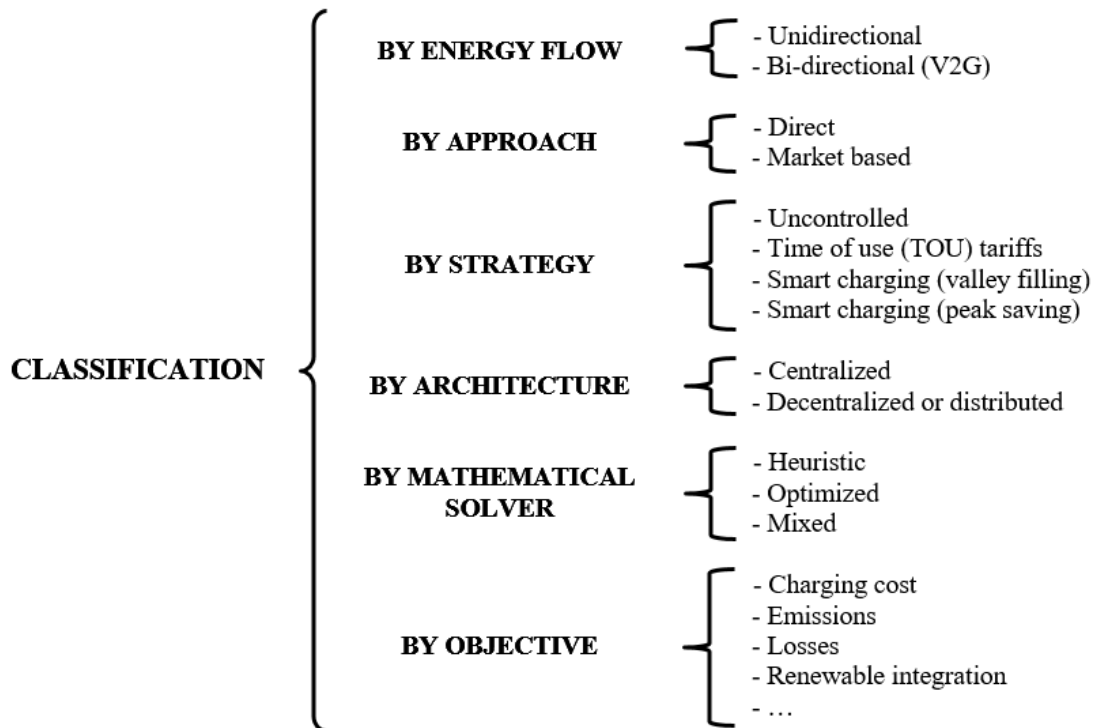
Figure 3.14. Classification of PEVs integration methods

B.   By approach: These smart charging strategies can be carried out using two different approaches, direct approach or market based approach. In the first one, the smart control is applied directly to set the charging profile of PEVs. In the second one, a smart algorithm is applied to modify market prices to change indirectly the charging profile of PEVs. One example of this last approach is usually called "dynamic pricing", which consists in modifying electricity cost depending on one or more factors, i.e., congestion level [43].

C.   By strategy used: Currently, most of the charging events are uncontrolled due to the very low PEVs penetration rate. Some countries have introduced TOU tariffs to encourage users to charge their PEVs at night. A further step is implementing smart charging strategies, in order to exploit distribution networks capacity. The main characteristics of these three options are:

1) Uncontrolled charging: Also known as dumb charging, PEVs are charged at maximum allowed power until their batteries are totally charged. So, no action is done in order to reduce or minimize impacts on distribution networks. PEV users tend to charge their vehicles when they arrived home, that is, at late afternoon, which coincides with peak hours, so impacts on distribution networks are larger. In addition, there is no possibility to provide additional services such as demand response, ancillary services or V2G.

2) TOU tariffs: Time of use tariffs is a pricing strategy in which electricity prices depend on the period of the day. Usually, the day is divided in two or three periods. This strategy is based on establishing regulated tariffs in which electricity is cheaper during off-peak hours. In contrast, charging at peak hours is penalized. This way, PEVs load demand is shifted from peak hours to off-peak hours. Figure 3.15 shows different TOU tariffs in Spain. The use of this strategy

improves PEVs integration respect to dumb charging and it is easy to implement. A simple time switcher can be used to accomplish this task. However, the charging of a large amount of PEVs at almost the same time can produce significant problems to distribution networks. Furthermore, deficit tariffs may arise if regulated tariffs prices are set below of the real electricity cost.
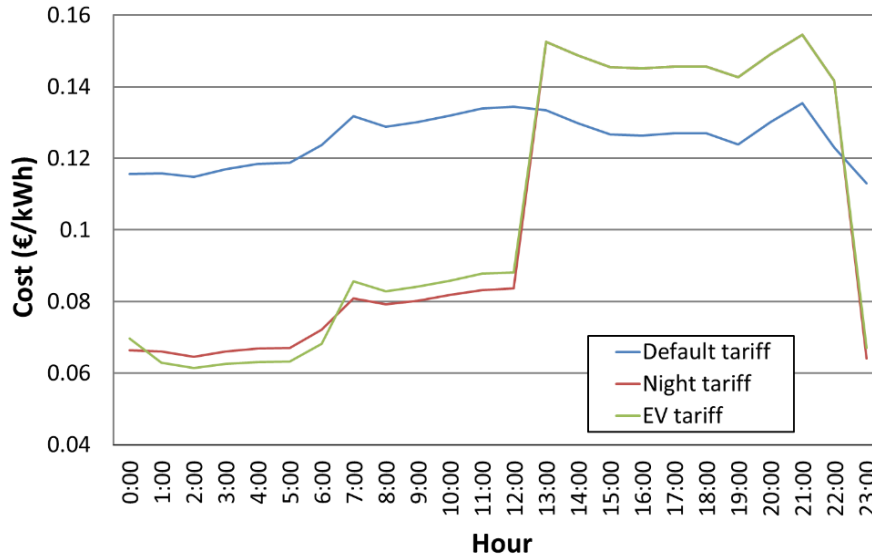
Figure 3.15. Example of different TOU tariffs in Spain

3) Smart Charging: Active charging management of PEVs can provide further advantages compared to uncontrolled and TOU approaches. Smart charging of PEVs allows customers and network operators to schedule PEVs charging profiles, in order to get technical and economic benefits, being considered a specific demand side management (DSM) of PEVs. That is, smart charging seeks active control of loads and it can be programmed with optimized or heuristic algorithms to achieve certain objectives. V2G concept can be considered as an extension of smart charging, allowing PEVs to be able to inject energy into the grid, acting as distributed generators or storage systems [44].

From this point of view, PEVs can be integrated with smart grids to sell demand response services such as reducing their charging rate or delivering energy into the grid. As market penetration of PEVs increases, it will be necessary to develop an active strategy or smart charging, which manages the charging of PEVs in an efficient way, and prevent or delay investments in reinforcing the grid. Besides, it can allow other objectives such as minimizing transmission losses and improving the integration of RES [45]. According to these strategies, and from the point of view of the network, a PEV can be considered as: a simple electrical load (uncontrolled and off-peak charging cases); a flexible electrical load (smart charging valley-filling case) or a distributed and mobile storage element (smart charging saving-peak case). Figure 3.16 shows the advantages and drawbacks of each strategy.

D.   By control architecture: Two different control schemes can be used to manage actively the charging of PEVs. On the one hand, centralized control consists in setting the charging profile of each PEV using an external entity. This entity has received

several names, such as aggregator, electric vehicles manager, electric vehicles fleet operator, etc. On the other hand, in decentralized or distributed control, charging decision is taken by each PEV, taking into account external information. Both architectures have advantages and disadvantages explained more in detail in section 4.3.3.
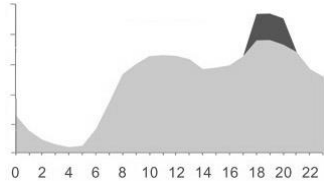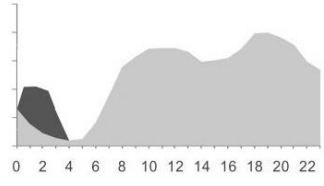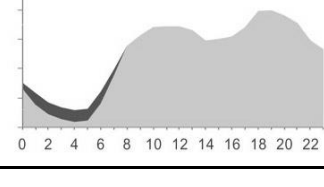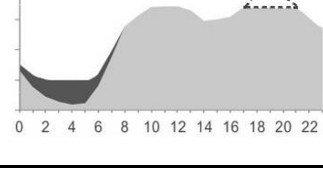
		Advantages	Drawbacks
Dumb Charging		✓ Easy to implement ✓ User friendly	✗ Overload of transformers and lines ✗ Voltage deviations ✗ Peak power increase ✗ Increase of electricity CO_2 intensity ✗ Electricity cost increase ✗ Needs to reinforce the grid
Off-peak Charging		✓ Easy to implement ✓ Demand profile flattened ✓ Better integration of wind energy at off-peak hours ✓ Delay in grid investments	✗ Imbalances due to rapid increase of power consumed by PEVs ✗ Possible overload of transformers and lines ✗ Possible voltage deviations ✗ Willingness of the customer required
Smart Charging (Valley filling)		✓ Ancillary services provision ✓ Demand profile flattened ✓ Better integration of wind energy at off-peak hours ✓ Delay in grid investments	✗ Complex implementation ✗ ICT technologies required ✗ Willingness of the customer required
Smart Charging (Peak saving)		✓ Ancillary services provision ✓ Peak power reduction ✓ Optimal integration of intermittent RES ✓ Reduction of electricity CO_2 intensity ✓ Less investments in network reinforcements	✗ Very complex implementation ✗ ICT technologies required ✗ Willingness of the customer required ✗ Premature degradation of batteries resulting of using V2G ✗ Energy losses in grid-battery-grid transmissions

Figure 3.16. Advantages and drawbacks of different strategies for PEVs integration

E. By mathematical solver: Intelligent integration of PEVs into distribution networks can become a very complex task from a mathematical point of view, especially when optimized algorithms and complex objective functions are involved. Three main approaches can be distinguished: heuristic, optimized and a mix of both.

1) Heuristic method is a technique to solving problems by using practical methodologies. Solutions provided by heuristic methods are not perfect but good enough for the problem presented.

2) Optimized methods consist in mathematical tools to obtain optimum solutions to problems which are defined with an objective function and a set of constraints. On the one hand, the objective function is a mathematical equation to be optimized (minimized or maximized) and expresses the relationship between a design vector "x" to be calculated and a criterion to be optimized, for example charging cost. On the other hand, constraints are technical or user requirements which should be met by the optimization method.

3) Mixed methods: Heuristic and optimized methods can be used at the same time with different purposes. Optimized methods are more used to improve well-defined parameters such as charging cost, while heuristic methods are more suited to keep distribution network within its operational limits.

F.   By objective: PEV charging methods can be classified by objectives. Researchers have proposed different objectives such as: reduce charging cost, electricity cost, GHG emissions, energy losses, voltage unbalances, improve load factor, renewable energy integration, limit distribution network impacts (voltage deviations, overloads, transformer lifetime degradation, etc.), increase profits for current or new business entities, supply ancillary services and others. Additionally, it is possible to improve more than one objective as some of them are interrelated or because a multi-objective control is used.

3.6   Opportunities in the integration of PEVs

Although integration of PEVs can lead problems to distribution networks, there are several opportunities to explore, such as:

- Increase of utility profits and CO_2 emission credits.
- Increase of load factor.
- Increase of renewable energy integration.
- Provision of demand response and ancillary services.
- Development of the vehicle to grid concept.

Charging a considerable amount of PEVs will lead an increase of energy consumption and, therefore, utilities will increase their profits. Considering a Nissan Leaf with a fuel economy of 0.212 kWh/km, an average daily distance travelled of 34.3 km [36] and an average energy cost of 0.208 €/kWh (average electricity cost in second semester of 2014 in Europe), the annual income per PEV will be approximately about 550€. Furthermore, in some countries electricity providers will receive Low Carbon Fuel Standard (LCFS) credits for refuel PEVs with electricity. Then, these credits can be sold in the LCFS credit market to high emissions companies which have to meet their carbon intensity reduction targets. Therefore, providing electric energy to PEVs can generate another source of income to electricity providers [46].

Current load factor is poor due to low energy demand at night and high energy demand at late afternoon. This fact will be worse as residential electricity demand grows. One of the most important characteristics of PEVs is that they are deferrable loads. This means that PEVs charging demand can be scheduled at low demand hours achieving the valley filling effect. Thus, load factor or utilization factor is increased and, as a consequence, base-load power plants can run during more time, reducing their operating costs.

Similarly happens with renewable energies such as wind and solar energy. On the one hand, wind energy is inherently intermittent, little unpredictable and does not match with load demand. On the other hand, solar energy is more predictable and better matched with load demand but does not provide energy at night. PEVs can absorb these generation intermittences by shifting their charging demand to periods of strong wind and solar energy production.

In this context, there are two mechanisms in order to cope with demand-generation deviations: demand side management and ancillary services. The first one is based on modifying the load demand so that it meets with generation while the second one is based on modifying supply side. Currently, ancillary services are widely used over DSM alternative. As commented before, PEVs are deferrable loads and they can perform DSM easily without affecting user comfort. DSM driven by PEVs is already working in the pilot project BMWi ChargeForward [47]. This project consists in sending load drop request (up to 100kW) from the utility (PG&E) to the BMWi server, which selects vehicles for delayed charging according to owners departure time. User can set its departure time by using a mobile phone app. BMWi server notifies to PEV owners if they want to participate or not in the load drop request. Users who participate in the load drop request are economically compensated.

Additionally, plug-in electric vehicles can provide ancillary services (Table 3.3), such as spinning reserve and frequency and voltage regulation, adding value to the PEV itself. Global ancillary services market involves approximately 33GW, with a total value estimated between 18,000M€ and 50,000M€ [48]. It is expected that this market will grow due to several reasons, being the increase of renewable energy generation one of the main reasons. PEVs are able to respond almost instantaneously to network changes, allowing them to participate in all types of ancillary services. Furthermore, they do not need external energy to be operative, so they have also black start capacity. In order to be able to participate in ancillary services market, PEVs should be integrated in coordination entities such as aggregators or PEVs fleet operators.

Table 3.3. Ancillary services description which can be provided by PEVs

Ancillary service	Description
Frequency control	Maintaining the frequency within the given margins by continuous modulation of active power
Voltage control	Maintaining voltage through injecting or absorbing reactive power by means of synchronous or static compensation
Spinning reserve	Increase or decrease in generation or reduction in consumption that can be provided at short notice, carried out by partially loaded generating units and interruptible customers
Standing reserve	Increase in generation or reduction in consumption that can be provided by those generating units that are not synchronously on-line, or by interruptible loads
Black start capability	The capability of a generating unit to start up without an external power supply, usually after a major failure on all or part of the network

Finally, V2G concept allows PEVs to work as distributed generation or distributed storage when they are connected to the grid. This way, PEV owners can obtain additional profits for trading energy (buy at low prices and sell it at high prices) within a dynamic electricity pricing market. Another possibility is storing energy from non-dispatchable energy sources such as wind energy and injecting it back when it is needed. However, this concept requires more reliable battery technology, bi-directional converters, smart meters and the support of smart grids technology. Current battery technology has a limited number of cycles before its EOL, so using PEV batteries for other applications, different from transport purposes, could have no sense from an economic point of view. As commented in subsection 2.5.1, battery cycle life depends on DoD value, among other parameters such as operating temperature. In order to limit battery degradation, V2G usage should be limited to a short amount of energy per PEV. Additionally, economic incentive for utilities is still not clear as they have to spend money on adapting their metering and distribution systems in order

to make V2G technically feasible. The only cost avoidance for utilities is the possibility of reducing the number of peak power plants, taking into account that utilities usually receive economic compensations to run and maintain these facilities.

3.7 Conclusions

Plug-in electric vehicles use electric grids to obtain the required energy to operate. This energy can be transferred using wires or through magnetic fields. Another possibility, but less feasible, is battery swapping. Among these three options, conductive charging is the most preferred one as it provides a very high efficiency at low cost. Several standards have been developed to define conductive charging systems and connectors, while inductive charging still has not a published one.

Even at low PEV penetration rate, it is expected that multiple issues will arise in electric distribution networks. These problems have been analyzed by several researchers. Most of them conclude that it is necessary to take actions towards an intelligent management of PEVs energy demand. In fact, several authors have analyzed impacts and proposed methods or techniques to avoid or reduce them. These impacts include: changes in load demand curve and generation portfolio, increase of voltage deviations and unbalances, congestion of lines and distribution transformers, increase of energy losses, GHG emissions, energy cost and harmonic distortion and decrease of distribution transformer lifetime.

One of the key points of PEVs integration is the influence of driving and charging behavior. Both factors, with PEV penetration rate and network characteristics, will determine the impact that PEVs will have on electric distribution networks. Thus, it is very important to have an approximated model of driving and charging behavior in order to schedule the operation of the network. Such type of driving and charging model depends on a quite large number of factors such as: country, type of area, climate and weather, type of day, type of vehicle, etc.

Moreover, smart metering has a critical role in the integration of electric vehicles. The deployment of smart meters allows utilities and grid operators to know the real time load consumption. Additionally, data obtained from smart meters will improve load demand forecast models, which are important to coordinate generation profile, demand side management and ancillary services. Finally, smart meters could provide a communication interface between distribution network operators and plug-in electric vehicles allowing the implementation of smart charging techniques.

A classification of charging approaches has been presented. Inside this classification, two concepts have particular relevance: smart charging and V2G. Smart charging deals with how to manage effectively a large amount of PEVs improving one or more objectives, while distribution network technical limits are not surpassed. V2G allows bi-directional flow of energy. This way, PEVs can act as distributed storage devices, improving electric grid efficiency. However, V2G concept has a number of problems to be addressed such as: battery degradation, lack of regulations, need of a bi-directional charger and smart meter, etc.

To conclude, opportunities that PEVs could bring to electric system have been explained. On the one hand, it is expected that utilities will increase their profits due to the growth of load demand and procurement of CO_2 emission credits. Additionally, utilities could introduce more renewable generation in their generation mix, further reducing GHG

emissions and improving their social and environmental image. On the other hand, PEV users could provide a set of services such as: demand response, ancillary and V2G services. PEVs are very suitable for performing these types of services due to several reasons: very fast response, relatively high room for manoeuvre, distributed location which allows local or global actions and high efficiency.

CHAPTER 4

ACTIVE INTEGRATION OF PEVS IN ELECTRIC DISTRIBUTION NETWORKS

4.1 - INTRODUCTION

4.2 - MATHEMATICAL PROGRAMMING

4.3 - SMART CHARGING

4.4 - DISTRIBUTED GENERATION AND PEVS

4.5 - PEVS INTEGRATION PROJECTS OVER THE WORLD

4.6 - CONCLUSIONS

4. ACTIVE INTEGRATION OF PEVS IN ELECTRIC DISTRIBUTION NETWORKS

4.1 Introduction

From the point of view of electric grids, PEVs are currently considered as simple loads due to their low market penetration. However, as the PEVs fleet grows, implementation of an intelligent management system will be necessary. This management system will avoid large capital expenditures in network reinforcements and negative effects on electric distribution networks, such as: voltage deviations, degradation of quality of supply, increase of power losses, overload of transformers and lines and increase of harmonics and fault currents [22], [49], [50]. It is estimated that the energy demand of 30 million PEVs may require about 100 TWh per day and an additional power of 35 GW [51]. Therefore, the smart integration of PEVs into the electric grids, together with the development of better and more efficient batteries, is one of the biggest challenges of electric mobility technology.

Additionally, PEVs will have to share space with the distributed generation in low voltage distribution networks, causing impacts on the grid [52], [53]. However, this pairing can produce some synergies, which might be developed in order to improve the competitiveness of both technologies.

Currently, due to the poor market penetration level of PEVs, no integration strategy is performed (dumb or uncontrolled charging) or a passive strategy is implemented. Among passive strategies, the most widely used is the off-peak charging, using TOU tariffs, which encourages the charging of PEVs during night. However, this solution has the drawback of producing sudden power demand increases because all PEVs charging processes would begin almost simultaneously [54].

Thus, researching how PEVs should be controlled, in a smart way, can be a very complex task considering the large number of variables that come into play. One of the most used methods to address this problem is mathematical optimization or programming.

In this chapter, after the basic mathematical background is explained (section 4.2), smart charging approaches are reviewed in section 4.3, distinguishing between centralized and decentralized control architectures. Then, a comparison between them is presented. In section 4.4, some solutions where PEVs are part of virtual power plants and microgrids are described. Following, the most important projects developed around the world concerning to PEVs and electric grids are presented in section 4.5. Finally, conclusions of this chapter are summarized in section 4.6.

4.2 Mathematical programming

Mathematical programming or mathematical optimization is a technique used to find the best solution from a set of possible solutions or alternatives. This mathematical method is widely used in economics, manufacturing and engineering. Considering electrical engineering, mathematical optimization is used in applications such as: power system planning, economic dispatch, unit commitment, network reconfiguration for losses reduction, etc. [55].

In general, a mathematical optimization process seeks to find the maximum or minimum of an objective function, also known as cost function, taking into account several

constraints which delimit the number of possible solutions. Mathematical programing problems can be classified attending to the characteristics of the objective function itself and its variables and constraints. A mathematical problem can be defined as:

- Binary integer linear programming (BILP): Linear problems with binary variables.
- Integer linear programming (ILP): Linear problems with integer variables.
- Linear programming (LP): Linear problems with continuous variables.
- Mixed integer programming (MILP): Linear problems with integer and continuous variables.
- Quadratic programming (QP): Quadratic problems with continuous variables.
- Quadratic programming (QCP): Quadratically constrained problems with continuous variables.
- Mixed integer quadratic programming (MIQP): Quadratic problems with integer and continuous variables.
- Non-linear programming (NLP).
- Others…

Moreover, inside mathematical programming, convex optimization is defined as a problem where all the constraints and the objective function are convex functions. These types of problems can be solved using specific algorithms which find the global optimum. For example, a LP problem can be solved by using the simplex algorithm or the interior point method.

Furthermore, meta-heuristic techniques can be also used to find the solution of an optimization problem. On the one hand, specific algorithms give the exact result but they are not suited to problems with a large number of variables. On the other hand, meta-heuristic techniques can solve very complex optimization problems, such as those that are non-convex problems, but achieving the optimal solution is not guaranteed. Examples of meta-heuristic solvers are: evolutionary algorithms, simulated annealing, particle swarm, tabu search, ant colony, etc. Additionally, optimization problems can be classified in two different groups, depending on the number of objective functions to be optimized.

4.2.1   Single objective optimization (SOO)

Optimization of a single-objective, such as cost minimization, is relatively common in engineering. It is used to find the best solution to a variable which correspond to the minimum or maximum value of a single objective function. Examples of this type of optimization are: minimization of cost, maximization of profits, minimization of fuel used, etc. A mathematical optimization problem can be stated as follows:

- Find a design vector:

$$x = (x_1, x_2, x_3, \dots, x_n) \tag{4-1}$$

- which minimize or maximize the objective function:

$$f(x) \tag{4-2}$$

- subject to a number *m* of inequality constraints:

$$g_j(x) \leq 0 \quad j \in \{1, \dots, m\} \tag{4-3}$$

- and p equality constraints:

$$l_j(x) = 0 \quad j \in \{1, \dots, p\} \tag{4-4}$$

Additionally, the design variable x can be limited to lower and upper bounds:

$$x_i^{(l)} \leq x_i \leq x_i^{(u)} \quad \forall i \in \{1, \dots, n\} \tag{4-5}$$

In practice, the set of constraints is usually called as S. Thus, it is said that a solution x meets the constraints if $x \in S$. For a minimization problem, the design vector (4-1) gives a global minimum if there is no another design vector $y \in S$ such:

$$f(y) \leq f(x) \quad x, y \in S \tag{4-6}$$

In contrast, for a maximization problem, the design vector $x \in S$ defines a global maximum if there is no another design vector $y \in S$ such:

$$f(y) \geq f(x) \quad x, y \in S \tag{4-7}$$

Additionally, a simple optimization problem can be graphically solved. Thus, Figure 4.1 shows a problem composed by a design vector of two variables and six constraints. The point is the optimal solution while the dotted arrows represent the direction of the optimization. In this type of problem, solutions are usually located in one of the extreme points of the feasible region.
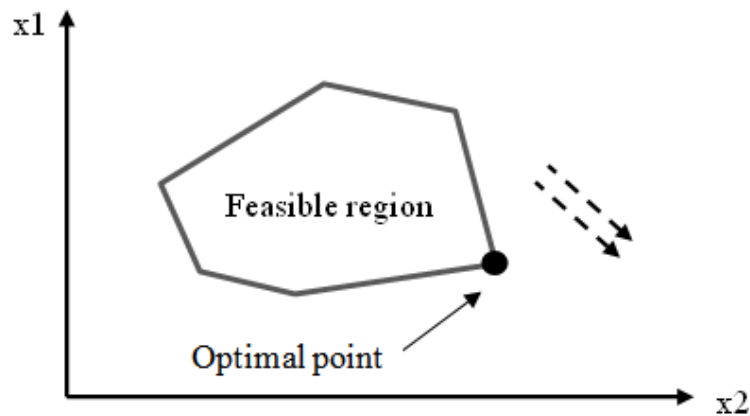
Figure 4.1. Optimization of a linear problem with two variables and six constraints

4.2.2 Multi-objective optimization

In the previous section, the problem was composed by one single objective function. However, in real world it is necessary to optimize more than one parameter, which requires a number of objective functions. In general, it is not possible to optimize all objectives at once. That is, an improvement of one of the objectives can be also a worsening of the others. This leads to make a trade-off between the different objectives.

The process of optimizing a set of objective functions is called multi-objective optimization (MOO) or vector optimization. A MOO problem can be stated as finding a design vector x which minimize or maximize J, as shown in equation (4-8).

$$J(x) = [f_1(x), f_2(x), \dots, f_k(x)] \quad x \in S \tag{4-8}$$

A feasible solution $x \in S$ is called as Pareto optimal (PO) if there is no another solution $y \in S$ such [56]:

$$J(y) \leq J(x) \text{ and} \qquad\qquad\qquad (4\text{-}9)$$

$$f_i(y) < f_i(x) \text{ for at least one i} \in \{1, \dots, k\} \qquad\qquad (4\text{-}10)$$

In contrast to single objective optimization, there is no a single solution in MOOs. In fact, a set of PO solutions can be achieved, often called as Pareto frontier, Pareto front or Pareto set (Figure 4.2). This Pareto frontier is bounded by a so-called Pareto boundary and it is contained in the objective space, which is divided by feasible and infeasible regions defined by the problem constraints.
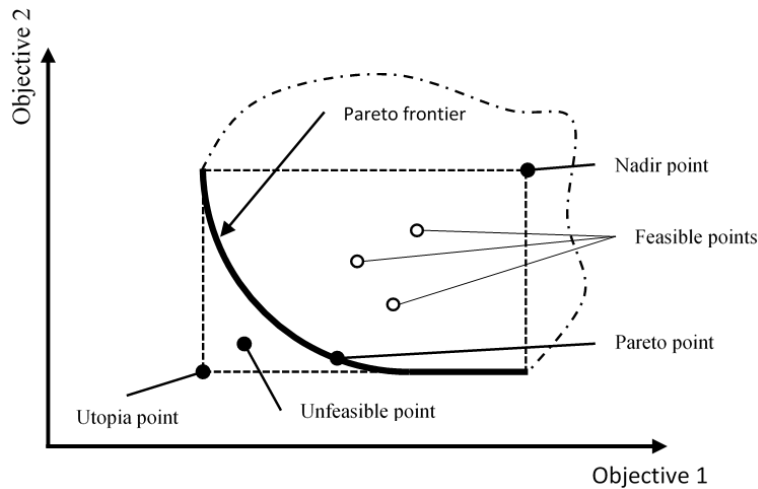
Figure 4.2. Pareto frontier of a bi-objective optimization

MOO optimization cannot be solved unless the different objective functions are combined in a single objective optimization. There are several approaches to carry out this transformation. Between them, the weighted sum method and the ε-constraint method are the most used ones. The weighted sum method is based on making an addition of objective functions multiplied by weights, as shown in equation (4-11) [57]. This way, SOO solving techniques can be used.

$$J(x) = \sum_{i=1}^{k} w_i \cdot f_i(x) \quad x \in S \qquad\qquad (4\text{-}11)$$

where:

- $J(x)$:   total objective function to minimize/maximize
- $f_i(x)$:   objective function i
- w_i: weight for objective function $f_i(x)$
- k: number of objective functions

Weights must be always positive or zero, as shown in equation (4-12). Using negative values will become the optimization problem unfeasible. In addition, it is usual to define the weight in function of the equation (4-13) but it is not compulsory.

$$w_i \geq 0 \qquad \forall i \in \{1, .., k\} \qquad\qquad (4\text{-}12)$$

$$\sum_{i=1}^{k} w_i = 1 \qquad i \in \{1,..,k\} \tag{4-13}$$

However, this type of optimization presents some drawbacks. On the one hand, each weight has to be defined by the user or decision maker (DM), so the results can be quite subjective. On the other hand, the objective functions usually have different dimensions, i.e. cost in euros and energy losses in kWh. Thus, it is necessary to normalize each objective function to convert it into a non-dimensional system. The most robust approach to normalize objective functions is given in equation (4-14) [56].

$$\theta_i = \frac{1}{Z_i^N - Z_i^U} \tag{4-14}$$

where:

- i: index of the objective function
- θ_i: normalization parameter for objective function i
- Z_i^N: nadir point of objective function i
- Z_i^U: utopia point of objective function i

Utopia and nadir points represent the ideal and anti-ideal points of the objective space of a MOO problem respectively. That is, utopia point is the optimal value obtained when each objective function of the MOO optimization is optimized individually, within the feasible region. In contrast, nadir point is the worst solution, that is, the maximization of a minimization problem or the minimization of a maximization problem. The normalization of a weighted sum objective function is important to reduce as much as possible the numerical deviation between the different objective functions. This way, if there is a change of one of the objective functions such as different electricity prices or different number of PEVs, the weighted sum objective function will be less affected.

An alternative to weighted sum method is the ε-constraint method. This approach is also called as bounded objective function method or hierarchical method. It is based on minimizing the most important objective function while all other objective functions are ranked and used as additional constraints. The general formulation is presented in equation (4-15).

$$\min_{x} f_1(x) \quad s.t. \quad f_2(x) \le \varepsilon_2$$
$$f_3(x) \le \varepsilon_3 \tag{4-15}$$
$$\cdots$$
$$f_k(x) \le \varepsilon_k$$

However, one of the drawbacks of this method is how to select the right values of the different ε parameters, especially when parameters of the objective functions are changed. In addition, this approach could be less intuitive than the weighted sum method. But, the normalization problem of weighted sum method is avoided.

Finally, there is a great number of alternatives to the two mentioned ones such as lexicographic method, weighted min-max method, exponential weighted criterion,

weighted product method and even, hybrid ones which combine weighted sum method with ε-constraint method, etc. [56].

In general, most of the proposed smart charging solutions for PEVs are based on mathematical programming technique. So, those smart charging algorithms, which can be found in the literature, are reviewed in the following sections.

4.3   Smart Charging

Smart charging of PEVs allows customers and distribution network operators to schedule PEVs charging profiles, in order to get technical and economic benefits. It can be considered as a specific demand side management (DSM) of PEVs. That is, smart charging seeks active control of loads and it can be programmed with optimized or heuristic algorithms to achieve certain objectives. This is possible because it is estimated that PEVs are parked 96% of the time [58].

Through V2G, PEVs can provide ancillary services (frequency control, load balance and spinning reserve services) [59], [60]. It is believed that the use of such a system could be used for "valley filling" (timing devices to draw power at times of low grid demand) and "peak shaving" (reducing the peak energy demand on the grid). Moreover, both smart charging and V2G can be an excellent tool to compensate for deviations caused by intermittent RES, such as wind power and solar photovoltaic [45], [61], [62].

Also, this concept could be competitive in the provision of ancillary services. Considering the long term, V2G may play a more important role as mass storage system, depending on the penetration of intermittent RES [58]. But, it is necessary to adapt the electronic devices that act as interface between the PEV and the EVSE to make the V2G concept possible. Additionally, the use of V2G will increase the battery degradation of PEVs and the energy losses [63].

Moreover, in order to make feasible the technical and economic management or the coordination of PEVs charge, a new entity may be required. In many papers this entity is known as aggregator [64]–[67]. Other names are EV fleet operator and EVs Management System. The aggregator function is to bind a significant amount of PEVs within a region and work as an interface between the different entities of the electrical system. The main objective is to give visibility to PEVs, both for technical management and for integration of these devices into the electricity market.

The control capacity of the aggregator will depend on the number of controllable PEVs connected and the flexibility provided by the users of those PEVs, which depends on their preferences. These aspects will be defined by the initial charge level, the connection time and the desired final charge level. As the number of PEVs increases, more flexibility can be available for the aggregator in order to achieve its goals and improve the economic benefits.

Another source of income for the aggregator is the provision of ancillary services, such as primary and secondary frequency regulation, given the capacity of batteries of reducing/increasing electricity demand almost instantaneously [68]. As an example, it is estimated that the annual market of ancillary services in the United States is 6.5 GW, with an estimated value in the range from 3 to 10 thousand million dollars [48].

Finally, the smart charging of PEVs can be implemented in two different control architectures, centralized and decentralized. The aggregator functions will vary according to the type of architecture. For example, in decentralized architectures the aggregator will have an auxiliary role while, in centralized solutions, the aggregator will be in charge of directly managing the charging of all PEVs. In both architectures, the functions of the aggregator could be assumed by the electricity supplier or utility.

In the following sections, centralized and decentralized controls are introduced. Additionally, a literature review of each approach is presented. The same nomenclature that appears in the papers has been used.

4.3.1 Centralized control architecture

Also known as direct control, the aggregator is responsible for managing directly the charge of all PEVs under its control. Furthermore, the aggregator can also control other external entities, such as an EVSE manager (EVSEM), which controls a group of EVSEs of a specific location such as a car park.

A possible market and technical operation of this centralized control architecture has been described in [65] and [69]. The aggregator, in addition to the technical management, is also responsible for PEVs participation in the electricity market. Thus, it must perform daily demand forecasts based on historical data, user's preferences, etc. Once the demand profile forecast of the whole controlled PEVs is obtained by the aggregator, this profile has to be communicated to the Distribution System Operator (DSO) for prior approval. The DSO will check whether the power demand profile compromises the safe operation of the distribution network. After receiving the approval of the DSO, the aggregator has to perform the power purchase bids directly in the day-ahead market or through a utility. After market negotiation, the Transmission System Operator (TSO) will evaluate and require changes in the demand profile, in case that any problem could arise in the transmission network. If this technical assessment is positive, the aggregator will provide the charging set-points to each connected PEV in real time, in order to meet the commitments made in the electricity market. Figure 4.3 shows the general scheme of a centralized control architecture.

In addition to the day-ahead and intraday markets, the aggregator can also participate in the ancillary services market. The aggregator will estimate the ability to offer these additional services, such as frequency regulation. In case of being accepted, the aggregator will provide these services when the TSO demands them.

If abnormal operation of the distribution system occurs, the aggregator, at the request of the DSO, will interrupt the operation of the system as scheduled by the market, and will perform the necessary corrective actions to return to safe operation of the distribution network. In this case, the aggregator will receive the compensations stipulated by providing these services.
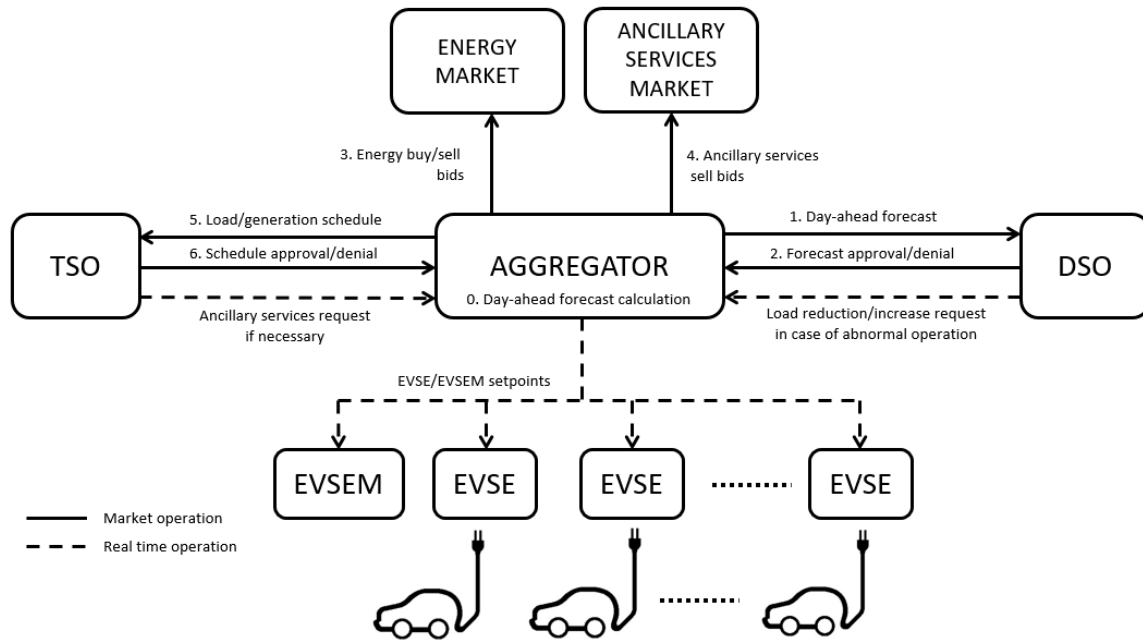
Figure 4.3. Centralized control architecture [65], [69]

In real-time operation, the aggregator must collect data from the PEVs that are connected to the grid, such as PEV identification (ID), EVSE or EVSEM identification, state of charge of the batteries (SOC) and user's preferences. With this PEV ID, the aggregator may access relevant data using databases (Figure 4.4). Likewise, the EVSE ID provides extra data such as the location and the power limits of the EVSE.
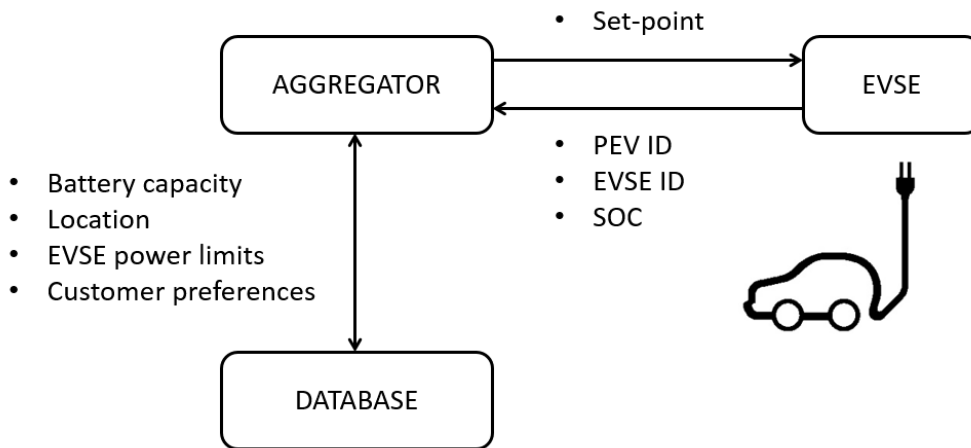
Figure 4.4. Information required for the aggregator operation in a centralized architecture

With this information, the aggregator will apply the necessary algorithms to achieve the proposed objectives, while meets the needs of the PEV owners. In order to do so, all set-points will be sent to the PEVs through the EVSEs. Within each PEV, the control unit will receive the set-point and act on the charger/inverter to set the required charging/discharging power (Figure 4.5).
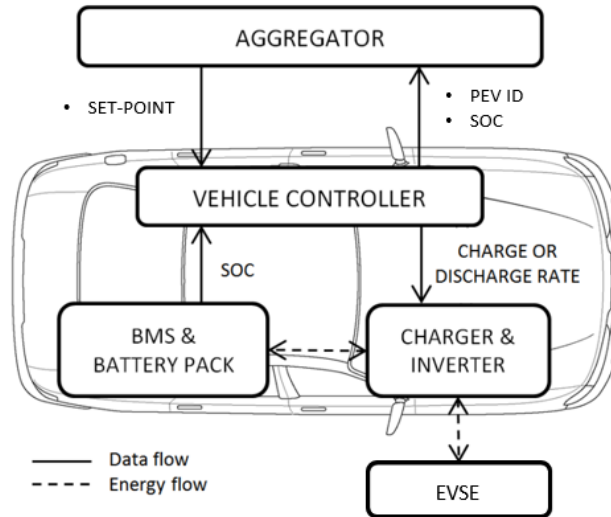
Figure 4.5. Interactions between different elements in the centralized control

In the literature, a wide range of algorithms to achieve certain objectives can be found. Focusing in the participation of the aggregator in the market, it is important to minimize deviations between the energy bought in the market and the real-time power demand from PEVs, which are divided in flexible PEVs and inflexible PEVs (not controlled). F.J. Soares et al. have proposed a linear programming technique [70], which is suitable for quasi-real time application due to the low computation time required. A heuristic method is also proposed based on power flow calculations in order to identify problematic feeders and buses. In this way, voltage and lines overloading problems could be solved. Although authors point out that there is no necessity of load demand forecasting for the optimization algorithm, in fact, it is necessary to know beforehand the PEVs load demand. This way, it is possible to minimize deviations between the energy bought in the market and the real-time power demand. However, this heuristic method could be problematic because it is necessary to know the load demand at every node, as well as the distribution network model. Furthermore, all PEVs are modelled as three-phase loads even though level 1 chargers are used. Thus, voltage unbalances are not considered in this paper.

In [71] a centralized multi-objective scheduling strategy is formulated for a MV/LV distribution networks. In this paper, two different objective functions are presented: total operational cost of a distribution network and CO_2 emissions. On the one hand, operational cost takes into account the electricity cost from main grid, cost of producing electric energy using distributed generators and cost of discharging from PEVs, as shown in equation (4-16). Thus, using V2G the overall cost of the distribution network could be reduced.

$$F^{cost} = \sum_{t=1}^{T} \left[P_{grid}(t) \cdot \Omega_t + \sum_{i=1}^{I}(C_{DG}(i,t) + SU(i,t)) + \sum_{v=1}^{Nv}\left(P_{EV}^{Dch}(v,t) \cdot C_{Dch}^{v,t}\right) \right] \qquad (4\text{-}16)$$

where:

- T: total number of time slots
- I: total number of DGs
- Nv: total number of PEVs
- $P_{grid}(t)$:   scheduled purchased power from the grid at time slot t
- Ω_t: electricity cost from the grid at time slot t

- $C_{DG}(i,t)$:   operation cost function of the i-th DG at time slot t
- $SU(i,t)$:   startup cost of the i-th DG at time slot t
- $P_{EV}^{Dch}(v,t)$:   discharging power rate of the v-th PEV at time slot t
- $C_{Dch}^{v,t}$:   cost of discharging for the v-th PEV in time slot t

On the other hand, the CO_2 emissions of the main grid and the DGs are considered, as shown in equation (4-17). The ϵ-constrained method is used to combine both objective functions in a single function, to be optimized.

$$F^{Emission} = \sum_{t=1}^{T} \sum_{i=1}^{I} \left(E_{CO_2}^{DG,i} \cdot P_{DG}(i,t) \right) + \sum_{t=1}^{T} \left(E_{CO_2}^{grid,t} \cdot P_{grid}(t) \right) \qquad (4\text{-}17)$$

where:

- $E_{CO_2}^{DG,i}$:   emissions of the i-th DG at time slot t
- $P_{DG}(i,t)$:   active power output of the i-th DG at time slot t
- $E_{CO2}^{grid,t}$:   average emission rate of the grid at time slot t
- $P_{grid}(t)$:   active power consumed from the grid at time slot t

A number of constraints are implemented in order to satisfy some technical limits, such as energy balancing, PEV energy needs, SOC limits of PEV batteries, DG capacity limits and voltage constraints. A Benders decomposition (convex optimization) is used to solve this large-scale problem. Then, a fuzzy solution is proposed to achieve the best compromise between the two objective functions. This way, both objectives can be enhanced. However, this proposed solution can present several problems for a real implementation. For example, this optimization is done with a day-ahead time horizon. That is, the central controller has to know the demand of the PEVs in a day-ahead time horizon. This implies that the PEV users must submit their expected trip distance and park time (arrive and departure time), something that can be difficult from the point of view of user willingness and privacy. Any deviation from expected trip distance or park time from the real ones will have an impact on the results. Moreover, in order to not violate distribution network technical constraints, such as voltage levels and capacity of lines, it is necessary to know beforehand the active and reactive power injected at each node as well as the admittance matrix of the distribution network. That is, load demand forecast per node and network characteristics must be known.

Charging a large number of PEVs may produce overloads of transformers and lines, power losses and voltage deviations. Therefore, this aspect is widely analyzed in the literature. In [65] a heuristic method is proposed to avoid overloads of lines and transformers, and improve voltage profiles, using an intelligent charging algorithm. This algorithm is executed by the DSO prior market negotiations. In a one hour basis, this algorithm calculates a power flow and analyses whether the operating conditions are suitable. Otherwise, algorithm recognizes whether the problem is due to a voltage deviation in a node or to an overload of some element and proceeds to stop charging a percentage of PEVs, adding them to a waiting list. When the electrical network conditions allow it, the charge of the affected PEVs will be restarted. After achieving a successful solution, DSO will communicate the amount of PEV load that should be shifted in order to guarantee a safe operation of the distribution network. In order to bring this solution to the real world, it is necessary to forecast not only conventional loads demand but also PEVs power

demand. Forecasting PEVs power demand can be even more difficult than conventional loads one.

Other authors have used Artificial Immune Systems algorithms (AIS) with a heuristic method [72]. In this paper, the IEEE 34 node test feeder is used to perform all simulations. Using AIS, authors seek the minimization of power losses while a heuristic method is implemented to avoid overloads and voltage limits violations. The heuristic method performs power flows in order to detect voltage or capacity limit violations in a real-time basis. This real-time operation requires a complex communication infrastructure to know the active and reactive power of residential loads and electric vehicles of each node as well as data about their SOC. Furthermore, PEVs are distributed in a balanced way between the three phases, so voltage unbalances due to PEVs charging is not analyzed. Moreover, although it is a real-time solution, authors do not mention the absolute computation time required. They only stated that computation time will be higher in wider distribution networks.

In a similar way, a real-time smart load management (RT-SLM) algorithm to coordinate the charging of PEVs is presented in [73]. This heuristic algorithm tries to reduce the charging cost and power losses. The proposed RT-SLM algorithm is based on sorting in a queue/list the PEVs in function of the priority levels and their impact on power losses (calculated previously through power flows). Then, PEVs are allowed to be charged in function of these factors as long as technical constraints are met, which are verified making power flows. Similar than in previous cases, using power flows as a part of the algorithm requires information of active and reactive power flows at each node, as well as distribution network data (lines, distances, etc.). Additionally, the proposed heuristic algorithm based on reducing charging cost will generate high variations in PEVs power load demand, only limited by voltage and capacity constraints.

Minimizing power losses is also the aim of [74]. In this case, three optimal charging algorithms are compared to know the relationship between them. First algorithm is designed to minimize power losses (4-18), second for minimizing load variance (4-19) and third for maximizing load factor (4-20). These three algorithms achieve a reduction of power losses in the network, but load variance minimization and load factor maximization are considered better solutions because they do not depend on the network topology. However, taking into account computation time, maximizing load factor is the best solution since it only requires half of the time that load variance algorithm. This is due to load variance algorithm is a quadratic function while load factor is a linear one. It should be pointed out that computation time is a key factor to achieve real-time solutions. Although this is true, it also should be pointed out that in decentralized architectures computation time do not depend on the number of PEVs. Thus, this fact is important only in centralized solutions.

$$\underset{I}{\text{minimize}} \sum_{t=1}^{T} \sum_{l=1}^{lines} \left(R_l \cdot I_{l,t}^2 \right) \tag{4-18}$$

where:

- T: total number of time slots
- $lines$: total number of lines in the distribution networks
- R_l: resistance of the line l
- $I_{l,t}$: current through line l at time slot t

$$\underset{S}{\text{minimize}} \sum_{t=1}^{T} \left(\frac{1}{T} \left(\sum_{m=1}^{nodes} (S_{m,t} \cdot \mu_D) \right)^2 \right) \qquad (4\text{-}19)$$

where:

- $nodes$:   total number of nodes
- $S_{m,t}$:   load of m-th node at time slot t
- μ_D: average distribution system load during T

$$\underset{S}{\text{maximize}} \frac{\max\left(\sum_{m=1}^{nodes} S_{m,t}\right)}{\mu_D} \qquad (4\text{-}20)$$

In a similar way, uncontrolled charging, minimization of charging cost (uncoordinated control), minimization of power losses and maximization of load factor are compared in [75]. The last two ones are coordinated controls. Three scenarios were analyzed: 10, 25 and 50% of PEV-PR. Authors also analyzed the voltage deviations produced by each algorithm. According to the authors, both coordinated algorithms provide similar results in terms of load factor and energy losses. Regarding to voltage deviations, coordinated methods improve voltage levels. However, nothing is mentioned about voltage unbalances as they have not been taken into account in this analysis.

L. Jian et al. have presented a centralized solution for optimizing load variance in [76]. This solution uses V2G and load forecasting in order to flatten the load profile of a distribution network. Researchers achieve good results in load variance reduction but some aspects of the proposed framework can be problematic. First, the centralized nature forces to PEV users to send information about the actual SOC, departure time and the amount of energy required for the next trips. This last information can be difficult to know beforehand for PEV users. Second, V2G operation is not limited, so involved PEVs could suffer high DoD and battery degradation would be higher. Third, there is no incentive for PEV users to participate in the proposed solution. Fourth, as number of PEVs increases, the optimization problem will be more and more complex to solve, due to centralized nature. Authors use a 15 minutes resolution time for scheduling the charging of PEVs. This way, they reduce the computational effort but, in turn, they lose accuracy as load demand can change substantially in 15 minutes. Finally, voltage issues are not mentioned in this paper.

A solution to reduce computational complexity is also proposed in [77] by L. Jian et al. They expose that with high number of PEVs the computational complexity will be very high. In order to handle this problem, a double layer optimal charging strategy which minimize the load variance is proposed. In this solution, a central control center (CCC) calculates the optimal power schedule for each charging station under its governance. The objective of the CCC is to minimize the overall load variance. Then, each charging station makes the dispatching of each charging post in order to meet the instructions of the CCC. In a similar way than before, authors use a 15 minutes resolution time. Adding control layers to reduce complexity in a centralized scheme is not new and does not solve the inherent problems of centralized solutions such as privacy and reliability. Additionally, this double layer framework, which minimizes the variance at high level, can cause problems in the elements located in the low layer such as LV distribution transformers. This is due to minimizing the load variance in the highest layer does not imply that load variance is optimized in LV distribution transformers of the lower layers.

Authors of [23] have used the quadratic (QP) and dynamic (DP) programming in order to minimize power losses and reduce voltage deviations. The IEEE 34 node distribution test feeder is used for the analysis. Authors perform a sequential series of optimizations and power flow calculations until the convergence of the algorithm is achieved. The QP and DP results have been compared, showing that they provide rather similar results but DP is slower and requires more data storage capacity. In order to minimize power losses and perform power flow calculations, the distribution network topology and the load forecast of the different nodes must be known. In this last aspect, authors are right when they introduce an error in load forecasting by using a stochastic approach to forecast load demand. Authors have pointed out that quality of the results obtained depends on the accuracy in forecasting the residential demand profile but they claim that the loss of efficiency is rather small.

In several papers, only heuristic methods are used. Thus, authors of [78] have compared three real-time control strategies based on queues: earliest deadline first (EDF), least laxity first (LLF) and receding horizon control (RHC). The main objective of the researchers is to reduce the reserve capacity needed in electric networks with high penetration of renewable energies. Using electric vehicles or deferrable loads, authors pursue to dispatch them when an excess of renewable energy generation happens. EDF is based on charging the PEVs which have the most imminent deadline or departure time. However, EDF does not take into account the energy requirement of the resources. In contrast, LLF consists in charging the PEVs which have the least flexibility factor between them. Finally, a RHC approach is analyzed. RHC is also known as model predictive control (MPC), which is based on making an optimization in each time step t, but only implementing the result of the current time step. This way, the optimization of current time step is made while the future states are taking into account. However, one of the main problems of this approach is that at each time step an optimization must be carried out, so computation time could be very high taking into account that it is a real-time control. Furthermore, if number of PEVs increases, computation time will increase accordingly due to the centralized nature. After analyzing the three options, authors consider that the control strategies RHC and EDF reduce the need for reserve capacity to cover non-dispatchable RES.

In [79] a heuristic real-time control with V2G is formulated. A priority of charging is assigned to each PEV according to EDF policy, but taking into account the energy requirements. Authors compare this real-time solution with an optimized method based on minimizing the deviation between PEVs power demand and a predefined day-ahead power demand reference, which is designed to achieve a valley-filling effect. Authors state that in a timing limitation context (less time available than required for charging the PEVs) EDF algorithm provides better results in number of missing deadlines (PEVs not totally charged). This is because the proposed EDF algorithm includes information about departure time of PEVs, while in the optimized version, time constraints have not been included. Thus, this comparison is not fair at all.

Authors of [68] have proposed a dynamic programming algorithm to achieve an optimized frequency regulation with V2G. In this case, the aggregator seeks maximizing its revenues by making frequency regulation and, at the same time, minimizing the charging cost. Authors have shown that charging rate should be 0 or 1 to achieve the optimal solution in terms of revenues. This aspect causes that the charging process of PEVs will be stopped when frequency regulation is well paid. Conversely, at low electricity prices, all PEVs will tend to charge. This behavior will lead to a sudden increase or decrease of energy demand

of PEVs (avalanche effects), which will have harmful effects in voltage levels at distribution networks.

Additionally, considering that low voltage distribution networks have low X/R ratio, the reactive power control is not so efficient to address voltage disturbances. Therefore, it is necessary to control the active power consumed by PEVs, in order to efficiently manage the voltage in such networks. This coordinated voltage control is complex when user's preferences are taken into account, since the coordinated control of voltage may cause delays in the charging process of PEVs. One solution to this problem is proposed in [80] using two control layers based on fuzzy logic. This scheme is designed to control the energy flow between the grid and PEVs, being possible the use of V2G. According to the authors, voltage stability of the distribution network is improved and it can be easily implemented in a real-time scenario. However, fuzzy logic control is rather a heuristic solution. Thus, optimal solution cannot be achieved using only fuzzy logic control. In addition, authors do not show results of a full day operation time, which is important to know the impact on the peak and off-peak periods. Furthermore, V2G operation is not limited which can lead to an increase of battery degradation. Finally, economic aspects are not taken into account.

With regard to this last point, aggregator can play an important role in reducing charging costs. In fact, aggregator can provide ancillary services such as downward reserve capacity. In [81] an objective function to minimize those charging costs as well as providing secondary reserve capacity is presented. This function is divided in three parts: cost of purchasing electricity in spot market, cost of charging with downward reserve and positive income for having reserve capacity available. Authors have made several simulations for two years (2009 and 2010). A thousand of PEVs were involved in this approach. According to the authors, an aggregator agent with an optimized bidding can reduce the charging costs in comparison with the dumb charging solution. In addition, participation in secondary downward reserve could be economically attractive for an aggregator. However, forecast of PEVs driving and charging behavior is needed, which can be difficult. Regarding to this point, authors have included forecasting errors. Taking into account these errors, results are worse but still provide significant benefit to the aggregator. This way, the aggregator could offer cheap charging cost to its customers. However, authors do not provide any information about the impacts of implementing this business case, in terms of voltage deviations and network congestions. Using only economic aspects, avalanche effects may happen in real operation conditions, unless additional actions are taken.

With the same idea, authors of [82] have presented two algorithms to be used by an aggregator. Both are designed to know how much energy should be bought in the day-ahead market. The first one is a typical charging cost minimization, taking into account hourly market prices. The second one is a modification based on increasing electricity cost as power demand increases. This way, the charging process of PEVs will be more distributed. However, this type of solutions could generate sudden power demand variations of PEVs, especially at hours with the lowest electricity prices. Moreover, authors point out that aggregators do not have any incentive to smooth PEVs power demand. Therefore, it is necessary to design new incentives, which is not addressed in this paper. In addition, possible voltage deviations and congestion problems are not analyzed.

Authors of [83] have developed an interesting approach for minimizing charging cost, while a power reference is tracked. In this case, they use MPC to achieve valid solutions in compliance with IEC 61851, which defines that the charging power of a PEV has to be semi-continuous. That is, charging power can be either zero or it can range from a minimum

positive value to a maximum positive value. The proposed MPC optimization consists of two weighted sum objective functions, as shown in equation (4-21), being μ the weight parameter.

$$J = J^{cost} + \mu \cdot J^{reg} \tag{4-21}$$

The first objective function is related to charging cost minimization and it considers not only the electricity prices but also a coefficient to model the battery degradation, as shown is equation (4-22).

$$J^{cost} = \sum_{m \epsilon M} \sum_{k=I}^{E_m} \Delta P_m T \left\{ C_k U_{mk} + C_m^{dep} |U_{mk}| \right\} \tag{4-22}$$

where:

- M: total number of PEVs
- I: current time interval
- E_m: departure time of m-th PEV
- U_{mk}: controlled power flow for the m-th PEV
- C_k: electricity price during k-th time interval
- C_m^{dep}: cost coefficient of battery degradation for m-th PEV
- ΔP_m: maximum power flow of m-th PEV
- T: discretization step of the optimal control problem

The battery degradation coefficient is a constant and it is multiply by the amount of energy flow from/to the battery. However, this approach to model the battery degradation is not accurate because battery degradation depends largely in DoD which is not linear, as shown in Figure 2.8. V2G is also included but buy/sell prices are considered to be the same. Equation (4-23) defines the second objective function, which is the error between PEVs power demand and a previously defined power reference. This way, DSO or other entity can manage the charging power of PEVs. A diagonal matrix has been introduced by the authors which gives different weights to the tracking error along the time horizon. That is, short-term tracking errors are more penalized than long-term ones.

$$J^{reg} = \left\| \Lambda (P - P^{ref}) \right\|_{\infty} \tag{4-23}$$

where:

- P: controlled aggregated power flow
- P^{ref}: reference power flow
- Λ: diagonal matrix

Because of the use of two different objective functions, a trade-off must be achieved between charging cost and tracking error. Thus, weight value should be selected carefully. In this context, authors have performed a sensitivity analysis to know the control answer to different weight values. However, this sensitivity analysis is only valid to a specific case because authors use the weighted sum method but they have not done the normalization of the objective function. Therefore, changes in prices or in power reference can change the obtained results, even if the same weights are used. In addition, the option of setting a power reference can be tricky and surely it will need forecasting the PEVs power demand. Finally, no considerations about voltage deviations have been made.

A summary of the analyzed centralized smart charging solutions can be found in Table 4.1.

Table 4.1. Characteristics analyzed in centralized control solutions

Papers' main objectives	References	
	No V2G	V2G
Frequency regulation	[78], [81]	[68]
Voltage regulation		[80]
Minimize generation cost		[71]
Minimize charging cost	[73], [81], [82]	[75], [83]
Maximize aggregator profits	[70], [82]	
Minimize power losses	[23], [72], [73], [74]	[75]
Maximize load factor	[74]	[75], [79], [83]
Minimize load variance	[74]	[76], [77]
Avoid network issues	[23], [65], [70], [72], [73]	
Minimize CO_2 emissions		[71]

Solver/tools used	References	
	No V2G	V2G
Convex optimization	[23], [70], [74], [81], [82]	[71], [75], [76], [77], [83]
Dynamic programming	[23]	[68]
Heuristic method	[65], [73], [78]	[79]
Meta-heuristic method	[72]	
Fuzzy logic		[71], [80]
Power flow	[23],[65],[70],[72],[73]	

It is clear that PEVs can be used to improve several aspects of electric power systems and researchers have proposed a great number of solutions to integrate those PEVs. Most of them are partial solutions due to the high complexity of the problem. In this context, mathematical programming is the most preferred method to achieve a certain objective or objectives but other approaches can be valid. However, few of them have addressed or analyzed voltage deviations problems and almost none of them have considered voltage unbalances.

To conclude this subsection, it should be noted that centralized control system presents several problems, due to the centralized nature of data management. The first one is due to the importance of the aggregator for the system to work properly. Therefore, it is necessary to have a backup system to minimize the risk of a possible system failure. The second one is due to the amount of data that must be handled by the aggregator. As the number of PEVs increases, the amount of information that have to be transmitted and processed by the aggregator can be significant, making difficult to manage it and needing an expensive communication system. Finally, in this type of centralized control privacy issues can arise, because the aggregator will access to data from PEVs and, consequently, to transport habits of users. Considering these aspects, it can be desirable to implement a decentralized control.

4.3.2   Decentralized control architecture

Also known as indirect, distributed or local control, the decision-making resides in each PEV, i.e. in each owner, rather than in an external entity. This aspect implies that each PEV must have some intelligence implemented. Although the decision of "when and how much should be charged" is taken by the PEV/owner itself, there are ways to influence these decisions. One of these ways is known as price signals which consist in dynamically modify electricity prices in function of some parameters such as energy demand level. The market

operation of a decentralized control architecture based on price signals has been described in [69]. Figure 4.6 shows the possible operation scheme of this system.
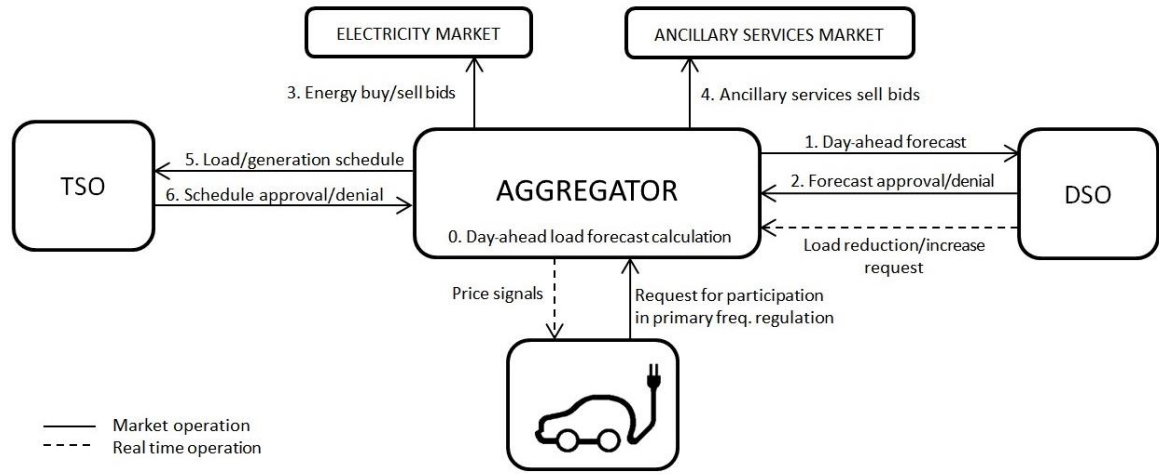
Figure 4.6. Decentralized control architecture using price signals [69]

Apart from price signals, other basic way to modify locally the charging power of a PEV is by measuring the local voltage and frequency at the connection node. Depending on these values, active and/or reactive power of PEVs can be modulated in order to control the local voltage or provide primary frequency regulation. This technique is known as droop control and it can work without any communication infrastructure.

Normally, PEVs are individually connected to low voltage networks, where R/X ratio is higher than in MV and HV electric networks. Therefore, it is more efficient to apply an active power control by reducing the power demand of PEVs and even injecting power into the grid, in case the V2G option is available [84], [85]. In addition, the primary frequency control is also possible by using the mentioned droop control, which consists in adjusting the power demand of the PEV, according to equation (4-24). In a similar way, local voltage control can be performed by using equation (4-25).

$$P = P_0 + (f - f_0)/k_p \qquad (4\text{-}24)$$

$$Q = Q_0 + (V - V_0)/k_q \qquad (4\text{-}25)$$

where:

- P, Q: active and reactive power output
- $f - f_0$:   frequency deviation
- $V - V_0$:   voltage deviation
- k_p, k_q: active and reactive power droop control characteristics (slope)
- P_0, Q_0:   active and reactive power offset

In this droop control, a dead zone should be added, where PEVs do not respond to changes in frequency to ensure the longevity of batteries. This dead zone and the slope of the droop control should be defined according to the characteristics of the distribution network where PEVs are connected. Additionally, the willingness of users to participate in system frequency regulation should be taken into account. Furthermore, both charging and discharging power (only with V2G) should be limited by the battery and the charger

characteristics. Finally, there must be an offset that represents the rated power consumption of PEVs when the system is operating without frequency deviations. Thus, for frequency deviations greater than the dead zone, PEVs' batteries will respond as it has been defined in the droop control. If frequency decreases, the battery consumption will be reduced in the first instance. If still this action is not enough, the battery will start to inject power into the grid. Conversely, if frequency increases, the battery consumption will increase, in an attempt to drain the power excess in the system. A droop frequency characteristic including the mentioned improvements can be seen in Figure 4.7 [45].
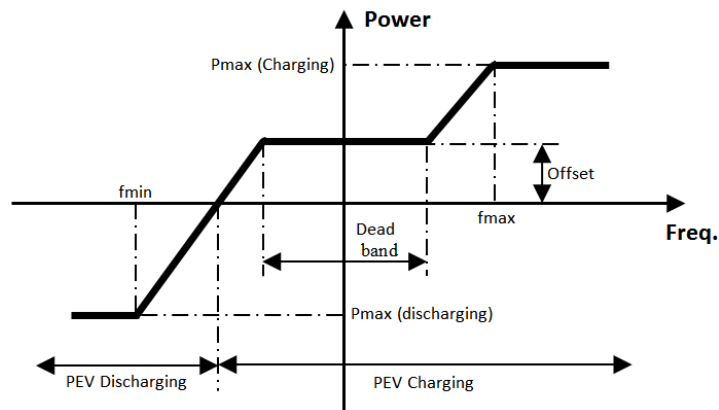
Figure 4.7. Frequency droop control with V2G [45]

Batteries of PEVs are very suitable to perform primary frequency and voltage control, due to their fast response and ramp up/down characteristics. To implement the primary frequency control in a market environment, users must notify to the utility their intention to participate as a primary reserve. After communication has been established, the PEV will be designated as primary reserve supplier and the local control will be activated. When the provision of this service is finished, the PEV will send a signal to the utility and will be compensated based on the time that it has been available as primary reserve.

Many authors have used this classical technique of control. In [86] the droop control method is used to achieve suppression of frequency and voltage fluctuation, without using any type of communication. The system includes not only electric vehicles but also electric water heaters. Possibilities of droop control to maximizes intermittent RES integration, using PEVs and V2G in islanded grids, is researched in [45]. The droop control of Figure 4.7 is used to define the active power output of an inverter. Several simulations have been carried out in Matlab/Simulink to know the response of such control when a sudden wind speed drop happens.

Also, in [87] V2G is used to provide frequency regulation in an islanded power system, with high penetration of wind power sources. Two droop methods were tested, one based on a proportional controller and the second one based on a PI controller with a high pass filter. The last one provides better results. According to the authors, 80% of frequency regulation reserves could be covered by PEVs with V2G, on average. Simulations were performed in the DIgSILENT PowerFactory software.

Katarina et al. [88] have implemented a reactive power control (RPC) based on droop control method. The LV distribution network used is based on a real distribution network located in Borup (Denmark). The data of this network has also been used in the methodology developed in this thesis. RPC is implemented not only in the electric vehicles

but also in the photovoltaic (PV) installations of the network. Six different scenarios were analyzed depending on the chosen season (winter or spring) and the possible combinations of control (no RPC, RPC in PVs and RPC in PVs and PEVs). Results obtained show that the RPC method improves voltages profile while energy losses do not vary significantly.

Frederik Geth et al. [89] have proposed an unidirectional droop method in order to limit under-voltage problems that can arise in residential distribution networks. A 400/230V network with 62 household was used. Four different cases were considered: no droop control and three different droop control characteristics. Unbalanced simulations were performed with Matlab. Authors suggest that droop control method can have an impact in the charging rate of PEVs, about 15% in the worst case, which is manageable. In contrast, voltage deviations can be significantly improved by approximately 46%. According to the authors, controllability of the voltage in the three phases is not equal due to unbalances generated by household loads.

A similar network to the previous paper is used in [90]. In this case, authors have added a coordinated charging to the droop control. This coordinated charging is based on charging at the minimum charging power to meet the user requirements, regarding to departure time. However, a minimum charging power to avoid low efficiency in chargers is taken into account. This minimum charging power was set to 25% of nominal charging power. Four cases were analyzed: uncoordinated charging, uncoordinated charging with droop control, coordinated charging and coordinated charging with droop control. As expected, the coordinated charging significantly reduces peak power compared to the uncoordinated cases. Droop control provides better values in terms of voltages. Also, voltage unbalances have decreased, especially in coordinated charging. The reason is that coordinated charging naturally synchronizes the charging of PEVs between all phases. However, this coordinated control increases charging time in more than three times. In addition, the proposed coordinated charging is not optimal. Therefore, some smart charging algorithms (such as losses or variance minimization or load factor maximization) can provide significant improvements.

Adaptive droop control method can offer interesting solutions. In [91] primary frequency control (PFC) is performed, while required charging level of customers is fulfilled. However, droop based PFC presents the drawback that charging power depends on the frequency level. That is, if the PEV is providing PFC and frequency is low during a long period of time, the PEV battery could not have enough stored energy for the next trip of the user. The authors of this paper address this problem proposing a decentralized V2G control (DVC), which consists in two different smart charging approaches. The first one, called battery SOC holder (BSH), consists in maintaining a minimum SOC, preselected by the user, during the PFC. The second one, called charging with frequency regulation (CFR), is used to charge the PEV without stopping the frequency regulation. The main idea of these control methods is to introduce two variables in the droop control method to define the slopes for charging and discharging, depending on the current SOC of the PEV and the minimum SOC required by the user. According to the authors, DVC can provide primary frequency regulation while charging demand of the PEV users is satisfied.

However, a drawback of the droop methods is that the effective gain of the control is affected by the number of connected PEVs. Therefore, it is necessary to update the gain of the droop control of each PEV, which participates on the primary frequency/voltage regulation, to achieve a constant effective gain and avoid fluctuations. In addition, the droop control method alone do not provide some important advantages given by the optimized

methods, such as load levelling, peak shaving, congestion management and charging cost reduction.

Some optimized and decentralized solutions can be considered as market based solutions, especially when price signals are part of the algorithm. In this case, the aggregator or utility iteratively update electricity prices (price signals) in order to modify the charging profile of PEVs. Thus, charging cost will depend on these price signals. One typical application is to relate the charging cost with power demand in order to avoid grid congestions. Thus, if power demand increases at certain time, electric prices for that time will increase, encouraging to recently connected PEVs to be charged in another period of time.

A large amount of papers that analyze decentralized control methods put the focus on achieving a valley-filling effect. Z. Ma et al. [92] have developed an algorithm based on a finite-horizon non-cooperative dynamic game. First, they define the electricity cost which depends on base load and load demanded by PEVs, divided by the network capacity, as shown in equation (4-26).

$$r_t = \left(\frac{d_t + avg(u_t)}{C} \right) \tag{4-26}$$

where:

- r_t: ratio of aggregated load demand and the generation capacity
- d_t: forecasted base load at time slot t
- u_t: charging power of PEVs at time slot t
- C: generation capacity

This electricity cost is broadcasted to all PEV agents. Then, each PEV agent tries to minimize its charging cost and the cost incurred in deviating from the average behavior of the PEV population (4-27).

$$J^n(u) \triangleq \sum_{t=0}^{T-1} \left\{ p(r_t) \cdot u_t^n + \delta \left(u_t^n - avg(u_t) \right)^2 \right\} \tag{4-27}$$

where:

- $p(r_t)$:   electricity retail price which depends on (4-26)
- u_t^n: charging power of n-th PEV at time interval t
- δ: tracking parameter
- T: number of time periods

After optimal charging strategy has been calculated, it is sent to the utility which update the aggregated PEVs power demand of (4-26) and send it back to all PEVs, repeating the process until the algorithm achieves the convergence. In this context, the tracking parameter of (4-27) has a relevant importance on the convergence of the algorithm. But, convergence is not assured if the tracking parameter is not well selected. This algorithm was tested for homogeneous and heterogeneous driving and charging behavior. In the homogeneous case, all PEVs have the same characteristics, energy requirements and arrive and departure time. According to the authors, algorithm converges in a few iterations for this homogeneous case. However, for the heterogeneous case, which is the realistic one, the algorithm does not achieve optimal solutions.

In a similar way, Lingwen Gan et al. [93] have proposed an iterative algorithm that tries to fill the off-peak hours optimally. The valley-filling effect is achieved by an iterative optimization. First, the utility will broadcast a control signal. This control signal is calculated from equation (4-28), as the sum of the forecasted base load and the PEVs power demand.

$$p^k(t) := \gamma U' \left(D(t) + \sum_{n \in \mathcal{N}} r_n^k(t) \right), t \epsilon \mathcal{T} \tag{4-28}$$

where:

- $p^k(t)$:   control signal of iteration k at time slot t
- γ: parameter to modulate the control signal value
- U':   Lipschitz function
- $D(t)$:   forecasted base load at time slot t
- $r_n^k(t)$:   charging rate of the n-th PEV at time slot t and iteration k
- $\mathcal{T}$:   scheduling time horizon

Taking into account this control signal and a penalty term, each PEV will minimize its cost function (4-29). The penalty term will penalize changes in the charging profile of the PEV between two consecutive iterations.

$$min\langle p^k, r_n \rangle + \frac{1}{2} \|r_n - r_n^k\|^2 \quad s.t. \ r_n \in \mathcal{F}_n \tag{4-29}$$

where:

- $\mathcal{F}_n$:   feasible space of the n-th PEV

After the optimization is performed, the charging profile will be sent to the utility which will update the control signal. This process continues until the convergence is achieved with the help of the penalty term. This optimization takes into account the user preferences in terms of energy charged and departure time. Authors also present a similar algorithm with the objective of tracking a predefined load curve in real-time operation. Additionally, they have compared their algorithm with the solution developed in [92], showing that their algorithm cope with the non-homogeneous driving and charging behavior better than the solution of [92]. However, authors do not provide any analysis about the impact of voltage levels.

In the same manner, but focusing in buildings [94], a decentralized control algorithm which tries to minimize costs for users as well as increase load factor, using a non-cooperative game approach for a building. In this solution, each PEV i receives data of the total load of the building, from a building controller. Then, PEV i finds the best optimized load profile, by minimizing equation (4-30), in order to pay as less as possible.

$$\min_{x_i \in \mathcal{X}_i} k_i \cdot \sum_{t=1}^{T} \delta \left(l^t + \sum_{j \neq i}^{N} (x_j^t) + x_i^t \right)^2 \tag{4-30}$$

where:

- k_i: energy demand of i-th PEV and total energy demand ratio
- δ: cost coefficient (€/kWh^2)
- l^t: forecasted base load demand at time slot t

- x_j^t: charging power of j-th PEV at time slot t
- x_i^t: charging power of i-th PEV at time slot t

This profile is sent to the building controller which updates the total building load profile and sends it to another user. This procedure is done in rounds and repeated until convergence is reached. Authors of this paper define that the charging cost is directly related with the total energy demand in the building, as shown in equation (4-30). This way, a smooth energy demand of the building is achieved. However, they do not include any real factor of electricity cost from the grid. Thus, PEVs could be charged at high electricity market prices.

Similarly, in [95] an algorithm is formulated to minimize the overall charging cost of all PEVs using a game theoretic approach and focusing in distribution networks. In this case, a complex cost function is developed including the generation capacity, as shown in equation (4-31).

$$cost_i = \int_a^b r_i(t) \cdot \gamma_{bt} \cdot \left(\frac{\sum_{j \in V} r_j(t) + L_{base}(t)}{G(t)} \right)^\alpha dt \qquad (4\text{-}31)$$

where:

- $r_i(t)$:   charging rate of i-th PEV in time t (to be calculated)
- $r_j(t)$:   charging rate of j-th PEV in time t
- V: set of already connected PEVs
- a, b: connection time interval
- γ_{bt}:   energy cost ($/kWh)
- $L_{base}(t)$:   forecasted base load demand in time t
- $G(t)$:   generation capacity in time t
- α: nonlinear cost coefficient between load and prices

In addition, authors have taken into account the PEV owners' driving patterns, which have been obtained from statistical data of 2009 NHTS [30]. Three different scenarios were simulated: 2, 15 and 70% of PEV-PR for a distribution network composed by 1,000 houses. They have assumed one PEV for household at maximum. According to the simulation performed, the proposed algorithm reduces peak load compared to uncontrolled scenario and improves load factor. As previous analyzed papers, authors do not analyze the impact of load forecasting errors on the results. In addition, possible voltage deviations are not analyzed.

Implementation and organization of a decentralized control architecture, where intelligence is distributed in each PEV, can be performed using a tool known as multi-agent system (MAS) [96]. A multi-agent system is a set of two or more intelligent entities, named agents, which interact in an environment. The purpose of this tool is to reduce the complexity of a problem, by dividing it into sub-problems. According to Wooldridge [97], an agent is a virtual or physical entity located in an environment that is able to react autonomously to changes in that environment. The basic functions that define an agent are:

- Autonomy. Ability to meet designated targets without the constant guidance of a user.
- Sensitivity. Ability to perceive the environment and respond to changes.
- Social ability. Ability to interact with other virtual or physical agents.

- Activeness. Ability to take decisions and start their own actions to meet designated goals.

Agents can cooperate and communicate with each other, so that an agent may influence another agent's decisions and the state of its environment, in order to meet its needs and those of the system. Each PEV will have its own agent, which will act in order to meet certain objectives, according to its status and environment. For instance, an agent can have the objective of charging with the minimum cost possible, while another agent may be programmed to have a minimum of SOC available, even whether it is penalized financially. Other types of agents can exist, like transformer agent which may be responsible for preventing overloads.

Karfopoulos et al. [98] have designed and modeled a MAS method for charging PEVs. The scheme is similar than those of previous analyzed papers, in which price signals are used. This scheme works as follows. Each PEV agent tries to minimize its charging cost, which depends on pricing policy. A regional aggregation unit (RAU) agent updates the pricing policy, according to equation (4-32), in order to reflect the load level of the distribution transformer. The higher the transformer load level is, the higher the electricity prices will be. This way, overloads can be avoided.

$$p(t) = f\left(\frac{D(t) + \sum_{i=1}^{N} P_i(t)}{P_{trans}}\right) \tag{4-32}$$

where:

- $P_i(t)$: optimal charging power of i-th at time t
- $D(t)$: forecasted base load at time t
- P_{trans}: transformer load capacity
- $p(t)$: RAU pricing policy at time t

Two different objective functions to be minimized by the PEV agent have been used. The first one, called uncoupled, is based on minimizing the charging cost, using equation (4-33). The second one, called weakly-coupled, is based on equation (4-27) of reference [92]. Charging optimization of PEVs is solved by using a hybrid PSO technique, while overall system is solved using a non-cooperative dynamic game. Authors suggest that with this solution an effective valley filling is achieved, reducing energy losses.

$$min\ F = \int_{t_0}^{t_0+T} p(t)P(t)dt \tag{4-33}$$

where:

- $P(t)$: charging power at time t
- t_0: starting time of charging
- T: charging period

According to the authors, the uncoupled version does not achieve the convergence, while the weakly-coupled converges in a few iterations. This last version is compared with a centralized solution, based on load variance minimization. As commented before, the centralized version achieves an optimal solution in only one iteration, but as number of PEVs increases, the computation time will be higher. The same conclusions are commented in this paper. Obviously, this is because the centralized nature of the algorithm. In addition,

load forecast errors are not taken into account. In this type of solutions, this error in load forecasting will have an important impact on charging cost of PEV users.

Hu et al. have proposed a MAS based on price signals [99]. This MAS is composed by four different agents: the DSO agent, the market operator agent (CMO), the fleet operator agent (FO) and the EV agent. The proposed solution works as follows: each PEV generates the charging schedule by minimizing equation (4-34) and taking into account the user requirements.

$$Min \sum_{i=1}^{N_T} \left(\phi_{j,i} + \varepsilon_i \cdot \Lambda(i) \right) P_{j,i} t \tag{4-34}$$

where:

- N_T: total number of time slots
- $\phi_{j,i}$:   predicted day-ahead electricity market price vector
- ε_i: weighting factor of the shadow prices
- $\Lambda(i)$:   shadow price
- $P_{j,i}$:   charging power of j-th PEV at time slot i
- t: length of each time slot

The obtained charging schedule is sent to the FO, which aggregates all charging schedules under its governance. The aggregated charging schedules of the different FOs are submitted to the DSO, which runs a power flow to check if any distribution network constraints are exceeded. If there is no problem, FOs could bid the energy scheduled for the next operation day. However, if the power flow reveals any congestion problem, the FOs will submit their aggregated charging schedules to the CMO agent. An iterative procedure between the CMO and the FOs is carried out in order to avoid those congestion problems. This procedure consists in calculating iteratively the power demand profile of each FO (equation (4-35)) and the necessary shadow prices (equation (4-36)) to avoid congestion problems and taking into account the maximum network capacity.

$$L = \sum_{k=1}^{N_B} \sum_{i=1}^{N_T} C_{k,i} \left(\tilde{P}_{k,i} - P^E_{k,i} \right)^2 + \sum_{i=1}^{N_T} \Lambda(i) \left(\sum_{k=1}^{N_B} \tilde{P}_{k,i} - P_{Cap}(i) \right) \tag{4-35}$$

where:

- N_B: number of FOs
- $C_{k,i}$:   weighting factor associated with power difference
- $\tilde{P}_{k,i}$:   power demand of FO k at time slot i to be calculated
- $P^E_{k,i}$:   accumulated charging profile of k-th FO at time slot i
- $P_{Cap}(i)$:   power capacity at time slot i

$$\Lambda(i)^{\omega+1} = \Lambda(i)^\omega + \alpha_\omega \sum_{k=1}^{N_B} \left(P^*_{k,i}(\Lambda^*) - P_{Cap}(i) \right) \tag{4-36}$$

where:

- $\Lambda(i)^{\omega+1}$:   shadow price to be calculated at time slot i
- $\Lambda(i)^\omega$:   shadow price of previous iteration ω at time slot i
- α_ω: step size
- $P^*_{k,i}(\Lambda^*)$:   optimal solution achieved using equation (4-35)

After convergence is achieved, each PEV performs the optimization of equation (4-34) taking into account the calculated shadow prices. This way, congestion management of distribution networks with high PEV-PRs can be performed.

A real-time multi-agent system based on price signals is carried out and tested experimentally at laboratory scale in [100]. As in the previous paper, four different agents are defined: DSO agent, coordinator agent, local area agent and PEV agent. The PEV agent sends PEV owner's preferences and receives charging set-points from the local area agent that had been previously calculated by minimizing a cost function. The coordinator agent aggregates the demand of the local area agents and sends it to the DSO agent which is responsible for the safe operation of the distribution network. The DSO will perform a power flow in order to know whether there is any congestion. If yes, a virtual price is added to the hours when congestions happen. The tests carried out by authors show that MAS can manage PEVs charging tasks avoiding overloads in distribution networks. This solution is slightly different because cost optimization is performed in the local area agent, instead on the PEV agent. Thus, PEVs agent must sent more information to local agent such as actual SOC, required final SOC, connection time, charging power, charger efficiency and battery efficiency. Furthermore, this type of solution can increase peak power and power losses as no optimal dispatch is used. As most of the papers, voltage problems have not been addressed.

An approach, based on congestion pricing of Internet traffic control, is proposed in [101] to develop a distributed demand response algorithm with PEVs in a residential scenario. Price of energy in a certain period of time depends on the aggregated demand. Moreover, each user agent declares a price per time slot that he is willing to pay (WTP). Thereby, users who pay more receive a better quality of service, i.e. they will charge their PEVs in less time. The formulated cost function is composed by two terms. The first one is referred as utility (user's quality of service) function which depends on the WTP parameter. The second one, called as cost function, is a price function which depends on aggregated demand. That is, the higher the overall demand, the more expensive the electricity will be. Hence, the objective of a user i is to maximize equation (4-37).

$$w_i \cdot \log(x_i(n)) - x_i(n) \cdot a \left(\frac{\sum_{i=1}^{N} x_i(n)}{C} \right)^k \qquad (4\text{-}37)$$

where:
- n: current time slot
- N: total number of PEVs
- $x_i(n)$: charging power at time slot n
- w_i: WTP at time slot i
- a, k: shape parameters
- C: market capacity

As a consequence of different WTPs between users, load levelling and peak saving can be achieved. Although it is an interesting approach, it can be complex to develop in real world. Users will have to define the WTP for each time period, which can be difficult to understand, especially because results do not depend only on the WTP scheme selected, but also on the aggregated PEVs power demand and other parameters defined by an external entity, such as a, k and C.

Another interesting approach to avoid network congestions, as well as voltage drops problems, is presented in [102]. Authors present a random access framework to schedule the PEVs charging. A network control center monitors load and voltage parameters of the different buses. When a PEV is plugged into a specific bus, a smart agent which makes decisions for the PEV will request data from that control center. The smart agent will schedule the PEV charging in function of two stochastic probabilities: access and suspend probability. The first one is designed to prevent the access to the network or resume the charging process, and the second one to suspend the charging process if any problem exists in the network. Both probabilities are divided in two parts, one designed to avoid load congestion and the other one developed to avoid voltage violations. Only the worst case between both probabilities is used. Equation (4-38) shows the access probability equation used by authors. A mechanism is also added to assure that PEV will reach the expected charging level before departure time is reached.

$$p_1(\gamma_c) = \begin{cases} k_1 e^{-\alpha_c(\gamma_c - v_{c1}) + \beta_c \cdot \omega/\omega_m} + \delta_1, & if \ \omega < \omega_m \\ 1, & if \ \omega = \omega_m \end{cases} \qquad (4\text{-}38)$$

where:
- $p_1(\gamma_c)$:   charging probability
- k_1:   global parameter to modulate the probability to start charging
- γ_c: loading ratio
- α_c: parameter to define how fast $p_1(\gamma_c)$ changes when $\gamma_c \rightarrow v_{c2}$
- v_{c1}:   value of threshold one for bus congestion (warning level)
- v_{c2}:   value of threshold two for bus congestion (emergency level)
- δ_1:   user preference parameter
- ω: current waited time
- ω_m: maximum tolerable waited time
- β_c: weight factor of waiting time

According to the authors, this approach maximizes the number of PEVs that can be integrated in a distribution network. This can be true, but the proposed approach does not have an optimal behavior with lower PEV-PRs. That is, it is designed to avoid load congestions and voltage violations but cannot reduce energy losses or peak power. In fact, in low loaded networks, it will tend to increase peak power until load congestions or voltage violations happen. Thus, energy losses will be higher compared with other optimal solutions already analyzed. Furthermore, these authors do not take into account economic aspects.

In [103] a stochastic process is also used. Authors design a Markov chain to model the user driving patterns. The probability of the vehicle of being used is considered in the decision process that determines when a PEV has to be charged, in order to minimize charging costs. A penalty term is introduced to model the flexibility level of the PEV user. That is, the less flexible the user is, the higher the penalty term will be. Therefore, the charging process of the PEV will be faster. Besides, two versions are analyzed: unidirectional and bidirectional (V2G). A stochastic dynamic programming is used to determine the optimal charging profile. According to the authors, it could achieve daily savings of approx. 19-47% in the G2V version, respect to dumb charging. This approach only addresses economic aspects and therefore, a real implementation can lead to avalanche effects as all PEVs will tend to be charged at hours with low prices.

Decentralized voltage control is introduced in [104], using an iterative algorithm called best response dynamics (BRD), based on non-cooperative game theory. Authors use a sensitivity matrix to evaluate deviations in voltages of pilot nodes, induced by changes in active and reactive power injections. The solution procedure works as follows: all PEVs send their charging profiles to an aggregator which calculates the voltage level on all the pilot nodes and sends this data back to each PEV. After that, each PEV updates its charging profile to minimize an objective function. Authors propose two objective functions. On the one hand, the minimization of voltage deviations for all pilot nodes (global approach), which objective function is presented in equation (4-39). On the other hand, the minimization of voltage deviations for only neighborhood pilot nodes (local approach), which objective function is presented in equation (4-40).

$$f^{global}(\Delta P_i, \Delta P_{-i}) = \sum_{p=1}^{N_p} f_V \left(V_p - V_{ref} + \sum_c S_{V_p, P_c} \cdot \Delta P_c \right) \tag{4-39}$$

where:

- ΔP_i: change in active power injection at instant i
- ΔP_{-i}:   change in active power injection at any instant (except i)
- N_p: total number of pilot nodes
- p: pilot node
- c: controlled node
- $f_V(V_p)$:   performance function
- V_p: voltage measured at pilot node p
- V_{ref}:   voltage reference
- S_{V_p, P_c}:   value of the sensitivity matrix V-P for pilot node p
- ΔP_c: variation of power at c-th controlled node

$$f_i^{local}(\Delta P_i, \Delta P_{-i}) = \sum_{p \in \mathcal{V}_i} f_V \left(V_p - V_{ref} + \sum_c S_{V_p, P} \cdot \Delta P \right) \tag{4-40}$$

where:

- $\mathcal{V}_i$:   local pilot nodes for i-th PEV
- ΔP: change in PEV active power injection

Simulations have been performed in the IEEE 34 distribution network model and results show that there is a significant improvement compared to the uncontrolled case. Furthermore, the proposed algorithms provide also better results than the droop method, which is also applied to the problem in order to compare with the two optimized methods. In general, local and global approaches give similar results. Obviously, the optimized methods need more information exchange than the voltage droop control approach. The proposed methods only act when a voltage value, at any pilot node, is out of 0.9-1.1 p.u. range. This is because $f_V(V_p)$ is equal to zero, when pilot node voltages are in their standard limits (0.9-1.1 p.u.). It could be more interesting if these controls would start to work gradually, before any pilot node surpasses the voltage limits. Moreover, distribution network topology, i.e. the admittance matrix, must be known in order to calculate the sensitivity matrix. Additionally, voltage unbalances problem is not analyzed in this paper.

All decentralized systems analyzed until now require that the intelligence should go installed onboard of the PEV, which means that there must be a dedicated hardware to process the data. The additional cost of this hardware can be avoided by using mobile agents concept. In the V2G concept, PEVs can be considered as distributed generation and distributed storage. But PEVs are also mobile devices. Therefore, the distribution network where the PEV is connected will demand nomadic computing capacity. This means that the PEV which is moving from an area to another one must be able to connect to different EVSEs and continue to experience the same level of service quality, concept known as roaming. This concept requires that the PEV must have the know-how of bidirectional power exchange with the network, the intelligence to take decisions based on the environment (SOC, market prices, system status, etc.) and an adequate computing power to run the required tasks. In other words, knowledge, intelligence and computing power must be on-board of the PEV.

This option requires the existence of an embedded system that allows the different charging strategies and market participation to be integrated. But embedded systems usually have a limited computing power. In order to adapt this limited potential to V2G concept, embedded system should be improved, which will increase the cost of PEVs. That cost increase can be avoided by transferring the computing capacity to an external system using the mobile agents concept [105], as shown in Figure 4.8.

Thus, locally, there is an agent which is part of the residential energy management. This agent contains all the information and intelligence needed for the charging/discharging control of the PEV batteries, at local level. Once the PEV leaves the residential zone, the battery will discharge depending on the distance travelled, traffic and driving behavior. In case that the battery SOC is greater than the travel needs of the user, and taking into account the possible degradation of the battery, the excess energy could be injected into the grid. To achieve a proper operation of the V2G concept, intelligence and data of the stationary agent, located in the residential EVSE, is required. Therefore, a migration of information and intelligence to the new EVSE is needed. The mobile agent technology allows this migration.
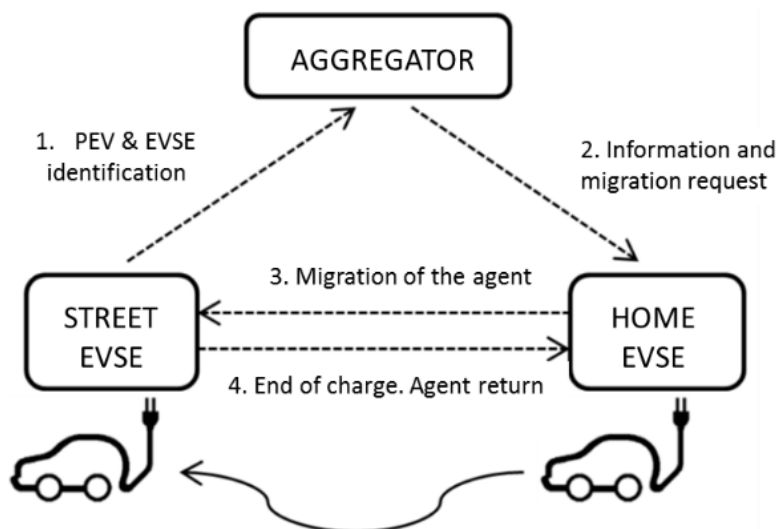
Figure 4.8. Application of mobile agent concept for PEVs

When the PEV is connected to a new EVSE, an identification message is sent to the aggregator. This message contains the identity of the PEV and the location of the EVSE. After receiving this information, the aggregator sends the location of the EVSE to the stationary agent, which is cloned and migrated to the new EVSE. When this process is complete, the agent returns from the new EVSE to the residential EVSE and updates the data of the stationary agent. This system is only feasible if there is some kind of communication infrastructure that can be installed on each EVSE. Additionally, privacy concerns may arise because private information is transmitted through an external entity (aggregator). Finally, it is expected that, in general, vehicles will have more computing power installed, due to the development of connected, intelligent and autonomous vehicles. Note that onboard CPUs will be free to execute smart charging algorithms because the vehicles are parked and most of these new services, such as autonomous drive, are not necessary.

In contrast to droop control methods, most of reviewed optimized algorithms are not focused on voltage and frequency regulation. Thus, some of the proposed algorithms will probably have an impact on voltage and congestion levels. In this context, it is necessary to analyze these aspects, something that several papers do not address.

Thus, it is necessary to implement optimized algorithms with some type of voltage control such as the droop control already proposed. However, mixing both controls, i.e. droop methods and optimized methods, could not be easy unless they focus in different variable controls such as active power for optimized algorithms and reactive power for droop control methods.

To finish this subsection, a summary of the analyzed decentralized smart charging solutions is presented in Table 4.2.

Table 4.2. Characteristics analyzed in the decentralized control solutions

Papers' main objectives	References	
	No V2G	V2G
Frequency regulation		[45], [86], [87], [91]
Voltage regulation	[89], [90], [104]	[86], [88]
Minimize charging cost	[95]	[103]
Load levelling (price signals)	[92], [93], [95], [98], [100], [101]	
Minimize load variance		[94]
Avoid network issues	[99], [100], [102]	

Solver/tools used	References	
	No V2G	V2G
Convex optimization	[92], [93], [99], [100], [104]	[94]
Dynamic optimization		[103]
Droop method	[89], [90]	[45], [86], [87], [88], [91]
Meta-heuristic	[98]	
Power flow	[99], [100]	
Stochastic algorithm	[102]	

4.3.3   Comparison between centralized and decentralized control approaches

This subsection compares the intrinsic characteristics of the two control architectures presented. In this aspect, some authors have published papers using and comparing these two approaches.

In [106], linear programming optimization is used in both architectures in order to charge PEVs within network constrains limits. The decentralized smart charging algorithm is based on maximizing the charging power without exceeding the local voltage and single-phase line loading limits, which are programmed as constraints. In the centralized case, the optimization objective is also to maximize the charging power without surpassing the observed node voltages and loading level of distribution transformer. Additionally, the objective function prioritizes the charging of PEVs with less SOC. Authors use Matlab to solve the optimization problem and PowerFactory to test and compare the obtained solutions. The main conclusions obtained in the simulations are that the centralized control approach makes a better use of the network capacity and achieves a better control of voltage, due to all network information is known by the central controller. However, this centralized control approach needs a more complex communication infrastructure.

Authors of [107] have developed and compared three different control systems: centralized control, decentralized with system-wide price signals and decentralized with nodal price signals. These control approaches are designed to optimize generating costs in a large-scale network. Low voltage network constraints are not considered. In the decentralized cases, PEV users seek to minimize their charging cost. Thus, the TOU tariffs which minimize generation cost are calculated. Simulation results show that the best solution, in terms of generation cost, is achieved with centralized control approach. However, the decentralized control with nodal prices obtains similar results. Therefore, the authors prefer the decentralized control approach, taking into account that it presents better consumer acceptance and requires a smaller communication infrastructure.

Thus, considering all the aspects analyzed in section 4.3, a comparison of these two control schemes and a set of advantages and drawbacks of each approach are presented (Table 4.3):

Table 4.3. Advantages and drawbacks of centralized and decentralized architecture controls

	Advantages	Drawbacks
Centralized control	✓ Well-known architecture ✓ Better utilization of network capacity ✓ Better ancillary services provision	✗ A complex and expensive communication infrastructure is required ✗ A central controller and a backup system is necessary ✗ Complexity increases with the number of PEVs ✗ Large amount of data to process ✗ Privacy issues
Decentralized control	✓ Scalable ✓ Improved fault tolerance ✓ Less communications infrastructure required ✓ Charge control remain in the user ✓ Higher consumer acceptance	✗ Uncertainty in the final result ✗ Limited ancillary services provision ✗ Necessity of predicting or forecasting the reaction of consumers ✗ Avalanche effects or simultaneous reactions may happen

- Optimization. In centralized control, application of optimization algorithms for PEVs charging is easier, since all system information is available at the same point. This aspect facilitates the management of the distribution network, maximizing the network capacity and the provision of ancillary services. However, it requires a large amount of data such as: desired final level of SOC, charging time available, battery capacity, etc. to reach the optimal solution. In practice, some of these data will be difficult to know in advance, therefore, the final solution will be affected.

  In the decentralized option, the global optimization is achieved through the influence of price or control signals over the PEVs. However, the final decision is taken by each PEV, which implies some uncertainty in the final result. Also, avalanche effects may occur, that is, a huge number of PEVs can change their charging power rate at the same time, in response to a fall/rise of electricity prices. This effect is more likely to occur if only economic aspects are taken into account.

- Information, communication and processing. In the centralized architecture the information is received and processed at a central control. This situation will be computationally-intensive, depending on the number of PEVs and the optimization algorithm applied. In contrast, in the distributed architecture, the information is processed in a distributed way. Thus, communication infrastructure and data processing requirements are lower. However, an on-board control unit is required in each PEV.

- Privacy. In the centralized control, privacy problems may exist because a third party will hold data about the PEV users' behavior. This problem does not occur in decentralized control because the information is locally processed.

- Modularity. In centralized control, connection of new PEVs in the system may require small adjustments in the control program of the aggregator. In the decentralized case, no changes are expected. In addition, computation effort do not vary as number of PEVs increases because the calculation process is made in a distributed way.

- Fault tolerance. The centralized control architecture is more sensitive to errors, especially when these errors occur in the central management entity; therefore, a backup system is necessary. In contrast, decentralized control can run autonomously because every PEV has an on-board controller.

4.4 Distributed generation and plug-in electric vehicles

In the last decade, the growth of distributed generation and renewable energy resources connected in low voltage networks has been remarkable, mainly due to environmental, commercial and regulatory aspects [108]. As example, the European Union countries have set a target of 20% of RES by 2020 [109]. Therefore, these technologies are expected to become more profitable. However, as PEVs, DG units do not have the minimum size to compete in the electricity market under the same conditions than conventional generation. One solution may be to group PEVs and DGs, giving the visibility needed for controlling them in a smart way. Currently, there are two solutions to integrate actively DG and PEVs, within the electrical system: virtual power plants (VPPs) and microgrids (MGs) [110].

4.4.1   Virtual power plants (VPP)

VPPs can be defined as a clustering model that tries to manage electrical generation and demand devices, geographically dispersed, as if they were a single entity for the system operator (Figure 4.9) [110]–[112]. Thus, a VPP has the advantage of reducing the financial risk regarding the individual participation of each distributed generator. In the future, it is expected that the VPP concept will maximize the benefits for owners of distributed generators and the system operator.

Within a VPP, PEVs may be considered as mobile distributed energy sources that have the potential to provide advantages in the power system. The main advantages are the absence of "on and off" costs, very fast response time, low cost in standby and high availability factors [68], [113]. Furthermore, the combination of VPP, RES and PEVs offers significant synergies that can allow an important reduction of CO_2 emissions [114], [115].
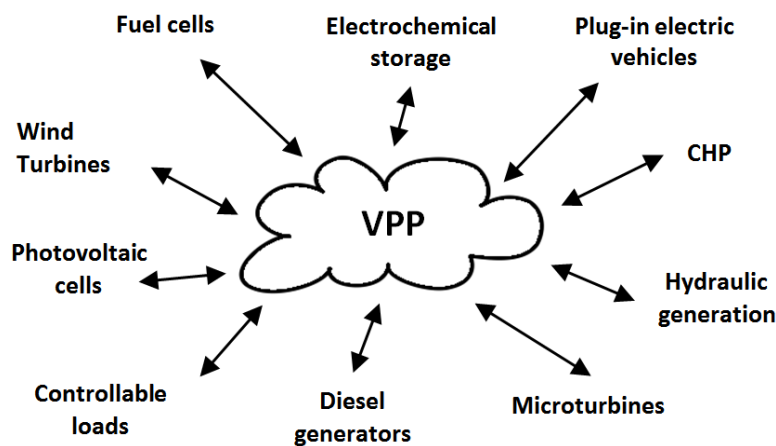
Figure 4.9. Technologies that can be integrated into a VPP

VPPs with PEVs appear shortly in the literature, but it should be taken into account that the aggregator concept can be considered as a specific VPP for PEVs. Thus, F. Raab et al. present a possible control architecture for VPPs with PEVs [116]. Authors classify control systems into three types: direct, hierarchical and distributed control. They also note that in a VPP, mixed control modules or specific modules can exist for each DG technology. In the latter case, there is a specific module for PEVs group control, associated with that VPP, which authors refer to as EV management module. Besides, the control of a significant amount of PEVs and geographically distributed DGs can be expensive and complex. In [117], the architecture and communications system necessary for a centralized hierarchical control of a VPP with PEVs is discussed.

Authors of [118] have developed an agent-based VPP, composed of wind generation and PEVs in order to address the intermittent character of wind power generation. According to these authors, wind generators may use the available capacity of the PEV batteries to store energy when the electricity price is low and sell part of this energy when the price is high. In the authors' approach, payment for PEVs storage service is provided in the form of charging entitlements rather than money, to take advantage of the price differential between wholesale market and retail market. Two optimization problems are presented: day-ahead optimization with the objective of maximizing VPP profits in the day-ahead electricity market and receding horizon control to cope with changes in scheduled wind power generation during the day of operation. The objective of this last control is to avoid

economic penalties due to deviations in power dispatching. According to the authors, it is economically profitable for wind farms and PEV users to be integrated in a VPP as the proposed one.

Skarvelis-Kazakos et al. propose a centralized optimization method to minimize CO_2 gas emissions of a VPP [115]. The main idea is to apply an environmental dispatch instead of a typical economic dispatch. Thus, partial load CO_2 emission curves of generators are used. In this context, electric vehicles give the flexibility necessary to prioritize the production of electricity from less contaminant generation technologies. Several types of generators have been taken into account, such as wind turbines, PVs, fuel cells, micro-CHPs and even the electric grid. Equation (4-41) presents the objective function to be minimized. Authors use Lagrange multipliers (λ), which are used to incorporate the constraints (C) into the objective function.

$$L = \sum_{t=1}^{T} \left(\sum_{i=1}^{N} F_{i,t}(P_{i,t}) \right) + \lambda \cdot C \qquad (4\text{-}41)$$

where:
- T: total number of time slots
- N: number of generators
- $F_{i,t}$: CO_2 emissions function of i-th generator
- $P_{i,t}$:   active power of i-th generator at time slot t

This optimized algorithm has been applied to a VPP with different distributed generation penetration levels. Authors claim that using this algorithm, a reduction up to 44% of CO_2 emissions can be achieved. However, in order to implement this optimized algorithm, it is necessary to forecast non-PEV load demand and PEVs power demand. The last one can be especially difficult to determine accurately.

4.4.2 Electric microgrids (MG)

The microgrid concept was first introduced in 1998 as a set of micro-generators and electrical storage devices that are able to work isolated from the grid [119]. Subsequently, the Consortium for Electric Reliability Technology Solutions (CERTS) defines a microgrid as a set of loads and micro-generators operating as a single system, which provides both electrical and heat energy [120].

In the European Union, the microgrid concept was developed in the project "MICROGRIDS - Large Scale Integration of Micro-Generation to Low Voltage Grids". In this project, MGs are defined as a low-voltage (LV) distribution system, on a modular basis, where small power generators with electric loads are associated. In addition, electrical MGs may also contain electric storage devices, controllable loads, communication and management devices and cogeneration plants (CHP) [121].

Unlike VPPs, devices that compose an electrical MG are geographically close to each other and can be operated isolated from the rest of the grid. In this way, the security of supply of loads integrated within the MG is increased.

Several authors have analyzed how to integrate PEVs within a MG. In [65] and [102] an architecture for the management of PEVs in a microgrid is described (Figure 4.10). In this

case, the element called microgrid central controller (MGCC) is responsible for the market participation of the microgrid, through the market operator (MO), to operate the microgrid in an optimal way. The vehicle controller (VC), the micro-source controller (MC) and the load controller (LC) are located at the field level. As in the VPP, the control system may be centralized or decentralized.
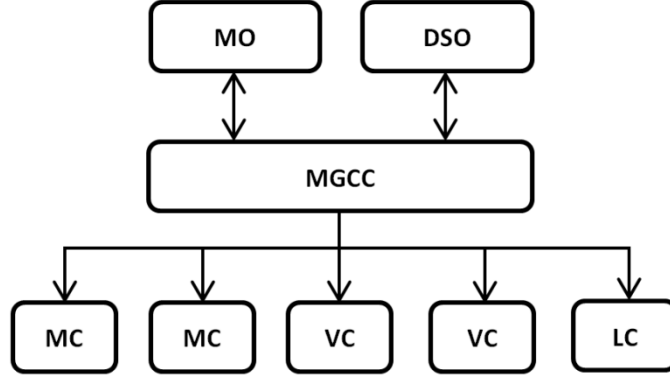
Figure 4.10. Architecture of a microgrid with PEVs

In [122] a centralized control architecture is used to integrate PEVs in MGs. Authors have designed an algorithm, called optimal power set-points calculator (OPSC), to minimize active power variance through the MV/LV substation. The OPSC calculates optimal load profiles for each PEV by using evolutionary particle swarm optimization tool, based on data such as battery technology, behavior of PEV owners, mobility patterns, etc. Equation (4-42) is used as objective function.

$$min\left(\sum_{h=1}^{24}\frac{(P_h - \sum_{h=1}^{24}(P_h)/24)^2}{24}\right) \tag{4-42}$$

where:

− P_h: power generated by DG units and demanded by loads and PEVs

The performance of the proposed algorithm was tested in a 24 node LV distribution network. A small number of PEVs (8 vehicles) were integrated in the network. Six of them were charged through a single-phase EVSE, while three-phase chargers were used in the other two PEVs. According to the authors, the load curve was flattened from uncontrolled charging. No analysis was done about voltage levels in the network. Implementing this algorithm to calculate the set-point of PEVs, with a time horizon of 24 hours, will require to forecast PEVs power demand, micro-generators power production and non-controlled load demand. Thus, load forecasting error will be very significant, especially when the aggregation level is so low. In addition, a resolution time of one hour could be very large.

Two different control approaches have been developed in [123]: a local control approach based on droop control without any communication system and a centralized control to reduce voltage unbalances in the microgrid. Both controls have been developed to work in an islanded microgrid. In addition, V2G is available. In the local control, the measurement of frequency and voltage at PEVs connection points are carried out to define two droop controls. The objective is to reduce frequency and voltage deviations. As commented before, R/X ratio in low voltage networks is high and, therefore, controlling reactive power

supply of PEVs could not be effective enough to limit voltage deviations. Thus, injecting or absorbing active power is more efficient to reduce those voltage deviations. Therefore, authors use both droop controls to define the active power of the corresponding PEV. The priority between the two droop control methods is given to frequency regulation, which is more important to maintain microgrid stability, especially when it works in islanded mode. Moreover, the centralized control, housed in the MGCC, which reduce the voltage unbalances is based on measuring the active power demand of the three phases. Taking into account this data, MGCC calculates in real-time the power set-points of each PEV connected in different phases, in order to reduce phase unbalances of the MG. Both control approaches have proven to be effective to tackle frequency deviations (local control) and voltage unbalances (centralized control). However, these types of control methods should be used only in emergency cases because they will impact on the charging process duration.

Decentralized MAS is also used in [124] to find optimal active power set-points for PEVs, distributed energy resources and loads. In the proposed system, the PEV agent transmits the EVSE capacity, the connection time, the initial and the final SOC to an external agent (called as optimizing agent) which is in charge of minimizing the objective function of equation (4-43). This objective function is partly based on equation (4-42), but adding a new term in order to model the operating cost of distributed generators.

$$min\left(\sum_{h=1}^{24} \frac{(P_h - \sum_{h=1}^{24}(P_h)/24)^2}{24}\right) + \sum_{j=1}^{N} C_j \qquad (4\text{-}43)$$

where:
- P_h: sum of DGs, loads and PEVs power demanded/produced
- N: total number of generators
- C_j: operating cost for the j-th DG

Authors use a meta-heuristic algorithm (AIS) to solve the optimization problem. Once calculation is finished, the optimizing agent sends the optimum set-points to each distributed energy resource, load and PEV. Although authors have described it as a decentralized method, using a single optimization agent converts it to a centralized control architecture more than a decentralized one. That is, all information is sent to the optimization agent, which calculates and returns the set-point of all controllable elements of the MG.

Authors of [125] present a strategy for congestion management in MGs with PEVs. This methodology is based on decentralized MAS architecture. Each agent solves an optimization problem to obtain the power dispatch needed to maximize its profits. After an auction, a power flow and an optimal power flow are carried out to check whether the final situation is technically feasible, regarding to overloaded lines. If not, the demand of the specified nodes will be reduced iteratively for each overloaded line, through changes in PEVs set-points, until congestion problem is cleared. In this case, PEVs are not optimally charged, that is, they are only managed when any line congestion happens.

4.5   PEVs integration projects over the world

Several projects have been developed for the integration of electric vehicles into electrical grids (Table 4.4). These projects focus on three main aspects: the impact on the grid, the

driving and charging behavior of users, and the technical and economic integration of PEVs. Following the most relevant projects are summarized:

- Grids for Vehicles (G4V). Formed by a consortium of 12 European entities, among which there were utilities (RWE, ENEL, EDF, etc.) and research institutions. The consortium aimed to explore the technical problems, the necessary regulation, business models and socio-environmental aspects, to make a set of recommendations for the implementation of PEVs in 2030 [126].

- Mobile Energy Resources in Grids of Electricity (MERGE). European project focused in the management and control concepts, to facilitate the massive integration of PEVs in the electrical grid. The project also explored the possibilities of integrating PEVs in MGs and VPPs and the possible synergies with the smart metering systems [127].

- EDISON Project. Funded by the Danish TSO and focused on integrating PEVs and RES technologies using open standards of Information and Communication Technologies (ICT). The aim of the project was to develop infrastructure that enables PEVs to intelligently communicate with the grid, to determine when charging and discharging can take place. Also, aimed to create a platform for testing and demonstration in the island of Bornholm [87], [128].

- SmartV2G project. European project that aims connecting the electric vehicle to the grid, by enabling controlled flow of energy and power through safe, secure, energy efficient and convenient transfer of electricity and data. Smart charging strategy is accomplished by a control system based on MPC theory, which optimally re-computes charge profiles for all the managed charging post, each time a new recharge starts. It takes into account the current state of the grid, possible demand side management orders received in the charging post central controller by external agents (DSO or TSO) and the PEV users preferences (final cost, charging time) [129].

- Green eMotion. International project to coordinate different ongoing regional and national electromobility initiatives, leveraging on the results and comparing the different technology approaches to promote the best solutions for the European market. It is composed by forty-three partners from industry, universities, research institutions, power supply companies and municipalities that have come together for the purpose of identifying the challenges of Europe-wide emissions-free transportation [27].

- Mobincity (Smart mobility in smart city). Related to integrate PEVs in smart cities, this project searches to define efficient and optimum charging strategies adapted to user and PEV needs and grid conditions [130].

- EV Project. Launched in 2009 as the biggest initiative to introduce PEVs and EVSEs in the United States. This project was funded by the U.S. Department of Energy and several partners, such as Nissan and Chevrolet. The project has recorded a lot of data to characterize the use of PEVs in different regions and climates. The effectiveness of charging infrastructure and possible business models have been evaluated for the implementation of public and commercial EVSEs. Until October 2012, the project had collected driving data corresponding to more than 64 million kilometers and logged more than one million charge events [131].

- Vehicle-to-grid demonstration project. This project aimed to demonstrate the feasibility and practicality of PEVs based grid regulation, and to assess the economic value based on real operating data and real market prices for the service being provided [59].

- NIKOLA project. The aim of this demonstration project is to investigate about the synergies between the electric vehicle and the power system. Using the appropriate control and communication technologies, it is possible to manage the power exchange between the PEV and the electric grid. This way, PEV can provide valuable services to the power system, the PEV owner and the society in general. Nikola project seeks to investigate about these services and the technologies needed to implement them.

Table 4.4. Integration projects of PEVs

Country/Region	Project Name	Project Manager	Duration	State
European Union:	G4V	RWE German utility	18 months	Finished
	MERGE	PCC Greek utility	24 months	Finished
	SmartV2G	ITE Spain R&D center	36 months	Finished
	Mobincity	ITE Spain R&D center	36 months	Finished
	Green eMotion	Siemens	48 months	Finished
Denmark:	EDISON	Danish Energy Association	24 months	Finished
	Nikola project	Technical University of Denmark (DTU)	36 months	Ongoing
United States:	EV project	ECOtality	48 months	Finished
	V2G Demonstration	University of Delaware	Unknown	Finished

4.6 Conclusions

This chapter has presented a review of the current literature about the active integration of PEVs into distribution networks. In general, smart charging algorithms are designed to accomplish two main tasks. On the one hand, smart charging algorithms should reduce system costs or improve system load factor. On the other hand, these smart charging algorithms must keep the distribution network within its operational limits. That is, transformers and lines thermal limits and voltage deviation limits must not be surpassed. Two main methods are used by researchers to implement a smart charging algorithm: heuristic techniques and mathematical programming. Between heuristic methods, droop control is one of the most used. However, droop control methods do not provide optimal results. Thus, most of the proposed smart charging solutions use mathematical programming.

Mathematical programming can be classified as single objective or multi-objective optimization. Single objective optimization only cope with optimizing one variable of the system while multi-objective optimization is used to achieve a trade-off between two or more variables of the system. Thus, in multi-objective optimization, a decision maker entity is necessary to select intelligently which variables are more important.

In order to implement a smart charging method, two types of control architectures can be used: centralized and decentralized. Currently, most of the electric systems are controlled by using a centralized architecture, which is a robust and well-known approach. In this type of architecture, a central controller or aggregator will decide the charging set-point of each PEV under its governance. However, this approach has several drawbacks, such as its poor scalability, privacy issues, complex communication system, etc. An important number of proposed centralized solutions are based on achieving a valley filling effect by minimizing power losses or load variance, but they usually do not deal with economic aspects. It is not

clear what the economic incentives to PEV users will be. Additionally, it is expected that PEV users will not give up the charging control of their vehicles.

Thus, a decentralized architecture control could be more adequate to manage a large number of PEVs. In this approach, users will keep the charging control of their PEVs. However, there are methods to influence indirectly the charging process of the PEVs. One of the most used methods is price signals. In general, PEV users seek to charge their vehicles at less cost as possible. Thus, modifying electricity prices will lead to a modification of the charging profile of the PEVs. Usually, researchers who use signal prices link electricity prices with total energy demand. By minimizing the charging cost of each PEV, a valley filling effect can be achieved while avalanche effect is avoided. But, although it is an interesting approach, linking electricity prices with the energy demand volume or network capacity could lead to significant impact on electricity price formation. Additionally, this operation scheme may lead to electricity price unbalances between different regions of the same electricity market.

Most of the proposed optimized solutions do not address the problem of voltage deviations. Some of them use the power flow tool to know whether there is any voltage violation or congestion issue. But using power flow may not be realistic at LV distribution network level because the lack of information about energy demand at each node and the network model. In this aspect, droop control methods are proposed to reduce voltage deviations and provide primary frequency regulation. However, this control is not optimal and a valley filling effect cannot be achieved using only this method. In addition, some type of coordination or adaptive control is needed to avoid fluctuations due to simultaneous control actions. Furthermore, voltage unbalances generated by the charging of a significant number of PEVs in LV distribution networks is almost not addressed.

Integration of PEVs in MGs or VPPs has been less analyzed in the literature. Many papers about intelligent management of PEVs have been presented but only few of them have considered the integration of PEVs in MGs. Some of them take advantages of PEV battery characteristics to reduce generation costs of distributed generators. Integrating wind energy generation and PEVs in a VPP could be a very interesting option in order to cope with wind energy intermittency. Another possibility is to use PEVs to improve MGs stability, when it is islanded, by using droop control methods.

Finally, active integration of PEVs can be a very complex task. In fact, many of the analyzed papers give solutions to technical or economic problems, omitting other important issues such as voltage deviations, lines and transformers overloading, etc. or vice versa. Thus, it is necessary to address this problem from an overall point of view and generate benefits to all stakeholders. That is, it is desirable to achieve a valley filling effect to reduce energy losses and improve load factor, which is the main interest of utilities and system operators, without forgetting the electricity cost in order to reduce charging cost for PEV users. In addition, the proposed solution must also analyze and address voltage issues to be a more realistic solution.

CHAPTER 5

PROPOSED METHODOLOGY

5.1- INTRODUCTION

5.2 - SIMULATION SETUP

5.3 - GRID TOPOLOGY AND PEVS MODELLING

5.4 - MODEL OF DRIVING AND CHARGING BEHAVIOR

5.5 - UNCONTROLLED CHARGING

5.6 - SMART CHARGING APPROACHES

5.7 - NEW PROPOSED SMART CHARGING METHODOLOGY

5.8 - COMPARATIVE ANALYSIS

5.9 - SYSTEM ARCHITECTURE

5.10 - CONCLUSIONS

5. PROPOSED METHODOLOGY

5.1 Introduction

In chapter 3, the relevance of integrating PEVs adequately in low voltage distribution networks has been discussed. Hence, researchers have been looking for a solution in order to address this complex problem. Throughout chapter 4, the existing solutions have been reviewed. In this context, a new decentralized multi-objective optimization methodology for integration of PEVs in electric distribution networks is presented in this thesis. This methodology has been verified through simulations.

This chapter is organized as follows. In section 5.2 the simulation setup is introduced. Simulations have been carried out using the software DIgSILENT PowerFactory. Control algorithms have been programmed in C++ using Microsoft Visual Basic software and Matlab. Also, IBM ILOG CPLEX Optimization Studio for Matlab has been used to solve the optimization problems. Unbalanced RMS simulations have been performed in PowerFactory while optimization problems have been solved in Matlab, at the same time as simulation is running in PowerFactory. This way, the control system can detect and respond to voltage deviations and re-scheduling the charge of PEVs when it is necessary and without interrupting the simulation process.

The distribution network model is introduced in section 5.3. This model is based on a real LV distribution network of Denmark. Additionally, real consumption data is used. Moreover, as mentioned in chapter 3, the impact that PEVs can have on low voltage electric grids is widely influenced by charging and driving patterns of PEV users. Thus, a new model has been also developed in this thesis (section 5.4) in order to test optimized control algorithms in different scenarios. Real data collected in 2009 NHTS in the United States of America are used to develop this model. Aspects such as type of day, season and type of area are taken into account.

Before introducing smart charging approaches, the consequences of using an uncontrolled charging strategy in the LV distribution network is analyzed in section 5.5. Six different PEVs penetration rates or levels have been considered. The results of the uncontrolled charging have been used as a reference case to know the advantages of the proposed smart charging algorithm. This new smart charging methodology has been designed starting from two already proposed methods, in particular the optimization of charging cost and variance. Thus, these control methods are analyzed more deeply in section 5.6 in order to achieve a better comprehension of the proposed algorithm and its advantages. The achieved solution could be defined as a trade-off between these two control methods. Additionally, the new proposed algorithm is ready for use V2G concept.

The proposed algorithm, which is presented in section 5.7, comprises two versions: one which uses load demand forecasting (MOO-WF) and the other one without using load demand forecasting (MOO-NF). Load forecasting is a powerful tool to improve not only PEVs but also intermittent renewable energy sources integration. However, load forecasting is not a trivial problem and its accuracy is not guaranteed. For this reason, a version of the proposed algorithm without load forecasting is also developed in this thesis. Additionally, a sensitive analysis is also carried out to know the influence of load forecasting error in the MOO-WF algorithm.

Charging PEVs can lead to problems in low voltage distribution networks. Among them, voltage deviations and unbalances are the most likely, so it is necessary to develop a mechanism in order to minimize these voltage deviations. Both approaches reduce voltage deviations indirectly by reducing overall load variance. However, a specific control method (VUR) to reduce voltage unbalances has also been proposed and integrated to MOO-WF and MOO-NF algorithms. Figure 5.1 shows the smart charging approaches and their different versions developed within this thesis. Between parentheses, the section number of each smart charging algorithm is indicated.
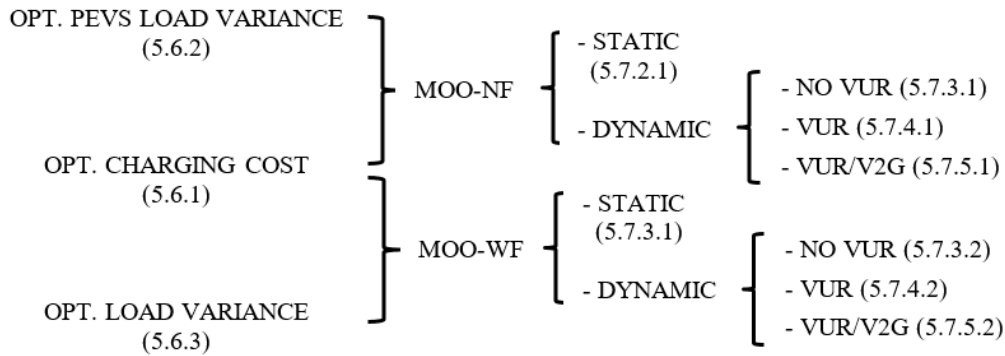
Figure 5.1. Smart charging approaches analyzed and proposed in this thesis

After obtaining all results, a comparative analysis is presented in section 5.8, showing the advantages of the new proposed methodology. Finally, a possible system architecture for implementing the proposed methodology is presented in section 5.9.

5.2   Simulation setup

The DIgSILENT PowerFactory is a powerful tool to simulate and analyze applications in generation, transmission, distribution and industrial systems. Furthermore, this software has the possibility of building new dynamic models through DIgSILENT Simulation Language (DSL) and programing of new scenarios with DIgSILENT Programming Language (DPL). The last one is especially useful to generate, place and model the charging and driving behavior of the PEVs under study.

Although DSL is a good tool to model new controllers and systems, it is very limited when data processing is needed. Fortunately, PowerFactory can work with C++ language, so users can program their own DSL functions in C++. In order to do so, digexfun.dll file has to be modified by the user. This way, data about each PEV can be processed in the C++ program. Additionally, other programs can be executed such as Matlab.

In this thesis, the following method is used. First of all, a DPL script is executed in order to create, place and assign main characteristics of the PEVs, such as: type of PEV, battery capacity, power of the charger, initial SOC, arrive and departure time, final SOC, EVSE power, phase, etc. This script contains the new driving and charging model developed in section 5.4. Second, an unbalanced RMS simulation of 24 hours is performed. In each simulation step, a C++ function is called by every PEV in the grid. This C++ script executes the control algorithm and return the charging set-point to the PEV. This set-point varies from -1 (discharging at full power) to 1 (charging at full power). If set-point is 0, no charging or discharging action will be required to the PEV. C++ program calls to Matlab

API (Application Programming Interface) for solving the mathematical functions (linear, quadratic programming, fuzzy control, etc.) or plotting the final results when it is required. The set-point calculated for each PEV in every time slot is applied to the unbalanced RMS simulation. A scheme of the used simulation setup is shown in Figure 5.2.
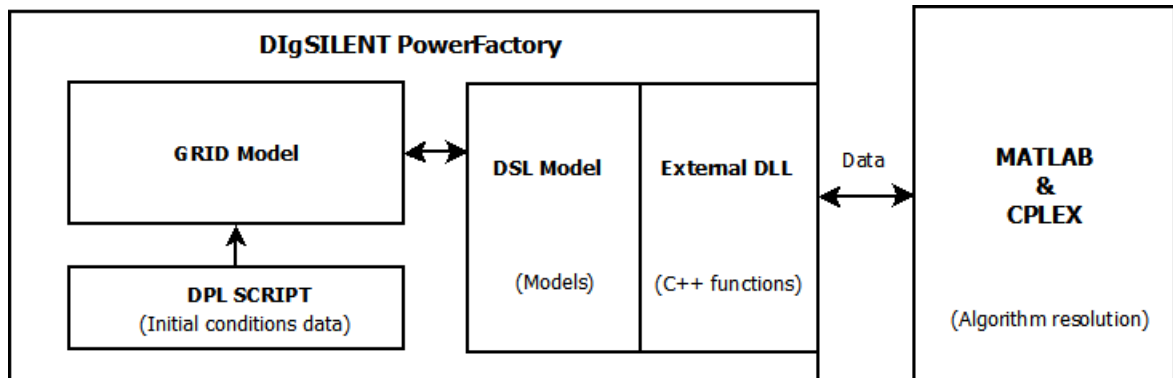
Figure 5.2. Simulation setup

Although Matlab has several tools for solving optimization functions, in this thesis IBM ILOG CPLEX under Matlab API environment has been used, because it provides better results in terms of convergence and calculation time. Finally, results are obtained not only from PowerFactory software but also from the Matlab API.

As mentioned above, simulation time covers 24 hours (starting from 12:00h), in order to represent one full charge event in the grid. For optimized algorithms, PEV set-points resolution time is set to 5 minutes, to limit the computation time of the algorithms.

5.3   Grid topology and PEVs modelling

Algorithms proposed and analyzed in this thesis have been applied to a real Danish low voltage distribution network located in the city of Borup, in the Zealand Island. The distribution network comprises 14 distribution nodes (301 and 601 to 613) and 43 houses. The single phase configuration of the low voltage network is given in Figure 5.3. Part A represents 17 houses located in Hørmarken Street while part B represents 26 households located in Græsmarken Street. There are also street lights connected to the grid in Græsmarken Street at node 608.
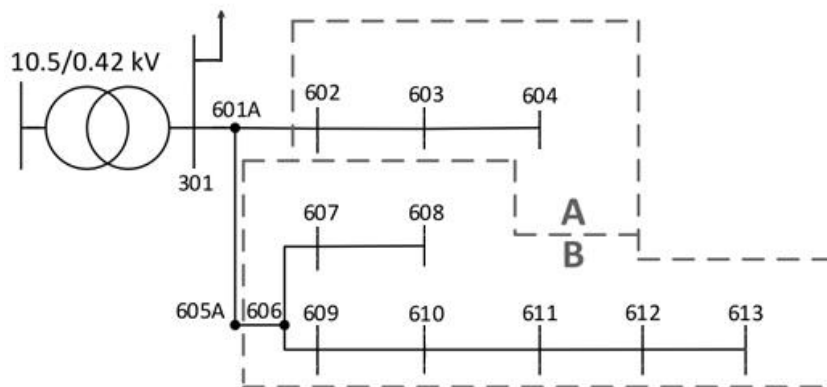
Figure 5.3 Single phase diagram of the modelled distribution network

The 43 households can be divided in two categories due to their different characteristics: (A) residential houses in Hørmarken Street, and (B) residential houses in Græsmarken Street. The first group has lower consumption profile during the winter season as a result of implemented district heating. Furthermore, none of the houses of this group have a PV installation. The second group covers households with PV installations, as well as with heat pumps and consequently it presents higher consumption during winter season. A detailed map of the distribution network location is presented in Figure 5.4 while an aerial view of the zone is presented in Figure 5.5.
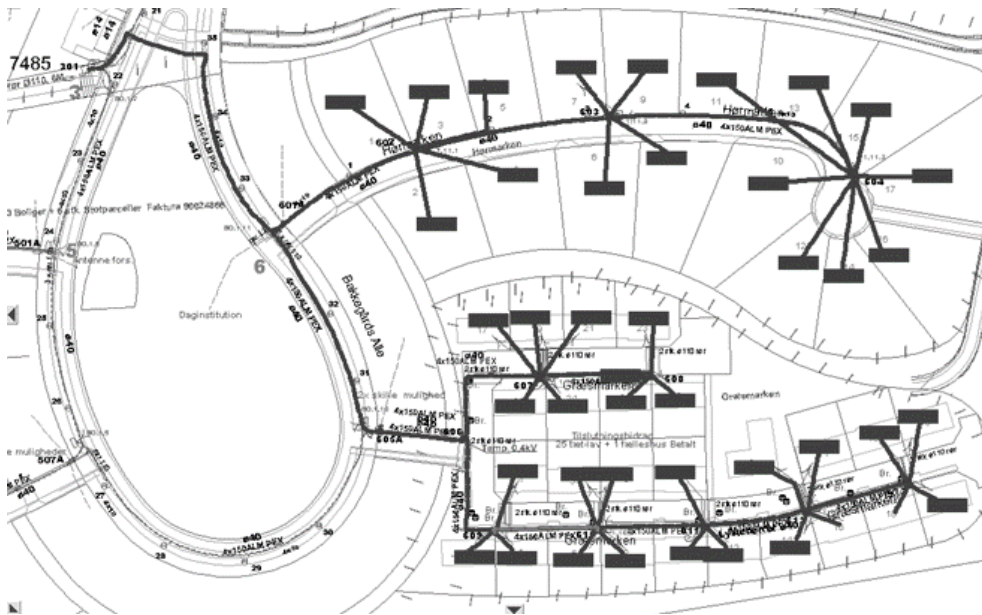
Figure 5.4 GIS map of the part of Borup distribution network used in this thesis

Figure 5.5 Satellite overview of the part of Borup town, where the distribution network used in this thesis is located

The distribution network is fed by an Alstom DCU 3631 H distribution transformer which characteristics are the following: 0.4MVA of nominal power, 10.5/0.42kV of nominal voltage, 50Hz and Dyn11 connection group. The secondary star point winding of the transformer has been directly connected to the ground. Short circuit power of external grid is 10MVA and the voltage set-point of the grid is 1 p.u.

The low voltage feeder bifurcates into three feeders, matching with physical streets where the households are located, and it runs in radial configuration. The line consists of 14 nodes and 13 line segments, with a total length of 681 meters. All segments between the distribution nodes are the same type of 4x150mm^2 aluminium PEX conductor, with R=0.207 Ω/km and X=0.073 Ω/km. The lengths of the lines and loads distribution are shown in Table 5.1.

Table 5.1. Distance between distribution nodes and loads distribution

From	To	Length (m)		Node	Loads
301	601	112		301	Rest of houses
601	602	49		602	Hørmarken 01 to 05
601	605	80		603	Hørmarken 06 to 09
602	603	64		604	Hørmarken 10 to 17
603	604	87		605	Empty
605	606	25		606	Empty
606	607	46		607	Græsmarken 17, 19, 21, 22 and 24
606	609	40		608	Græsmarken 23, 26, 28 and street lights
607	608	37		609	Græsmarken 01, 02 and 04
609	610	35		610	Græsmarken 03, 05 and 08
610	611	36		611	Græsmarken 07, 10 and 12
611	612	35		612	Græsmarken 09, 11, 14 and 16
612	613	35		613	Græsmarken 13, 15, 18 and 20

Additionally, there are other three feeders with the rest of houses (~130) under the same distribution transformer. However, only aggregated data for these feeders are available. Thus, they have not been considered to hold electric vehicles.

PV installations are mostly located in Græsmarken (only one located in Hørmarken) and all of them are connected through single-phase inverters. The modelled network contains 27 PV installations: 24 installations with a peak power of 2.96 kWp and 3 upgraded installations with a peak power of 4.07 kWp, which are connected through 3.6 kWp and 5.4 kWp inverters, respectively. The number of PVs connected to a particular phase is not known, so the installations have been connected randomly taking into consideration that the overall production on each phase should be approximately the same. The PV production has been measured separately for every house on an hourly basis along with the consumption data.

The node 613 is located at the furthest point from distribution transformer (398 meters) and, normally, it has the lowest voltage of the network. So, this node 613 has been selected as the worst case node in order to know the impact that the charging algorithms will have on voltage deviations in the grid.

Consumption profiles are based on real metering data read on hourly basis through a period of one year (from March 2012 until March 2013). However, measured power flows correspond to all phases. That is, there is no disaggregated information of individual phase consumption. Therefore, it is assumed that the household loads are equally distributed and

symmetrically balanced between the phases. Additionally, the lack of unbalances generated by the household loads will ease the analysis of unbalances produced by PEVs. With regard to reactive power, there is no data available for the reactive power component, so the minimum required power factor has been taken as the reference value for all households (cos φ = 0.95).

A typical winter day has been selected, with high energy consumption and almost no PV production. As commented before, simulations have been carried out from 12:00h to 12:00h of the next day. Thus, partial data of two days are necessary. In this case, the days 14th and 15th of January were selected (Monday and Tuesday). Figure 5.6 shows the load demand at the transformer level and the voltage profile at node 613, for the observed period. The maximum peak power during this period is 206kW while total energy demand of households is 3.04MWh. Line-neutral voltages at node 613 reaches a minimum value of 0.946 p.u.

(a)   (b)
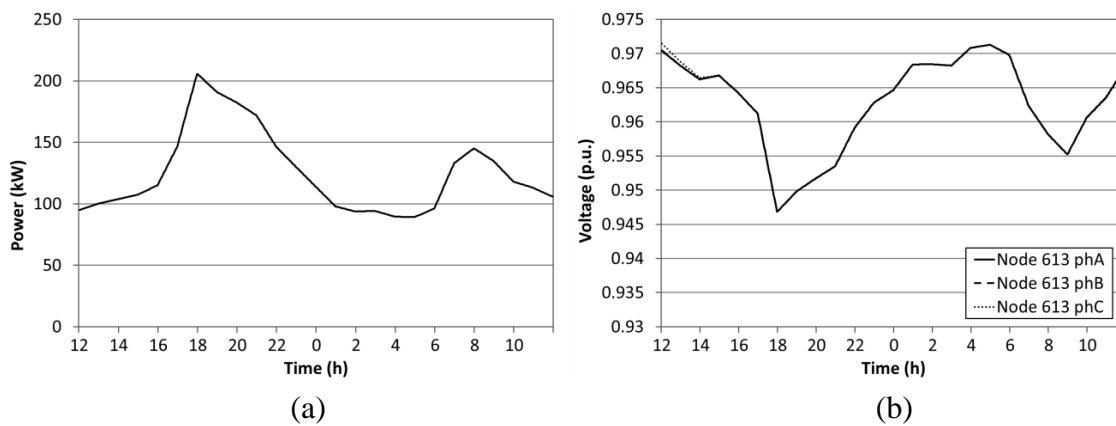
Figure 5.6. No PEVs case: (a) Distribution transformer load and (b) line-neutral voltages at node 613

Finally, PEVs are modelled in PowerFactory as static generators (ElmGenstat), working as current sources (Figure 5.7). The power set-point is controlled by the d-axis and q-axis current reference, being both in p.u. Li-ion batteries are charged using a CC/CV profile. However, in this thesis, this charging profile is not considered because power demand of a battery pack not only depends on the battery characteristics and CC/CV profile but also on temperature, battery degradation, balancing processes, etc. Rather than modelling this complex process, the worst case scenario for LV distribution networks is used. Thus, electric vehicles have been considered as constant power loads which is considered the worst case scenario [132]. Constant power loads have specific consequences for distribution networks. When voltage decreases, demanded current of constant loads increases, to maintain the power demand constant, leading an additional voltage drop. Thus, constant power loads have more harmful effects, in terms of voltage drops, than any other load model. Moreover, the SOC of PEV batteries is calculated using the integral of the absorbed energy. Efficiency of the charging process is also taken into account. Besides, this efficiency has been considered constant in all power range of the charger.

As mentioned in subsection 4.3.2, reactive power control can be used for reducing voltage deviations but, in low voltage networks, the X/R ratio is low. Thus, voltage drops mainly depend on active power flow [84]. In contrast to active power control, reactive power control could not be efficient enough to deal with voltage drops. Furthermore, reactive power control can increase power losses. Taking into account this aspect, in this thesis,

reactive power control of PEVs has not been considered. That is, q axis reference has been set to 0 in all study cases. However, it should be pointed out that implementing a reactive power control to complement an active power control might be interesting.
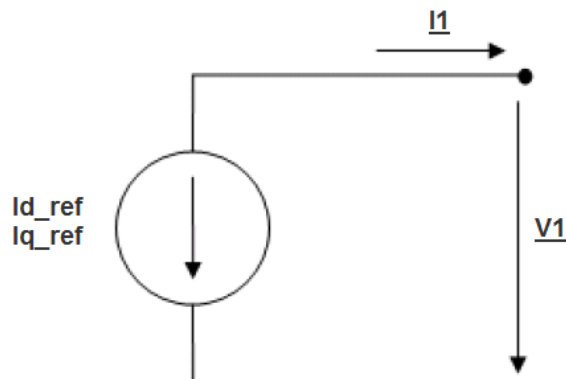
Figure 5.7. Model of the current source for PEV characterization

With regard to PEV models, the most three sold PEVs have been considered in this thesis: Chevrolet Volt, Nissan Leaf and Tesla S. Table 5.2 provides the main characteristics of these PEVs and the probability of occurrence in the model, which has been calculated taken into account market sales of each PEV [133]. Charger efficiency has been set according to report [134]. Similar efficiency values are obtained in [135].

Table 5.2. Characteristics of used PEVs

	Type	Battery Cap. (kWh)	Range (km)	Fuel Economy (Wh/km)	Charger Efficiency (%)	Charge P. (kW)	Probability (%)
Nissan Leaf	BEV	24	121	212	86.4	3.7 (1 phase)	53
Chevrolet Volt	PHEV	10.3*	610**	239***	83.7	3.7 (1 phase)	27
Tesla S	BEV	60	335	237	86.4	11 (3 phase)	20

*Usable battery capacity   ** Total extended range   *** Electric consumption in extended mode

5.4 Model of driving and charging behavior

Social patterns have a significant influence when a smart charging algorithm is tested in a specific distribution grid. Thus, some aspects have to be modelled in order to reduce errors as much as possible. Modelling social patterns of drivers can be a difficult task, especially if few data are available. The report 2009 NHTS from the U.S. Department of Transportation provides a huge amount of data about social patterns of ICEV drivers, which can be accessed publicly. However, no data are included about PEVs. So, some assumptions have to be made until specific data about PEV drivers are available.

Raw data provided by 2009 NHTS is divided in four Excel files: HHV2PUB.xls contains information on households; PERV2PUB.xls provides data on people; VEHV2PUB.xls contains information on household' vehicles and, finally, DAYV2PUB.xls provides information on trips done. Table 5.3 shows the main characteristics of these files.

Table 5.3. Data provided in the 2009 NHTS

Document	Number of items	Number of variables
HHV2PUB.xls	150,147 houses	42
PERV2PUB.xls	308,901 people	116
VEHV2PUB.xls	309,163 vehicles	61
DAYV2PUB.xls	1,048,572 trips	112

The amount of data has been reduced by eliminating those that do not have interest for this analysis, as trips made by public transport or other means of transport. This way, only trips done by private cars have been taken into account. In order to do so, variable TRPTRANS has to be 1. Thus, trip data have been reduced to 537,022. Table 5.4 shows the list of variables used in this analysis.

Table 5.4. Description of variables used

Variable	Description
DWELTIME	Calculated time at destination
ENDTIME	End time of the trip
HHVEHCNT	Count of household vehicles
STRTTIME	Start time of the trip
TDWKND	Trip on weekend
TDAYDATE	Date of travel day
TDTRPNUM	Travel day trip number
TRPMILES	Calculated trip distance in miles
TRPTRANS	Transportation mode used on trip
TRVLCMIN	Calculated travel time
URBRUR	Household is in rural or urban area
VEHID	Vehicle number used for trip

Starting from a specific grid with a number of households, the number of vehicles per house has to be determined. Two categories are distinguished, rural and urban households. This information is obtained through two columns in the HHV2PUB.xls file (HHVEHCNT and URBRUR). Distributions obtained are shown in Figure 5.8.
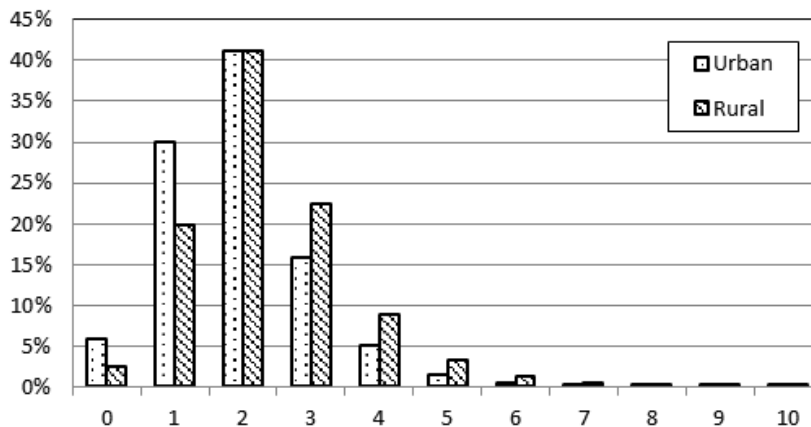
Figure 5.8. Distribution of number of vehicles per house

In the urban case, there is an average of 1.93 vehicles per household with a variance of 1.22. In contrast, in rural areas there is an average of 2.35 vehicles per household with a variance of 1.55.

Departure and arrive time are analyzed for eight cases, depending on time of year and the type of day, i.e. weekday or weekend day. In this case, data of the DAYV2PUB.xls file are analyzed and specifically STRTTIME, ENDTIME, TDWKND, TDAYDATE and TDTRPNUM variables are used. For departure time distributions, only first trip of day has been taken into account while for arrive time only last trip of day.

In Figure 5.9 to Figure 5.12 the departure and arrive time distributions are represented. All these distributions are fitted to Generalized Extreme Value (GEV) distributions because of their good fit with analyzed data. Table 5.5 shows the main parameters of these distributions.
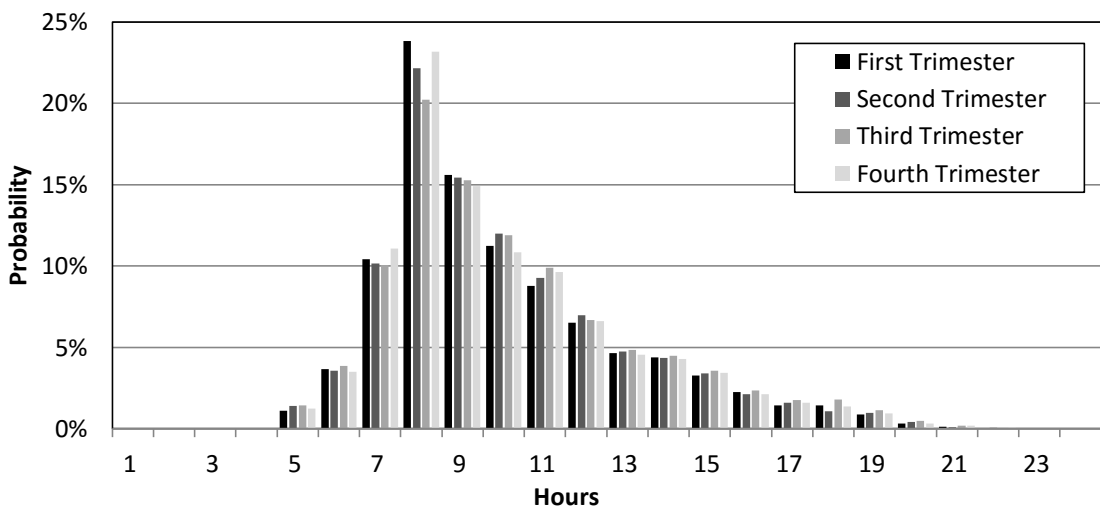
Figure 5.9. Distribution of departure time in weekdays
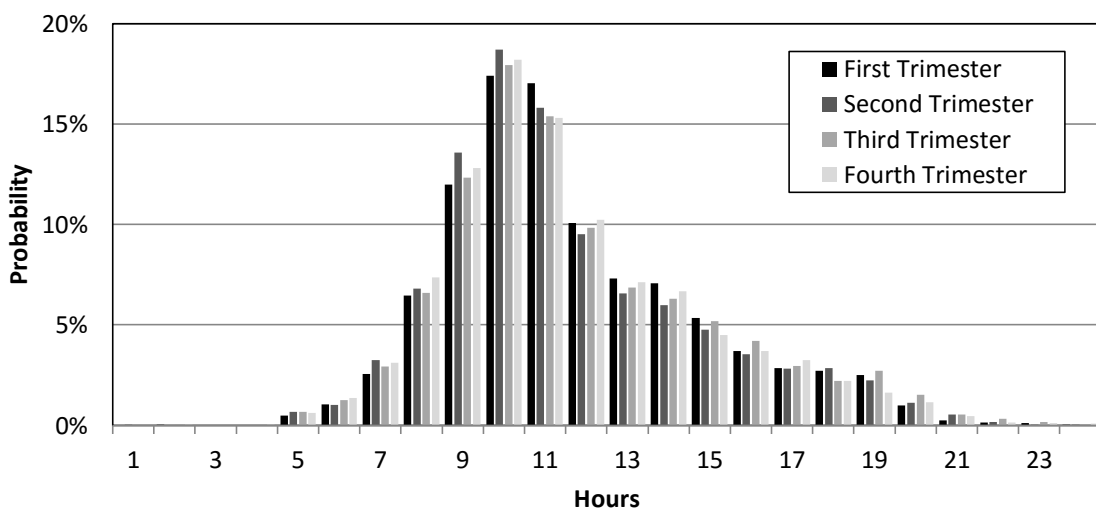
Figure 5.10. Distribution of departure time in weekend days
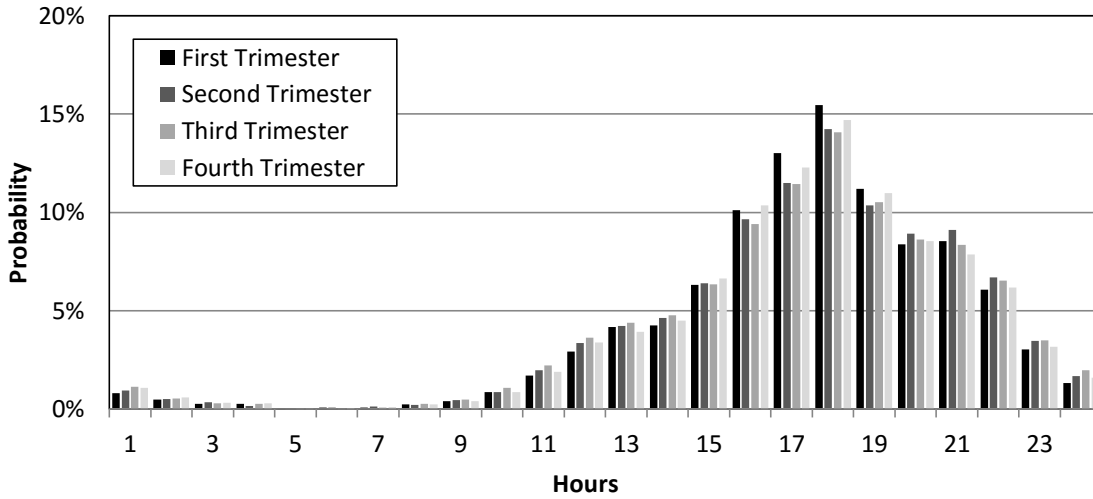
Figure 5.11. Distribution of arrive time in weekdays
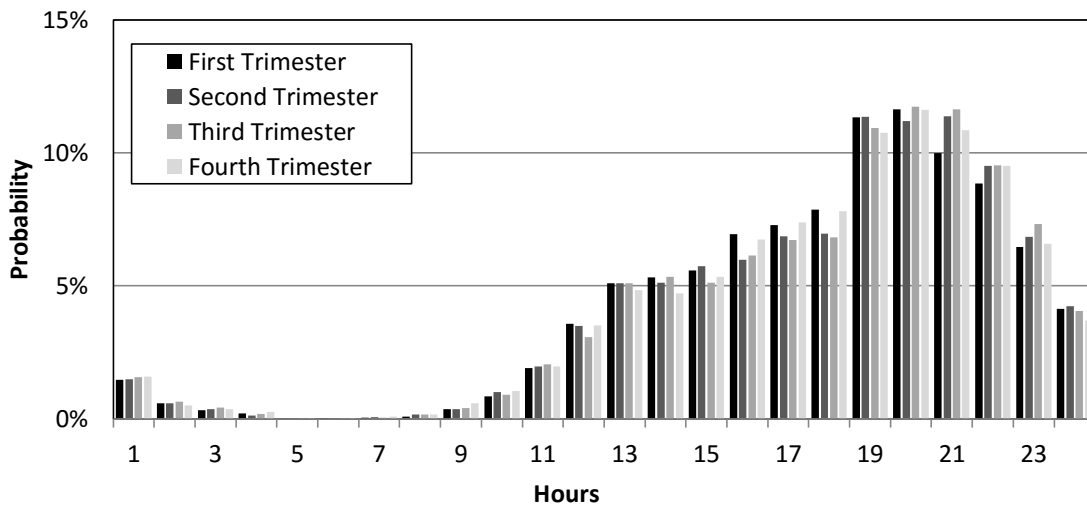
Figure 5.12. Distribution of arrive time in weekend days

Table 5.5. Departure and arrive time distributions (in minutes)

	Departure time		Arrive time	
	Weekday	Weekend day	Weekday	Weekend day
1st Trimester	μ = 481.66 σ = 126.83 ξ = 0.07216	μ = 586.9 σ = 153.93 ξ = -0.06192	μ = 953.88 σ = 240.14 ξ = -0.4962	μ = 989.48 σ = 282.96 ξ = -0.6292
2nd Trimester	μ = 485.34 σ = 131.46 ξ = 0.045	μ = 576.03 σ = 156.24 ξ = -0.05644	μ = 953.72 σ = 251.07 ξ = -0.5163	μ = 995.59 σ = 284.93 ξ = -0.6414
3rd Trimester	μ = 489.61 σ = 136.82 ξ = 0.05572	μ = 583.88 σ = 161.67 ξ = -0.05694	μ = 947.14 σ = 258.64 ξ = -0.5246	μ = 997.77 σ = 288 ξ = -0.6524
4th Trimester	μ = 483.66 σ = 132.1 ξ = 0.04543	μ = 574.65 σ = 153.76 ξ = -0.05118	μ = 945.78 σ = 252.78 ξ = -0.5106	μ = 988.83 σ = 285.3 ξ =-0.6347

These distributions refer on how many kilometers are done when travel duration is known. In order to do so, all day trips of one vehicle have to be combined in a single day trip. Additionally to previous variables, four new variables are used: VEHID, DWELTIME,

TRPMILES and TRVLCMIN. Duration of travel does not only refer to driving time but also to time at destination (working, shopping, etc.). Figure 5.13 and Figure 5.14 show the distribution of distance travelled in function of travel duration for weekdays and weekend days.
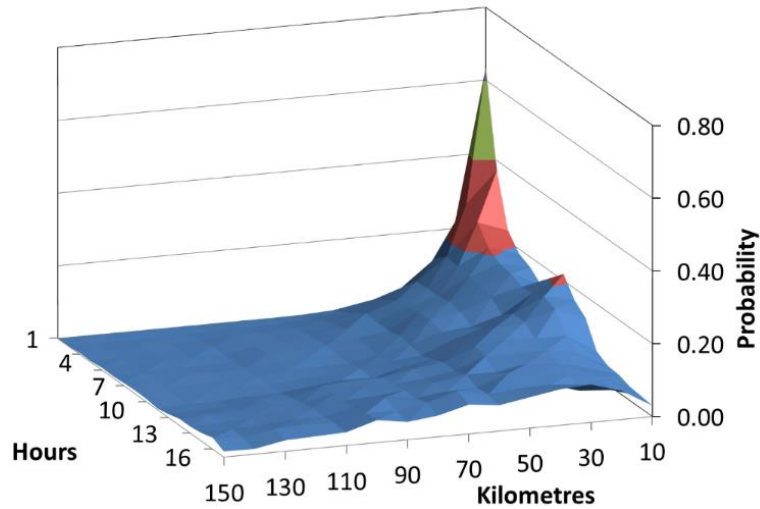
Figure 5.13. Distribution of distance travelled in function of travel time for weekdays
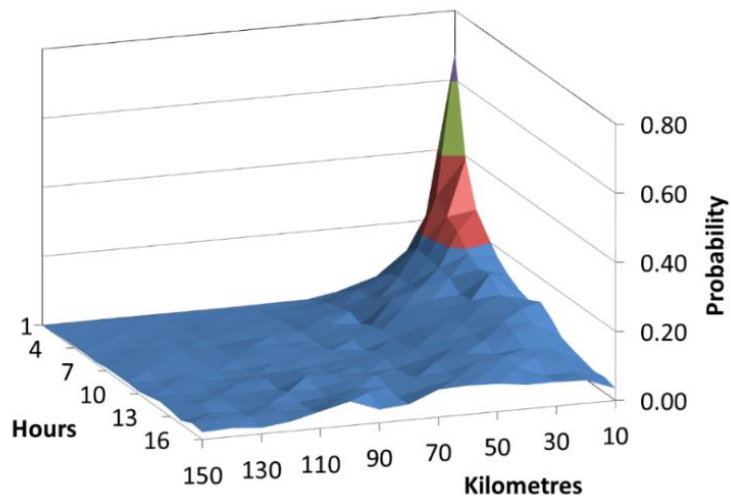
Figure 5.14. Distribution of distance travelled in function of travel time for weekend days

5.4.1 Proposed algorithm to model driving and charging behavior

In order to develop an algorithm to define driving and charging patterns, some assumptions have to be done due to lack of data. First of them, driving behavior of PEV owners has been considered similar to ICEV owners. That is, daily travel patterns will not change with the use of PEVs. Surely, this aspect will not be totally true because of the PEV autonomy limits. It is expected that for short daily distances, model error will be negligible. Instead, error may be larger for long daily distances. In fact, calculated daily distance can be larger than its respective PEV autonomy. In these cases, daily distance has to be recalculated. Respect to departure and arrive time, it is expected that there will be no difference between ICEV and PEV drivers.

Second assumption is that all vehicles are connected to the grid when users arrive at home and disconnected only when the first trip of day starts. This assumption is considered because no data about when drivers charge their PEVs are available. The last assumption is that PEVs will be charged once per day (after last trip of day). Again, this last assumption is taken because of lack of data. However, the study developed in [136] indicates that, on average, PEV drivers will charge their vehicles once per day.

The algorithm proposed in Figure 5.15 works as follow: from grid data, the number of houses in the grid is known and also the type of area (rural or urban). Number of vehicles is obtained according to distribution in Figure 5.8. Then, penetration rate of PEVs in the grid and time data (time of year and type of day) have to be provided. These data can be considered as variables, in order to know smart charging algorithm ability to control PEVs under different scenarios. With the PEVs penetration rate value, the number of PEVs is obtained (variable N).
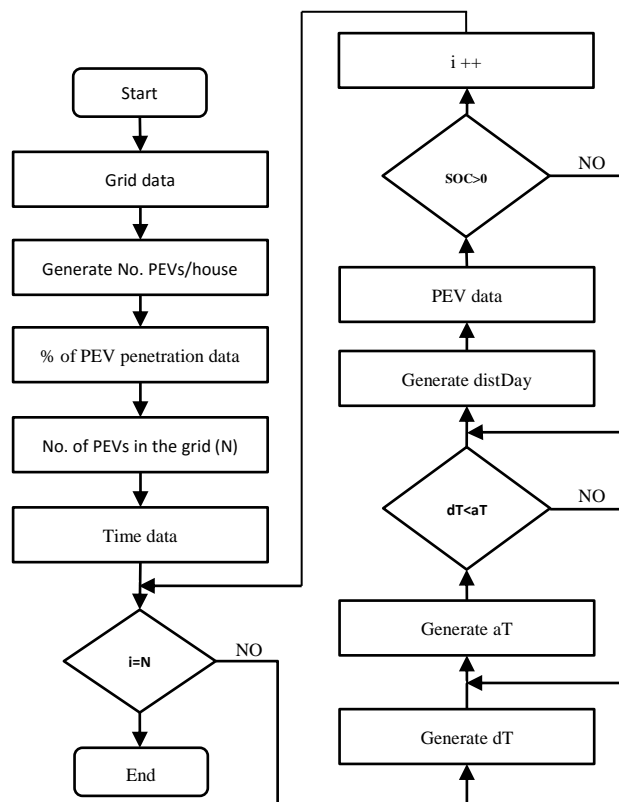
Figure 5.15. Flow chart of the proposed algorithm

Once the number of PEVs is calculated, departure time (*dT*) and arrive time (*aT*) are generated for each PEV. One technique to generate random numbers, according to a given distribution, is using the inverse of cumulative distribution function (CDF) or quantile function.

Quantile function is calculated inverting the CDF function. Then, probability *y* has to be generated randomly, according to the uniform distribution. Finally, value *x* is computed using the calculated distribution parameters and the generated probability value. As mentioned previously, departure and arrive time have been fitted to GEV distributions,

which inverse CDF is presented in equation (5-1). GEV distributions parameters can be found in Table 5.5.

$$x = f(y|\mu, \sigma, \xi) = \mu + \sigma \cdot \left\{ \frac{[-ln(y)]^{-\xi} - 1}{\xi} \right\} \quad \begin{cases} y \in [0,1] \\ \mu \in \mathbb{R} \\ \sigma > 0 \\ \xi \in \mathbb{R} \end{cases} \quad (5\text{-}1)$$

where:

- μ: location of the GEV distribution function
- σ: scale of the GEV distribution function
- ξ: shape of the GEV distribution function
- y: probability

Inverse CDF of GEV distribution and departure time data in weekdays, for the first trimester, are presented in Figure 5.16, showing a very good fit.
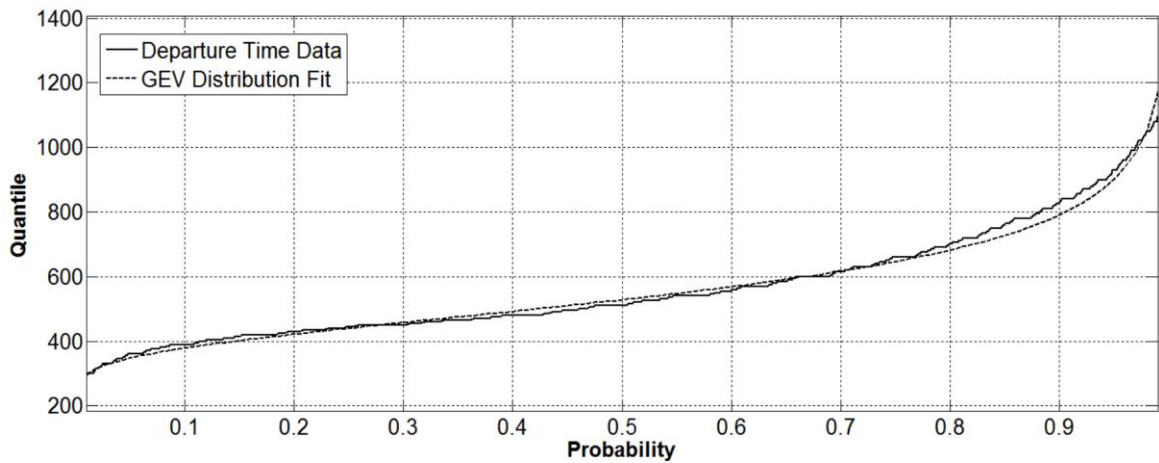
Figure 5.16. Inverse CDF of GEV distribution fitted to departure time data

If generated departure time is less than arrive time, then travel duration is calculated (*aT-dT*). If not, arrive time is re-calculated until the above condition is fulfilled. Knowing travel duration, distance travelled during the day (distDay) is generated in a similar way than departure and arrive time. In this case, inverse CDF of Weibull distribution is used, as shown in equation (5-2).

$$x = f(y|k, \lambda) = \lambda \cdot \sqrt[k]{-ln(1 - y)} \quad \begin{cases} y \in [0,1] \\ k > 0 \\ \lambda > 0 \end{cases} \quad (5\text{-}2)$$

where:

- λ: scale of the Weibull distribution function
- k: shape of the Weibull distribution function

Weibull distributions parameters have been obtained from Inverse CDF of Weibull distribution. Figure 5.17 shows the distribution of distance travelled of trips which duration is less than an hour.
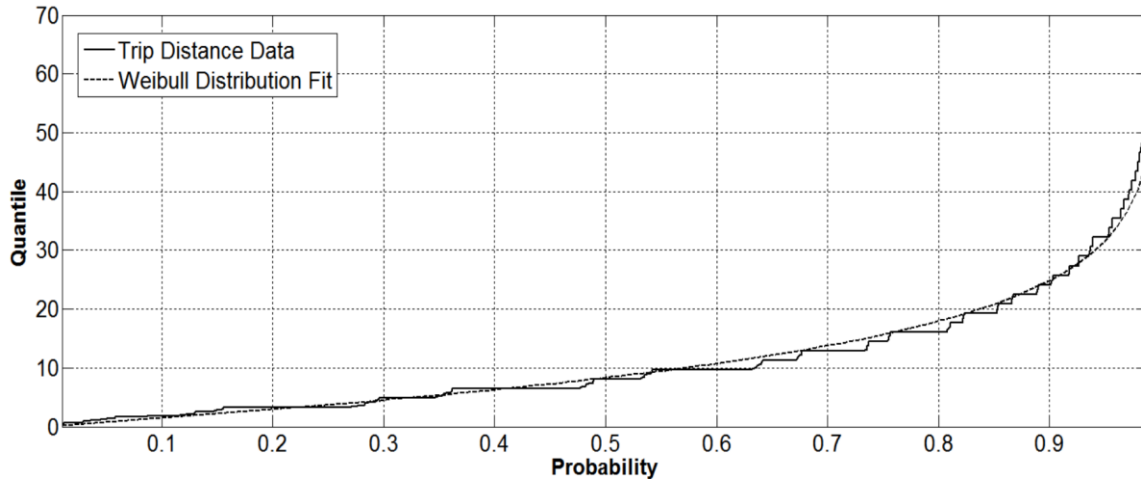
Figure 5.17. Inverse CDF of Weibull distribution fitted to trip distance data

After distance travelled is generated, PEV data have to be added, especially charging power, charger efficiency, energy consumption per kilometer and battery capacity. With distance travelled and PEV data, the initial SOC of the battery is calculated. If this initial SOC is less than zero, in other words, if distance travelled is greater than PEV autonomy, "distDay" parameter has to be recalculated until the initial SOC value is greater than zero. Finally, the last step of the algorithm is to check whether all PEVs have been modelled ($i=N$).

5.4.2   Simulation results

The algorithm proposed has been implemented in DIgSILENT PowerFactory software in order to validate its adequacy. This algorithm has been applied to the distribution network and PEV models presented in section 5.3.

In order to validate the proposed driving and charging model, unbalanced RMS simulations have been carried out for 24 hours, starting from 12:00h to 12:00h of the next day. This period of time has been selected because, in general, home charging will be carried out mostly at night. Following, the results obtained for 4 different cases are presented.

Case 1: Comparing different PEV penetration rates

In this first case, different PEV penetration rates are compared (10, 30, 50, 70, 90 and 100%). Simulation is performed as a rural distribution grid, while a workday of the first trimester is selected as day type.

Mean results obtained from the simulations are presented in Table 5.6. Maximum charge demand usually occurs around 21:00h. PEVs power demand along simulation time for 10, 30, 50 and 70% of PEV-PRs are presented in Figure 5.18.
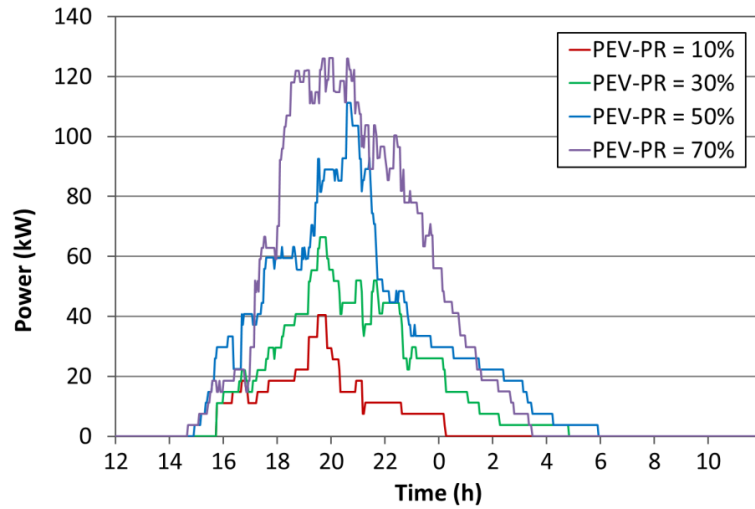
Figure 5.18. PEVs power demand for 10, 30, 50 and 70%

Table 5.6. Mean results obtained from case 1

PEV-PR	No. PEVs	km/PEV	Connection time	Max. demand	Energy demand	Time at Max. Demand
10%	10	45.3	12.5 h	40 kW	0.138 MWh	20:00 h
30%	29	43.3	12.13 h	66 kW	0.337 MWh	20:00 h
50%	53	42	12.88 h	111 kW	0.584 MWh	21:00 h
70%	72	41.4	12.83 h	126 kW	0.788 MWh	21:00 h
90%	93	40.7	12.59 h	182 kW	1.01 MWh	21:00 h
100%	97	41.1	12.54 h	190 kW	1.06 MWh	21:00 h

Case 2: Comparing rural or urban grids

In general, there are more vehicles in rural houses compared to urban ones. This is due to the greater availability of public transport facilities in cities and, therefore, private cars are less necessary. The simulation results show this difference, considering the same level of PEV-PR (50%). Specifically, there are 13 more PEVs in the rural case than in the urban case (Table 5.7). As a consequence, energy demand of PEVs will be greater in rural areas than in urban areas. PEVs power demand profile obtained from the simulation is presented in Figure 5.19.
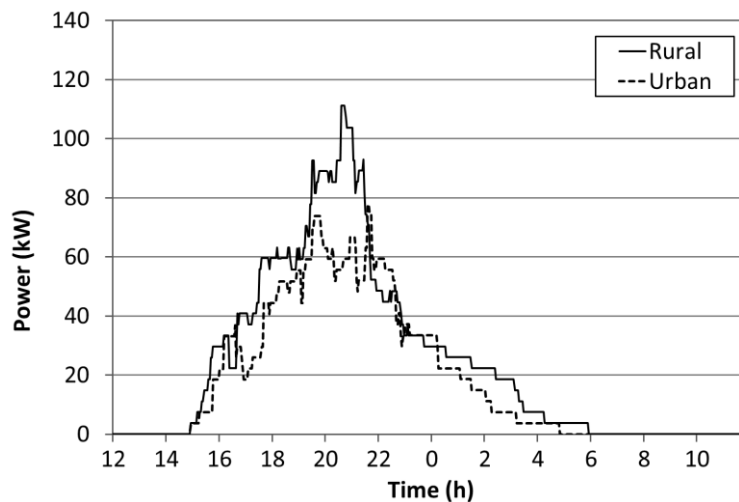
Figure 5.19. PEVs power demand profile in case 2

Table 5.7. Mean results obtained from simulation case 2

	No. PEVs	km/PEV	Connection time	Max. demand	Energy demand	Time at Max. Demand
Rural area	53	42	12.88 h	111 kW	0.584 MWh	21:00 h
Urban area	40	42	12.27 h	78 kW	0.454 MWh	21:00 h

Case 3: Comparing weekdays and weekend days

In weekdays PEVs tend to be charged at mid of the afternoon, while in weekend days this happens later because the mean value of departure and arrive times are higher, as shown in Table 5.5. Moreover, mean distance travelled in weekdays is less than in weekend days. As a consequence, PEVs energy demand is often greater at weekend days. In this case, PEV-PR has been set to 50% in a rural grid. Results of case 3 are presented in Figure 5.20 and Table 5.8.
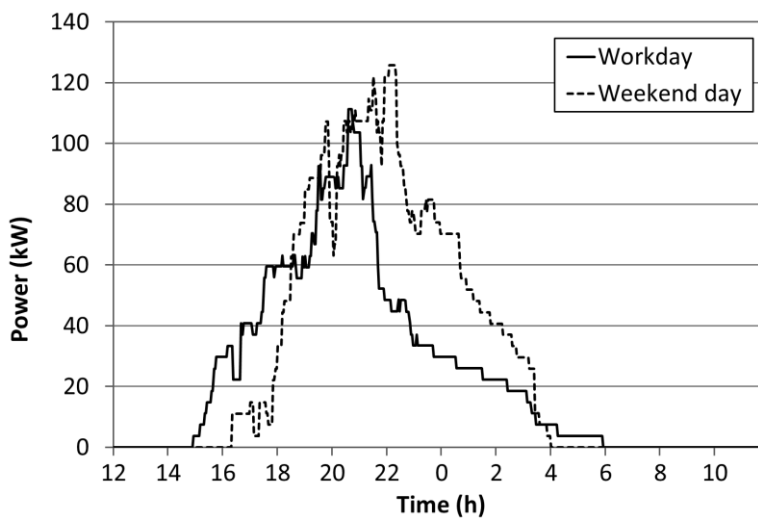
Figure 5.20. PEVs power demand in case 3

Table 5.8. Mean results obtained from simulation case 3

	No. PEVs	km/PEV	Connection time	Max. demand	Energy demand	Time at Max. Demand
Weekday	53	42	12.88 h	111 kW	0.584 MWh	21:00 h
Weekend day	53	53.6	12.7 h	126 kW	0.725 MWh	22:00 h

Case 4: Comparing different time of year

In this case, the effect of different season of year in PEVs power demand is analyzed. As in the previous case, penetration rate has been set to 50% in a rural grid. Also, type of day has been set as weekday.

Few variations can be observed in Figure 5.21, between the different seasons, in agreement with the calculated parameters of distributions (Table 5.5). According to this analysis, season of year has little effect on driving behavior. Only in the summer season, an increase of standard deviation can be observed. However, it must be pointed out that in winter or cold weather, electric vehicles tend to spend more energy because of the use of heater and other auxiliary equipment. This effect has not been taken into account in this algorithm as

no data is available. Table 5.9 presents the mean results collected from the performed simulations.
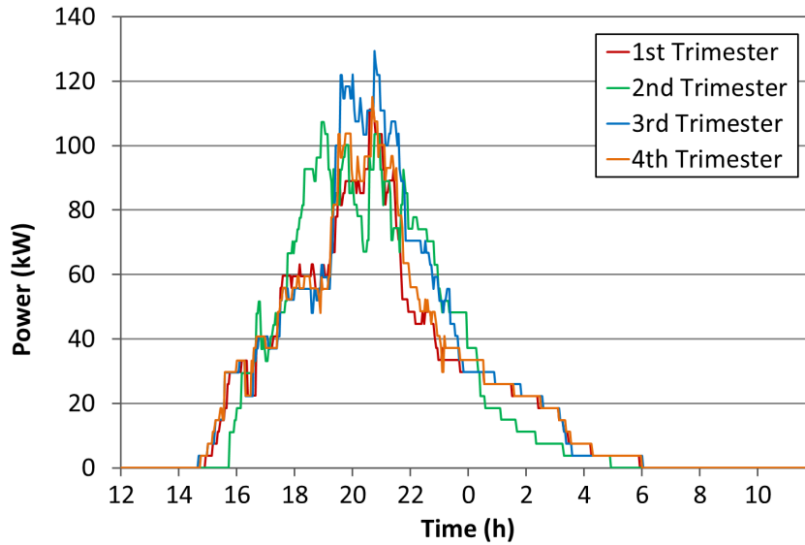
Figure 5.21. PEVs power demand profile in case 4

Table 5.9. Mean results obtained from simulation case 4

	No. PEVs	km/PEV	Connetion time	Max. demand	Energy demand	Time at Max. Demand
1st Trimester	53	42	12.88 h	111 kW	0.584 MWh	21:00 h
2nd Trimester	53	43.7	12.4 h	107 kW	0.625 MWh	19:00 h
3rd Trimester	53	47	12.8 h	129 kW	0.668 MWh	21:00 h
4th Trimester	53	43.8	12.9 h	115 kW	0.613 MWh	21:00 h

Once driving and charging patterns are modelled, in the following subsections uncontrolled and smart charging approaches are presented.

5.5 Uncontrolled charging

Grid architecture and driving and charging patterns have been introduced in previous sections. Before introducing smart charging approaches, uncontrolled charging is analyzed so as to take it as the reference case. This way, improvements achieved with the different smart charging approaches can be quantified. In an uncontrolled charging scenario, PEVs will be charged as soon as they arrive home from the last trip of the day. Charging power is set to the maximum allowed by the specified PEV (3.7kW for Leaf and Volt and 11kW for Tesla S).

PEVs have been randomly distributed along the nodes and phases and they are charged until one of these conditions become true: final SOC is fulfilled or departure time is reached. In this research work, final SOC is set to 1, i.e. 100%. Because of this random distribution and taking into account that most of PEVs are charged using a single-phase charger, different energy demand per phase and voltage unbalances will be generated. Table 5.10 shows the number, model distribution and the energy demand per phase for the different PEV-PR cases. As mentioned before, PEVs load demand per phase is randomly distributed, giving different unbalance levels.

Table 5.10. Data about the different PEV-PR cases and energy demand of PEVs

PEV-PR	Number of PEVs	Model distribution	PEVs energy demand (MWh)	Energy demand per phase (kWh)	Load per phase (%)
10%	11	Leaf: 5 Volt: 3 Tesla: 3	0.138	Phase A: 37 Phase B: 67 Phase C: 34	Phase A: 27 Phase B: 49 Phase C: 24
30%	29	Leaf: 14 Volt: 11 Tesla: 4	0.337	Phase A: 109 Phase B: 148 Phase C: 80	Phase A: 32 Phase B: 44 Phase C: 24
50%	52	Leaf: 25 Volt: 21 Tesla:6	0.584	Phase A: 250 Phase B: 202 Phase C: 132	Phase A: 45 Phase B: 35 Phase C: 23
70%	72	Leaf: 43 Volt: 16 Tesla: 13	0.788	Phase A: 204 Phase B: 285 Phase C: 300	Phase A: 26 Phase B: 36 Phase C: 38
90%	93	Leaf: 48 Volt: 33 Tesla: 12	1.01	Phase A: 356 Phase B: 335 Phase C: 318	Phase A: 35 Phase B: 33 Phase C: 31
100%	97	Leaf: 50 Volt: 34 Tesla: 13	1.06	Phase A: 397 Phase B: 342 Phase C: 322	Phase A: 37 Phase B: 32 Phase C: 30

Some aspects must be taken into account before presenting simulation results of the different approaches:

- European Standard EN50160 has been taken as a reference to define the acceptable range of RMS of the supply voltage. The standard indicates that line to neutral or line to line voltage should be within ±10% of nominal voltage for 95% of time of a week. As simulations are performed for 24h, line-neutral RMS voltage should not be out of the ±10% of the nominal voltage for more than 72 minutes.

- Charging and discharging efficiency of the charger is considered to be equal and constant along all power range of the charger. Additionally, the charger of the PEVs must allow different charging rates and V2G, if this concept is used.

- The IEC 61851 which defines that the charging rate must be semi-continuous, that is, the charging rate can be either zero or within a range defined by a minimum (different from zero) and a maximum charging power. This statement has not been considered for simplification purposes. This assumption will not have noticeably impact on the overall results. The analyzed algorithms will schedule PEVs in such a way that final results will not be affected. This fact is especially true as the number of PEVs connected to the network increases.

- Driving and charging patterns have been set to workday, winter and rural area, in order to facilitate the comparison between the different solutions. Only PEV-PR is modified. Simulations have been performed for six different PEV-PR (10, 30, 50, 70, 90 and 100%), which have been already presented in case 1 of section 5.4.2. In Annex 1, more information about each PEV-PR case can be found.

- Simulations have been carried out using real consumption data of Borup grid, for 14th and 15th of January of 2013. Simulations start at midday of 14th to midday of 15th, for a total of 24 hours simulation time. In these days there is almost no PV production.

Uncontrolled charging usually adds power demand at peak hours (Figure 5.22-a), leading a decrease of system load factor and increasing energy losses. For 30% of PEV-PR, peak load is increased from 206kW to 253kW. Furthermore, voltage levels at peak hours are affected by the extra load and the unbalance between phases generated by the charging of PEVs, as can be seen in Figure 5.22-b.

(a)   (b)
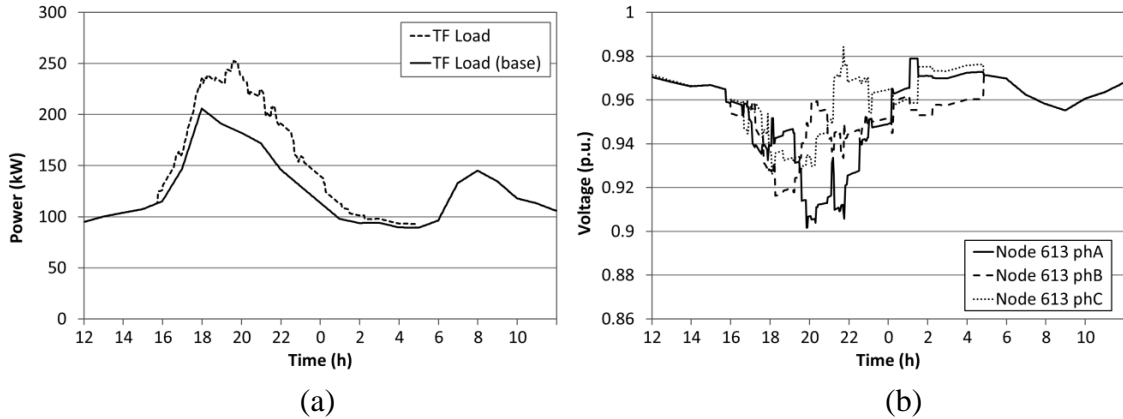
Figure 5.22. Uncontrolled charging for 30% of PEV-PR. (a) Total load of distribution transformer and (b) line-neutral voltages at node 613

In Figure 5.23-a, the PEVs power demand and the electricity cost are shown. PEVs are partly charged when electricity cost is high, increasing unnecessarily the total charging cost. PEVs are charged from initial SOC to final SOC, in this case 1 p.u., i.e. 100% (Figure 5.23-b). The evolution of the SOC of all PEVs indicates that they are charged without any type of coordination. Furthermore, their charging rates do not vary during the charging process.

(a)   (b)
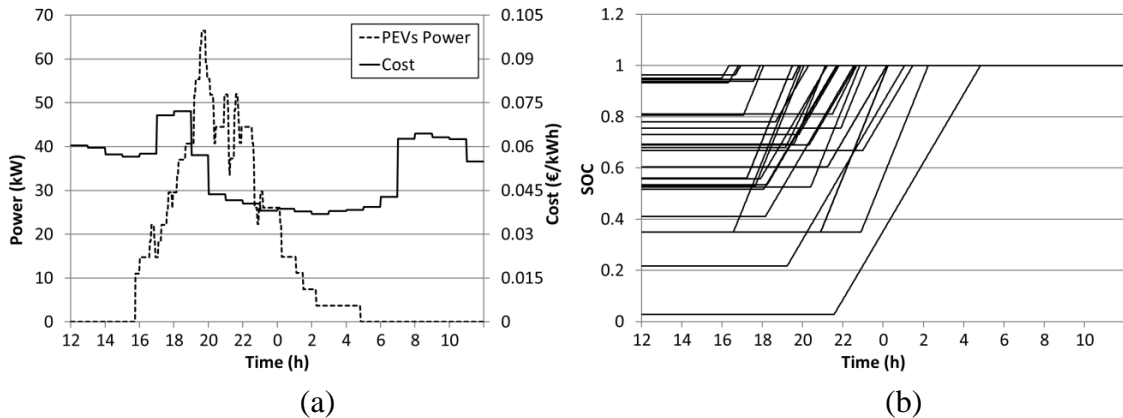
Figure 5.23. Uncontrolled charging for 30% of PEV-PR. (a) PEVs power demand compared to electricity cost and (b) evolution of SOC of each PEV

Uncontrolled charging has negative impact on charging cost, peak power, load variance and voltages. However, the distribution network analyzed can withstand this situation with a limited quantity of PEVs. From 30% of PEV-PR onwards, voltage violations may occur as can be seen in Table 5.11. Values in bold indicate that a limit has been surpassed. On the one hand, a peak power limit of 400kW has been set according to distribution transformer nominal power. On the other hand, line-neutral voltages must not be out of the ±10% of nominal voltage during more than 72 minutes (95% of the time within ±10%).

Energy losses produced in the lines and the distribution transformer have been calculated. Without any PEV in the LV distribution network, the energy losses were 56kWh. However, in the case of 100% of PEV-PR, these energy losses have a value more than double (137kWh).

Table 5.11. Uncontrolled charging results for the analyzed PEV-PRs

Case of study	Overall charging cost (€)	Overall load variance (kW²)	PEVs power variance (kW²)	Overall peak power (kW)	PEVs peak power (kW)	Energy losses (kWh)	Min. 613 node voltage (p.u.)	Time below 0.9p.u. (min)
No PEVs	-	1039	-	206	-	56	0.9468	0
Uncontrolled (10%)	7.39	1599	81	227	40	63	0.92	0
Uncontrolled (30%)	16.53	2266	327	253	66	74	0.9016	0
Uncontrolled (50%)	28.75	3340	839	290	111	85	**0.8816**	**102**
Uncontrolled (70%)	38.97	5244	1870	320	126	106	**0.8537**	**132**
Uncontrolled (90%)	47.46	6409	2770	367	182	132	**0.8106**	**247**
Uncontrolled (100%)	49.85	6842	3063	375	189	137	**0.8125**	**262**

Thus, analyzing the results obtained from uncontrolled charging, it is necessary to develop new smart charging approaches to improve PEVs integration in LV distribution networks.

5.6 Smart charging approaches

In this section, the smart charging approaches that have led to the algorithm proposed in this thesis are presented. The new algorithm proposed is composed by two different smart charging methods: charging cost minimization and variance minimization. So, it is interesting to analyze the behavior of each algorithm in different study cases, in order to know the characteristics, advantages and drawbacks of each algorithm.

All smart charging algorithms developed in this thesis have a resolution time of 5 minutes. That is, charging set-point of PEVs are defined in a 5 minutes time basis. Thus, the 24 hours of the simulation time is discretized in 288 time slots or intervals. Let $t \in \mathbb{N}$ denote the discretization step of the time of day and let $T \in t$ be the total number of time slots, as can be seen in equation (5-3).

$$t = \{1, 2, 3, \dots, 287, T\} \tag{5-3}$$

In addition, let $n \in \mathbb{N}$ be the number of a PEV connected to the distribution network, being $N \in n$ the total number of PEVs currently connected to the distribution network, as shown in equation (5-4).

$$n = \{1, 2, 3, \dots, N\} \tag{5-4}$$

Let $aT, dT \in t$ denote the time slot when the PEV is connected to the network (arrive time) and the time slot when PEV is disconnected (departure time), respectively. Then, let $cT \in \mathbb{N}$ be the number of time slots in which the PEV remains connected to the network (connection time), as defined in equation (5-5).

$$cT = dT - aT \tag{5-5}$$

Two important definitions must be introduced before starting to describe the smart charging methods used in this thesis. The first one is the vehicle charging profile (VCP), which is

the charging set-point vector along the connection time (cT) of the n-th PEV, as it is defined in equation (5-6).

$$VCP_n = \{x_{n,aT}, x_{n,aT+1}, x_{n,aT+2}, \dots, x_{n,dT}\} \quad aT, dT \in t \tag{5-6}$$

where:

− VCP_n: vehicle charging profile of n-th PEV
− aT: arrive time of n-th PEV
− dT: departure time of n-th PEV
− $x_{n,t}$:   power set-point of the n-th PEV at time slot t

The second one is the accumulated charging profile (ACP) which is the total power demand of PEVs during the all day, as shown in equation (5-7).

$$ACP = \left\{ \sum_{n=1}^{N} x_{n,1}, \sum_{n=1}^{N} x_{n,2}, \dots, \sum_{n=1}^{N} x_{n,T-1}, \sum_{n=1}^{N} x_{n,T} \right\} \tag{5-7}$$

Following, charging cost and variance optimization algorithms are explained. Within the variance optimization algorithm, two different alternatives can be distinguished: the minimization of PEVs load variance and the minimization of overall load of the network. In the first one, the VCP of each PEV is calculated knowing the ACP of the other PEVs that are already connected to the grid. In the second one, the VCP is calculated knowing not only the ACP but also the load forecasting of the distribution network. This load forecasting can include estimation of distributed generation production. Both alternatives require a coordination system to work properly through the use of ACP. In contrast, cost optimization algorithm does not require of any coordination system. Furthermore, V2G concept can be implemented in each algorithm. So, the effect of these aspects in the PEVs integration has been analyzed.

5.6.1   Optimization of charging cost

Cost optimization is one of the simplest decentralized smart controls that can be used to charge PEVs. This optimization is based on the minimization of the cost of charging, especially in hourly discrimination tariffs. This way, PEVs only draw energy from the grid when prices are low. V2G capabilities enhance charging cost by selling part of the energy stored when prices are higher. This option is particularly advantageous when there is a large difference between prices at peak and off-peak hours. However, it should be taken into account other aspects, like taxes and battery degradation. With regard to the last one, the algorithm developed in this thesis can limit the energy injected back to the grid.

The objective function, presented in equation (5-8), for this smart charging is the product of energy consumed/injected by the PEV and the electricity prices in that period of time. The objective function is minimized in order to reduce the charging costs.

$$J = \sum_{t=aT}^{dT} \left(C_t^{ch} \cdot x_{n,t}^{ch} - C_t^{dch} \cdot x_{n,t}^{dch} \right) \cdot P_n \tag{5-8}$$

where:

- n: the n-th PEV to be optimized
- $x_{n,t}^{ch}$:   charging set-point at time slot t of the n-th PEV
- $x_{n,t}^{dch}$:   discharging set-point at time slot t of the n-th PEV
- C_t^{ch}:   purchase prices of electricity at time slot t
- C_t^{dch}:   sell prices of electricity at time slot t
- P_n: maximum energy absorbed by the n-th PEV for a time slot

Two set-point variables are considered: $x_{n,t}^{ch}$ for charging and $x_{n,t}^{dch}$ for discharging. After the optimization process is done, these two variables are subtracted to determine the final set-point for the corresponding PEV, as shown in equation (5-9). This optimization problem is solved using a linear programming technique and its results are the set-point of the PEV charger at each time period t, being -1 discharging at maximum power, 0 no power transfer and 1 charging at maximum power.

$$x_{n,t} = x_{n,t}^{ch} - x_{n,t}^{dch} \tag{5-9}$$

The optimization process is done for every n-th PEV when it is connected to the distribution network. Hence, there is no need for an aggregator entity. Only information about electricity prices is required. For the approach developed in this thesis, Nord Pool spot prices have been taking as reference, specifically in the DK2 region where Borup is located. The prices correspond with the real data of load demand (14th and 15th of January of 2013). No taxes have been considered and purchase prices (C_t^{ch}) and sell prices (C_t^{dch}) are considered equal.

The objective function of equation (5-8) is subject to different constraints in order to satisfy user preferences and technical limits, such as final SOC required. These constraints can be expressed in two forms: as equality or as inequality constraint. When an objective function is minimized, inequality constraints must be defined as less or equal form instead of higher or equal form. Following, the linear constraints used in this approach are described:

- SOC must be less or equal than 1 (equivalent to 100% of SOC) at any time slot, as shown in equation (5-10). This way, over-charge of PEV batteries is avoided. Other maximum SOC value can be selected to reduce battery degradation.

$$\sum_{t=aT}^{dT} \left(P_n \cdot \eta_n \cdot x_{n,t}^{ch} - \frac{P_n \cdot x_{n,t}^{dch}}{\eta_n} \right) \leq (Q_n - q_n) \cdot BC_n \quad \forall t \tag{5-10}$$

- SOC must be higher or equal than zero at any time slot, as shown in equation (5-11). This constraint is necessary in order to avoid over-discharge when PEV is injecting energy back to the network (V2G). Other higher minimum SOC value can be selected in function of battery characteristics.

$$\sum_{t=aT}^{dT} \left(\frac{P_n \cdot x_{n,t}^{dch}}{\eta_n} - P_n \cdot \eta_n \cdot x_{n,t}^{ch} \right) \leq q_n \cdot BC_n \quad \forall t \tag{5-11}$$

- SOC must be equal to final SOC at final charging time dT, as shown in equation (5-12). It defines the final SOC requested by the user. In this approach, this final SOC is set to

1 for all PEVs, but lower values can be selected in order to reduce battery degradation. In contrast, the total autonomy of the PEV will be reduced.

$$\sum_{t=aT}^{dT} \left(P_n \cdot \eta_n \cdot x_{n,t}^{ch} - \frac{P_n \cdot x_{n,t}^{dch}}{\eta_n} \right) = (Q_n - q_n) \cdot BC_n \qquad (5\text{-}12)$$

- Variables $x_{n,t}^{ch}$ and $x_{n,t}^{dch}$ must be between 0 and 1, as shown in equation (5-13).

$$0 \leq x_{n,t}^{ch} \leq 1 \qquad 0 \leq x_{n,t}^{dch} \leq 1 \qquad \forall t \qquad (5\text{-}13)$$

- Energy injected back to the grid must be less than the maximum allowed by the user, which is set through Z value, as shown in equation (5-14). The value of Z limits the battery capacity portion destined to V2G, being $Z=0$ no V2G allowed and $Z=1$ the 100% of battery capacity can be used to provide V2G.

$$\sum_{t=aT}^{dT} \frac{P_n \cdot x_{n,t}^{dch}}{\eta_n} \leq Z_n \cdot BC_n \qquad (5\text{-}14)$$

where:

- η_n: charging/discharging efficiency of the n-th PEV
- BC_n: battery capacity of the n-th PEV
- Q_n: final SOC required for the n-th PEV
- q_n: initial SOC for the n-th PEV
- Z_n: portion of battery capacity reserved for V2G operation of n-th PEV

PEV user can limit V2G provision through changing variable Z. This option does not necessary imply that the mentioned percentage of battery capacity will be delivered but it is the maximum one allowed by the user. For example, if Z is set to 0.1, V2G provision is limited to 10% of the battery capacity. Obviously, PEVs can deliver energy only when SOC is above 0% due to constraint (5-11).

Cost optimization is a linear programming problem. In this case, the objective function is minimized using the simplex method in CPLEX software for Matlab. Linear programming problems can be expressed by equation (5-15).

$$\min_x C'x \quad s.t. \quad \begin{cases} A_{ineq} \cdot x \leq b_{ineq} \\ A_{eq} \cdot x = b_{eq} \\ l_b \leq x \leq u_b \end{cases} \qquad (5\text{-}15)$$

where:
- x: vector of variables to be determined
- C: vector of coefficients of x
- A_{ineq}: matrix with the coefficients of the inequality constraints
- A_{eq}: matrix with the coefficients of the equality constraints
- b_{ineq}: vector with the independent variables of the inequality constraints
- b_{eq}: vector with the independent variables of the equality constraints
- l_b: vector with the lower bounds of x
- u_b: vector with the upper bounds of x

Table 5.12 shows simulation results of different PEV-PR cases. At low PEV-PR, cost optimization algorithm provides better results in terms of cost and overall load variance but from PEV-PR of 50% both solutions are not feasible due to voltage limits violations. With regard to energy losses, only in the 10% of PEV-PR case the energy losses are reduced but only in 1kWh. For the rest of cases, energy losses increase compared to uncontrolled case, especially at high PEV-PR cases.

Table 5.12. Uncontrolled charging and cost optimization results without using V2G

Case of study (PEV-PR)	Overall charging cost (€)	Overall load variance (kW²)	PEVs power variance (kW²)	Overall peak power (kW)	PEVs peak power (kW)	Energy losses (kWh)	Min. 613 node voltage (p.u.)	Time below 0.9p.u. (min)
No PEVs	-	1039	-	206	-	56	0.9468	0
Uncontrolled (10%)	7.39	1599	81	227	40	63	0.92	0
Cost opt. (10%)	5.08	896	187	206	63	62	0.9264	0
Uncontrolled (30%)	16.53	2266	327	253	66	74	0.9016	0
Cost opt. (30%)	12.51	1261	985	236	137	75	0.9107	0
Uncontrolled (50%)	28.75	3340	839	290	111	85	**0.8816**	**102**
Cost opt. (50%)	21.82	2921	2992	345	234	95	**0.7965**	**155**
Uncontrolled (70%)	38.97	5244	1870	320	126	106	**0.8537**	**132**
Cost opt. (70%)	29.21	6067	6001	**475**	344	132	**0.7499**	**145**
Uncontrolled (90%)	47.46	6409	2770	367	182	132	**0.8106**	**247**
Cost opt. (90%)	37.54	10420	9419	**576**	413	191	**0.6094**	**190**
Uncontrolled (100%)	49.85	6842	3063	375	189	137	**0.8125**	**262**
Cost opt. (100%)	39.53	11675	10307	**610**	434	203	**0.4493**	**200**

Following, some figures obtained in different simulation cases are presented. In the first case V2G is not allowed, so variable Z has been set to 0. In Figure 5.24-a, the total load of distribution transformer for base case (no PEVs) and 30% of PEV-PR case are presented. A peak demand of 236kW is produced by the charging of PEVs. In Figure 5.24-b, the line-neutral voltages at node 613 are shown. As can be seen in this figure, unbalances between phases are only induced by the charging of PEVs. In general, this type of optimization tends to concentrate the charge of all PEVs in a short period. In fact, this linear decentralized optimization generates avalanche effects as all PEVs are induced to be charged at the same time when prices are the lowest ones.

(a)   (b)
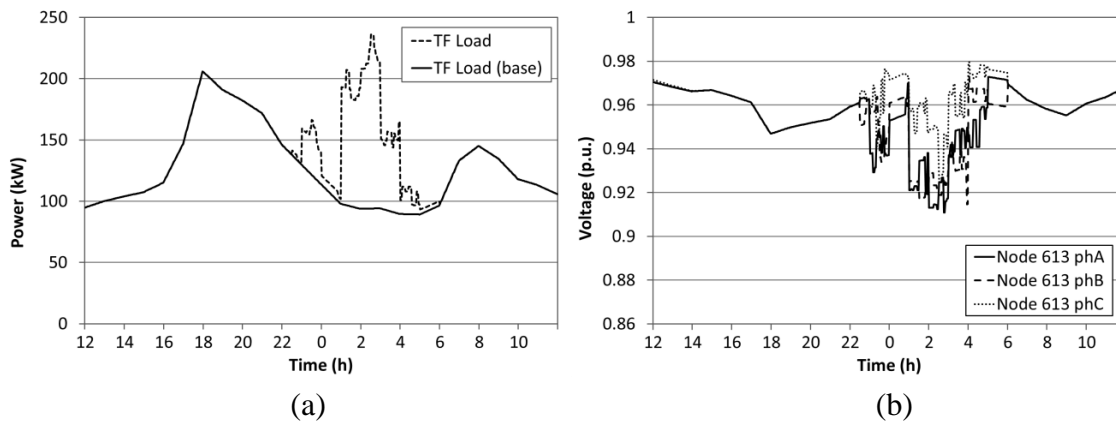
Figure 5.24. Optimization of charging cost (no V2G case) for 30% of PEV-PR. (a) Load in the distribution transformer and (b) line-neutral voltages at node 613

PEV charging profile and electricity prices are presented in Figure 5.25-a, showing clearly that this algorithm tends to accumulate the charge of all PEVs at hours of lower electricity prices. Electricity cost is higher between 00:00 to 01:00h compared to 23:00 to 00:00h. That is why almost no PEVs are charged between 00:00 to 01:00h. In this case, the maximum charging power of PEVs reaches 137kW.

Figure 5.25-b shows the evolution of the SOC of all PEVs, during the charging process. This evolution indicates that they are charged almost at the same time (from 01:00 to 04:00h) as well as their charging power do not vary during the charging process. The slope of the SOC curve indicates the charging rate of the battery. The greater the slope, the higher the charging power is, while no slope means no charging.

| (a) | (b) |
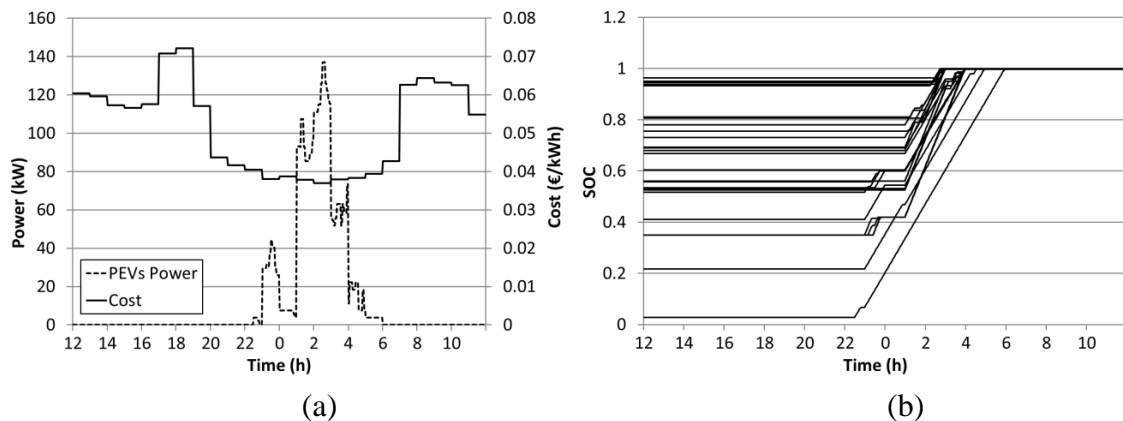
Figure 5.25. Optimization of charging cost (no V2G case) for 30% of PEV-PR. (a) PEVs load compared to electricity cost and (b) evolution of SOC of each PEV

Introducing V2G concept reduces overall charging cost, i.e. from 12.51 to 11.36€ for 30% of PEV-PR. However, it is less efficient and grid impacts are usually higher than the cost optimization algorithm without using V2G. In addition, energy losses are always greater using V2G concept due to the increase of energy flows. Anyway, both approaches do not give valid solutions for high PEV-PRs, as can be seen in Table 5.13.

Table 5.13. Results of no V2G and V2G cases, for the cost optimization algorithm

Case of study (PEV-PR)	Overall charging cost (€)	Overall load variance (kW²)	PEVs power variance (kW²)	Overall peak power (kW)	PEVs peak power (kW)	Energy losses (kWh)	Min. 613 node voltage (p.u.)	Time below 0.9p.u. (min)
No PEVs	-	1039	-	206	-	56	0.9468	0
Cost opt. (10%)	5.08	896	187	206	63	62	0.9264	0
Cost opt. V2G (10%)	4.45	711	371	198	63	63	0.9281	0
Cost opt. (30%)	12.51	1261	985	236	137	75	0.9107	0
Cost opt. V2G (30%)	11.36	1275	1642	236	137	80	0.9122	0
Cost opt. (50%)	21.82	2921	2992	345	234	95	**0.7965**	**155**
Cost opt. V2G (50%)	19.89	3954	5031	349	238	109	**0.7965**	**195**
Cost opt. (70%)	29.21	6067	6001	**475**	344	132	**0.7499**	**145**
Cost opt. V2G (70%)	26.04	9277	10372	**489**	355	164	**0.7407**	**200**
Cost opt. (90%)	37.54	10420	9419	**576**	413	191	**0.6094**	**190**
Cost opt. V2G (90%)	34.87	14798	14439	**591**	423	238	**0.6438**	**250**
Cost opt. (100%)	39.53	11675	10307	**610**	434	203	**0.4493**	**200**
Cost opt. V2G (100%)	36.67	16762	15973	**622**	446	255	**0.5804**	**240**

Using V2G, the PEV users can act as energy traders, selling energy when it is expensive and buying it when it is cheap. In this context, Figure 5.26 and Figure 5.27 show the results obtained for minimizing charging cost when V2G provision is allowed. In this case, all PEVs are limited to provide less or equal than 20% of the battery capacity ($Z=0.2$).

Selling electricity prices have been set equal to buying electricity prices, so there is no additional incentive to sell energy, except for the obtained by trading. Obviously, the existence of other economic incentive must be taken into account in the objective function. This energy trading through V2G produces a sharp and short decrease of load in the distribution transformer, as shown in Figure 5.26-a. In addition, PEVs energy demand is higher than in previous case where V2G was not allowed (332 to 373kWh), because of the energy losses produced by the use of V2G. Voltages are increased at node 613 (in an unbalanced way) when energy is injected back to the network, as shown in Figure 5.26-b.

(a)   (b)
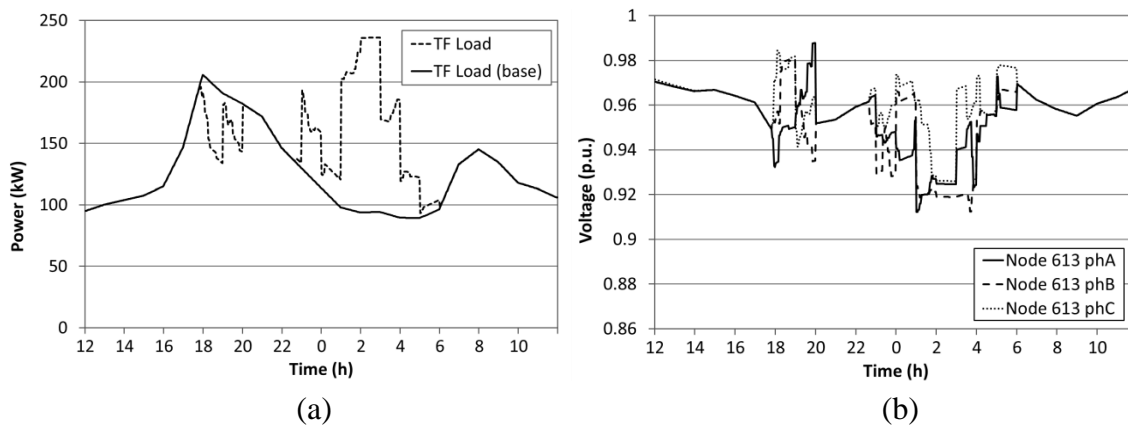
Figure 5.26. Optimization of charging cost (V2G case) for 30% of PEV-PR. (a) Load in the distribution transformer and (b) voltages at node 613

This minimization algorithm searches for the most expensive hours to sell energy and the cheapest hours to buy it, while the user requirements are accomplished (Figure 5.27-a). The SOC of PEVs (Figure 5.27-b) shows also the initial decrease of the SOC (negative slope) because of the injection of energy from PEV batteries to the distribution network, at around 18:00-20:00h and a later increase to satisfy the final SOC constraint.

(a)   (b)
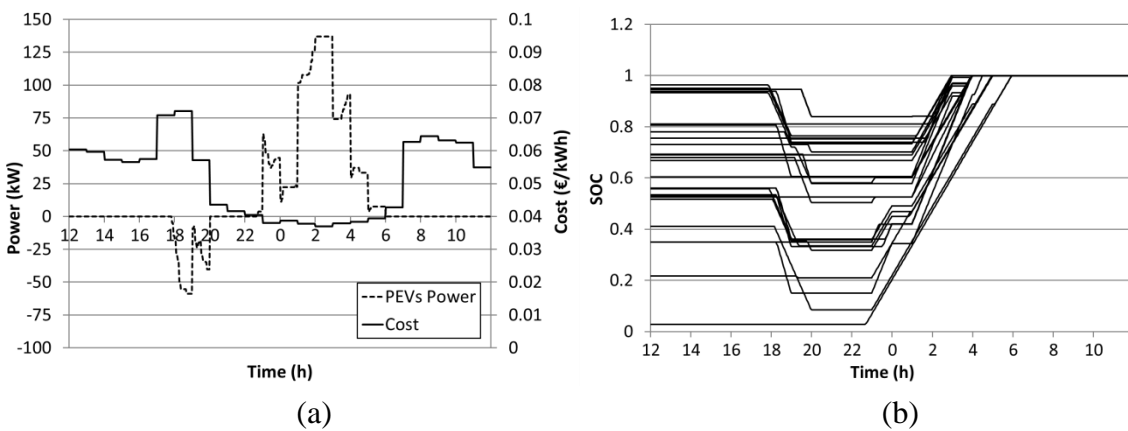
Figure 5.27. Optimization of charging cost (V2G case) for 30% of PEV-PR. (a) PEVs load compared to electricity cost and (b) evolution of SOC of each PEV

As mentioned before, PEV customers can set the percentage of battery capacity limit (Z) for V2G provision, according to their preferences. As Z value increases, more energy is available to be injected back to the network, but energy only will be injected back if it reduces the charging cost of the PEV. Figure 5.28 shows the PEVs power demand for 30% of PEV-PR at different Z values. As can be seen in this figure, there is almost no difference between Z=0.6 and Z=0.4 options.
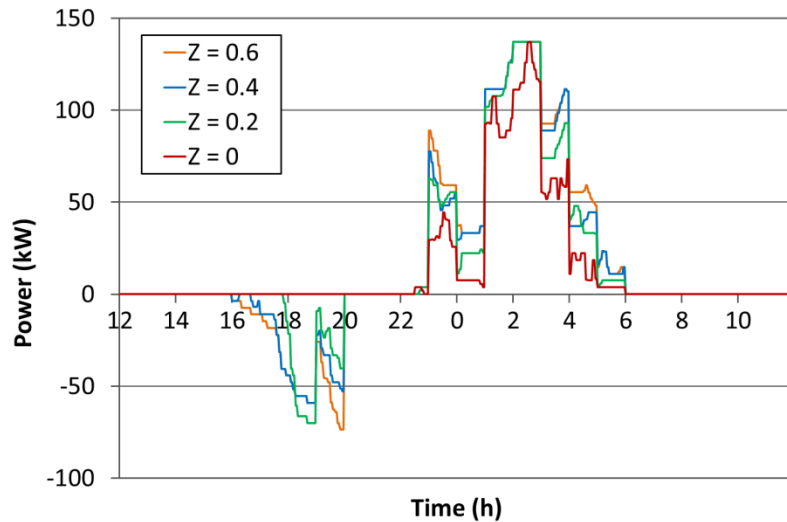
Figure 5.28. PEVs power demand at different Z values for PEV-PR of 30%

With regard to charging cost, a significantly improvement is made from uncontrolled strategy (16.53€) to cost optimization algorithm (12.51€). Furthermore, increasing Z value reduces also charging cost. But, this reduction has a limit because of the charger efficiency and the electricity prices. So, only discharging at specific hours can decrease charging cost and increasing value of Z does not have any extra effect, as shown in Figure 5.29.
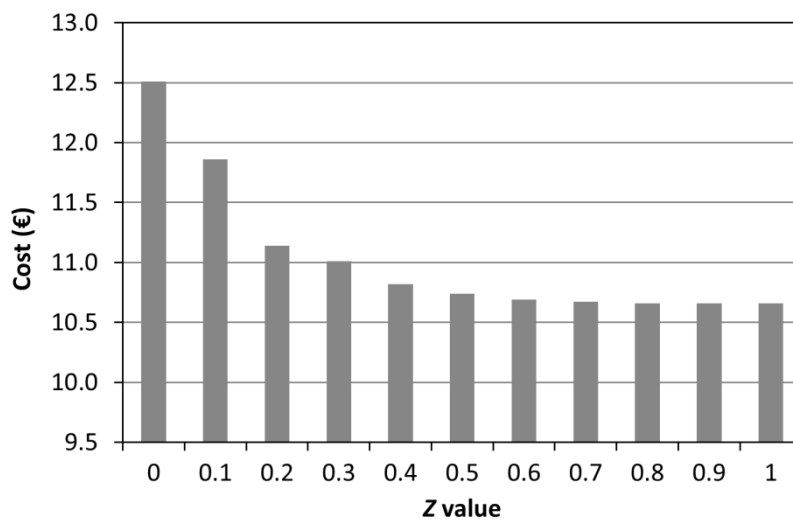
Figure 5.29. Overall PEVs charging cost at different Z values for PEV-PR of 30%

As a conclusion, this algorithm provides a useful tool to reduce PEVs charging cost but it has the drawback that affects largely the distribution network reliability due to the avalanche effect, even at low penetration rates of PEVs. The use of V2G concept decreases more the charging cost but it also has more impacts on the network. There are several

solutions to address avalanche effects, most of them are based on applying a coordinated control system. In this thesis, a solution for this problem is introduced in the proposed smart charging algorithm. Additionally, other types of algorithms can be used in order to reduce grid impacts. One of them is the minimization of PEVs load variance, which is presented in the next subsection.

5.6.2 Optimization of PEVs load variance

The variance is an indicator of the spread out of a set of data. So, if variance is minimized, the fluctuation of the set of data will be reduced. This technique can be useful to smooth the overall load demand or the power demand of a set of PEVs in a distribution network. Furthermore, minimizing load variance is equivalent to reduce power losses of the distribution network, as well as increase the load factor. The equation (5-16) is used to calculate the variance of a set of values x.

$$s^2 = \frac{1}{N}\left[\sum_{n=1}^{N}(x_n)^2\right] - \left[\frac{1}{n}\sum_{i=1}^{n}x_n\right]^2 \tag{5-16}$$

where:

- s^2:   the variance
- N: the total number of samples
- x_n: the n-th sample

Researchers usually tend to use this optimization technique to minimize the overall load variance, neglecting the possibility of using it only for smoothing the power demand of PEVs. The objective function to minimize is presented in equation (5-17). This function has a quadratic form and, therefore, linear programming cannot be used. Constraints remain the same as previous case.

$$J = \frac{1}{cT}\sum_{t=aT}^{dT}\left[P_n \cdot \left(x_{n,t}^{ch} - x_{n,t}^{dch}\right) + ACP_t\right]^2 - \mu^2 \tag{5-17}$$

in which:

$$\mu = \frac{1}{cT}\sum_{t=aT}^{dT}\left[P_n \cdot \left(x_{n,t}^{ch} - x_{n,t}^{dch}\right) + ACP_t\right] \tag{5-18}$$

where:

- cT: total number of time slots during the connection time
- P_n: maximum energy absorbed by the n-th PEV in a time slot
- $x_{n,t}^{ch}$:   charging set-point of the n-th PEV at time slot t
- $x_{n,t}^{dch}$:   discharging set-point of the n-th PEV at time slot t
- ACP_t: accumulated PEVs charging demand at time slot t

The objective function of equation (5-17) is subject to constraints shown in equations (5-10), (5-11), (5-12), (5-13) and (5-14). Quadratic programming is used to solve this optimization problem, which equation is presented in (5-19).

$$\min_x \frac{1}{2} x'Hx + f'x \quad s.t. \quad \begin{cases} A_{ineq} \cdot x \le b_{ineq} \\ A_{eq} \cdot x = b_{eq} \\ l_b \le x \le u_b \end{cases} \quad (5\text{-}19)$$

where:

− x: variables to be calculated
− H: symmetric matrix with quadratic coefficients of x
− f: vector with coefficients of x

This optimization process requires of a coordination system. In this case, each PEV has to upload their VCP to an aggregator entity. This way, the ACP of the PEVs can be calculated. When a new PEV is connected, this overall ACP will be downloaded from the aggregator, in order to be used in the optimization algorithm. After the algorithm is executed, the calculated VCP is sent to the aggregator and the ACP is updated.

In contrast to uncontrolled and cost optimization approaches, PEVs load demand variance optimization allows that 70% of PEV-PR case do not surpassing any voltage limit. In addition, this algorithm reduces peak power and charging cost and improves overall load variance when it is compared with uncontrolled charging approach. However, charging cost savings are not so noticeably compared to using a cost optimization algorithm. For PEV-PR of 90 and 100%, this algorithm cannot give valid solutions. Furthermore, this algorithm tends to increase peak power. For example, peak power grows from 206kW to 225kW for 100% of PEV-PR case.

PEVs load demand variance minimization algorithm reduces also energy losses compared to uncontrolled charging in all cases. This reduction can achieve a 17% (from 137 to 114kWh) in the 100% of PEV-PR case. Table 5.14 shows the results obtained from applying the optimization of PEVs load demand variance for the six different PEV-PR cases.

Table 5.14. Uncontrolled charging and PEVs power demand variance optimization results, without V2G

Case of study (PEV-PR)	Overall charging cost (€)	Overall load variance (kW²)	PEVs power variance (kW²)	Overall peak power (kW)	PEVs peak power (kW)	Energy losses (kWh)	Min. 613 node voltage (p.u.)	Time below 0.9p.u. (min)
No PEVs	-	1039	-	206	-	56	0.9468	0
Uncontrolled (10%)	7.39	1599	81	227	40	63	0.92	0
PEVs var. opt. (10%)	6.04	1044	17	210	10	62	0.9426	0
Uncontrolled (30%)	16.53	2266	327	253	66	74	0.9016	0
PEVs var. opt. (30%)	15.17	1057	89	212	24	70	0.9204	0
Uncontrolled (50%)	28.75	3340	839	290	111	85	**0.8816**	**102**
PEVs var. opt. (50%)	26.74	1158	254	218	40	78	0.9299	0
Uncontrolled (70%)	38.97	5244	1870	320	126	106	**0.8537**	**132**
PEVs var. opt. (70%)	36.48	1335	433	225	51	92	0.8942	20
Uncontrolled (90%)	47.46	6408	2770	366	182	132	**0.8106**	**247**
PEVs var. opt. (90%)	45.86	1529	816	222	70	111	**0.8724**	**85**
Uncontrolled (100%)	49.85	6842	3063	375	189	137	**0.8125**	**262**
PEVs var. opt. (100%)	48.17	1613	909	225	74	114	**0.8701**	**85**

From the point of view of the LV distribution network reliability, there is an important improvement in this type of optimization process. The charging of PEVs is distributed as much as possible over time, while users' requirements are met. However, a little increase of peak power is produced, as can be seen in Figure 5.30-a. Also, voltages in the network are slightly affected, as shown in Figure 5.30-b. In these figures, the PEV-PR of 30% has been used.

(a)   (b)
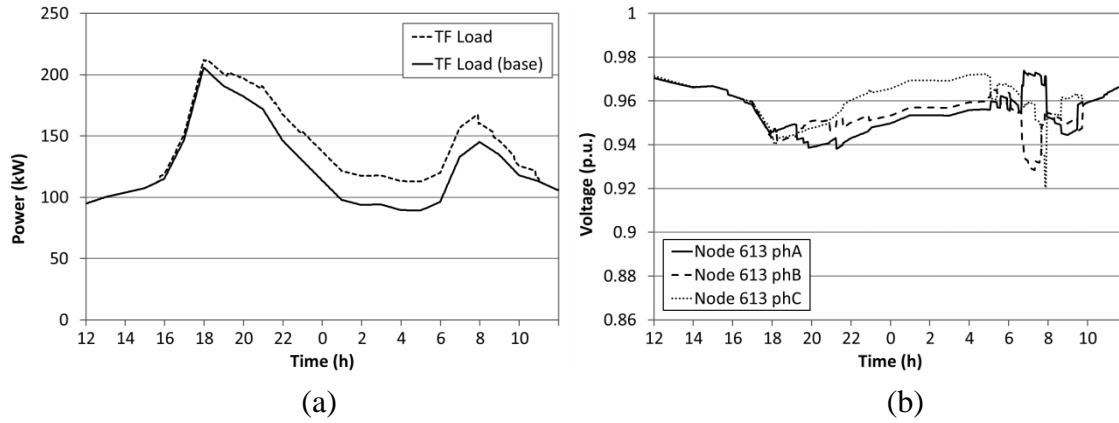
Figure 5.30. Optimization of PEVs load variance (no V2G case) for 30% of PEV-PR. (a) Load in the distribution transformer and (b) line-neutral voltages at node 613

The most important characteristic of this type of control is that maximum PEVs power demand is widely decreased, reaching only 24kW (Figure 5.31-a). In contrast, this value reaches 66kW for uncontrolled charging strategy and 137kW for optimization of charging cost. In addition, this algorithm starts the charging process of the PEVs when electricity is expensive due to electricity cost is not considered in the algorithm. The evolution of the SOC demonstrates that every PEV is charged at different power rates, in order to minimize PEVs power demand variance, as shown in Figure 5.31-b. All of them reach the final SOC required at departure time, which is set by the user. This type of optimization reduces also battery degradation because the charging process is done at lower charging rates than uncontrolled and cost optimization strategies.

(a)   (b)
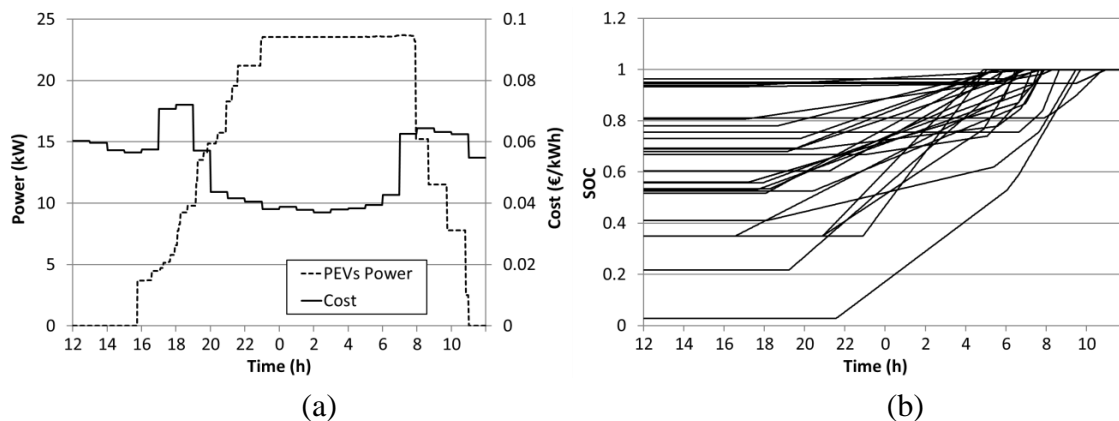
Figure 5.31. Optimization of PEVs load variance (no V2G case) for 30% of PEV-PR. (a) PEVs power demand versus electricity cost and (b) evolution of the SOC of each PEV

In this variance optimization algorithm, V2G concept is also introduced in order to determine the possibilities of V2G in this type of algorithm. In Table 5.15, no V2G and V2G options of PEVs power demand variance minimization are presented. Both solutions

provide similar results. This is due to the fact that the use of V2G tends to increase the PEV load variance value. That is, using V2G requires more energy from the network because there are more energy losses induced mainly by the limited efficiency of the charger.

Table 5.15. Comparing no V2G and V2G approaches of PEVs power demand variance optimization

Case of study (PEV-PR)	Overall charging cost (€)	Overall load variance (kW²)	PEVs power variance (kW²)	Overall peak power (kW)	PEVs peak power (kW)	Energy losses (kWh)	Min. 613 node voltage (p.u.)	Time below 0.9p.u. (min)
No PEVs	-	1039	-	206	-	56	0.9468	0
PEVs var. opt. (10%)	6.04	1044	17	210	10	62	0.9426	0
PEVs var. opt. V2G (10%)	6.56	1045	12	210	10	62	0.9416	0
PEVs var. opt. (30%)	15.17	1057	89	212	24	70	0.9204	0
PEVs var. opt. V2G (30%)	16.25	1056	84	212	23	71	0.926	0
PEVs var. opt. (50%)	26.74	1158	254	218	40	78	0.9299	0
PEVs var. opt. V2G (50%)	27.10	1159	258	218	40	79	0.9234	0
PEVs var. opt. (70%)	36.48	1335	433	225	51	92	0.8942	20
PEVs var. opt. V2G (70%)	37.35	1321	430	225	52	93	0.8849	50
PEVs var. opt. (90%)	45.86	1529	816	222	70	111	**0.8724**	**85**
PEVs var. opt. V2G (90%)	46.76	1539	831	222	71	112	**0.8842**	**85**
PEVs var. opt. (100%)	48.17	1613	909	225	74	114	**0.8701**	**85**
PEVs var. opt. V2G (100%)	49.30	1630	927	225	74	115	**0.879**	**80**

Thus, using V2G has little effect on the optimization of PEVs power demand variance (Figure 5.32). In this simulation case, Z has been set to 0.2 and the 30% of PEV-PR case has been used.

(a)   (b)
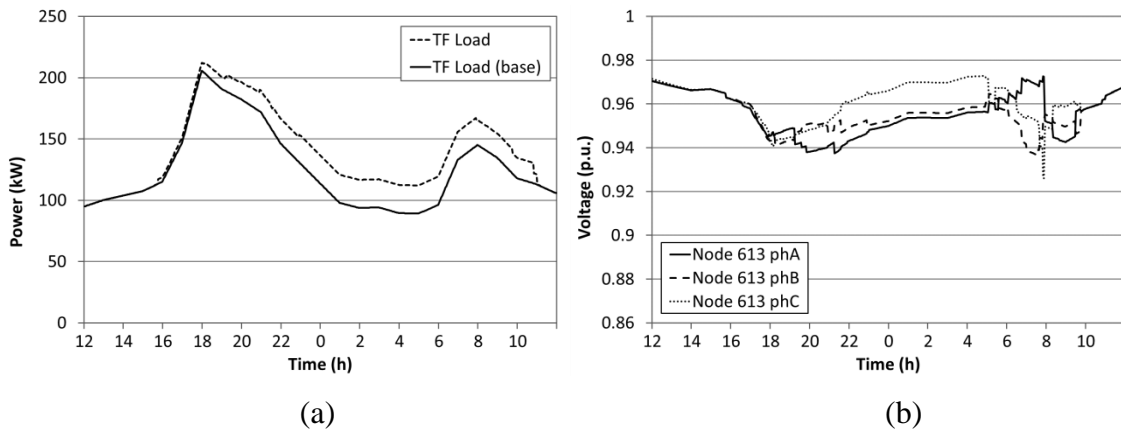
Figure 5.32. Optimization of PEVs load variance (V2G) for 30% of PEV-PR. (a) Load in the distribution transformer and (b) line-neutral voltages at node 613

Few PEVs inject energy back to the grid, as shown in Figure 5.33-b. Additionally, charging cost is increased when V2G is used (from 15.17 to 16.25€) while there are not any improvement in terms of overall load variance. Thus, using V2G has no practical value in this optimization algorithm.

(a)   (b)
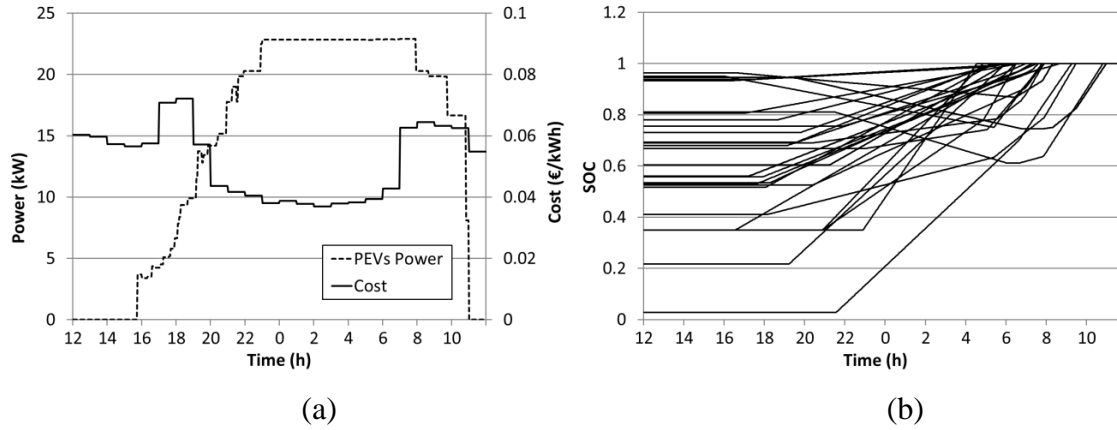
Figure 5.33. Optimization of PEVs load variance (V2G case) for 30% of PEV-PR. (a) PEVs power demand versus electricity cost and (b) evolution of the SOC of each PEV

Summarizing, minimization of PEVs power demand variance is a good solution to reduce impacts on the distribution network, but this technique has also some drawbacks such as: it could increase power demand at peak hours, V2G concept is useless and it does not take into account electricity prices. The first two drawbacks may be fixed through the use of an algorithm to minimize overall load variance, as it is explained in the following subsection.

5.6.3   Optimization of overall load variance

As mentioned above, the optimization of PEVs load variance presented in the previous subsection has the unintended consequence that it can increase the overall peak power. In order to avoid this problem, it is interesting to minimize the overall load of the system. A method to achieve this objective is to use load demand forecasting. This way, PEVs tend to charge when distribution network load is low, producing the called valley filling effect.

The hourly load demand forecast (LF) used in this case is obtained directly from the transformer load, without PEVs. Thus, it can be considered as an ideal forecast. This simplification is done in order to remove the influence of load demand forecasting errors from the results, thereby facilitating the comparison between the different algorithms. Anyway, influence of load forecasting errors is analyzed in subsection 5.7.7.

In this case, the objective function to minimize shown in equation (5-20) is similar to the previous case, but a variable LF_t is added, which represents the LF values at each time slot t. Constraints remain the same as in the previous cases.

$$J = \frac{1}{cT} \sum_{t=aT}^{dT} \left[P_n \left(x_{n,t}^{ch} - x_{n,t}^{dch} \right) + ACP_t + LF_t \right]^2 - \mu^2 \tag{5-20}$$

in which:

$$\mu = \frac{1}{cT} \sum_{t=aT}^{dT} P_n \left(x_{n,t}^{ch} - x_{n,t}^{dch} \right) + ACP_t + LF_t \tag{5-21}$$

Using load forecasting avoid increasing the peak power, improves load factor and reduces energy losses. Additionally, as can be seen in Table 5.16, peak power is 206kW for all PEV-PRs when load variance optimization is used. Furthermore, overall load variance is widely improved, being at least half of the uncontrolled case and reaching more than four time less in 100% PEV-PR case. Charging cost is also improved, giving better results than

PEVs power demand variance optimization. Additionally, analyzed algorithm improves voltage results for 70% of PEV-PR, being phase-neutral RMS values above 0.9 p.u. at any time. However, at higher PEV-PRs (90 and 100% cases), voltages exceed the low limits.

Table 5.16. Uncontrolled charging and load variance optimization algorithm results

Case of study (PEV-PR)	Overall charging cost (€)	Overall load variance (kW²)	PEVs power variance (kW²)	Overall peak power (kW)	PEVs peak power (kW)	Energy losses (kWh)	Min. 613 node voltage (p.u.)	Time below 0.9p.u. (min)
No PEVs	-	1039	-	206	-	56	0.9468	0
Uncontrolled (10%)	7.39	1599	81	227	40	63	0.92	0
Load var. opt. (10%)	5.17	774	97	206	27	62	0.9434	0
Uncontrolled (30%)	16.53	2266	327	253	66	74	0.9016	0
Load var. opt. (30%)	13.31	652	366	206	50	71	0.9386	0
Uncontrolled (50%)	28.75	3340	839	290	111	85	**0.8816**	**102**
Load var. opt. (50%)	24.07	759	787	206	73	80	0.9161	0
Uncontrolled (70%)	38.97	5244	1870	320	126	106	**0.8537**	**132**
Load var. opt. (70%)	33.56	904	1093	206	85	94	0.9088	0
Uncontrolled (90%)	47.46	6409	2770	367	182	132	**0.8106**	**247**
Load var. opt. (90%)	42.96	1328	1728	206	105	115	**0.8888**	**230**
Uncontrolled (100%)	49.85	6842	3063	375	189	137	**0.8125**	**262**
Load var. opt. (100%)	45.24	1437	1870	206	109	118	**0.8824**	**250**

Valley filling effect is clearly achieved through this control algorithm, as can be seen in Figure 5.34-a. However, phase-neutral voltages at node 613 are affected (Figure 5.34-b), mainly due to unbalances produced by the charging processes of PEVs. Although load level is noticeably lower at off-peak hours, the voltage level at phase b is lower than at peak hours. These results illustrate that voltage unbalances produced by PEVs are a very important factor to take into account.

(a)   (b)
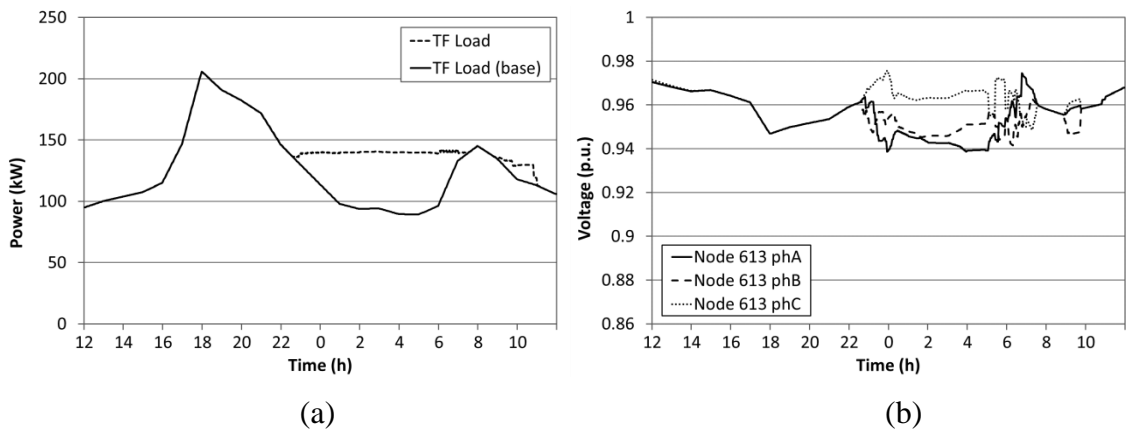
Figure 5.34. Optimization of overall load variance (no V2G case). (a) Load in the distribution transformer and (b) voltages at node 613

Almost all PEVs are charged at off-peak hours, which is indicated by LF, in order to reduce overall load variance, as can be seen in Figure 5.35-a and Figure 5.35-b. The maximum power demand of PEVs reaches 50kW which is considerable higher than the value reached in PEVs load variance optimization algorithm (24kW).

(a)   (b)
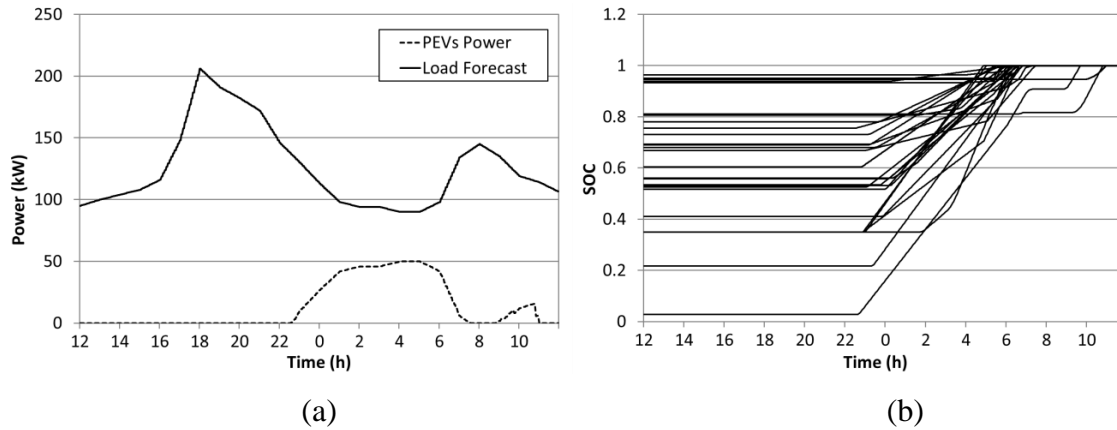
Figure 5.35. Optimization of overall load variance (no V2G case). (a) PEVs power demand versus load forecast and (b) evolution of the SOC of each PEV

In the PEVs power demand variance optimization, V2G does not offer any improvement. In order to achieve a better use of the V2G concept, load forecasting should be done. So, in the following case the use of LF and V2G is analyzed. In this case, Z variable has been set to 0.2.

Introducing V2G in the overall load variance minimization algorithm provides a reduction of load variance at low PEV-PRs, but an increase at high PEV-PRs. For example, load variance is reduced from 652 to 423kW^2 for 30% of PEV-PR but, in contrast, load variance grows from 1438 to 1738kW^2 for 100% of PEV-PR, as can be seen in Table 5.17. This effect is because the optimization algorithm is executed once per PEV. As a consequence, first PEVs connected to the network use V2G to reduce peak power, as well as to increase energy demand at off-peak hours. This situation is correct when there are not too many PEVs connected to the network. However, when the number of PEVs to be charged is high enough, injecting energy by using V2G may be counterproductive because energy demand at off-peak hours could be higher than typical peak power demand.

Table 5.17. Overall load variance optimization results for no V2G and V2G cases

Case of study (PEV-PR)	Overall charging cost (€)	Overall load variance (kW²)	PEVs power variance (kW²)	Overall peak power (kW)	PEVs peak power (kW)	Energy losses (kWh)	Min. 613 node voltage (p.u.)	Time below 0.9p.u. (min)
No PEVs	-	1039	-	206	-	56	0.9468	0
Load var. opt. (10%)	5.17	774	97	206	27	62	0.9434	0
Load var. opt. V2G (10%)	5.04	483	274	186	38	63	0.9412	0
Load var. opt. (30%)	13.31	652	366	206	50	71	0.9386	0
Load var. opt. V2G (30%)	14.23	432	790	183	62	75	0.9269	0
Load var. opt. (50%)	24.07	759	787	206	73	80	0.9161	0
Load var. opt. V2G (50%)	24.64	743	1412	176	84	85	0.9089	0
Load var. opt. (70%)	33.56	904	1093	206	85	94	0.9088	0
Load var. opt. V2G (70%)	34.39	976	1778	188	95	100	0.9188	0
Load var. opt. (90%)	42.96	1328	1728	206	105	115	**0.8888**	**230**
Load var. opt. V2G (90%)	43.99	1593	2515	209	115	124	**0.8727**	**315**
Load var. opt. (100%)	45.24	1437	1870	206	109	118	**0.8824**	**250**
Load var. opt. V2G (100%)	46.52	1733	2665	213	119	127	**0.8696**	**340**

This problem can be solved by performing more than one algorithm execution per PEV. This way, the earliest PEVs connected to the grid will have better information of the distribution network status, through updated ACP. Such improvement can be easily introduced by sending new ACPs to the connected PEVs, every predefined period of time or when a predefined condition is met. This solution could be defined as iterative approach and it is especially useful when dealing with the V2G concept. In this thesis, this solution has not been implemented.

The application of V2G reduces peak power and increase the charge demand of PEVs in off-peak hours, as can be seen in Figure 5.36-a. Voltages profile at node 613 (Figure 5.36-b) are improved at peak hours (from 18:00 to 22:00h). As in the no V2G case, there is no valid solution for 90 and 100% of PEV-PRs, mainly due to voltage unbalances generated by the charging of PEVs.

(a) (b)
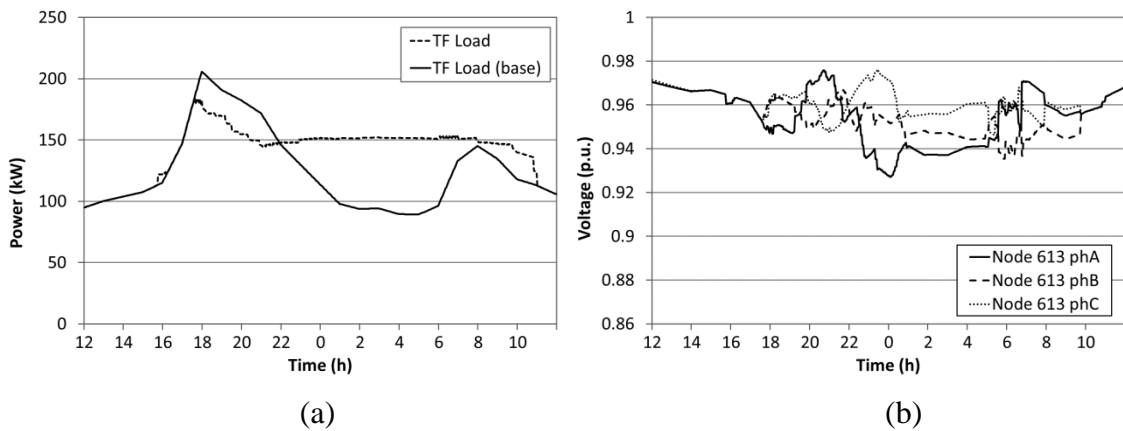
Figure 5.36. Optimization of overall load variance (V2G case). (a) Load in the distribution transformer and (b) voltages at node 613

Figure 5.37-a shows the LF and PEVs power demand. PEVs deliver energy back to the grid when load demand is high at peak hours. Thus, peak power is reduced from 206kW to 183kW, for 30% of PEV-PR. Evolution of the SOC for each PEV (Figure 5.37-b) also shows this behavior, with a first part where PEVs are injecting energy to the network and a second part where PEVs are being charged. All PEVs take part in reducing the overall load variance.

(a) (b)
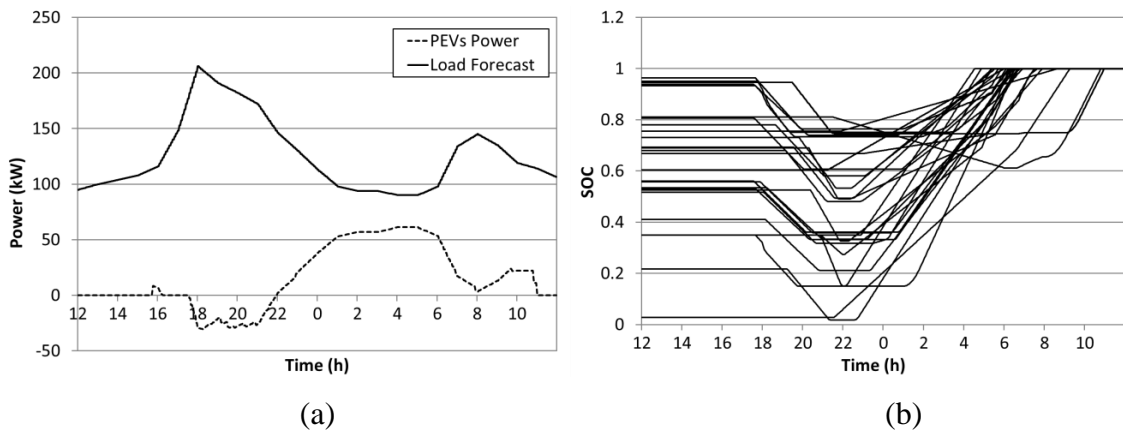
Figure 5.37. Optimization of overall load variance (V2G case). (a) PEVs power demand versus load forecast and (b) evolution of the SOC of each PEV

It is interesting to know the effect of varying the Z value in charging cost and overall load variance. Thus, several simulations have been carried out using the 30% of PEV-PR. As expected, when Z value increases, the overall load variance decreases. However, this variance reduction is more noticeable at low Z values (between 0.1 and 0.3). In contrast, the overall cost of charge of PEVs increases almost linearly, from 13.31 to 15.09€ (Figure 5.38). So, in this case, increasing Z beyond 0.2 is not profitable in terms of overall load variance.
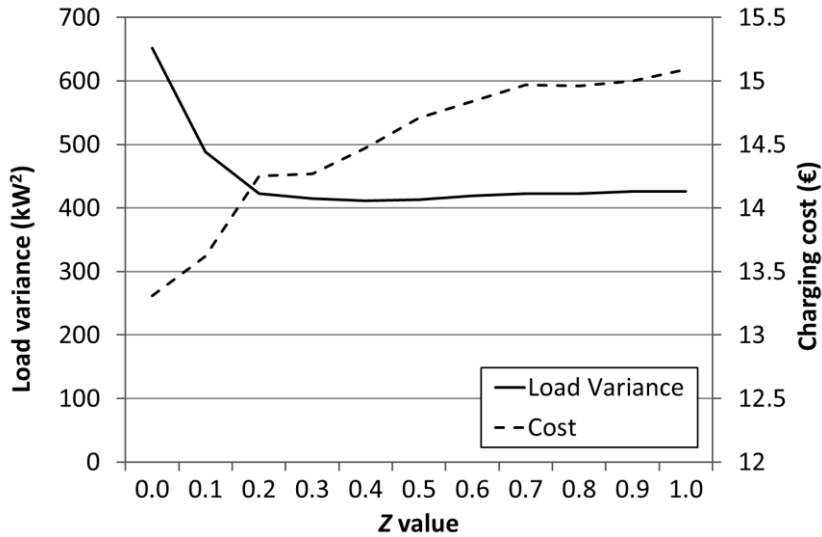
Figure 5.38. Overall load variance and total charging cost, at different Z values

Figure 5.39 shows PEVs power demand at different Z values. Note that there is no huge differences between PEVs power demand for Z equal to 0.2 and 0.3.
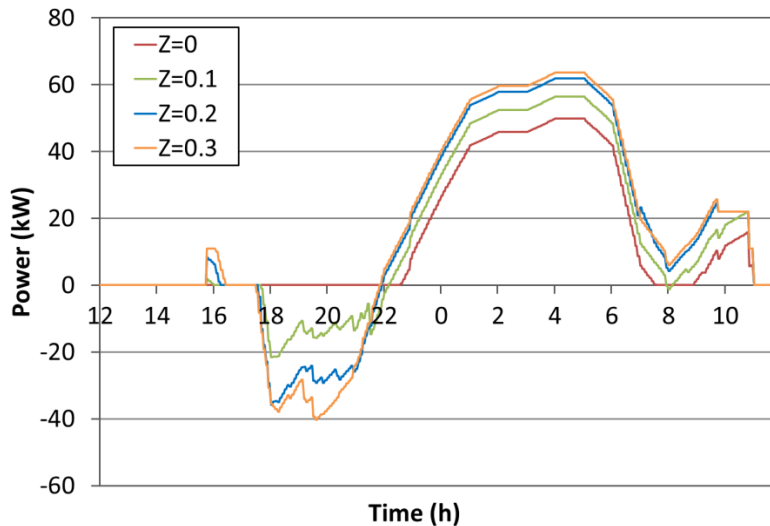
Figure 5.39. PEVs power demand at different Z values

Although there is no important improvement in overall load variance when Z reaches values higher than 0.2, observing the peak power value, there is a decrease as Z increases until 0.7. This way, peak power is reduced from 206kW to 165kW, as can be seen in Table 5.18.

Table 5.18. Simulation results obtained from varying Z value, in overall load variance optimization

Case of study (PEV-PR)	Overall charging cost (€)	Overall load variance (kW²)	PEVs power variance (kW²)	Overall peak power (kW)	PEVs peak power (kW)	V2G peak power (kW)	Min. 613 node voltage (p.u.)	Time below 0.9p.u. (min)
Load var. opt. (Z=0.0)	13.31	652	366	206	50	-	0.9386	0
Load var. opt. (Z=0.1)	13.62	488	577	190	56	-22	0.9319	0
Load var. opt. (Z=0.2)	14.25	423	828	183	62	-36	0.9269	0
Load var. opt. (Z=0.3)	14.27	415	931	179	64	-40	0.9294	0
Load var. opt. (Z=0.4)	14.47	411	1010	175	65	-45	0.9361	0
Load var. opt. (Z=0.5)	14.71	413	1056	171	66	-50	0.9323	0
Load var. opt. (Z=0.6)	14.84	419	1088	169	66	-53	0.9294	0
Load var. opt. (Z=0.7)	14.97	423	1105	166	67	-55	0.926	0
Load var. opt. (Z=0.8)	14.96	423	1119	165	67	-55	0.9265	0
Load var. opt. (Z=0.9)	15	426	1127	165	68	-55	0.9258	0
Load var. opt. (Z=1)	15.09	426	1129	165	68	-55	0.9263	0

Summarizing, overall load variance minimization improves load factor as well as system efficiency. Furthermore, if V2G concept is implemented better results could be achieved, especially for low values of Z. In contrast, charging cost of PEVs will be increased and load demand forecasting is needed. Load demand forecasting at small-scale can be complex because LV distribution networks are characterized by having higher variability than MV distribution networks. Electricity demand not only depends on number of customers, region, type of day, etc. but also depends on the behavior of individual customers and the influence of local phenomena, i.e., weather, special events, etc. So, errors in load forecasting can result in unwanted behavior in PEVs charging process that may impact the quality of supply. However, the introduction of smart meters is allowing the analysis of energy consumption at household level. In recent years, new techniques for load demand forecasting are being introduced. For example, support vector regression technique (SVR) has become an effective tool for load demand forecasting [137], [138]. This technique is based on support vector machine (SVM), which is a set of learning algorithms to solve classification and regression problems.

5.7   New proposed smart charging methodology

Two main objective functions have been considered in the previous section, cost minimization and variance minimization. Both have several advantages and drawbacks. On the one hand, cost optimization is best suited to reduce charging cost, which is the main interest of PEV users, but it has a very poor integration on LV distribution networks. Even at low PEV-PRs, cost optimization tends to concentrate in small period of time the charging of all PEVs. As a consequence, it produces sharp increase of PEVs power demand at off-peak hours that can be worse than typical peak power demand of homes. Voltages are also widely affected and it is usual that 0.9 p.u. voltage limit is surpassed at furthest nodes. Use of V2G can reduce the charging cost but, conversely, it produces a sharp fall of power demand at hours with the highest electricity prices that normally coincides with peak hours. This problem is due to the optimal behavior of PEVs and the lack of coordination between them (avalanche effect). In order to reduce this problem, two new constraints have been added to limit the rate of change of PEVs power demand.

On the other hand, variance minimization algorithm tends to disperse as much as possible the charging of PEVs. This way, the impact on the LV distribution network is decreased allowing the integration of a higher amount of PEVs than the cost minimization algorithm. However, it has the following drawbacks: the charging of PEVs slightly increases the peak power of the distribution network, valley filling is not completely achieved and cost of electricity is not taken into account. The first two problems can be cleared up by using load forecasting. The use of V2G can bring further improvements in peak power saving and valley filling but it is only feasible when load forecasting is taken into account in the algorithm.

As a conclusion, these two objective functions behave differently. One of them tends to concentrate the charging of PEVs and is focused in reducing charging cost for customers. The other one tends to disperse the charging of PEVs and is focused on reducing distribution network impacts. In addition, both approaches have voltage problems at high PEV-PRs. In this context, it is necessary to develop a new smart charging algorithm in order to address these problems as well as reducing as much as possible the complexity and requirements of the system and the charging costs and improve LV distribution network reliability. Following, a new decentralized multi-objective algorithm is presented.

5.7.1   Algorithm methodology

Taking into account the aspects commented before, a MOO algorithm has been developed in this thesis to efficiently integrate PEVs in LV distribution networks, reducing as much as possible the system requirements as well as improving the network reliability. This algorithm is a combination of the previously presented cost and variance optimization, through the use of weighted sum of objective functions.

As mentioned in section 4.2.2, an objective function based on weighted sum method must be normalized in order to make it dimensionless. In addition, a weight value must be added so as to give more relevance to one or another objective, i.e. to minimization of charging cost or to minimization of load variance. Variables w_1 and w_2 of equation (5-22) include not only the weights established by the DM (variable u) but also the normalization parameters (θ_1 and θ_2) of equation (4-14). The weight u can only take values from 0 to 1. Through varying weight variable u, DM can give more importance to cost minimization or to variance minimization objective.

$$w_1 = \theta_1 \cdot u = \frac{u}{Z_1^N - Z_1^U} \qquad w_2 = \theta_1 \cdot (1 - u) = \frac{1 - u}{Z_2^N - Z_2^U} \qquad (5\text{-}22)$$

Apart from normalizing, two new constraints are defined to limit the rate of change of PEVs power demand, based on the derivative of the ACP. One of the constraints is used for limiting upward gradient, and the other one the downward gradient. Upward/downward gradient limitation parameter (GL) is set to 20kW. This way, the number of PEVs that can start or stop their charging process in the same time slot is limited. The value of GL has been selected to be high enough to allow the starting or stopping the charging process of at least one PEV but low enough to avoid avalanche effects. It should be taken into account that the maximum charging power is 11kW for Tesla Model S.

These new constrains may be in conflict with constraints shown in equations (5-10) and (5-11), which limit the SOC value during the charging process, in function of the initial SOC value. In this case, optimization problem will be unfeasible. In order to make it

feasible, a relax factor (RF) is introduced in the constraints, shown in equations (5-23) and (5-24). This factor takes a value equal to 0 in the initial conditions but if the optimization is unfeasible, RF will be increased by 0.2, every time, until optimization problem became feasible. Thus, final rate of change will depend on several factors such as: GL parameter, charging power and relax factor value.

$$P_n \cdot \left(x_{n,t}^{ch} - x_{n,t}^{dch} \right) \leq GL - (ACP_t - ACP_{t-1}) + RF \cdot P_n \quad \forall t \tag{5-23}$$

$$P_n \cdot \left(x_{n,t}^{ch} - x_{n,t}^{dch} \right) \leq GL + (ACP_t - ACP_{t-1}) + RF \cdot P_n \quad \forall t \tag{5-24}$$

Where:
- t: current time slot
- GL: gradient limitation parameter in kW
- ACP_t: accumulated charging profile at time slot t
- RF: relax factor

In general, constraints of equations (5-23) and (5-24) will only affect to algorithms heavily dependent on cost minimization, which has avalanche effect problems. The final objective function, including both load variance and cost minimization with normalization parameters, is presented in equation (5-25).

$$J = w_1 \cdot J^{var} + w_2 \cdot J^{cost} \tag{5-25}$$

in which:

$$J^{var} = \frac{1}{cT} \sum_{t=aT}^{dT} \left(P_n \left(x_{n,t}^{ch} - x_{n,t}^{dch} \right) + ACP_t + LF_t \right)^2 - \left[\frac{1}{cT} \sum_{t=aT}^{dT} \left(P_n \left(x_{n,t}^{ch} - x_{n,t}^{dch} \right) + ACP_t + LF_t \right) \right]^2 \tag{5-26}$$

$$J^{cost} = \sum_{t=aT}^{dT} \left(C_t^{ch} \cdot x_{n,t}^{ch} - C_t^{dch} \cdot x_{n,t}^{dch} \right) P_n \tag{5-27}$$

The objective function of equation (5-25) is subject to the constraints of equations (5-10), (5-11), (5-12), (5-13), (5-14), (5-23) and (5-24). Before the optimization of equation (5-25) is carried out, utopia and nadir points must be calculated. So, the process has two sequential phases:

- Firstly, u is set to 0 and minimization of (5-25) is carried out. Evaluating the vector of results obtained in equation (5-26), the utopia point of cost optimization is calculated. Also, evaluating the vector of results in equation (5-27), an approximation of nadir point of the variance is obtained.

- Secondly, u is set to 1 and minimization of (5-25) is carried out. Evaluating the vector of results obtained in equation (5-26), the nadir point of cost optimization is calculated and evaluating the vector of results in equation (5-27), the utopia point of the variance is obtained.

Once the objective function has been totally defined, a mathematical development is carried out in order to obtain the different vectors and matrixes that are necessary to apply the quadratic programming technique of equation (5-19). Following, the vectors and matrixes calculated not only for the objective function but also for the constraints are presented:

- Vector X: The design vector to be determined, that is, the set-point of PEVs. It contains pairs of x^{ch} and x^{dch} set-points for each time slot. As commented, x^{ch} variable is the charging set-point while x^{dch} is the discharging set-point for V2G implementation.

$$X' = [x_{aT}^{ch} \quad x_{aT}^{dch} \quad x_{aT+1}^{ch} \quad x_{aT+1}^{dch} \quad \ldots \quad \ldots \quad x_{dT}^{ch} \quad x_{dT}^{dch}] \tag{5-28}$$

- Matrix H: Symmetric matrix with the quadratic coefficients of x^{ch} and x^{dch}. Indexes of the matrix are defined as i for rows and j for columns. Four different terms can be distinguished:

  ○ $x_i^{ch} \cdot x_j^{ch}$ or $x_i^{dch} \cdot x_j^{dch}$, being $i=j$:

$$A = \frac{2 \cdot w_1 \cdot (cT - 1)}{cT^2} \tag{5-29}$$

  ○ $x_i^{ch} \cdot x_j^{dch}$, being $i=j$:

$$B = \frac{2 \cdot w_1 \cdot (1 - cT)}{cT^2} \tag{5-30}$$

  ○ $x_i^{ch} \cdot x_j^{ch}$ or $x_i^{dch} \cdot x_j^{dch}$, being $i \neq j$:

$$C = \frac{-2 \cdot w_1}{cT^2} \tag{5-31}$$

  ○ $x_i^{ch} \cdot x_j^{dch}$, being $i \neq j$:

$$D = \frac{2 \cdot w_1}{cT^2} \tag{5-32}$$

Equation (5-33) shows the symmetric matrix H, which size depends on the total number of variables. In this case, two variables (x^{ch} and x^{dch}) are calculated per time slot. The total number of time slots depends on the connection time of the PEV (cT). Thus, it should be pointed out that dimension of all matrixes and vectors will change from PEV to PEV, depending on the connection time into the distribution network. For example, taking into account that, on average, PEVs will be connected for approximately 13 hours (as shown in subsection 5.4.2) and one hour has 12 periods of 5 minutes length (calculation period), cT will be 156 and the dimension of the H matrix will be 312x312.

$$H = \begin{bmatrix} A & B & C & D & \ldots & C & D \\ B & A & D & C & \ldots & D & C \\ C & D & A & B & \ldots & C & D \\ D & C & B & A & \ldots & D & C \\ \ldots & \ldots & \ldots & \ldots & \ldots & \ldots & \ldots \\ C & D & C & D & \ldots & A & B \\ D & C & D & C & \ldots & B & A \end{bmatrix} \tag{5-33}$$

- Vector f: It contains the linear coefficients of x^{ch} and x^{dch} and its size must be in line with matrix H. In order to simplify the representation of this vector, parameter k_t is defined as the sum of the accumulated charging profile (ACP_t) and the load forecast (LF_t).

$$f = \begin{bmatrix} \dfrac{2w_1[k_{aT}(cT-1) - \sum_{t=aT}^{dT}(k_t) - k_{aT}] + w_2 \cdot cT^2 \cdot C_{n,aT}^{ch}}{cT^2} \\[2ex] \dfrac{2w_1[k_{aT}(1-cT) + \sum_{t=aT}^{dT}(k_t) - k_{aT}] - w_2 \cdot cT^2 \cdot C_{n,aT}^{dch}}{cT^2} \\[2ex] \dfrac{2w_1[k_{aT+1}(cT-1) - \sum_{t=aT}^{dT}(k_t) - k_{aT+1}] + w_2 \cdot cT^2 \cdot C_{n,aT+1}^{ch}}{cT^2} \\[2ex] \dfrac{2w_1[k_{aT+1}(1-cT) + \sum_{t=aT}^{dT}(k_t) - k_{aT+1}] - w_2 \cdot cT^2 \cdot C_{n,aT+1}^{dch}}{cT^2} \\[1ex] \dots \\ \dots \\ \dots \\ \dfrac{2w_1[k_{dT}(cT-1) - \sum_{t=aT}^{dT}(k_t) - k_{dT}] + w_2 \cdot cT^2 \cdot C_{n,dT}^{ch}}{cT^2} \\[2ex] \dfrac{2w_1[k_{dT}(1-cT) + \sum_{t=aT}^{dT}(k_t) - k_{dT}] - w_2 \cdot cT^2 \cdot C_{n,dT}^{dch}}{cT^2} \end{bmatrix} \qquad (5\text{-}34)$$

- Matrix A_{eq} (5-35) and vector b_{eq} (5-36) represent the equality constraint of equation. Their sizes depend on the number of variables and equality constraints. In this case, only the equality constraint of equation (5-12) has been used.

$$A_{eq} = \left[P_n C_{n,aT}^{ch} \eta_n - \frac{P_n C_{n,aT}^{dch}}{\eta_n} \quad \dots \quad \dots \quad P_n C_{n,dT}^{ch} \eta_n - \frac{P_n C_{n,dT}^{dch}}{\eta_n} \right] \qquad (5\text{-}35)$$

$$b_{eq} = [(Q_n - q_n) \cdot BC_n] \qquad (5\text{-}36)$$

- Matrix A_{ineq} (5-37) and vector b_{ineq} (5-38) represent the inequality constraints of equations (5-10), (5-11), (5-14), (5-23) and (5-24). Except for constraint of equation (5-14), the other constraints are defined as a set of equations. This is due to these constraints must be accomplished at each time slot t. However, constraint of equation (5-14) only has to be met at departure time.

$$A_{ineq} = \begin{bmatrix}
P_n\eta_n & -P_n/\eta_n & 0 & 0 & \dots & 0 & 0 & 0 & 0 \\
P_n\eta_n & -P_n/\eta_n & P_n\eta_n & -P_n/\eta_n & \dots & 0 & 0 & 0 & 0 \\
\dots & \dots & \dots & \dots & \dots & \dots & \dots & \dots & \dots \\
P_n\eta_n & -P_n/\eta_n & P_n\eta_n & -P_n/\eta_n & \dots & P_n\eta_n & -P_n/\eta_n & 0 & 0 \\
P_n\eta_n & -P_n/\eta_n & P_n\eta_n & -P_n/\eta_n & \dots & P_n\eta_n & -P_n/\eta_n & P_n\eta_n & -P_n/\eta_n \\
-P_n\eta_n & P_n/\eta_n & 0 & 0 & \dots & 0 & 0 & 0 & 0 \\
-P_n\eta_n & P_n/\eta_n & -P_n\eta_n & P_n/\eta_n & \dots & 0 & 0 & 0 & 0 \\
\dots & \dots & \dots & \dots & \dots & \dots & \dots & \dots & \dots \\
-P_n\eta_n & P_n/\eta_n & -P_n\eta_n & P_n/\eta_n & \dots & -P_n\eta_n & P_n/\eta_n & 0 & 0 \\
-P_n\eta_n & P_n/\eta_n & -P_n\eta_n & P_n/\eta_n & \dots & -P_n\eta_n & P_n/\eta_n & -P_n\eta_n & P_n/\eta_n \\
P_n & -P_n & 0 & 0 & \dots & 0 & 0 & 0 & 0 \\
0 & 0 & P_n & -P_n & \dots & 0 & 0 & 0 & 0 \\
\dots & \dots & \dots & \dots & \dots & \dots & \dots & \dots & \dots \\
0 & 0 & 0 & 0 & \dots & P_n & -P_n & 0 & 0 \\
0 & 0 & 0 & 0 & \dots & 0 & 0 & P_n & -P_n \\
-P_n & P_n & 0 & 0 & \dots & 0 & 0 & 0 & 0 \\
0 & 0 & -P_n & P_n & \dots & 0 & 0 & 0 & 0 \\
\dots & \dots & \dots & \dots & \dots & \dots & \dots & \dots & \dots \\
0 & 0 & 0 & 0 & \dots & -P_n & P_n & 0 & 0 \\
0 & 0 & 0 & 0 & \dots & 0 & 0 & -P_n & P_n \\
0 & P_n/\eta_n & 0 & P_n/\eta_n & \dots & 0 & P_n/\eta_n & 0 & P_n/\eta_n
\end{bmatrix} \qquad (5\text{-}37)$$

$$b_{ineq} = \begin{bmatrix} (Q_n - q_n) \cdot BC_n \\ (Q_n - q_n) \cdot BC_n \\ \dots \\ (Q_n - q_n) \cdot BC_n \\ (Q_n - q_n) \cdot BC_n \\ q_n \cdot BC_n \\ q_n \cdot BC_n \\ \dots \\ q_n \cdot BC_n \\ q_n \cdot BC_n \\ GL - (ACP_{aT+1} - ACP_{aT}) + RF \cdot P_n \\ GL - (ACP_{aT+2} - ACP_{aT+1}) + RF \cdot P_n \\ \dots \\ GL - (ACP_{dT-1} - ACP_{dT-2}) + RF \cdot P_n \\ GL - (ACP_{dT} - ACP_{dT-1}) + RF \cdot P_n \\ GL + (ACP_{aT+1} - ACP_{aT}) + RF \cdot P_n \\ GL + (ACP_{aT+2} - ACP_{aT+1}) + RF \cdot P_n \\ \dots \\ GL + (ACP_{dT-1} - ACP_{dT-2}) + RF \cdot P_n \\ GL + (ACP_{dT} - ACP_{dT-1}) + RF \cdot P_n \\ Z_n \cdot BC_n \end{bmatrix} \qquad (5\text{-}38)$$

- Vectors l_b and u_b (5-39) represent the bounds of result values (x^{ch} and x^{dch}), from 0 (no charging) to 1 (charging/discharging at nominal power). Dimension must be in line with the vector of variables to be determined.

$$l_b = \begin{bmatrix} 0 \\ 0 \\ \dots \\ 0 \end{bmatrix}; \quad u_b = \begin{bmatrix} 1 \\ 1 \\ \dots \\ 1 \end{bmatrix} \qquad (5\text{-}39)$$

The variable u is the key factor to balance the response of this optimization algorithm. A low value of u implies a predominance of cost optimization part over variance optimization part. As value of weight u increases, the variance optimization part will have more influence in the control response. In fact, if $u=0$ the same results as cost optimization algorithm will be obtained. In contrast, if $u=1$ results of variance minimization algorithm will be obtained. In this new MOO algorithm two approaches have been analyzed. In the first one no load forecasting is considered (MOO-NF) while in the second one load forecasting is used (MOO-WF).

5.7.2 Static weight

In this subsection, MOO algorithms have been tested in order to know how they behave at different PEV-PRs, using static values of weight u. That is, the weight u does not change during the charging process and is the same for all PEVs connected to the distribution network. Firstly, the MOO-NF algorithm which does not use load forecasting is analyzed.

5.7.2.1 MOO-NF

No load forecasting is used in this solution and, therefore, parameter *LF* of equation (5-25) is set to zero. A set of simulations has been carried out in order to determine the behavior of MOO-NF when the u value is modified, from 0 to 1 in steps of 0.1.

From Table 5.19 to Table 5.24 results obtained from the simulation of the MOO-NF smart charging algorithm, for 10, 30, 50, 70, 90 and 100% of PEV-PR, are presented. These tables show the values obtained for the different parameters of interest such as charging cost, overall load variance, peak power, etc. With regard to charging cost, it should be pointed out that only spot market prices are taken into account. If taxes are added, the charging cost will be significantly higher. In addition, the minimum line-neutral voltage achieved in any of the three phases of the node 613 is also presented. Finally, the time in minutes during which this voltage is below to 0.9 p.u. is also included in the last column of the tables.

Table 5.19 shows the values obtained for 10% of PEV-PR (11 PEVs). As value of u increases, overall charging cost increases and PEVs power demand variance is reduced, as expected. All values of u outperforms the uncontrolled case. For example, charging cost is reduced at least 18% while overall load variance is reduced by 35%. In addition, peak power is also reduced from 227kW to at least 210kW. With regard to line-neutral voltages at the furthest node, they are increased to similar values than the case where no PEVs are charged in the distribution network.

Table 5.19. MOO-NF: comparative analysis of results obtained with 10% of PEV-PR

Case of study	Overall charging cost (€)	Overall load variance (kW²)	PEVs power variance (kW²)	Overall peak power (kW)	PEVs peak power (kW)	Min. 613 node voltage (p.u.)	Time below 0.9p.u. (min)
No PEVs	-	1039	-	206	-	0.9468	0
Uncontrolled	7.39	1599	81	227	40	0.92	0
MOO-NF u=0	5.08	890	181	206	62	0.927	0
MOO-NF u=0.1	5.08	882	167	206	50	0.9309	0
MOO-NF u=0.2	5.11	832	101	206	37	0.9409	0
MOO-NF u=0.3	5.17	848	68	206	27	0.9468	0
MOO-NF u=0.4	5.21	871	55	206	23	0.9447	0
MOO-NF u=0.5	5.24	888	47	206	21	0.9416	0
MOO-NF u=0.6	5.3	911	42	206	19	0.9409	0
MOO-NF u=0.7	5.38	935	37	206	16	0.9398	0
MOO-NF u=0.8	5.55	970	30	208	13	0.941	0
MOO-NF u=0.9	5.76	1001	24	209	12	0.9379	0
MOO-NF u=1	6.04	1045	17	210	10	0.9426	0

Table 5.20 presents the results of 30% of PEV-PR (29 PEVs). All solutions are feasible because they do not exceed maximum power supply of the distribution transformer neither the minimum voltage at furthest node. Best solution is achieved when u takes a value of 0.2, being peak power equal than no PEV case (206kW), while minimum voltage at node 613 is approximately 0.93 p.u. Charging cost is also reduced around 22% and overall load variance in approximately 75%, respect to the uncontrolled case. It can be pointed out the increase of peak power in the case of u equal to zero, due to the influence of charging cost optimization part of the objective function.

Table 5.20. MOO-NF: comparative analysis of results obtained with 30% of PEV-PR

Case of study	Overall charging cost (€)	Overall load variance (kW²)	PEVs power variance (kW²)	Overall peak power (kW)	PEVs peak power (kW)	Min. 613 node voltage (p.u.)	Time below 0.9p.u. (min)
No PEVs	-	1039	-	206	-	0.9468	0
Uncontrolled	16.53	2266	327	253	66	0.9016	0
MOO-NF u=0	12.53	1193	921	220	122	0.9105	0
MOO-NF u=0.1	12.59	972	644	206	101	0.9181	0
MOO-NF u=0.2	12.92	807	295	206	52	0.931	0
MOO-NF u=0.3	13.43	871	217	206	40	0.9318	0
MOO-NF u=0.4	13.79	915	179	206	34	0.9308	0
MOO-NF u=0.5	14.15	919	148	207	32	0.9276	0
MOO-NF u=0.6	14.34	952	134	209	30	0.9268	0
MOO-NF u=0.7	14.68	986	115	211	28	0.9257	0
MOO-NF u=0.8	14.85	1008	107	211	27	0.9278	0
MOO-NF u=0.9	14.99	1036	100	212	25	0.9237	0
MOO-NF u=1	15.17	1056	89	212	24	0.9204	0

At 50% of PEV penetration (Table 5.21), 23 PEVs more have been added from previous case, making a total of 52 PEVs. The value of weight u of 0.2 is also the better solution in terms of overall load variance (978kW²). Using this value, charging cost is reduced nearly 19% and overall load variance more than 70%, respect to uncontrolled case. Weight values below 0.2 do not provide valid solutions due to low voltages achieved at node 613.

Table 5.21. MOO-NF: comparative analysis of results obtained with 50% of PEV-PR

Case of study	Overall charging cost (€)	Overall load variance (kW²)	PEVs power variance (kW²)	Overall peak power (kW)	PEVs peak power (kW)	Min. 613 node voltage (p.u.)	Time below 0.9p.u. (min)
No PEVs	-	1039	-	206	-	0.9468	0
Uncontrolled	28.75	3340	839	290	111	**0.8816**	**102**
MOO-NF u=0	21.88	2439	2579	315	209	**0.8006**	**160**
MOO-NF u=0.1	21.97	1724	1898	278	176	**0.8385**	**90**
MOO-NF u=0.2	23.36	978	721	206	91	0.8786	10
MOO-NF u=0.3	24.1	1016	516	207	65	0.9103	0
MOO-NF u=0.4	24.79	1056	416	210	55	0.9176	0
MOO-NF u=0.5	25.48	1078	351	212	51	0.9174	0
MOO-NF u=0.6	25.86	1105	322	214	47	0.9229	0
MOO-NF u=0.7	26.2	1128	295	215	43	0.9253	0
MOO-NF u=0.8	26.42	1141	280	216	42	0.9285	0
MOO-NF u=0.9	26.59	1147	268	217	41	0.9266	0
MOO-NF u=1	26.74	1158	254	218	40	0.9299	0

At 70% of PEV-PR (72 PEVs), valid solutions have been achieved for values of weight u between 0.2 and 1, as can be seen in Table 5.22. In this case, best result in terms of overall load variance is obtained when u is 0.3 (1259kW²). A saving of almost 16% (from 38.97 to 32.89€) of charging cost can be achieved while a reduction of approximately 76% of load variance is obtained. Only u values from 0.3 to 0.7 maintain the minimum line-neutral voltages, at node 613, above 0.9 p.u.

Table 5.22. MOO-NF: comparative analysis of results obtained with 70% of PEV-PR

Case of study	Overall charging cost (€)	Overall load variance (kW²)	PEVs power variance (kW²)	Overall peak power (kW)	PEVs peak power (kW)	Min. 613 node voltage (p.u.)	Time below 0.9p.u. (min)
No PEVs	-	1039	-	206	-	0.9468	0
Uncontrolled	38.97	5244	1870	320	126	**0.8537**	**132**
MOO-NF *u*=0	29.32	4542	4828	**412**	292	**0.8045**	**140**
MOO-NF *u*=0.1	29.73	2589	3013	334	226	**0.8478**	**150**
MOO-NF *u*=0.2	30.86	1422	1409	230	132	0.8712	30
MOO-NF *u*=0.3	32.89	1259	869	216	97	0.9037	0
MOO-NF *u*=0.4	33.46	1261	756	216	90	0.9084	0
MOO-NF *u*=0.5	34.47	1265	630	216	81	0.9163	0
MOO-NF *u*=0.6	35	1282	578	216	75	0.907	0
MOO-NF *u*=0.7	35.49	1314	537	217	70	0.9038	0
MOO-NF *u*=0.8	35.90	1319	494	219	63	0.896	20
MOO-NF *u*=0.9	36.34	1319	448	222	54	0.8915	50
MOO-NF *u*=1	36.48	1335	433	225	51	0.8942	20

When PEV-PR is increased to 90% (93 PEVs), valid solutions are reduced to 0.4, 0.5, 0.6 and 0.7 values of weight *u*. Best value in this case is achieved when *u* is 0.5, in terms of overall load variance, providing an improvement in overall load variance of 77% and a reduction of 7% in charging cost. Peak power value achieves 224kW which is totally manageable for the distribution transformer, currently installed in the network. It should be pointed out that high values of *u* start to give not valid results due to low voltages achieved at 613 node, as shown in Table 5.23.

Table 5.23. MOO-NF: comparative analysis of results obtained with 90% of PEV-PR

Case of study	Overall charging cost (€)	Overall load variance (kW²)	PEVs power variance (kW²)	Overall peak power (kW)	PEVs peak power (kW)	Min. 613 node voltage (p.u.)	Time below 0.9p.u. (min)
No PEVs	-	1039	-	206	-	0.9468	0
Uncontrolled	47.46	6408	2770	366	182	**0.8106**	**247**
MOO-NF *u*=0	37.69	7382	7393	**499**	357	**0.6982**	**350**
MOO-NF *u*=0.1	38.09	4426	5048	398	277	**0.7663**	**460**
MOO-NF *u*=0.2	41.21	1742	1803	247	146	**0.8513**	280
MOO-NF *u*=0.3	41.20	1713	1610	223	114	**0.8951**	**100**
MOO-NF *u*=0.4	42.96	1527	1205	224	100	0.9006	0
MOO-NF *u*=0.5	44.15	1484	1021	224	86	0.8771	40
MOO-NF *u*=0.6	44.55	1495	966	223	80	0.8741	20
MOO-NF *u*=0.7	45.04	1489	905	222	76	0.878	65
MOO-NF *u*=0.8	45.36	1500	872	221	74	**0.8786**	**100**
MOO-NF *u*=0.9	45.55	1506	847	221	72	**0.8859**	**87**
MOO-NF *u*=1	45.86	1528	817	222	70	**0.8724**	**85**

Finally, for 100% of PEV-PR, which implies the charging of 97 PEVs, values for weight *u* of 0.3 to 0.6 and 0.9 provide valid solutions of voltages at node 613 (Table 5.24). Among them, weight value of 0.5 is the best in terms of overall load variance. In this case, load

variance is reduced from 6842kW^2 of uncontrolled case to 1579kW^2, achieving a reduction of 77% while charging cost is reduced around 7%.

Table 5.24. MOO-NF: comparative analysis of results obtained with 100% of PEV-PR

Case of study	Overall charging cost (€)	Overall load variance (kW²)	PEVs power variance (kW²)	Overall peak power (kW)	PEVs peak power (kW)	Min. 613 node voltage (p.u.)	Time below 0.9p.u. (min)
No PEVs	-	1039	-	206	-	0.9468	0
Uncontrolled	49.85	6842	3063	374	189	**0.8125**	**262**
MOO-NF *u*=0	39.67	7987	7980	**501**	362	**0.6881**	**380**
MOO-NF *u*=0.1	39.95	4840	5522	**402**	282	**0.7701**	**480**
MOO-NF *u*=0.2	42.63	1961	2114	250	149	**0.8535**	**360**
MOO-NF *u*=0.3	43.66	1809	1695	228	122	0.8954	5
MOO-NF *u*=0.4	45.71	1596	1250	228	101	0.8989	5
MOO-NF *u*=0.5	46.28	1579	1148	228	91	0.884	5
MOO-NF *u*=0.6	46.81	1581	1070	227	84	0.8949	5
MOO-NF *u*=0.7	47.32	1577	1005	226	80	**0.8702**	**85**
MOO-NF *u*=0.8	47.67	1587	969	225	77	**0.7829**	**185**
MOO-NF *u*=0.9	47.85	1591	943	225	76	0.8789	70
MOO-NF *u*=1	48.17	1612	909	225	74	**0.8701**	**85**

From the results presented in Table 5.20 and Table 5.24, the relationship between charging cost and PEVs power variance can be determined (Figure 5.40) for 30 and 100% of PEV-PR respectively. As can be observed, this curve is not constant and will vary from case to case, because it depends on parameters such as: number of PEVs connected to the network, charging and driving behavior, electricity prices, etc.

(a)   (b)
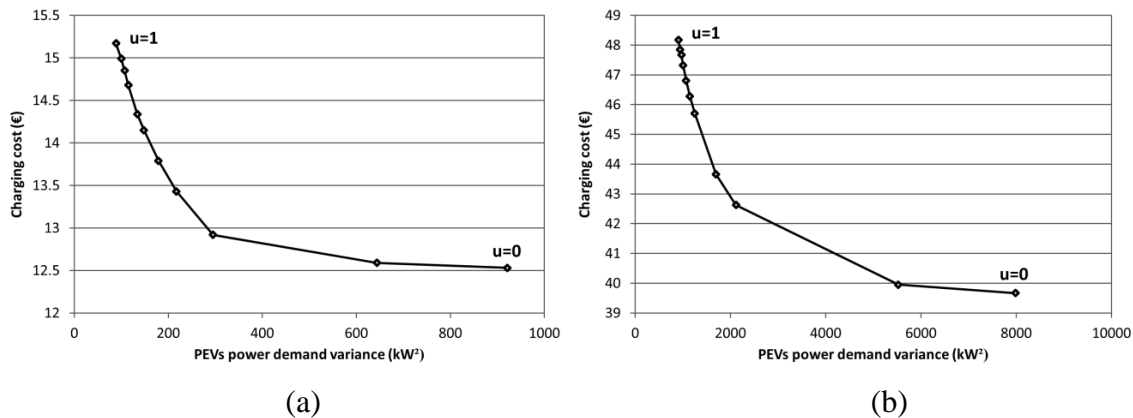
Figure 5.40. Evolution of charging cost and PEVs power demand variance in function of weight *u* for the MOO-NF algorithm: (a) 30% of PEV-PR and (b) 100% of PEV-PR

Additionally, apart from charging cost and PEVs power demand variance, it is important to know the behavior of overall load variance, because it is an indicator of how good the solution is for distribution system operation. Figure 5.41 shows the overall load variance for 30 and 100% of PEV-PR, using different values of weight *u*. For the 30% PEV-PR case, overall load variance decreases with high values of *u* until approximately 0.2, where a minimum is achieved. After this point, overall load variance increases again, as can be seen in Figure 5.41-a. In contrast, for 100% of PEV-PR (Figure 5.41-b), *u* values from 0.4 to 1 provide similar results in terms of overall load variance.

(a)

(b)
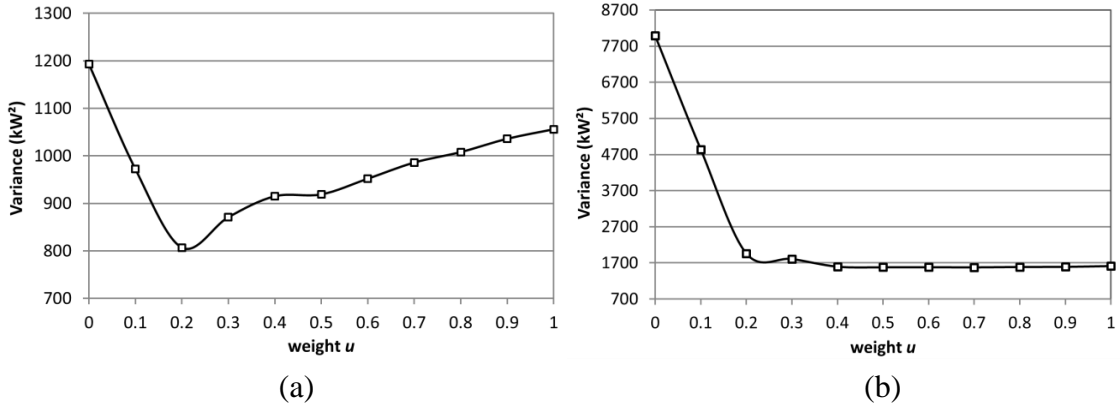
Figure 5.41. Evolution of overall load variance for the MOO-NF algorithm: (a) 30% of PEV-PR and (b) 100% of PEV-PR

Figure 5.42 and Figure 5.43 show the results obtained when applying a value of u equal to 0.2, while in Figure 5.44 and Figure 5.45 results are presented for u equal to 0.8. In these figures, the PEV-PR case of 30% has been used. When u is equal to 0.2, no increase of peak power is produced while valley filling is achieved, as can be seen in Figure 5.42-a. Also, an increase of PEVs power demand is noticeable when electricity prices are low. With regard to voltages at node 613 (Figure 5.42-b), the charge of the PEVs does not get worse the voltage profile at night time compared to cost optimization algorithm, where voltages reaches values below 0.92 p.u. (see Figure 5.24-b). However, there is an important voltage unbalance because of the charging process of PEVs.

(a)

(b)
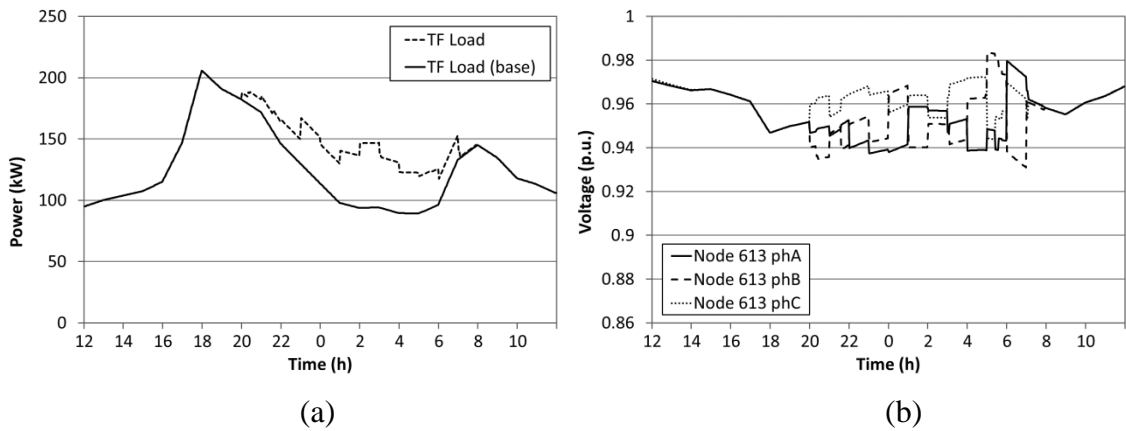
Figure 5.42. MOO-NF case with $u=0.2$: (a) Load in the distribution transformer and (b) line-neutral voltages at node 613

PEVs peak power reaches about 52kW when electricity prices are the lowest of the day. Then, sharps reductions of PEVs power demand appear at 06:00 and 07:00h, as can be seen in Figure 5.43-a. In addition, it is noticeable that PEVs are charged during hours of lower electricity prices. Evolution of the SOC of each PEV shows that every PEV is charged as expected and, unlike in cost optimization algorithm (Figure 5.25-b), the charge of PEVs is more distributed along the time, as can be seen in Figure 5.43-b.

(a)   (b)
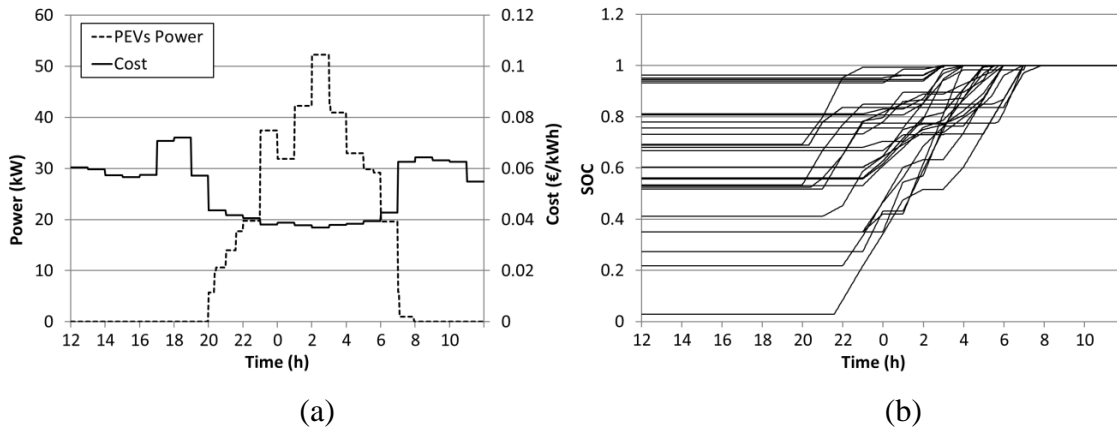
Figure 5.43. MOO-NF case with u=0.2: (a) PEVs power demand and electricity cost and (b) evolution of SOC of each PEV

Increasing the value of u to 0.8 provides a wider distribution of the charge of PEVs, at the expense of slightly increasing overall peak power (Figure 5.44-a). As a consequence, a worsening of voltage profile at node 613 happens at peak hours (Figure 5.44-b).

(a)   (b)
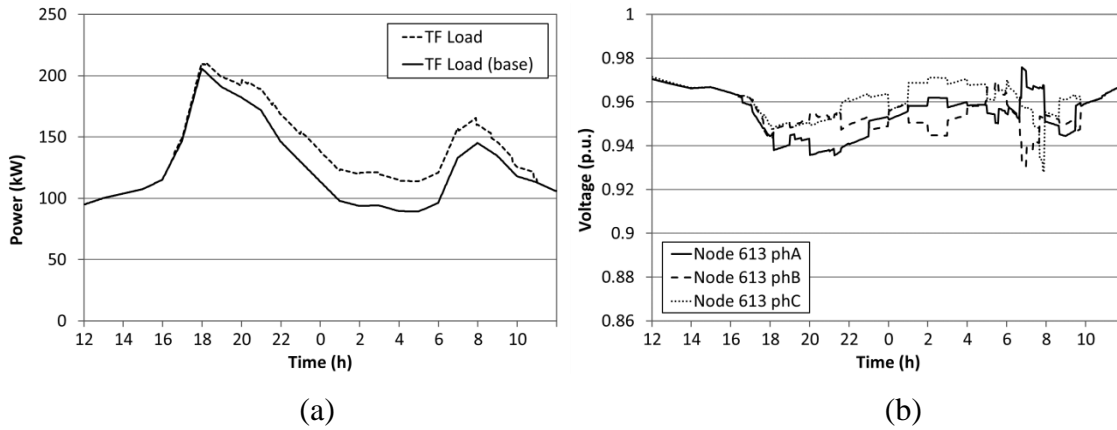
Figure 5.44. MOO-NF case with u=0.8: (a) Load in the distribution transformer and (b) line-neutral voltages at node 613

The maximum PEVs power demand is reduced from 52kW to 30kW (Figure 5.45-a). With regard to the SOC evolution of PEVs (Figure 5.45-b), it is more distributed than in the previous case (Figure 5.43-b), showing that a higher value of u reduces the load variance.

(a)   (b)
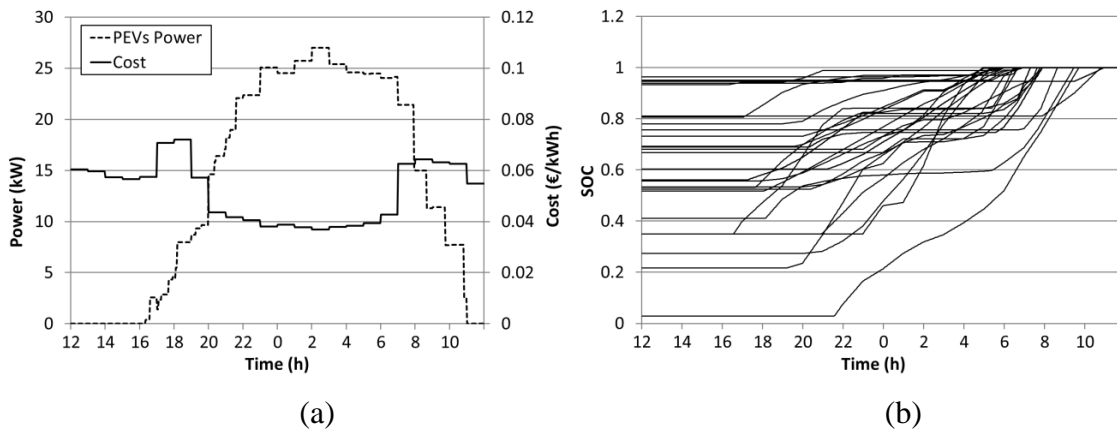
Figure 5.45. MOO-NF case with u=0.8: (a) PEVs power demand and electricity cost and (b) evolution of SOC of each PEV

Figure 5.46 shows the PEVs power demand for values of u of 0, 0.2, 0.6 and 1. As expected, PEV peak power demand is reduced when u tends to 1. However, increasing the value of weight u can overlap PEVs power demand with households load demand, increasing this way the peak power. In contrast, when using low values of weight u, the peak power is produced by cost optimization part of MOO-NF algorithm at off-peak hours and it can be greater than household load demand peak power, depending on the PEV-PR. Thus, a trade-off between charging too many PEVs at off-peak hours or partly increase the peak power must be considered.
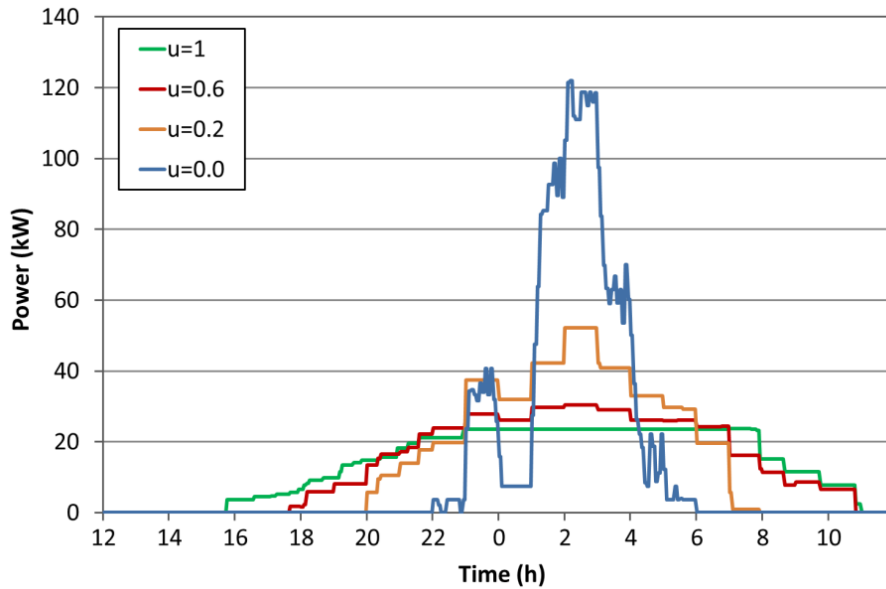
Figure 5.46. MOO-NF case. PEVs power demand for different values of u, with 30% of PEVs penetration rate

The main limiting factors for the safe integration of PEVs in LV distribution networks are the voltage drops and the unbalances that they produce. With regard to the last one, Figure 5.47 shows the different power demand of PEVs per phase, for two different cases. It can be seen that PEV charging process will produce voltage unbalances.

(a)   (b)
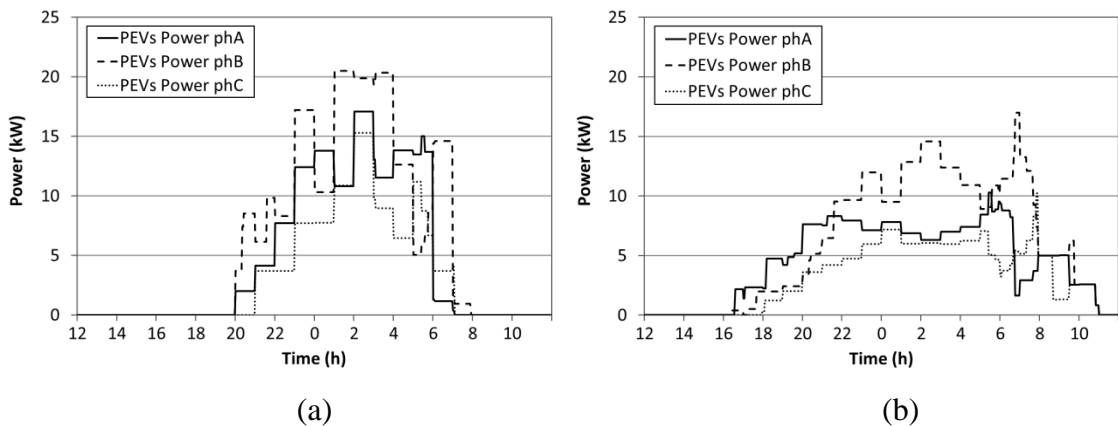
Figure 5.47. PEV power demand per phase using the MOO-NF algorithm with a PEV-PR of 30%: (a) Weight u equal to 0.2 and (b) weight u equal to 0.8

As a conclusion, the proposed MOO-NF algorithm has proven its ability to manage the multiple charging of PEVs. Additionally, no load forecast is used while charging cost and

overall load variance is improved respect to uncontrolled case. However, when PEV-PR increases, it is necessary to select adequately the numerical value of variable u. With regard to this aspect, *u* values from the range between 0.2 and 0.5 provide feasible solutions in terms of overall load variance, peak power and voltage at furthest node. Additionally, this short range of only 0.3 indicates that normalization of the objective function has been carried out correctly.

5.7.2.2   MOO-WF

In contrast to the MOO-NF algorithm, the MOO-WF algorithm uses load forecasting. Thus LF vector of the objective function shown in equation (5-25) is not zero. Including load forecasting may improve significantly load variance and reduce power losses. From Table 5.25 to Table 5.30 results from the simulation of the MOO-WF smart charging algorithm, for 10, 30. 50, 70, 90 and 100% of PEV-PR, are presented.

Table 5.25 shows the results obtained from a PEV-PR of 10%. Due to the low penetration rate, all values of the weight *u* provide valid solutions. As expected, best value in terms of overall load variance is achieved when *u* is one. This fact is kept throughout all PEV-PRs due to the usage of load forecasting. However, charging cost is the highest between all possible *u* values (5.17€). Anyway, a charging cost reduction of 30% and an overall load variance reduction around 52% is achieved, when value of weight *u* takes one, respect to the uncontrolled case. In all *u* values, overall peak power demand remains the same that the case where no PEVs are charged. With regard to line-neutral voltages at node 613, best values are achieved when *u* is 0.8 or more.

Table 5.25. MOO-WF: comparative analysis of results obtained with 10% of PEV-PR

Case of study	Overall charging cost (€)	Overall load variance (kW²)	PEVs power variance (kW²)	Overall peak power (kW)	PEVs peak power (kW)	Min. 613 node voltage (p.u.)	Time below 0.9p.u. (min)
No PEVs	-	1039	-	206	-	0.9468	0
Uncontrolled	7.39	1599	81	227	40	0.92	0
MOO-WF *u*=0	5.08	891	181	206	62	0.927	0
MOO-WF *u*=0.1	5.08	887	179	206	50	0.9296	0
MOO-WF *u*=0.2	5.08	882	175	206	50	0.9309	0
MOO-WF *u*=0.3	5.08	878	172	206	50	0.9309	0
MOO-WF *u*=0.4	5.08	871	167	206	50	0.9309	0
MOO-WF *u*=0.5	5.08	858	159	206	50	0.9309	0
MOO-WF *u*=0.6	5.09	841	145	206	47	0.9309	0
MOO-WF *u*=0.7	5.11	814	119	206	39	0.9272	0
MOO-WF *u*=0.8	5.12	791	106	206	35	0.9399	0
MOO-WF *u*=0.9	5.15	780	93	206	27	0.9415	0
MOO-WF *u*=1	5.17	774	97	206	27	0.9434	0

Also, all weight values give valid solutions when PEV-PR is 30%, as can be seen in Table 5.26. However, low *u* values increase overall peak power (220kW for *u*=0). It can be seen that reducing value of weight *u* leads to an increase of PEVs peak power demand. For example, for *u* equal to zero, the PEVs peak power demand reaches 122kW, 72kW more than the other extreme case, that is, when *u* value takes one. In this last case, a decrease of 71% of overall load variance and 20% of charging cost is achieved when is compared with the uncontrolled case.

Table 5.26. MOO-WF: comparative analysis of results obtained with 30% of PEV-PR

Case of study	Overall charging cost (€)	Overall load variance (kW²)	PEVs power variance (kW²)	Overall peak power (kW)	PEVs peak power (kW)	Min. 613 node voltage (p.u.)	Time below 0.9p.u. (min)
No PEVs	-	1039	-	206	-	0.9468	0
Uncontrolled	16.53	2266	327	253	66	0.9016	0
MOO-WF u=0	12.53	1193	921	220	122	0.9105	0
MOO-WF u=0.1	12.56	1088	812	208	111	0.9022	0
MOO-WF u=0.2	12.6	1000	739	206	107	0.9012	0
MOO-WF u=0.3	12.6	894	650	206	100	0.9172	0
MOO-WF u=0.4	12.63	820	576	206	87	0.9125	0
MOO-WF u=0.5	12.7	732	493	206	70	0.9121	0
MOO-WF u=0.6	12.74	706	471	206	65	0.9132	0
MOO-WF u=0.7	12.88	679	428	206	55	0.9143	0
MOO-WF u=0.8	13.01	666	406	206	52	0.9222	0
MOO-WF u=0.9	13.14	660	386	206	51	0.9241	0
MOO-WF u=1	13.31	652	366	206	50	0.9386	0

In the case of 50% of PEV-PR (Table 5.27), values of u from 0.4 to 1 provide feasible solutions in terms of maximum peak power and minimum voltages at node 613. First valid solution (u=0.4) provides a cost reduction of 22% and an overall load variance reduction of 68% respect to uncontrolled case. In contrast, when value of weight u takes one, it provides a charging cost reduction of 16% and an overall load variance reduction of 77%.

Table 5.27. MOO-WF: comparative analysis of results obtained with 50% of PEV-PR

Case of study	Overall charging cost (€)	Overall load variance (kW²)	PEVs power variance (kW²)	Overall peak power (kW)	PEVs peak power (kW)	Min. 613 node voltage (p.u.)	Time below 0.9p.u. (min)
No PEVs	-	1039	-	206	-	0.9468	0
Uncontrolled	28.75	3340	839	290	111	**0.8816**	**102**
MOO-WF u=0	21.88	2439	2578	315	209	**0.8006**	**160**
MOO-WF u=0.1	21.96	1755	1964	275	172	**0.8312**	**145**
MOO-WF u=0.2	22.13	1447	1699	261	159	**0.8453**	**150**
MOO-WF u=0.3	22.23	1265	1521	247	147	**0.8615**	**130**
MOO-WF u=0.4	22.37	1048	220	220	122	0.8792	50
MOO-WF u=0.5	22.94	891	1056	206	101	0.8691	10
MOO-WF u=0.6	23.37	813	929	206	83	0.8956	5
MOO-WF u=0.7	23.82	776	832	206	74	0.9078	0
MOO-WF u=0.8	23.87	774	822	206	74	0.9061	0
MOO-WF u=0.9	23.92	772	812	206	73	0.9086	0
MOO-WF u=1	24.07	759	787	206	73	0.9161	0

With regard to 70% of PEV-PR (Table 5.28), valid solutions are 0.2, 0.4 and 0.6 to 1 of weight u values. On the one hand, when weight u is equal to 0.2, a reduction of charging cost about 24% and a reduction of 61% in terms of overall load variance is achieved. On the other hand, when u takes a value of 1, the solution provides a reduction around 14% of charging cost and 82% of overall load variance. Voltages at node 613 are improved as u

value get close to one. Regarding to peak power, solutions with 0.6 to 1 do not add extra power demand.

Table 5.28. MOO-WF: comparative analysis of results obtained with 70% of PEV-PR

Case of study	Overall charging cost (€)	Overall load variance (kW²)	PEVs power variance (kW²)	Overall peak power (kW)	PEVs peak power (kW)	Min. 613 node voltage (p.u.)	Time below 0.9p.u. (min)
No PEVs	-	1039	-	206	-	0.9468	0
Uncontrolled	38.97	5244	1870	320	126	**0.8537**	**132**
MOO-WF *u*=0	29.32	4541	4827	**412**	292	**0.7928**	**160**
MOO-WF *u*=0.1	29.42	3207	3726	358	246	**0.8324**	80
MOO-WF *u*=0.2	29.71	2022	2626	299	195	0.8567	40
MOO-WF *u*=0.3	30.48	1538	2048	262	161	**0.8833**	80
MOO-WF *u*=0.4	31.72	1163	1545	224	126	0.8922	70
MOO-WF *u*=0.5	31.71	1147	1498	216	118	**0.8862**	80
MOO-WF *u*=0.6	32.19	1070	1378	210	113	0.8762	65
MOO-WF *u*=0.7	32.77	998	1258	206	103	0.8891	20
MOO-WF *u*=0.8	33.18	956	1179	206	93	0.9055	0
MOO-WF *u*=0.9	33.30	926	1137	206	87	0.9025	0
MOO-WF *u*=1	33.56	905	1093	206	85	0.9088	0

Finally, Table 5.29 and Table 5.30 show the results for 90 and 100% of PEV-PR, respectively. In both cases, no feasible solution can be achieved because of the low voltages reached at node 613. Taking into account this situation, for high values of weight *u* (from 0.7 to 1), the overall load variance is relatively low and the peak power is the same than in the no PEVs case. Therefore, it is necessary to introduce a mechanism to improve the voltage profile of the distribution network.

Table 5.29. MOO-WF: comparative analysis of results obtained with 90% of PEV-PR

Case of study	Overall charging cost (€)	Overall load variance (kW²)	PEVs power variance (kW²)	Overall peak power (kW)	PEVs peak power (kW)	Min. 613 node voltage (p.u.)	Time below 0.9p.u. (min)
No PEVs	-	1039	-	206	-	0.9468	0
Uncontrolled	47.46	6408	2770	366	182	**0.8106**	**247**
MOO-WF *u*=0	37.69	7382	7393	**499**	357	**0.6982**	**180**
MOO-WF *u*=0.1	37.97	4740	5357	**408**	285	**0.6956**	**190**
MOO-WF *u*=0.2	38.55	3169	3964	344	230	**0.7204**	**185**
MOO-WF *u*=0.3	39.43	2211	2970	284	180	**0.8364**	**185**
MOO-WF *u*=0.4	40.71	1726	2380	239	139	**0.8262**	**147**
MOO-WF *u*=0.5	41.27	1558	2137	223	123	**0.8306**	**180**
MOO-WF *u*=0.6	41.68	1473	2008	213	115	**0.8634**	**180**
MOO-WF *u*=0.7	42.23	1399	1873	206	109	**0.8702**	**105**
MOO-WF *u*=0.8	42.47	1379	1824	206	108	**0.8753**	**180**
MOO-WF *u*=0.9	42.66	1355	1784	206	107	**0.8814**	**125**
MOO-WF *u*=1	42.99	1329	1730	206	105	**0.8888**	**230**

Table 5.30. MOO-WF: comparative analysis of results obtained with 100% of PEV-PR

Case of study	Overall charging cost (€)	Overall load variance (kW²)	PEVs power variance (kW²)	Overall peak power (kW)	PEVs peak power (kW)	Min. 613 node voltage (p.u.)	Time below 0.9p.u. (min)
No PEVs	-	1039	-	206	-	0.9468	0
Uncontrolled	49.85	6842	3063	374	189	0.8125	262
MOO-WF u=0	39.67	7988	7980	501	361	0.6881	205
MOO-WF u=0.1	39.9	5397	5991	428	302	0.6756	215
MOO-WF u=0.2	40.6	3217	4093	338	227	0.7485	180
MOO-WF u=0.3	41.8	2271	3056	285	180	0.8184	185
MOO-WF u=0.4	42.92	1829	2512	241	141	0.8381	140
MOO-WF u=0.5	43.64	1658	2264	224	124	0.8266	175
MOO-WF u=0.6	43.89	1599	2172	218	119	0.8627	180
MOO-WF u=0.7	44.39	1523	2044	211	113	0.8751	180
MOO-WF u=0.8	44.73	1497	1978	207	112	0.8665	212
MOO-WF u=0.9	44.92	1467	1932	206	111	0.8769	190
MOO-WF u=1	45.24	1437	1870	206	109	0.8824	250

Figure 5.48 presents the charging cost and the overall load variance for 30 and 100% of PEV-PR, using different values of u. Both figures present similar shapes. However, for 30% of PEV-PR (Figure 5.48-a) has a better distribution of solution points than for 100% of PEV-PR. In the last case, solution points are concentrated near to the left side of the Figure 5.48-b (high cost and low variance). The reason is that as PEV-PR grows, low values of u increase exponentially the value of overall load variance. Thus, u values below 0.5 should not be considered for a real implementation, especially at high PEV-PRs.

(a)   (b)
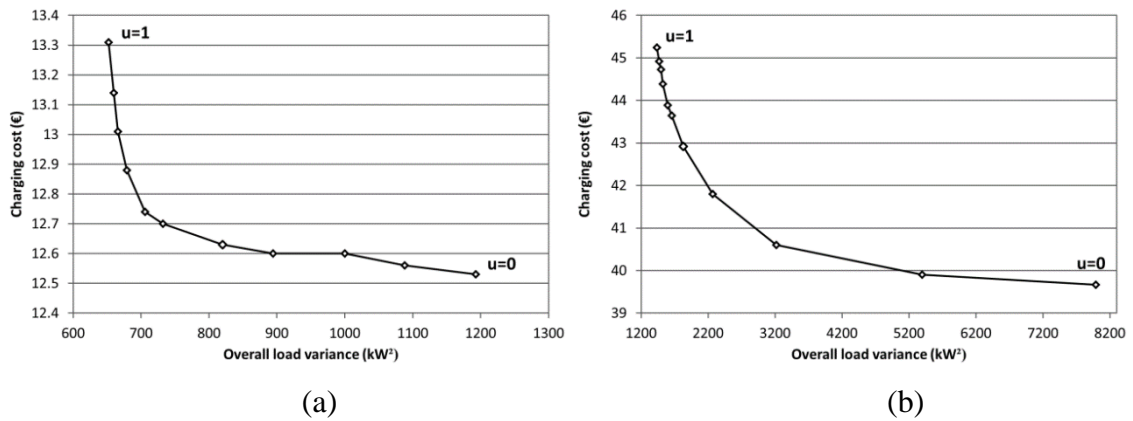
Figure 5.48. Evolution of charging cost and overall load variance in function of weight u for the MOO-WF algorithm (a) 30% of PEV-PR and (b) 100% of PEV-PR

Following, two specific cases of 30% PEV-PR are presented, specifically for weight u equal to 0.2 and 0.8. For the 0.2 case a noticeable increase of PEVs power demand happens because of the influence of cost optimization algorithm (Figure 5.49-a). This peak power is almost as high as household peak and reaches a value of 204kW. As a consequence, line-neutral voltage of phase A at node 613 are also reduced to 0.9 p.u. approximately, as can be seen in Figure 5.49-b. In addition, the effect of slope limit constraints is also noticed as PEVs power increase and decrease are not done instantaneously.

(a)   (b)
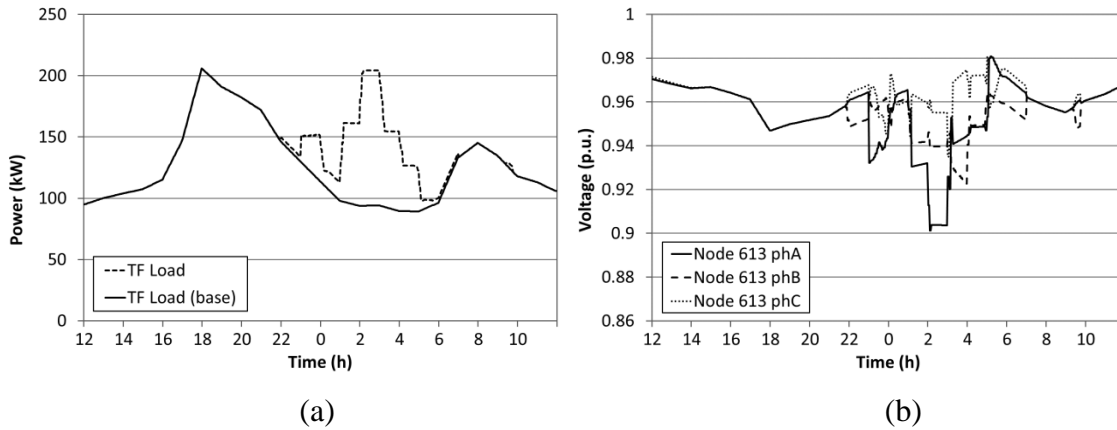
Figure 5.49. MOO-WF case with u=0.2. (a) Load in the distribution transformer and (b) line-neutral voltages at node 613

Similar conclusions can be obtained from Figure 5.50-a and Figure 5.50-b. Most of the PEVs are charged between 01:00 and 05:00h when the hourly electricity prices are the lowest ones. PEVs peak power reaches a value of 107kW between 02:00 and 03:00h. Two hours later, at 05:00h, almost all PEVs are totally charged, as shown in Figure 5.50-b, resulting in an important fall of PEVs power demand. The minimum power demand of PEVs is around 100kW during the nighttime. Almost all PEVs are charged at maximum charging power to take advantage of low electricity prices. As results have shown, a u value of 0.2 has harmful effects on the distribution network due to the concentration of PEVs power demand.

(a)   (b)
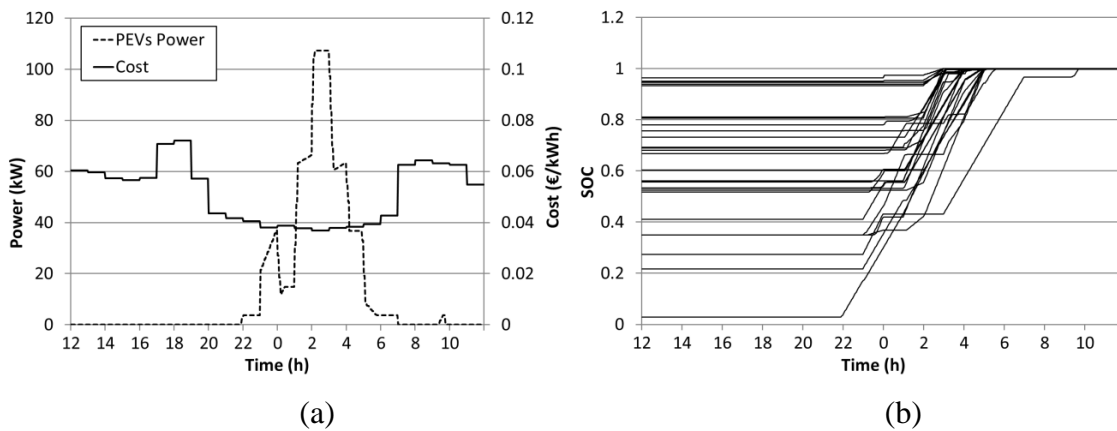
Figure 5.50. MOO-WF case with u=0.2. (a) PEVs power demand and electricity cost and (b) evolution of the SOC of each PEV

Increasing the weight u to 0.8 gives more relevance to overall load variance minimization part of the algorithm. Thus, night peak is reduced from previous 207kW to 144kW as well as minimum load demand is established at about 130kW during nighttime (Figure 5.51-a), allowing a better integration of renewable energies. Line-neutral voltages at node 613 remain above 0.92 p.u. during all simulation time (Figure 5.51-b). As in the previous cases, voltage unbalances appear during PEVs charging time.

(a)   (b)
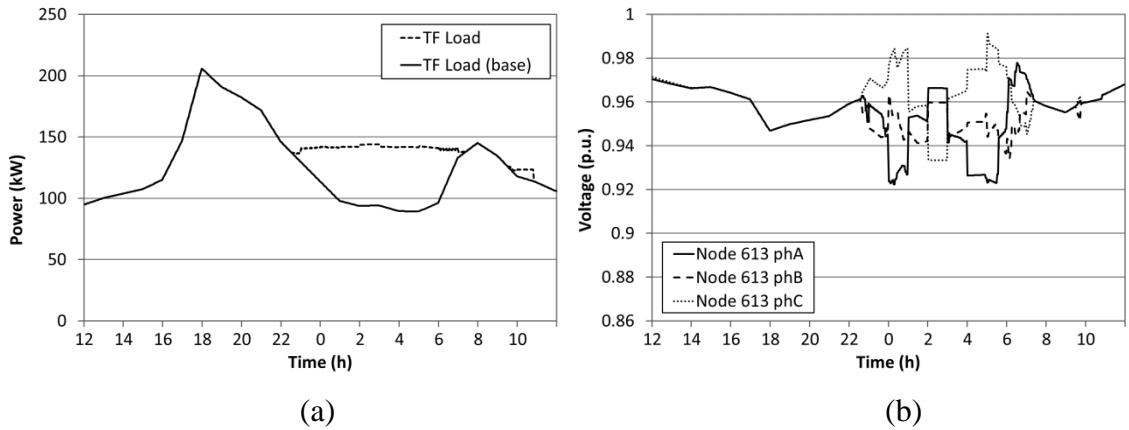
Figure 5.51. MOO-WF case with *u*=0.8. (a) Load of distribution transformer and (b) line-neutral voltages at node 613

Additionally, in contrast to the previous case, a significant number of PEVs start their charging process between 23:00 and 01:00h, as shown in Figure 5.52-a. Also, PEVs peak power is reduced from previous 107kW to 51kW. The evolution of the SOC of each PEV during the simulation verifies that all PEVs are charged in a more distributed way, as can be seen in Figure 5.52-b.

(a)   (b)
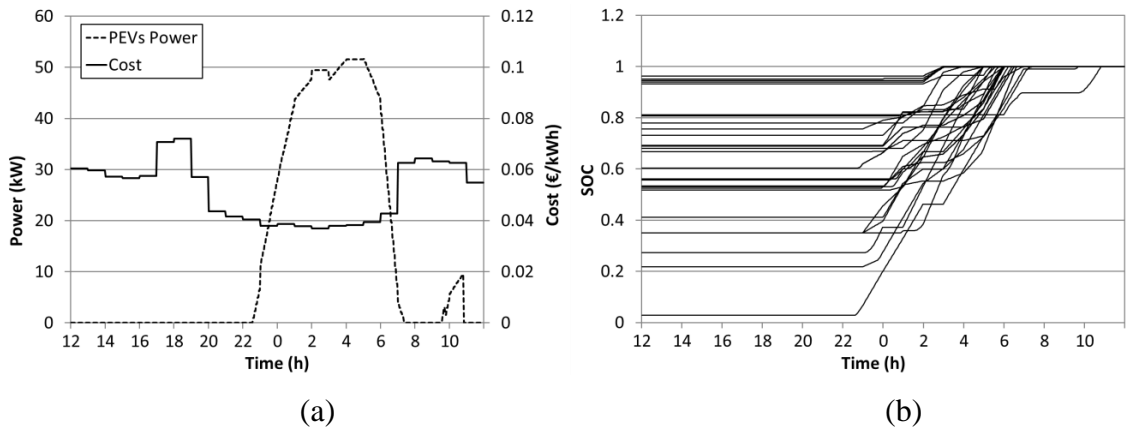
Figure 5.52. MOO-WF case with *u*=0.8. (a) PEVs power demand and electricity cost and (b) evolution of the SOC of each PEV

Figure 5.53 shows the PEVs power demand for *u* values of 0, 0.2, 0.6 and 1. As expected, PEVs peak power is reduced when *u* tends to 1. Because of load forecasting is used, increasing *u* to 1 does not increase the power demand at peak hours as it happens in the MOO-NF algorithm.

Thus, the best solution in terms of network reliability is achieved when *u* is 1. Note that in all cases, the PEVs charging process start almost at the same time (23:00h), while in the MOO-NF solution, it depends largely on the weight *u* value and ranges between 16:00 to 23:00h, as shown in Figure 5.46.
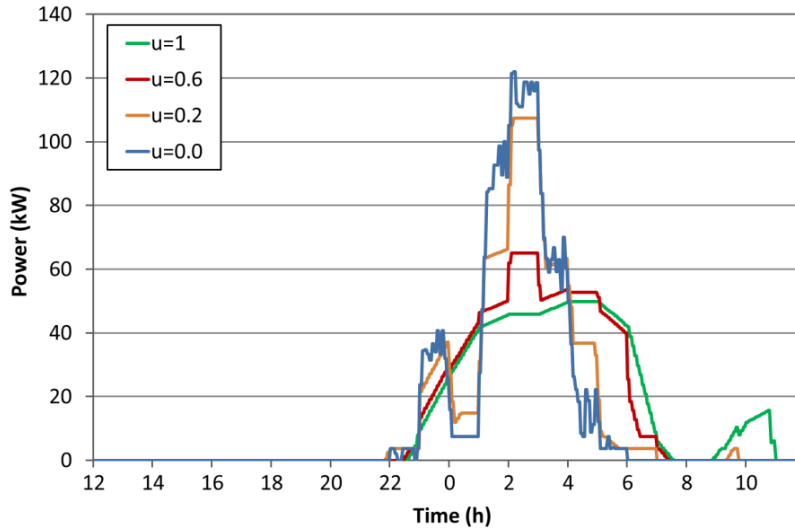
Figure 5.53. MOO-WF case. PEVs power demand for different u values, with 30% of PEV-PR

Therefore, including load forecasting to load variance minimization algorithm avoid adding more power demand at typical peak hours and achieves better results to carry out a valley filling effect. However, load forecasting is needed and the lack of accuracy on this forecast may affect to final results. Additionally, although the charging of PEVs are optimally dispatched, there are problems due to voltage unbalances generated by the charging of PEVs. Finally, a mechanism to select the value of weight u must be designed. In this context, fuzzy control technique can be used.

5.7.3   Dynamic weight selection

A set of different optimized results can be obtained when variable u is modified. So, it is necessary to design an automated weight control which can modify that weight u in function of several parameters. In this thesis, two different control strategies based on fuzzy control are presented, one for the MOO-NF algorithm and the other one for the MOO-WF algorithm.

5.7.3.1   MOO-NF

A control strategy for the MOO-NF algorithm, in function on voltage level at PEV connection point and electricity prices, has been developed. Electricity prices can be used as an indicator of how much loaded is the network, i.e. the highest hourly prices usually correspond with peak hours. Moreover, voltage level can be measured easily at the connection point of the PEV. Depending of electricity price and voltage level values, four cases can be distinguished:

1. Low voltage at high price hours: It is the most common case. This situation indicates that distribution network is high loaded at peak hours. So, in order to delay the charging of the PEVs, weight u must be low. This way, price optimization cost is more relevant in the MOO, which has the effect of delaying the charging of the PEVs to off-peak hours.

2. Low voltage at low price hours: It is the contrary case of the previous one. This situation indicates that there is too much connected load at low prices because of excessive

charging of PEVs at off-peak hours. The variable u should be increased in order to smooth the charging profile of the PEVs

3. High voltage at high price hours: This situation indicates excessive generation at peak hours. It can be caused by the use of distributed generation or the use of V2G for trading energy. This is the less common case. The variable u should be increased in order to add charging power demand of PEVs at peak hours.

4. High voltage at low price hours: As previous case, an excessive generation of distributed generators, such as wind generators, can produce an increase of voltage at off-peak hours. In this case, the variable u should be decreased in order to give more importance to minimization of charging cost. This way, voltage will be reduced due to the increase of PEVs charging demand at off-peak hours.

So, taken into account these four cases, a DM has been developed based on the fuzzy control method. This control is performed continuously, that is, every change in electricity prices or in the node voltage may lead the execution of the MOO-NF algorithm. This way, each PEV will execute the optimization algorithm more than once. However, the execution of this method must be limited in order to reduce the fluctuations. Hence, in the following cases, the MOO-NF algorithm will not be executed:

- If departure time happens in less than an hour.
- If the difference between the new calculated values of weight u is less than 0.05, compared to the last value of u used.
- If an execution of the MOO-NF algorithm has been already done in that time slot.

As commented before, the fuzzy control output depends on the node voltage in which each PEV is connected to and the electricity cost. Voltage limits have been selected in line with EN50160 European Standard. Moreover, limits values of weight u (0.1 to 0.6) have been set taking into account the results obtained in section 5.7.2.1. Best results for fixed weight values were achieved when the weight u was between 0.2 and 0.5. An additional margin of 0.1 has been added to those limits. Figure 5.54 shows the fuzzy control surface which defines the value of the weight u. Electricity cost is limited between minimum value of the day (0.03692€/kWh) and maximum value of the day (0.0721€/kWh).

Table 5.31 shows the results achieved from simulating the dynamic value selection of weight u for the four PEV-PR cases, compared to best achieved results using static values of weight u. With some exceptions, charging cost is higher using the automatic weight selection. With regard to overall load variance, automatic weight selection does not improve it in all cases. Furthermore, voltages at node 613 are worse than in the fixed cases, especially at high PEV-PRs. The reason is that voltage unbalances are bigger when several algorithm executions are made per PEV, as shown in Table 5.31.

It is noticeably that in the only case where voltage of dynamic weight selection is better than with static weight selection (PEV-PR of 50%), the voltage unbalance factor (VUF) is also better. For PEV-PR of 70, 90 and 100%, VUF is relatively higher and voltages at node 613 are lower than the limit established by EN50160, taking into account only a period of 24h instead of the whole week. Later, an improvement in this aspect will be presented.
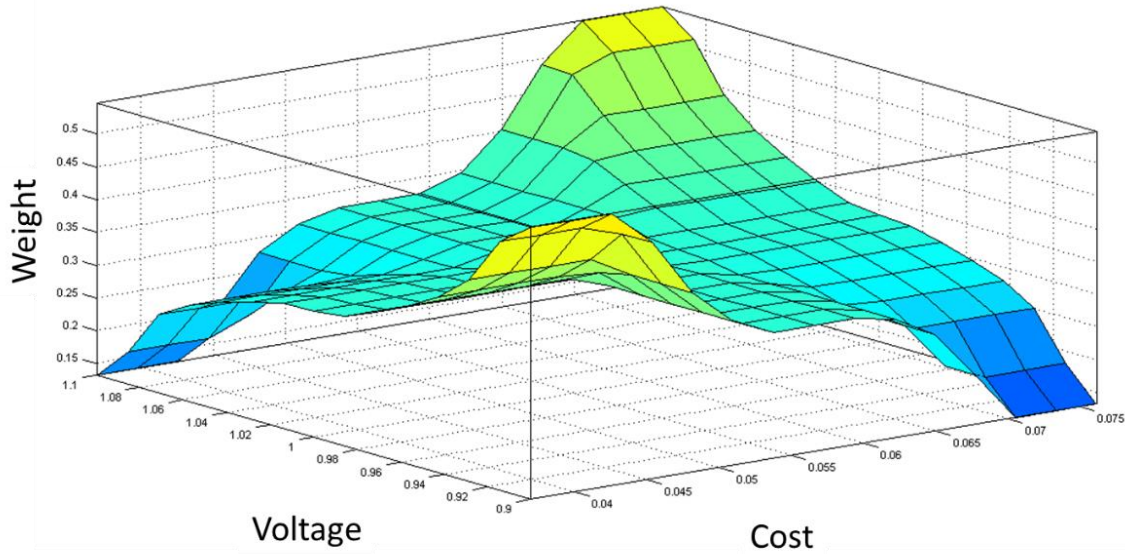
Figure 5.54. Fuzzy control surface for the MOO-NF algorithm

Table 5.31. Results obtained from automatic weight control for MOO-NF algorithm

Case of study (PEV-PR)	Overall charging cost (€)	Overall load variance (kW²)	PEVs power variance (kW²)	Overall peak power (kW)	Energy losses (kWh)	Max. VUF (%)	Min. 613 node voltage (p.u.)	Time below 0.9p.u. (min)
No PEVs	-	1039	-	206	56	0.011	0.9468	0
MOO-NF u=0.2 (10%)	5.11	832	37	206	62	0.348	0.9409	0
MOO-NF auto (10%)	5.16	844	70	206	62	0.366	0.9398	0
MOO-NF u=0.2 (30%)	12.92	807	295	206	71	0.596	0.931	0
MOO-NF auto (30%)	13.66	900	206	192	71	0.665	0.9269	0
MOO-NF. u=0.2 (50%)	23.36	978	721	206	80	1.182	0.8786	10
MOO-NF auto (50%)	25.13	1031	417	209	79	0.839	0.9098	0
MOO-NF u=0.4 (70%)	32.89	1259	869	216	97	0.873	0.9037	0
MOO-NF auto (70%)	34.31	1159	659	214	93	1.387	**0.8699**	**75**
MOO-NF u=0.5 (90%)	44.15	1484	1021	224	112	1.165	0.8771	40
MOO-NF auto (90%)	43.82	1557	1119	230	113	1.483	**0.8636**	**105**
MOO-NF u=0.5 (100%)	46.28	1579	1148	228	115	1.021	0.884	5
MOO-NF auto (100%)	46.49	1705	1220	238	116	2.372	**0.8306**	**72**

Figure 5.55 shows the load of the distribution transformer for 10, 30, 50, 70, 90 and 100% of PEV-PR cases, respectively. For PEV-PRs lower than 70%, there is not an increase of peak power. However, at higher PEV-PRs, peak power is increased to almost 230kW. Nonetheless, the MOO-NF algorithm provides feasible solutions except for 90 and 100% of PEV-PR cases. As an example, at 70% of PEV-PR, the MOO-NF reduces charging cost by approximately 14%, overall load variance by 76% and overall peak power by 32%, respect to the uncontrolled case.
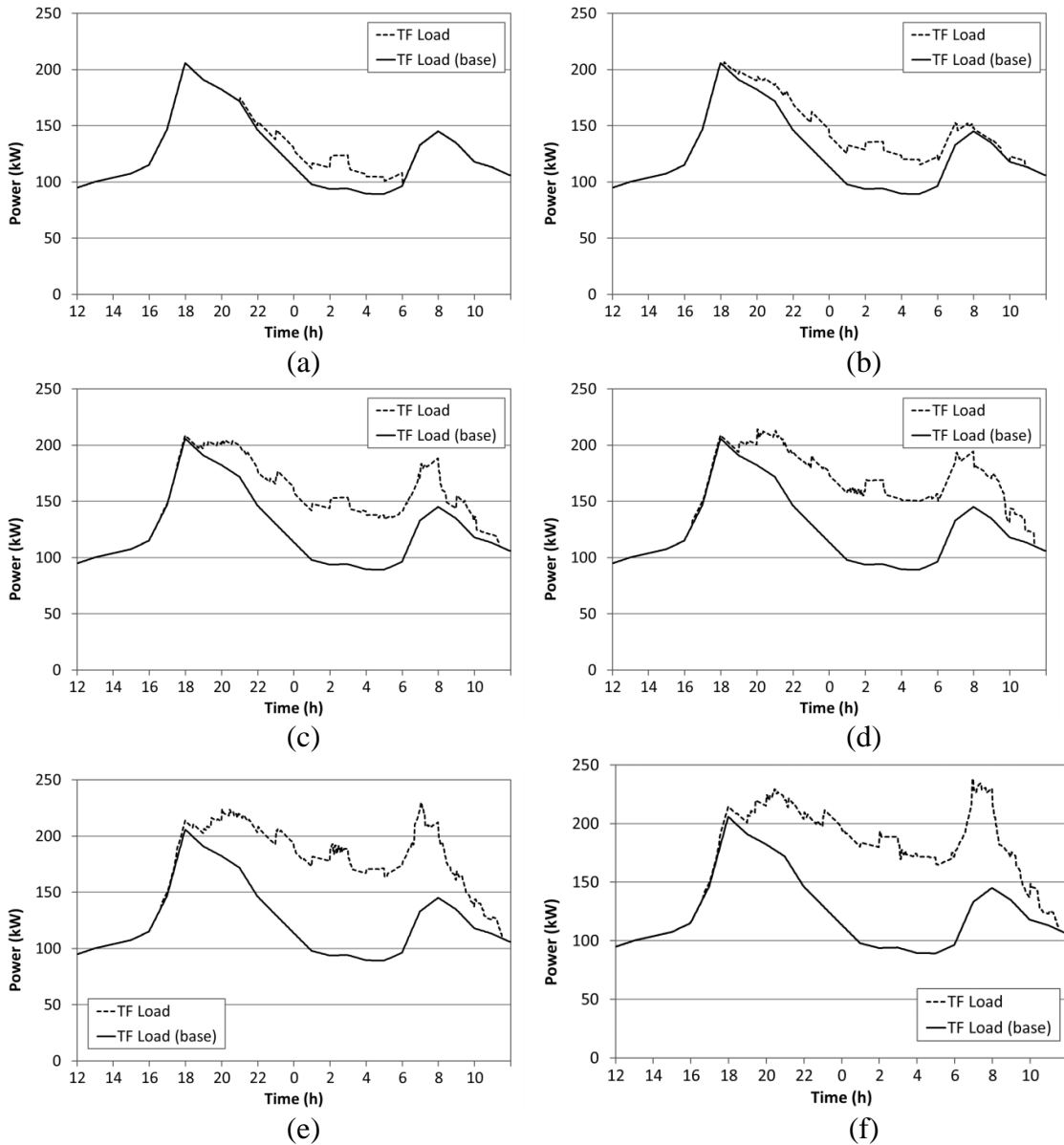
Figure 5.55. Distribution transformer load for different PEV-PR using MOO-NF algorithm: (a) 10%, (b) 30%, (c) 50%, (d) 70%, (e) 90% and (f) 100%

Thus, the MOO-NF algorithm has proven to be an effective one for reducing impacts at low penetration rates, without using load forecasting. However, at high penetration rates it tends to increase voltage unbalances and overall peak power. Thus, it is necessary to reduce the voltage unbalances. Furthermore, it is not easy to predict what the charging profile of all PEVs connected to the distribution network will be. Thus, it is necessary to introduce load forecasting in order to improve these aspects. In the following subsection the analysis of the MOO with load forecasting is presented.

5.7.3.2   MOO-WF

In this case, load forecasting has been included. Additionally, fuzzy control system has been modified to improve the algorithm results. Fuzzy control has been defined based on the local calculation of average power and load variance from the ACP and LF data, which is sent to each PEV. This way, the PEV controller can obtain an overall status of the distribution network and schedule its charging profile, in order to improve load variance

and charging cost. In contrast to the MOO-NF solution, this optimization algorithm is only executed once per PEV, when it is connected to the distribution network. This way, it is easier to an external entity, such as a DSO, to know beforehand the power demand of PEVs. In addition, the amount of data interchanged between the PEVs and the aggregator is reduced.

Fuzzy control has been designed to reduce overall load variance when its value is high or the distribution network is highly loaded. Thus, weight u takes high values for these two cases. In contrast, charging cost is improved only if both load variance and average load level are low, as can be seen in Figure 5.56. In this case, weight u has been limited from 0.5 to 1, taking into account the results obtained in subsection 5.7.2.2.
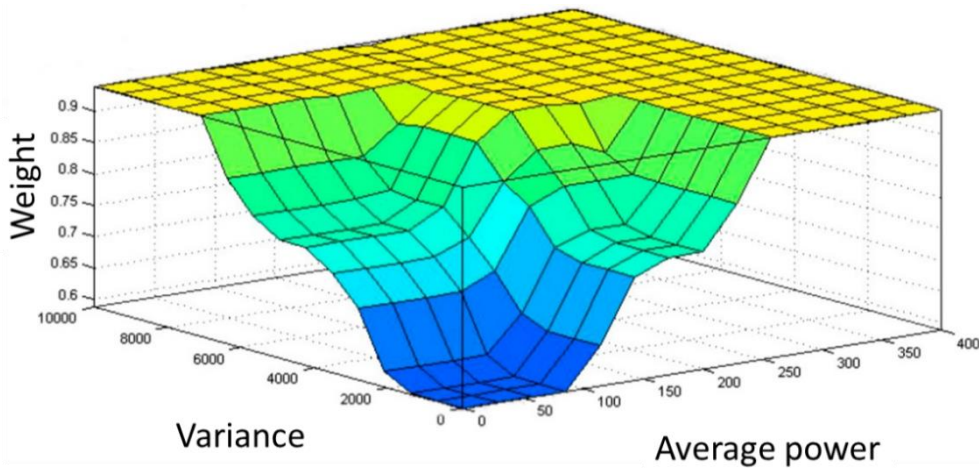
Figure 5.56. Fuzzy control surface for the MOO-WF algorithm

Table 5.32 shows the results achieved from simulating the automatic weight selection for the four cases of PEV-PRs. In all cases, charging cost is reduced compared to static weight u solutions but, in turn, overall load variance is slightly increased. For the analyzed cases, charging cost is reduced about 2% compared to static weight solution.

Table 5.32. Results obtained from automatic weight control for the MOO-WF algorithm

Case of study (PEV-PR)	Overall charging cost (€)	Overall load variance (kW²)	Overall peak power (kW)	PEVs peak power (kW)	Energy losses (kWh)	Max. VUF (%)	Min. 613 node voltage (p.u.)	Time below 0.9p.u. (min)
No PEVs	-	1039	206	-	56	0.011	0.9468	0
MOO-WF *u*=1 (10%)	5.17	774	206	27	61	0.396	0.9434	0
MOO-WF auto (10%)	5.11	816	206	39	62	0.611	0.9272	0
MOO-WF *u*=1 (30%)	13.31	652	206	50	71	0.48	0.9386	0
MOO-WF auto (30%)	12.97	671	206	53	71	0.802	0.9186	0
MOO-WF. *u*=1 (50%)	24.07	759	206	73	80	0.729	0.9161	0
MOO-WF auto (50%)	23.86	775	206	74	80	0.89	0.9066	0
MOO-WF *u*=1 (70%)	33.56	905	206	85	94	0.745	0.9088	0
MOO-WF auto (70%)	33.13	958	206	97	95	1.032	**0.8885**	**80**
MOO-WF *u*=1 (90%)	42.99	1329	206	105	115	0.949	**0.8888**	230
MOO-WF auto (90%)	42.43	1384	206	108	116	1.517	**0.8684**	180
MOO-WF *u*=1 (100%)	45.24	1437	206	109	118	1.141	**0.8824**	250
MOO-WF auto (100%)	44.66	1502	207	112	120	1.43	**0.8643**	215

In terms of overall peak power, both solutions give the same value (206kW). Thus, there is no increase of peak power in all cases, providing better results than the MOO-NF algorithm. Regarding to node 613 line-neutral voltages, only PEV-PRs of 90 and 100% are out of the boundaries established in this thesis. In this aspect, both the MOO-NF and the MOO-WF algorithms do not give valid solutions.

Finally, Figure 5.57 presents the load in the distribution transformer for the different analyzed cases. It is noticeably the influence of the charging cost part of the MOO-WF algorithm, especially at low PEV-PRs.

Figure 5.57. Distribution transformer load for different PEV-PR using the MOO-WF algorithm: (a) 10%, (b) 30%, (c) 50%, (d) 70%, (e) 90% and (f) 100%

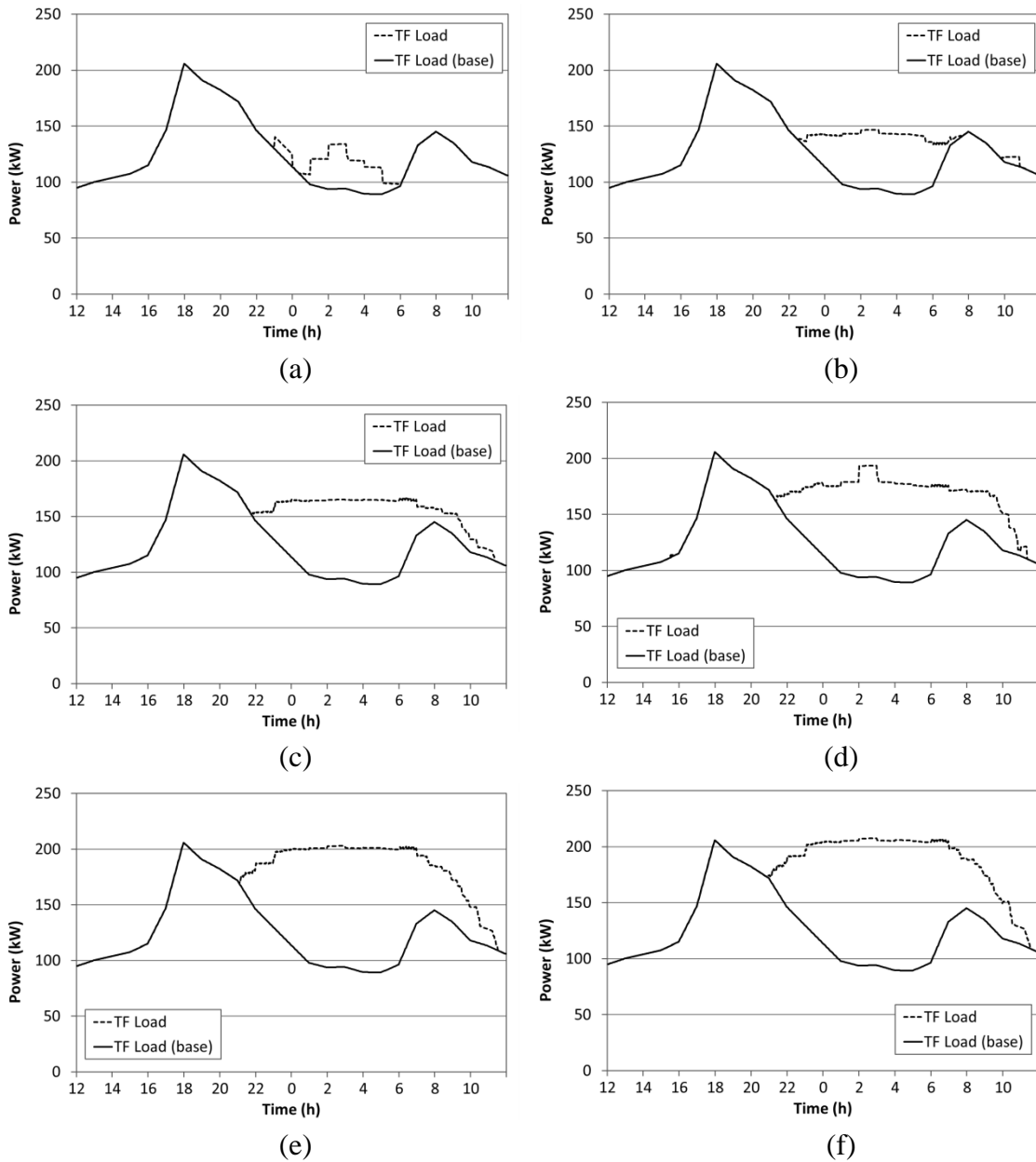However, as PEV-PR increases the charging cost part of the algorithm is less important. This way, impacts generated by PEVs charging process are reduced and the ability of the designed fuzzy controller to cope with different number of PEVs has been proven. As

expected, voltages at node 613 are lower in the MOO-WF case, compared to fixed or static weight solution. The reason is that voltage unbalances are increased when dynamic weight selection is used because the different values used of weight u between the PEVs.

To conclude, a fuzzy controller as a DM has proven to be a feasible method to control the charging process of multiple PEVs. However, there are voltage values under the limit established in the EN50160 standard. One option to reduce these voltages deviations is to implement a mechanism to minimize load unbalances between the three phases.

5.7.4   Voltage unbalance reduction (VUR)

Voltage unbalances induced by the charging of a significant number of PEVs can produce several problems, such as power losses in lines and increase of core losses in induction motors and power transformers [139], [140]. Voltage unbalances are measured using the Voltage Unbalance Factor (VUF), which is the percentage of the negative sequence voltage (V_2) divided by the positive sequence voltage (V_1), as can be seen in equation (5-40). According to the EN50160 standard, this value should be below 2%, for 95% of the time of a week.

$$VUF(\%) = \frac{V_2}{V_1} \cdot 100 \qquad\qquad (5\text{-}40)$$

Two types of voltages unbalances generated by PEVs can be distinguished: one generated by the random distribution of PEVs along the three phases (different energy demand per phase) and the other one due to different charging scheduling between phases (lack of coordination). This last one can be reduced by coordinating the PEVs charging processes at the same time, as cost and variance optimization is carried out. This way, voltage unbalances will be reduced and voltage profile of the distribution network will be improved.

The new factor introduced to achieve the mentioned control is based on splitting the ACP in four parts, one per phase and other one which is the sum of the other three. When a three phase charger is used, the overall ACP data will be used for the optimization algorithm. However, for single-phase charger the corresponding ACP, according to the phase, will be used. This way, overall variance is not only improved but also the variance of each phase. Furthermore, PEVs charging power at each phase will be equitably distributed and voltage unbalances and deviations will be limited.

Additionally, in low voltage distribution networks with high natural unbalances, different load forecasting per phase can be used. Thus, voltage unbalances produced by household or other loads could be reduced. In this case, household loads have been considered balanced. This assumption has been made to analyze the unbalanced induced by the charging of PEVs. In case of unbalanced household loads, the results will be different, better or worse, depending on the unbalances produced by the combination of PEVs and household loads.

5.7.4.1   MOO-NF

The VUR method has been applied to the MOO-NF and the MOO-WF algorithms. Table 5.33 shows the results obtained for the MOO-NF algorithm. In all PEV-PRs, voltages at node 613 are improved, especially at high PEV-PRs. In fact, after applying this method, all cases have met the EN50160 regulation.

The proposed VUR method achieves an important reduction of negative sequence component and voltage unbalance factor. In addition, a noticeably improvement in charging cost is also obtained in all cases. Overall peak power is also reduced, especially at high PEV-PRs. Regarding to energy losses, VUR algorithm version gives similar values than no VUR version.

Table 5.33. Summary of results using VUR method for the MOO-NF algorithm

Case of study (PEV-PR)	Overall charging cost (€)	Overall load variance (kW²)	Overall peak power (kW)	Energy losses (kWh)	Max. neg. sequence voltage node 613 (p.u.)	Max. VUF (%)	Min. 613 node voltage (p.u.)	Time below 0.9p.u. (min)
MOO-NF (10%)	5.16	844	206	62	0.0035	0.366	0.9398	0
MOO-NF (10%) VUR	5.11	835	206	62	0.0028	0.292	0.9456	0
MOO-NF (30%)	13.66	900	206	71	0.0063	0.665	0.9269	0
MOO-NF (30%) VUR	12.99	809	206	71	0.004	0.423	0.9342	0
MOO-NF (50%)	25.13	1031	209	79	0.008	0.839	0.9098	0
MOO-NF (50%) VUR	24.32	950	206	79	0.0051	0.532	0.9281	0
MOO-NF (70%)	34.31	1158	214	93	0.013	1.387	**0.8699**	**75**
MOO-NF (70%) VUR	32.44	1181	212	94	0.0089	0.945	0.8965	10
MOO-NF (90%)	43.82	1557	230	113	0.0139	1.483	**0.8636**	**105**
MOO-NF (90%) VUR	42.78	1502	220	113	0.0059	0.636	0.9093	0
MOO-NF (100%)	46.49	1705	238	116	0.0219	2.372	**0.8306**	**72**
MOO-NF (100%) VUR	44.74	1651	224	117	0.0089	0.965	0.8981	5

Figure 5.58 and Figure 5.59 present the line-neutral voltages at node 613 and the PEVs power demand per phase, for no VUR and VUR algorithms respectively. Results correspond to a PEV-PR of 30%. The minimum voltage achieved for no VUR case is 0.9267 p.u. in phase b, while for VUR case, this minimum is 0.9344 in phase a. With regard to VUF, it is reduced from 0.665 to 0.423. Note that PEVs load demand is more concentrated and balanced for VUR case than for no VUR case. In both cases, the energy demanded per phase of PEVs is the same.

(a) (b)

Figure 5.58. MOO-NF without VUR, for 30% of PEV-PR: (a) Line-neutral voltages of node 613 and (b) PEV power demand per phase

(a)   (b)

Figure 5.59. MOO-NF with VUR, for 30% of PEV-PR: (a) Line-neutral voltages of node
613 and (b) PEV power demand per phase

Figure 5.60 and Figure 5.61 present similar results, but for 100% of PEV-PR. In this case,
voltage improvement is more noticeably. Minimum voltage is enhanced from 0.8369 p.u.
of no VUR to 0.889 p.u. of VUR case, both for phase b. In Annex B, more results of all
PEV-PR cases can be found.

(a)   (b)

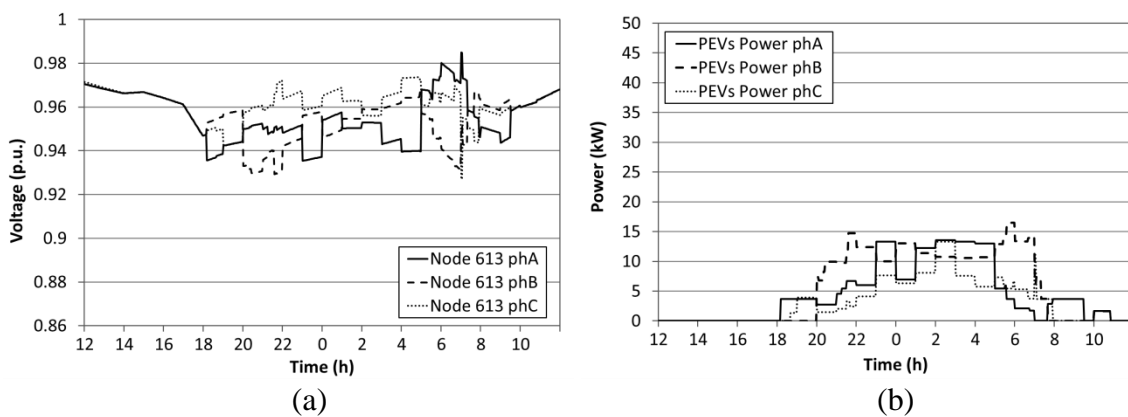Figure 5.60. MOO-NF without VUR, for 100% of PEV-PR: (a) Line-neutral voltages of
node 613 and (b) PEV power demand per phase

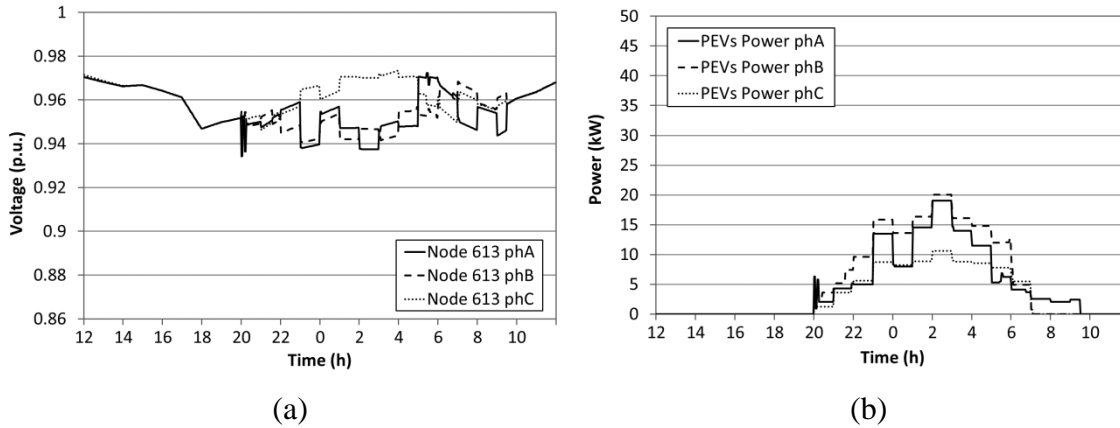(a)   (b)

Figure 5.61. MOO-NF with VUR, for 100% of PEV-PR: (a) Line-neutral voltages of
node 613 and (b) PEV power demand per phase

5.7.4.2   MOO-WF

In a similar way, VUR is also applied to the MOO-WF algorithm. Table 5.34 shows the obtained results. A reduction of negative sequence component has been achieved for all cases, without any exception. PEV-PRs of 90 and 100% deserve a special mention. An important reduction of negative sequence voltage has been achieved, which has led an increase of the minimum voltage at node 613. In addition, a little improvement in total charging cost is achieved in all cases, except for 10% of PEV-PR, while overall load variance and energy losses are almost not affected.

Table 5.34. Summary of results using VUR method for the MOO-WF algorithm

Case of study (PEV-PR)	Overall charging cost (€)	Overall load variance (kW²)	Overall peak power (kW)	Energy losses (kWh)	Max. neg. sequence voltage node 613 (p.u.)	Max. VUF (%)	Min. 613 node voltage (p.u.)	Time below 0.9p.u. (min)
MOO-WF (10%)	5.11	816	206	62	0.0058	0.611	0.9272	0
MOO-WF (10%) VUR	5.12	802	206	62	0.003	0.316	0.9462	0
MOO-WF (30%)	12.97	671	206	71	0.0076	0.802	0.9186	0
MOO-WF (30%) VUR	12.78	688	206	71	0.0038	0.397	0.9292	0
MOO-WF (50%)	23.86	775	206	80	0.0084	0.89	0.9066	0
MOO-WF (50%) VUR	23.62	788	206	80	0.0053	0.563	0.9205	0
MOO-WF (70%)	33.13	958	206	95	0.0098	1.032	**0.8885**	**80**
MOO-WF (70%) VUR	32.56	978	206	95	0.0051	0.533	0.9238	0
MOO-WF (90%)	42.43	1384	206	116	0.0141	1.518	**0.8684**	**180**
MOO-WF (90%) VUR	42.04	1409	206	116	0.0064	0.691	0.9051	0
MOO-WF (100%)	44.66	1502	207	120	0.0133	1.43	**0.8643**	**215**
MOO-WF (100%) VUR	44.35	1522	210	119	0.0067	0.726	0.9052	0

On the one hand, Figure 5.62 and Figure 5.63 show the line-neutral voltages at node 613 and the PEVs power demand per phase for no VUR and VUR versions of the MOO-WF algorithm respectively. Results correspond to the PEV-PR of 30%. The minimum voltage achieved for no VUR case is 0.9186 p.u. while for VUR case is 0.9292 p.u., both in phase a. On the other hand, Figure 5.64 and Figure 5.65 present the results for 100% of PEV-PR. In this case, an important increase of minimum voltage is achieved (from 0.8642 to 0.9052 p.u.). In Annex C, more results of all PEV-PR cases can be found.

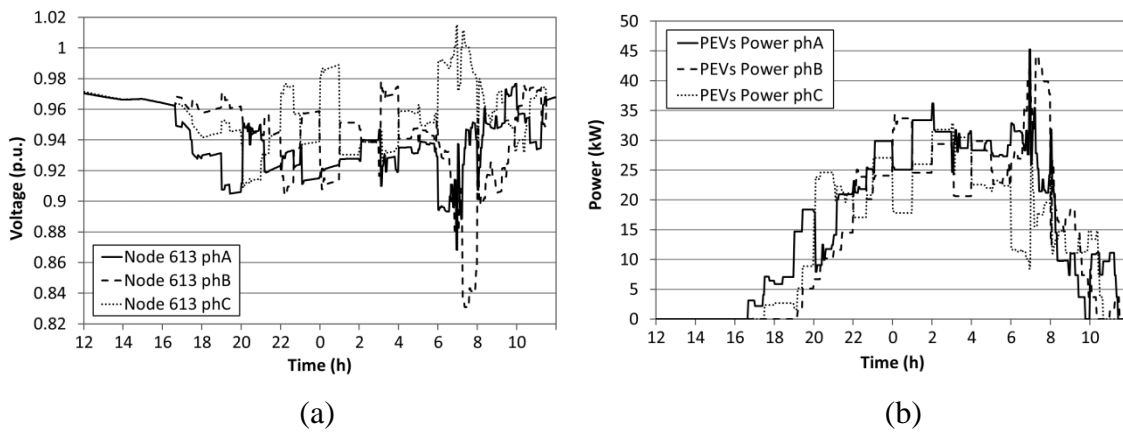(a)   (b)
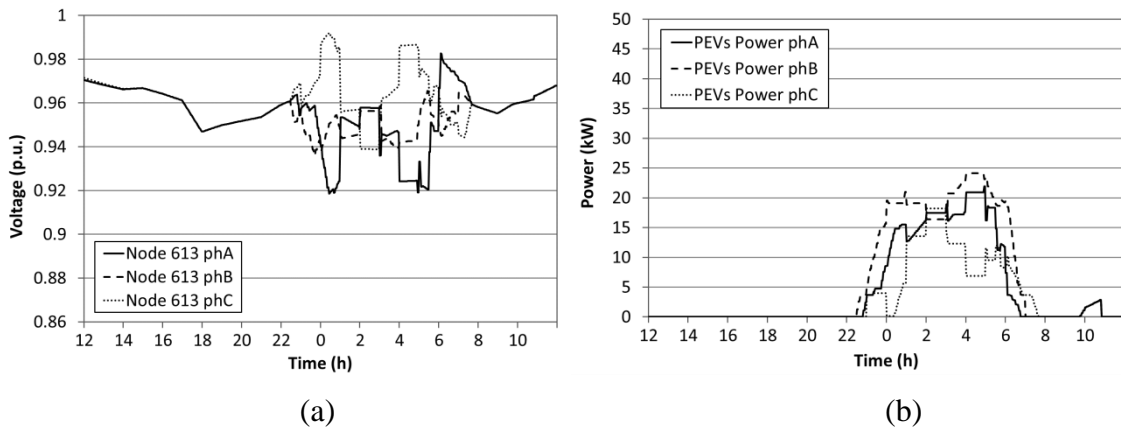
Figure 5.62. MOO-WF without VUR, for 30% of PEV-PR: (a) Line-neutral voltages of node 613 and (b) PEV power demand per phase
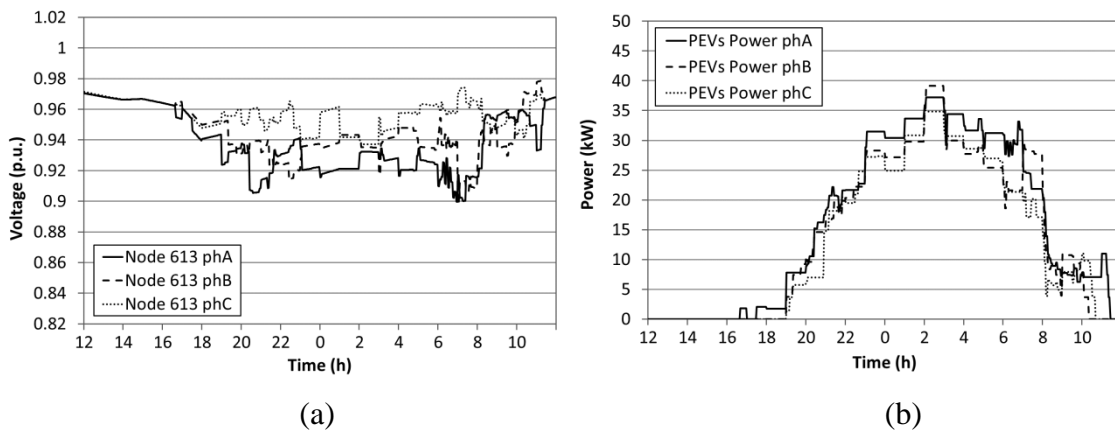
(a)   (b)
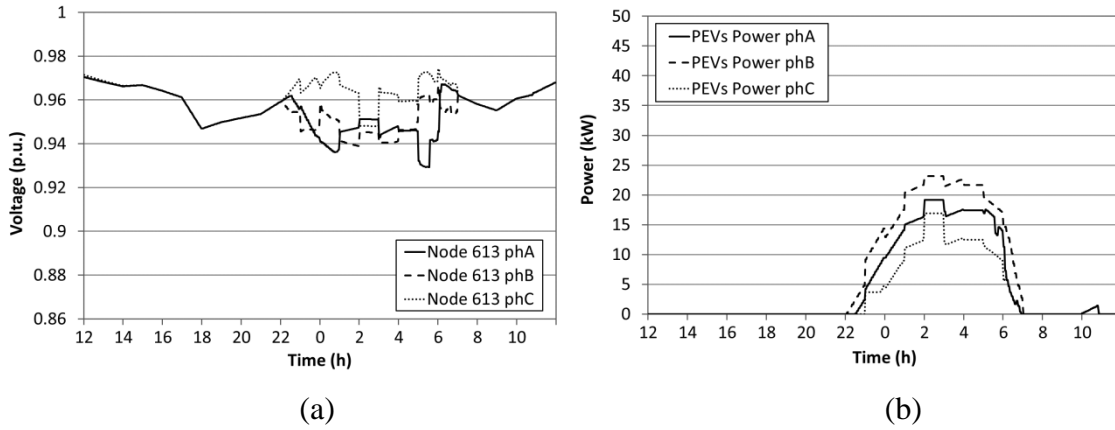
Figure 5.63. MOO-WF with VUR, for 30% of PEV-PR: (a) Line-neutral voltages of node 613 and (b) PEV power demand per phase

(a)   (b)
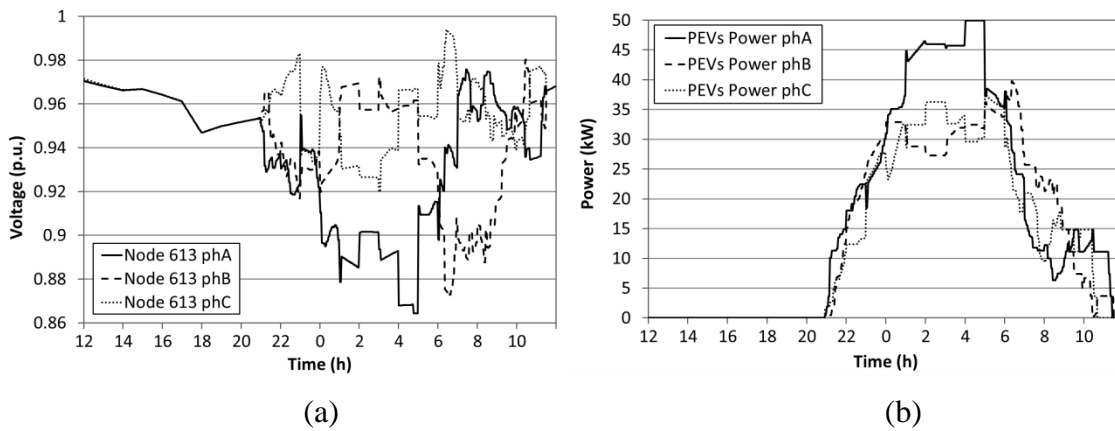
Figure 5.64. MOO-WF without VUR, for 100% of PEV-PR: (a) Line-neutral voltages of node 613 and (b) PEV power demand per phase

(a)   (b)
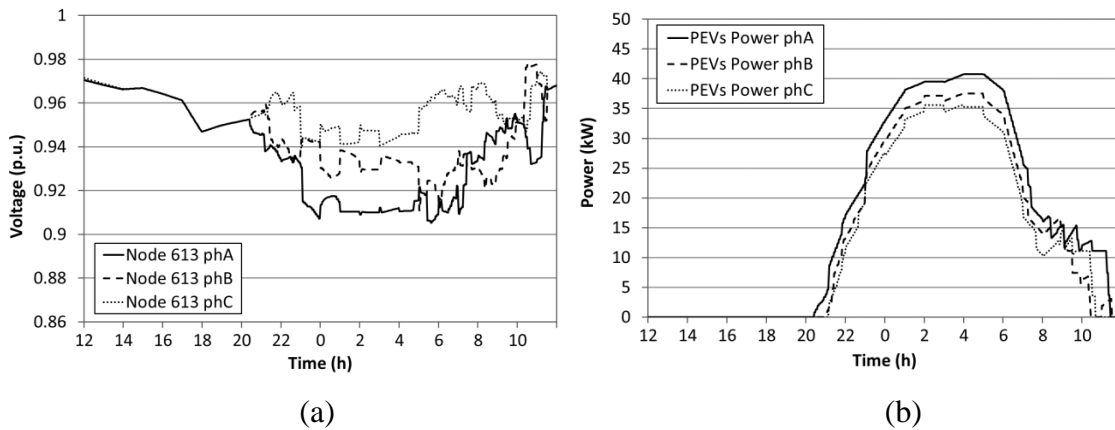
Figure 5.65. MOO-WF with VUR, for 100% of PEV-PR: (a) Line-neutral voltages of node 613 and (b) PEV power demand per phase

To conclude, voltage unbalance reduction method has proven to be an excellent approach to reduce VUF in both algorithms (MOO-NF and MOO-WF) and at different PEV-PR rates. It can reduce VUF without modifying the energy demand per phase and only coordinating the PEVs power demand between the three phases. Furthermore, a slightly improvement in charging cost is also achieved, without worsening overall load variance results.

5.7.5 Vehicle to Grid

V2G concept could bring extra enhancements for PEVs integration in distribution networks. V2G can reduce charging cost and overall load variance in function of the type of algorithm applied, as shown in sections 5.6.1 and 5.6.3. Additionally, V2G could bring further advantages such as providing backup power and ancillary services. At household level, users may be interested in backup power in order to avoid getting without electric power when an unexpected electric outage happens. Also, V2G can be used for saving peak power. However, V2G operation increases power losses at local level, mainly due to the inherent charger and battery efficiency. Furthermore, long-term battery degradation must be taken into account.

Both algorithms presented in this thesis can limit the V2G operation by setting a parameter called Z. After some simulations performed and results presented in sections 5.6.1 and 5.6.3 (see Figure 5.29 and Figure 5.38), it was determined that a Z value of 0.2, i.e. 20% of battery capacity, is enough to obtain noticeably improvements, while battery degradation is limited. In addition, these algorithms permit setting a minimum SOC to be met at any time. In this context, both MOO algorithms have been tested in order to know the influence of V2G in each one using different PEV-PRs.

5.7.5.1 MOO-NF

Using V2G in the MOO-NF algorithm improves total charging cost at any PEV-PR. Regarding to overall load variance, positive effects are achieved at low PEV-PR (10 and 30%) but at high PEV-PR, overall variance increases, as shown in Table 5.35. For the last case (100% of PEV-PR), V2G application causes a voltage deviation higher than permitted. Figure 5.66 and Figure 5.67 present two cases, PEV-PR of 30% and 100% respectively. VUR concept is used in all simulations performed in this section.

Table 5.35. Comparative between using Z=0 and Z=0.2 (V2G) in the MOO-NF algorithm

Case of study (PEV-PR)	Overall charging cost (€)	Overall load variance (kW²)	Overall peak power (kW)	V2G peak power (kW)	Energy losses (kWh)	Max. VUF (%)	Min. 613 node voltage (p.u.)	Time below 0.9p.u. (min)
MOO-NF (10%)	5.11	835	206	-	62	0.292	0.9456	0
MOO-NF (10%) V2G	4.68	690	198	-17	62	0.262	0.9405	0
MOO-NF (30%)	12.99	809	206	-	71	0.423	0.9342	0
MOO-NF (30%) V2G	12.95	693	198	-37	73	0.518	0.9383	0
MOO-NF (50%)	24.32	950	206	-	79	0.532	0.9281	0
MOO-NF (50%) V2G	23.83	982	217	-44	83	1.062	0.9145	0
MOO-NF (70%)	32.44	1181	212	-	94	0.945	0.8965	10
MOO-NF (70%) V2G	31.09	1697	228	-106	104	1.088	0.8847	55
MOO-NF (90%)	42.78	1502	220	-	113	0.636	0.9093	0
MOO-NF (90%) V2G	42.58	1819	234	-38	121	0.909	0.8911	35
MOO-NF (100%)	44.74	1651	224	-	117	0.965	0.8981	5
MOO-NF (100%) V2G	44.15	2078	244	-50	125	1.202	**0.8737**	**80**

(a)   (b)

Figure 5.66. MOO-NF and V2G (*Z*=0.2) with 30% of PEV-PR: (a) distribution
transformer load and (b) voltage at node 613

(a)   (b)

Figure 5.67. MOO-NF and V2G (*Z*=0.2) with 100% of PEV-PR: (a) distribution
transformer load and (b) voltage at node 613

5.7.5.2   MOO-WF

Table 5.36 shows the results from the simulation of the six different PEV-PRs, using the MOO-WF algorithm with VUR and V2G. At 10 and 30% of PEV-PR, charging cost, peak power and load variance are improved respect to the no V2G case. However, at higher PEV-PR, V2G provides worse results than the no V2G case, in terms of total charging cost and overall load variance. Peak power demand is better in V2G cases until 90% of PEV-PR.

This behavior is due to two reasons: on the one hand, the high ratio level between the PEVs energy demand (1.06MWh for the 100% PEV-PR case) and the households load demand (3.04MWh) and, on the other hand, the decentralized nature of the system control. That is, the earliest PEVs connected to the network use V2G to reduce charging cost and overall variance which, in turn, produces an increase of the energy demand at off-peak hours. In principle, this increase is beneficial to improve both objective functions, as can be seen in 10 and 30% PEV-PR cases. However, when the ratio between PEVs load demand and household load demand is high enough, the extra energy required for V2G operation adds load demand to the already overloaded off-peak hours, worsening overall results.

Table 5.36. Comparative between using Z=0 and Z=0.2 (V2G) in MOO-WF algorithm

Case of study (PEV-PR)	Overall charging cost (€)	Overall load variance (kW²)	Overall peak power (kW)	V2G peak power (kW)	Energy losses (kWh)	Max. VUF (%)	Min. 613 node voltage (p.u.)	Time below 0.9p.u. (min)
MOO-WF (10%)	5.12	802	206	-	62	0.316	0.9462	0
MOO-WF (10%) V2G	4.62	546	190	-26	62	0.319	0.9401	0
MOO-WF (30%)	12.78	688	206	-	71	0.397	0.9292	0
MOO-WF (30%) V2G	11.97	515	179	-43	75	0.535	0.9342	0
MOO-WF (50%)	23.62	788	206	-	80	0.563	0.9205	0
MOO-WF (50%) V2G	23.61	791	181	-55	86	0.504	0.9206	0
MOO-WF (70%)	32.56	978	206	-	95	0.533	0.9238	0
MOO-WF (70%) V2G	33.42	1116	200	-58	102	0.638	0.9146	0
MOO-WF (90%)	42.04	1409	206	-	116	0.691	0.9051	0
MOO-WF (90%) V2G	43.41	1713	214	-54	126	0.829	0.891	60
MOO-WF (100%)	44.35	1522	210	-	119	0.726	0.9052	0
MOO-WF (100%) V2G	45.77	1865	218	-57	129	0.927	**0.8889**	**100**

The decentralized control system cannot cope with this effect because it is impossible for the already connected PEVs knowing beforehand how many PEVs will be connected in the following hours into the network. A possible solution for this problem is to re-compute the MOO-WF algorithm, in all PEVs, when a new PEV is connected to the network. The aggregator can update and send new ACPs to the connected PEVs. This way, each PEV will schedule its charging profile knowing the current state of the network and not only the state of the network when it was connected.

Other similar possibility is re-computing the MOO-WF algorithm from time to time. Figure 5.68 and Figure 5.69 show the simulation results for 30 and 100% of PEV-PRs. As can be seen, the MOO-WF algorithm with V2G injects energy back to the distribution network when electricity prices are the highest ones in order to reduce as much as possible charging cost. Then, this energy, plus energy losses due to V2G operation, is recovered during off-peak hours.

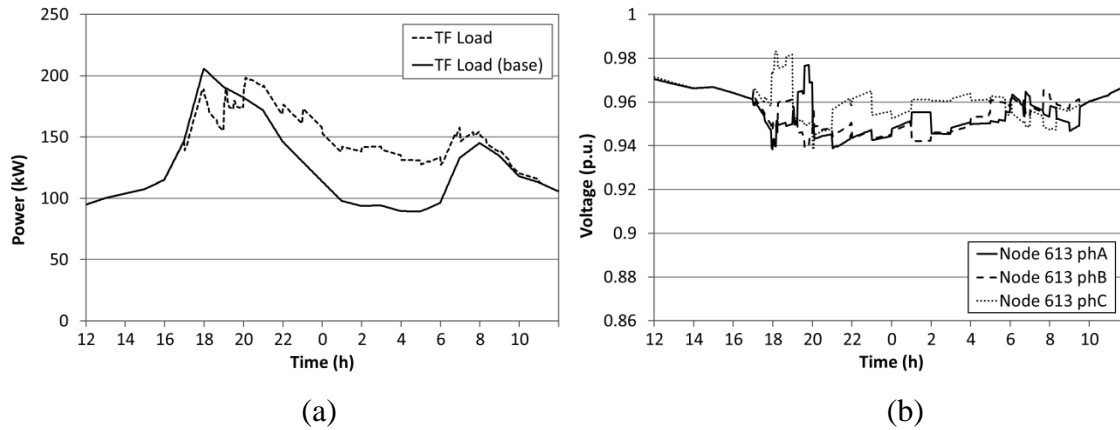(a)   (b)

Figure 5.68. MOO-WF and V2G (Z=0.2) with 30% of PEV-PR: (a) distribution transformer load and (b) voltage at node 613
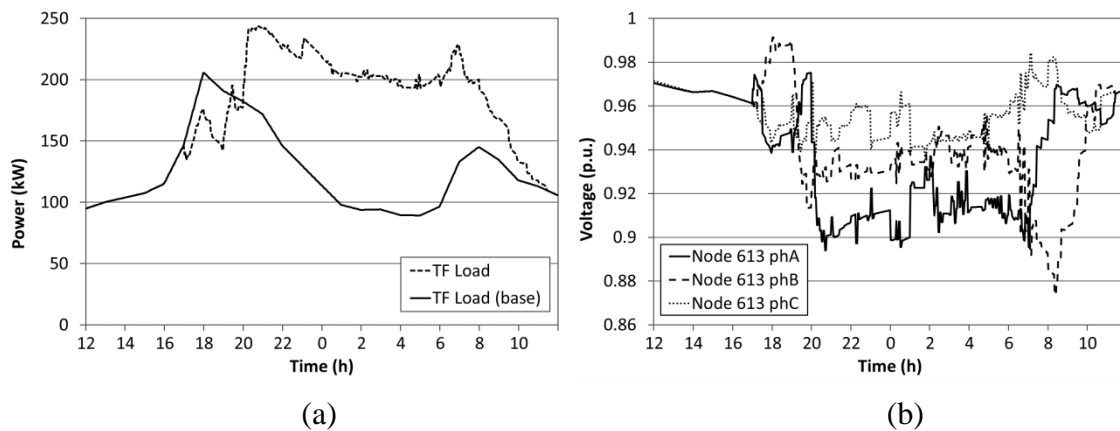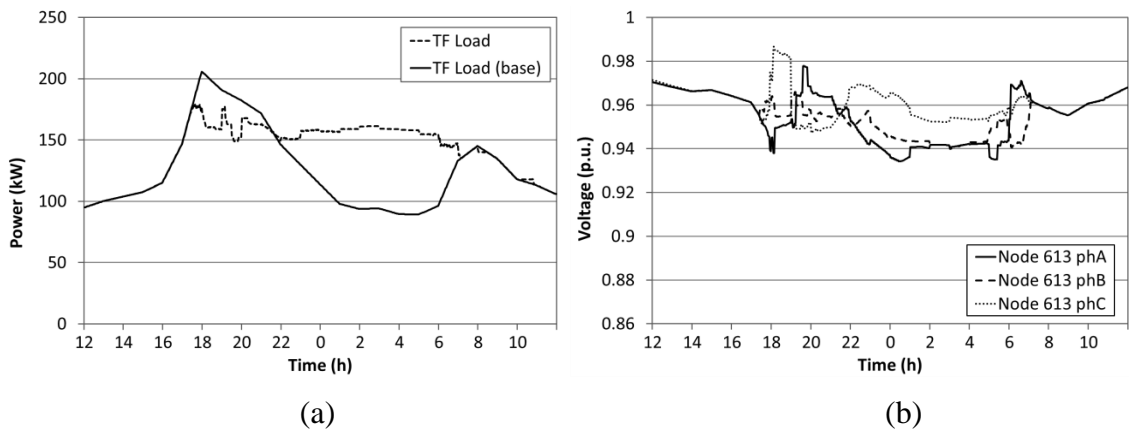
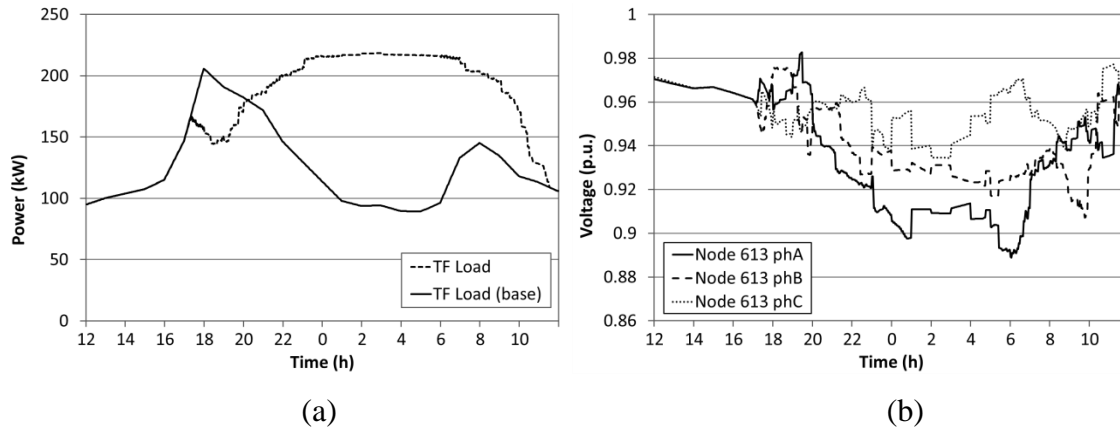(a)   (b)

Figure 5.69. MOO-WF and V2G (Z=0.2) with 100% of PEV-PR: (a) distribution
transformer load and (b) voltage at node 613

5.7.6   DSM services provision

Demand-side management is becoming a powerful tool in order to cope with renewable energy intermittency and other unexpected events, such as loss of electric generation or sudden increase of load demand. The proposed algorithm allows this management through modifying the ACP stored in the aggregator. This way, DSM can be done easily without directly managing the charging process of each PEV.

The operation of such a system has to be coordinated by the DSO, which will demand DSM services. Two types of orders can be distinguished: regulation up or down. In regulation up frequency is increased, so load must be reduced. This can be made in two different ways, reducing charging power of PEVs or using V2G concept. In contrast, regulation down is only achieved increasing charging power of PEVs.

The process begins with a petition from the DSO to the aggregator to modify the ACP. Once the ACP has been updated, the aggregator send it to each PEV connected to the distribution network. Then, each PEV executes the MOO algorithm, taking into account the new received ACP. After this process, a new VCP is obtained in each PEV, which is sent back to the aggregator in order to update the ACP.

Figure 5.70-a shows the result of a DSM petition at 01:00h, which consists in a load increase of 30kW between 01:00 and 02:30h. PEVs power demand is increased about 33kW at 01:00h and decreased approximately 30kW at 02:30h, respect to no DSM case. In contrast, in Figure 5.70-b the DSM petition is a reduction of 30kW between 01:30 and 02:30h. In this case, PEVs power demand only drops approximately 15kW at 01:30h, then it is increased about 30kW at 02:30h. Both simulations have been performed for 50% of PEV-PR and the MOO-WF algorithm.

The accuracy of the response to DSM petitions depends on several factors such as: the fuzzy control response, the PEVs capacity to increase or reduce their charging power and the availability of V2G. However, this configuration has the advantage that the DSO can monitor the accumulated charging profiles (through ACP), so the DSO can determine beforehand what the results obtained from the DSM petition are going to be.
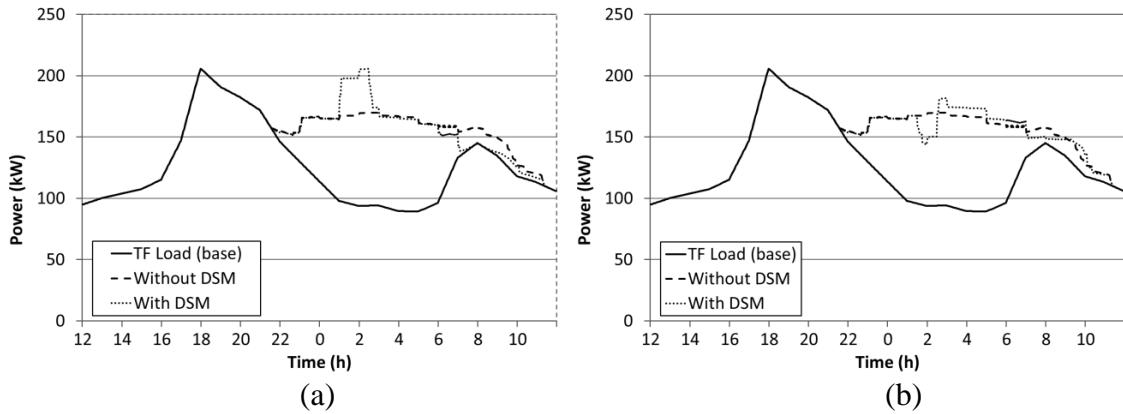
Figure 5.70. PEVs power demand under DSM petitions: (a) regulation up of 30kW and (b) regulation down of 30kW

5.7.7 Load forecast sensitivity analysis

The MOO-WF algorithm uses load forecasting, which mostly is not perfect. Load forecasting error may worsen the results obtained by the application of the MOO-WF algorithm. Accuracy in load forecasting depends on several factors such as: type of algorithm used to calculate it, time horizon (for few hours to a week ahead), aggregation level (at MV/LV, local LV feeder and end-user), etc. Error in load forecasting can be measured using the mean absolute percentage error (MAPE), defined by equation (5-41). A perfect forecast is defined by a 0% of MAPE error.

$$MAPE(\%) = \frac{1}{T} \sum_{t=1}^{T} \left| \frac{R_t - F_t}{R_t} \right| \cdot 100 \qquad (5\text{-}41)$$

where:

- R_t: the real load demand
- F_t: the forecasted load demand
- T: total number of forecasted periods

In this case, T is 25 for the 24h load forecasting. Authors of [141] use smart meter data from 1,600 Danish customers, for making a day-ahead load forecasting. According to the authors, MAPE can be in the range of 4-5% for MV/LV level (few hundred of customers) or 9-10% for LV feeder level (few tens of customers). Authors also use data of 6,500 Irish customers showing worse results in terms of MAPE (8-9% for MV/LV level and 15-16% at LV feeder).

Taking into account this data and knowing that the analyzed distribution network is composed by 170 households, ten different erroneous load forecasts have been tested for the MOO-WF algorithm. The MAPE of these load forecasts are between 10 to 12.6%. These erroneous load forecasts have been applied to the 100% of PEV-PR case. VUR has been also applied. Results obtained using these erroneous load forecast data are shown in Table 5.37, while Figure 5.71 shows the analyzed erroneous load forecasts.

Table 5.37. Results from using erroneous load forecast data for the 100% of PEV-PR case

Case of study	MAPE (%)	Overall charging cost (€)	Overall load variance (kW²)	Overall load peak power (kW)	PEVs peak power (kW)	Energy losses (kWh)	Max. VUF (%)	Min. 613 node voltage (p.u.)	Time below 0.9p.u. (min)
Case 0	0	44.35	1522	210	114	119	0.7256	0.9052	0
Case 1	10.6	45.59	1658	229	135	120	0.8072	0.8995	10
Case 2	11.3	44.95	1669	223	129	121	1.0615	0.8946	50
Case 3	11.06	44.97	1607	225	121	120	0.8701	0.8948	5
Case 4	12.56	44.95	1473	221	116	117	0.6867	0.9033	0
Case 5	10.58	45.19	1568	216	116	120	1.022	0.8961	5
Case 6	10.03	44.7	1649	225	131	121	0.7803	0.8965	12
Case 7	10.29	45.45	1674	231	126	121	0.9516	0.8961	5
Case 8	11.39	44.84	1662	236	123	121	0.9247	0.8904	70
Case 9	11.04	45.79	1547	233	113	119	0.8226	0.9030	0
Case 10	10.67	45.62	1477	223	99	117	0.7705	0.8974	15
Average	10.95	45.2	1598	226	121	120	0.8697	0.8971	17
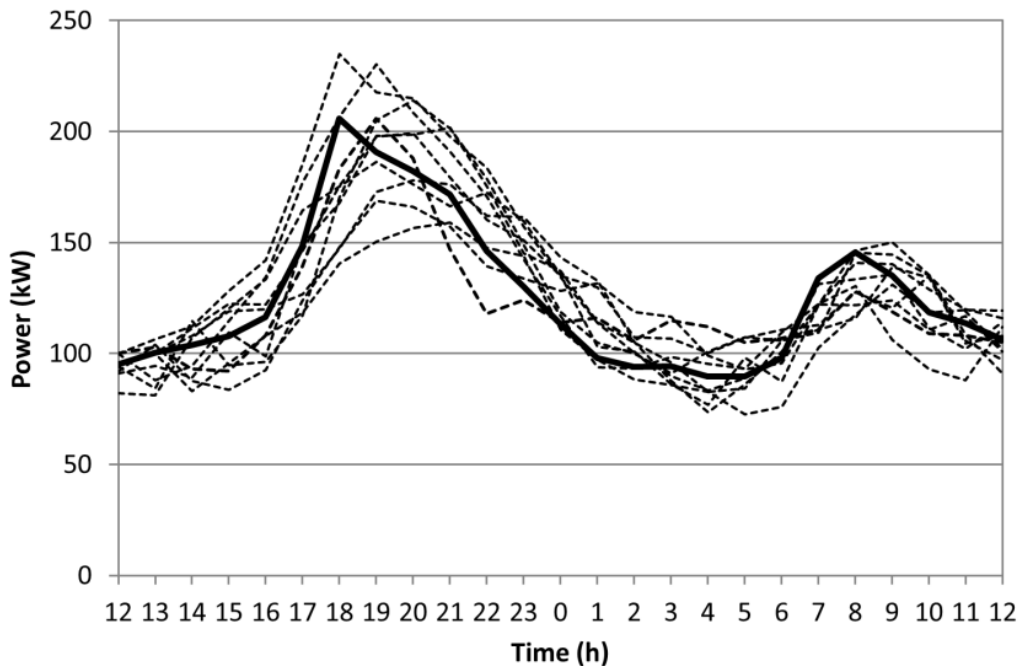
Figure 5.71. Perfect load forecast and erroneous load forecasts

As expected, load forecasting errors have a relative impact on results. In all cases, cost of charging is increased (2% on average), while overall load variance is also increased (5% on average). Peak power is more affected, reaching about a 7.5% higher value than applying a perfect load forecast. Obviously, voltages and VUF are also affected negatively but they still are within the EN50160 standard limits. In addition, a higher MAPE does not always imply worse results because it also depends on the shape of the erroneous load forecast, as can be seen in Figure 5.72 which presents two different cases. In the Annex D, more figures can be found with regard to this sensitivity analysis.

Figure 5.72. Two examples of load forecasting errors and their influence in the distribution transformer load. (a) Case 4 and (b) Case 8

Finally, MAPE depends on time horizon. Thus, using a shorter time horizon forecast will lead in better MAPEs and better algorithm results. A time horizon of 12h (average connection time) can be enough. In addition, the aggregator 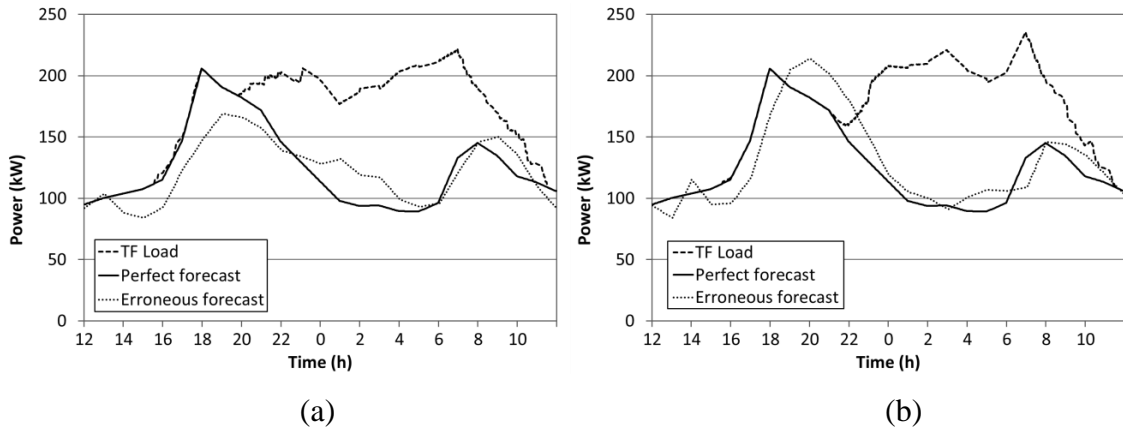could provide frequent updated LF and requests re-computing of smart charging algorithm of each PEV connected to the distribution network. This way, load forecasting errors will be reduced and overall results will be improved.

5.8   Comparative analysis

In this section, the analyzed smart charging algorithms are compared, in terms of cost and network impacts. Load forecasting errors have not been taken into account except for 100% of PEV-PR and only for the MOO-WF algorithm. Table 5.38 shows the numeric results obtained for the different simulations performed with 10% of PEV-PR (11 PEVs).

Table 5.38. Comparative analysis of results obtained for 10% of PEV-PR

Case of study	Overall charging cost (€)	Overall load variance	Load peak power (kW)	PEVs peak power (kW)	Energy losses (kWh)	Max. VUF (%)	Min. 613 node voltage (p.u.)	Time below 0.9p.u. (min)
No PEVs	-	1039	206	-	56	0.011	0.9468	0
Uncontrolled	7.39	1599	227	40	63	0.404	0.92	0
Cost opt.	5.08	896	206	63	62	0.605	0.9264	0
Cost opt. V2G	4.45	711	198	63	63	0.603	0.9281	0
PEVs var. opt.	6.04	1044	210	10	62	0.302	0.9426	0
PEVs var. opt. V2G	6.56	1045	210	10	62	0.163	0.9416	0
Load var. opt.	5.17	774	206	27	63	0.397	0.9434	0
Load var. opt. V2G	5.04	483	186	38	63	0.403	0.9412	0
MOO-NF	5.16	844	206	29	62	0.366	0.9398	0
MOO-NF VUR	5.11	835	206	39	62	0.292	0.9456	0
MOO-NF VUR/V2G	4.68	690	198	33	62	0.262	0.9405	0
MOO-WF	5.11	816	206	39	62	0.611	0.9272	0
MOO-WF VUR	5.12	802	206	35	62	0.316	0.9462	0
MOO-WF VUR/V2G	4.62	546	190	42	62	0.319	0.9401	0

As commented before, charging cost optimization provides an important reduction of costs respect to the uncontrolled case (-31%). Furthermore, if V2G concept is used this saving could reach almost 43%. Additionally, overall load variance is reduced almost to a half of the uncontrolled case (-44%), outperforming the overall load variance obtained when PEVs power variance optimization algorithm is used.

Moreover, overall load variance optimization improves not only load variance (-52%) but also total charging cost (-30%). Regarding to energy losses, they are similar in all cases. Additionally, if V2G is available further improvements could be achieved in overall load variance and charging cost (5.17 to 5.04€).

With regard to the MOO-NF algorithm with automatic weight selection, it also provides good results, -30% of charging cost and -48% of overall load variance, respect to the uncontrolled case, without using load forecasting. However, the best overall results are obtained by using the MOO-WF algorithm with V2G. It has one of the lowest charging cost (4.62€) while peak power is reduced to 190kW and load variance to 546kW^2.

In the case of 30% of PEV-PR (Table 5.39), PEVs variance optimization outperforms the value of load variance achieved with charging cost minimization. This trend continues along the rest of PEV-PR cases. Furthermore, charging cost minimization algorithm starts to increase peak power due to the high concentration of PEVs charging demand.

Table 5.39. Comparative analysis of results obtained for 30% of PEV-PR

Case of study	Overall charging cost (€)	Overall load variance	Load peak power (kW)	PEVs peak power (kW)	Energy losses (kWh)	Max. VUF (%)	Min. 613 node voltage (p.u.)	Time below 0.9p.u. (min)
No PEVs	-	1039	206	-	56	0.011	0.9468	0
Uncontrolled	16.53	2266	253	66	74	0.905	0.9016	0
Cost opt.	12.51	1261	236	137	75	0.849	0.9107	0
Cost opt. V2G	11.36	1275	236	137	80	0.79	0.9122	0
PEVs var. opt.	15.17	1057	212	24	70	0.633	0.9204	0
PEVs var. opt. V2G	16.25	1056	212	23	71	0.539	0.926	0
Load var. opt.	13.31	652	206	50	71	0.481	0.9386	0
Load var. opt. V2G	14.23	432	183	62	75	0.575	0.9269	0
MOO-NF	13.66	900	206	40	71	0.665	0.9269	0
MOO-NF VUR	12.99	809	206	55	71	0.423	0.9342	0
MOO-NF VUR/V2G	12.95	693	198	52	73	0.518	0.9383	0
MOO-WF	12.97	671	206	53	71	0.802	0.9186	0
MOO-WF VUR	12.78	688	206	59	71	0.397	0.9292	0
MOO-WF VUR/V2G	11.97	515	179	68	75	0.535	0.9342	0

As expected, load variance optimization is a good solution to reduce load variance but it is noticeably that V2G option increases charging cost (from 13.31 to 14.23€), which does not occur in the MOO-NF (13.66 to 12.95€) and the MOO-WF algorithms (12.97 to 11.97€). In a similar way than before, the MOO-WF with VUR/V2G can be considered as the best solution because of its balanced results in all aspects. Anyway, at this PEV-PR, all algorithms are valid from the point of view of voltage limits.

Table 5.40 presents a summary of results for 50% of PEV-PR. At this level (52 PEVs), uncontrolled and cost minimization algorithms do not provide valid solutions. PEVs power

demand variance algorithm leads to an increase of peak power (206 to 218kW) and a relatively high charging cost (26.74€).

Table 5.40. Comparative analysis of results obtained for 50% of PEV-PR

Case of study	Overall charging cost (€)	Overall load variance	Load peak power (kW)	PEVs peak power (kW)	Energy losses (kWh)	Max. VUF (%)	Min. 613 node voltage (p.u.)	Time below 0.9p.u. (min)
No PEVs	-	1039	206	-	56	0.011	0.9468	0
Uncontrolled	28.75	3340	290	111	85	1.203	**0.8816**	**102**
Cost opt.	21.82	2921	345	234	95	2.511	**0.7965**	**155**
Cost opt. V2G	19.89	3954	349	238	109	2.511	**0.7965**	**195**
PEVs var. opt.	26.74	1158	218	40	78	0.6	0.9299	0
PEVs var. opt. V2G	27.10	1159	218	40	79	0.711	0.9234	0
Load var. opt.	24.07	759	206	73	80	0.729	0.9161	0
Load var. opt. V2G	24.64	743	176	84	85	0.764	0.9089	0
MOO-NF	25.13	1031	209	58	79	0.839	0.9098	0
MOO-NF VUR	24.32	950	206	73	79	0.532	0.9281	0
MOO-NF VUR/V2G	23.83	982	217	69	83	1.062	0.9145	0
MOO-WF	23.86	775	206	74	80	0.89	0.9066	0
MOO-WF VUR	23.62	788	206	76	80	0.563	0.9205	0
MOO-WF VUR/V2G	23.61	791	181	88	86	0.504	0.9206	0

Results of the MOO-NF algorithm are between the charging cost and the PEVs power demand variance optimization algorithms but it adds an additional improvement in overall load variance. Specifically, a reduction of 18% is achieved when the proposed MOO-NF algorithm is compared to the PEVs power demand variance optimization algorithm (from 1158 to 950kW^2). Even if it is compared with load variance optimization, which uses load forecasting, the MOO-NF with VUR performs slightly worse in terms of charging cost (24.07 to 24.32€) but gives similar results in energy losses. Taking into account that no load forecasting is used in the MOO-NF algorithm, it can be considered that it provides relatively good results. Regarding to the MOO-WF algorithm, it provides good results even if V2G is used. The MOO-WF with VUR/V2G has the lowest peak power of all algorithms (181kW). No difference has been found in charging cost and load variance between the MOO-WF with VUR and MOO-WF with VUR/V2G options. However, VUR/V2G version increases energy losses in 6kWh.

Increasing the PEV-PR to 70% (72 PEVs) starts to have harmful effects on voltages of the furthest node of the distribution network, as shown in Table 5.41. Almost all algorithms reach line-neutral voltage values below to 0.9 p.u. except for overall load variance optimization and VUR versions of the MOO-WF. Furthermore, at this PEV-PR, V2G get worse results than no V2G versions, increasing distribution network impacts. The MOO-WF algorithm provides a reduction of 15% in charging cost, 81% in overall load variance and 23% in energy losses, compared to the uncontrolled charging case. When the MOO-WF is compared to the MOO-NF (both with VUR), the last one achieves better results on charging cost (32.56 to 32.44€), but overall load variance get worse (978 to 1181kW^2). However, energy losses are similar in both cases. MOO-NF algorithm increases the peak power in 6kW compared to MOO-WF algorithm.

Table 5.41. Comparative analysis of results obtained for 70% of PEV-PR

Case of study	Overall charging cost (€)	Overall load variance	Load peak power (kW)	PEVs peak power (kW)	Energy losses (kWh)	Max. VUF (%)	Min. 613 node voltage (p.u.)	Time below 0.9p.u. (min)
No PEVs	-	1039	206	-	56	0.011	0.9468	0
Uncontrolled	38.97	5244	320	126	106	1.466	**0.8537**	**132**
Cost opt.	29.21	6067	**475**	344	132	2.311	**0.7499**	**145**
Cost opt. V2G	26.04	9277	**489**	355	164	2.527	**0.7407**	**200**
PEVs var. opt.	36.48	1335	225	51	92	0.976	0.8942	20
PEVs var. opt. V2G	37.35	1321	225	52	93	1.173	0.8849	50
Load var. opt.	33.56	904	206	85	94	0.745	0.9088	0
Load var. opt. V2G	34.39	976	188	95	100	0.768	0.9188	0
MOO-NF	34.31	1158	214	87	93	1.387	**0.8699**	**75**
MOO-NF VUR	32.44	1181	212	74	94	0.945	0.8965	10
MOO-NF VUR/V2G	31.09	1697	228	104	104	1.088	0.8847	55
MOO-WF	33.13	958	206	97	95	1.032	**0.8885**	**80**
MOO-WF VUR	32.56	978	206	97	95	0.533	0.9238	0
MOO-WF VUR/V2G	33.42	1116	200	103	102	0.638	0.9146	0

Benefits of VUR implementation are obvious for 90% of PEV-PR, as show in Table 5.42. Only solutions where VUR is applied are able to achieve valid solutions at this high penetration level. In fact, the MOO-WF with VUR improves minimum line-neutral voltage level from 0.8636 to 0.9093 p.u. while VUF is reduced from 1.48 to 0.63%. Additionally, the MOO-WF VUR provides very good results in terms of charging cost and load variance (42.04€ and 1409kW^2), achieving a reduction of 11 and 12% in charging cost and energy losses. Regarding to overall peak power, the MOO-WF VUR algorithm keeps the peak power at 206kW. In contrast, the MOO-NF VUR increases it to 220kW.

Table 5.42. Comparative analysis of results obtained for 90% of PEV-PR

Case of study	Overall charging cost (€)	Overall load variance	Load peak power (kW)	PEVs peak power (kW)	Energy losses (kWh)	Max. VUF (%)	Min. 613 node voltage (p.u.)	Time below 0.9p.u. (min)
No PEVs	-	1039	206	-	56	0.011	0.9468	0
Uncontrolled	47.46	6409	367	182	132	1.683	**0.8106**	**247**
Cost opt.	37.54	10420	**576**	413	191	5.636	**0.6094**	**190**
Cost opt. V2G	34.87	14798	**591**	423	238	4.761	**0.6438**	**250**
PEVs var. opt.	45.86	1529	222	70	111	1.214	**0.8724**	**85**
PEVs var. opt. V2G	46.76	1539	222	71	112	1.045	**0.8842**	**85**
Load var. opt.	42.96	1328	206	105	115	0.95	**0.8888**	**230**
Load var. opt. V2G	43.99	1593	209	115	124	1.203	**0.8727**	**315**
MOO-NF	43.82	1557	230	99	113	1.483	**0.8636**	**105**
MOO-NF VUR	42.78	1502	220	111	113	0.636	0.9093	0
MOO-NF VUR/V2G	42.58	1819	234	121	121	0.909	0.8911	35
MOO-WF	42.43	1384	206	108	116	1.517	**0.8684**	**180**
MOO-WF VUR	42.04	1409	206	110	116	0.691	0.9051	0
MOO-WF VUR/V2G	43.41	1713	214	120	129	0.829	0.891	60

Results for 100% of PEV-PR are presented in Table 5.43. In this case, only VUR solutions are within voltage limits. None of the V2G cases are valid. If the MOO-NF and the MOO-WF are compared, the last one is slightly better in total charging cost (44.74 to 44.35€), load variance (1651 to 1522kW^2) and peak power (224 to 210kW). However, if load forecasting error is added to the MOO-WF algorithm, charging cost is increased to 45.2€, load variance to 1598kW^2 and load peak power to 226kW. Energy losses in both cases are similar (117kWh for MOO-NF and 120kWh for MOO-WF). Taking into account these results, it can be said that the MOO-NF algorithm provides similar results in this case. In addition, voltages at node 613 are in the same range.

Table 5.43. Comparative analysis of results obtained for 100% of PEV-PR

Case of study	Overall charging cost (€)	Overall load variance	Load peak power (kW)	PEVs peak power (kW)	Energy losses (kWh)	Max. VUF (%)	Min. 613 node voltage (p.u.)	Time below 0.9p.u. (min)
No PEVs	-	1039	206	-	56	0.0114	0.9468	0
Uncontrolled	49.85	6842	375	189	137	1.899	**0.8125**	**262**
Cost opt.	39.53	11675	**610**	434	203	9.8974	**0.4493**	**200**
Cost opt. V2G	36.67	16762	**622**	446	255	6.5689	**0.5804**	**240**
PEVs var. opt.	48.17	1613	225	74	114	1.2077	**0.8701**	**85**
PEVs var. opt. V2G	49.30	1630	225	74	115	1.0671	**0.879**	**80**
Load var. opt.	45.24	1437	206	109	118	1.1397	**0.8824**	**250**
Load var. opt. V2G	46.52	1733	213	119	127	1.2599	**0.8696**	**340**
MOO-NF	46.49	1705	238	102	116	2.372	**0.8306**	**72**
MOO-NF VUR	44.74	1651	224	115	117	0.965	0.8981	5
MOO-NF VUR/V2G	44.15	2078	244	118	125	1.202	**0.8737**	**80**
MOO-WF	44.66	1502	207	112	120	1.43	**0.8643**	**215**
MOO-WF VUR	44.35	1522	210	114	119	0.726	0.9052	0
MOO-WF VUR (LF error)	45.2	1598	226	121	120	0.8697	0.8971	17
MOO-WF VUR/V2G	45.77	1865	218	124	129	0.927	**0.8889**	**100**

Finally, the computation time of each optimized algorithm is presented in Table 5.44. The optimization problems have been solved using a 3.40GHz Intel i7-2600 CPU with 8GB of RAM. All algorithms have been executed in a very short period of time. In a real implementation, slower and cheaper CPUs can accomplish the optimization tasks without any problem.

Table 5.44. Computational time of the different algorithms presented in this thesis

Case of study	Average execution time (s)	Maximum execution time (s)
Cost opt.	0.14	0.21
PEVs var. opt.	0.19	0.24
Load var. opt.	0.19	0.23
MOO-NF	0.56	0.74
MOO-NF VUR	0.59	0.75
MOO-WF	0.61	0.74
MOO-WF VUR	0.62	0.8

5.9 System architecture

In this section, the implementation of the proposed smart charging architecture is presented (Figure 5.73). Being a decentralized architecture, most of the requirements have to be located in the PEV itself. These requirements are listed below:

- PEVs must support charging at different rates. This aspect depends mainly on battery charger and Battery Management System (BMS). V2G support is optional. However, the proposed algorithms can be also implemented in chargers with a limited range of charging power. That is, chargers that have a minimum charging/discharging power, apart from the standby status.

- PEVs have to execute the proposed smart charging algorithm internally, so they must have a processor unit on-board.

- PEVs must have a communication system in order to receive the corresponding ACP, the LF (MOO-WF case) and the electricity prices of the day. After optimization is carried out, each PEV must send its VCP and the charging post identifier to the aggregator. This VCP calculated in the vehicle has to take into account the estimated efficiency of the charger.

- PEVs need to measure the voltage at the connection point to use it in the dynamic u variable selection (only in MOO-NF version).

The other main component of the proposed system is the aggregator, which will manage one or more ACPs. The aggregator must have a database of charging post identifiers in order to know which phase and therefore, which ACP correspond for each PEV. This aggregator can be managed by a utility or DSO directly, which manages the distribution network. This way, the DSO or the utility can monitor the PEVs power demand. So, they can take further actions if it is necessary, in order to ensure the correct operation of the distribution network. Among these actions, managing available on-load tap changers (OLTC) and/or making DSM petitions can be found.

AGGREGATOR:
- Receive VCPs
- Update ACP
- Update ACP with DSM petitions
- Send ACP
- Send LF (MOO-WF)

DSO:
- Send DSM petitions
- ACP monitoring
- Further control actions

PEV:
- Get ACP
- Get LF (MOO-WF)
- Get electricity prices
- Measure voltage at EVSE (MOO-NF)
- Execute MOO algorithm
- Send calculated VCP and EVSE ID

USER:
- Define departure time
- Define final SOC required
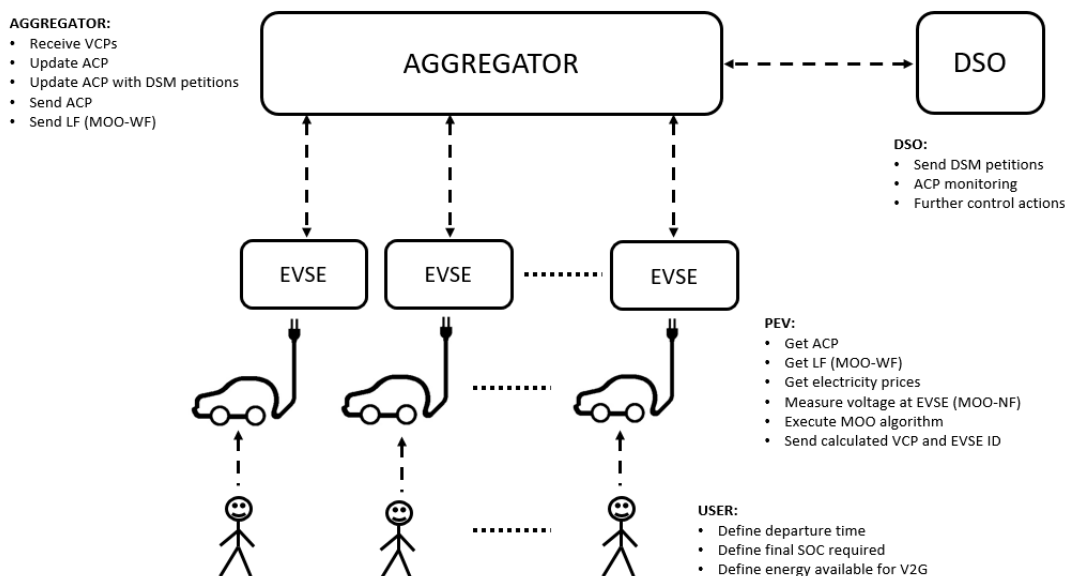- Define energy available for V2G

Figure 5.73. Proposed decentralized architecture

The normal operation of this system, based on the proposed methodology is as follows:

1. User sets the expected departure time for the next trip before connecting the PEV into the electric network. Additionally, user can define the percentage of battery capacity reserved to V2G and the final SOC required if it is different to 100%.
2. When the PEV is plugged into the network, its EVSE identifier (ID) will be sent to the aggregator.
3. From the EVSE identifier, the aggregator will know the location of the EVSE and the phase where the EVSE is connected (needed to implement the VUR enhancement). As answer, the aggregator will send the corresponding ACP and LF to the PEV.
4. Then, the PEV processor unit will execute the MOO-WF algorithm taking into account the user requirements, the ACP, the LF (MOO-WF only), the electricity prices and the voltage value at the connection point (MOO-NF only).
5. When optimization is finished, the PEV will send its VCP to the aggregator, which will update the corresponding ACP and wait to other PEVs.

The initial calculated VCP can be altered under the following four circumstances:

- An anticipated disconnection of the PEV, which will be communicated to the aggregator including the EVSE ID.
- A change in the VCP because of an automatic adjustment of the u value (MOO-NF).
- A modification of user's parameters, such as departure time or final SOC.
- A DSM petition from the DSO.

In these four cases, the aggregator must delete the old VCP of the PEV and update the corresponding ACP. Figure 5.74 shows the operation process for the MOO-WF algorithm with an unexpected disconnection event. With regard to DSM operation, it is quite similar but a re-computing request must be sent from the aggregator to each PEV (with the updated ACP and LF).
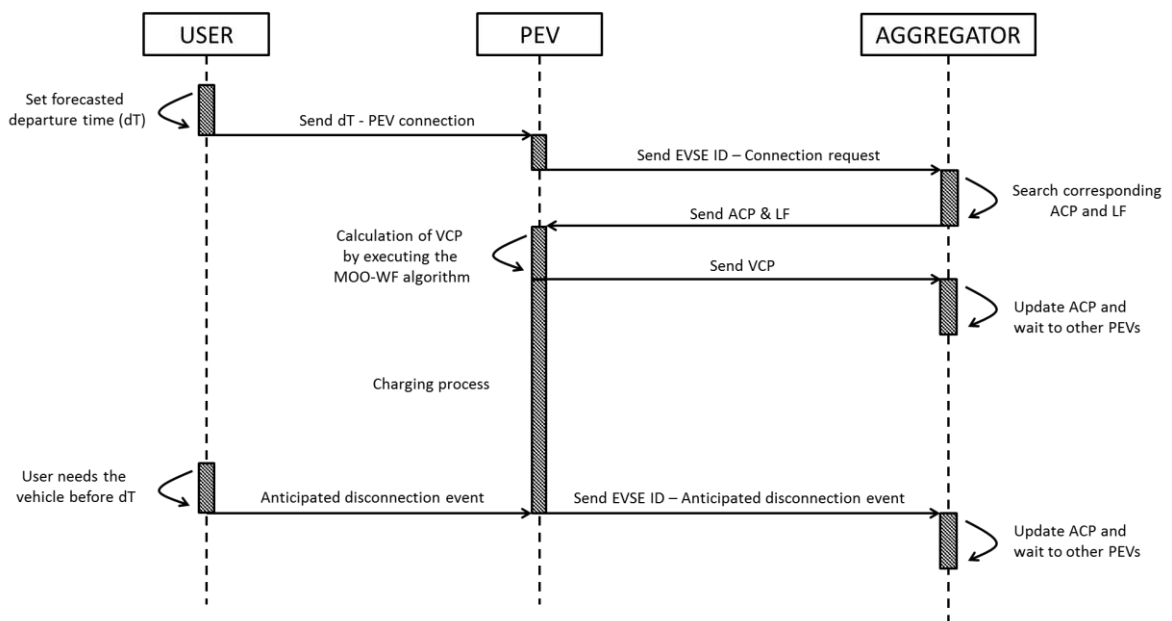
Figure 5.74. Operation scheme of the MOO-WF algorithm with an anticipated disconnection event

With regard to system reliability, PEVs will continue charging even though the aggregator is offline. Two cases can be distinguished: if the PEV is already connected to the network or not. In the first case, the PEV will be charged with the last valid ACP sent by the aggregator. In the second case, the PEV will be charged without using the ACP (because it has no received any ACP from the aggregator). That is, the PEV will perform the same MOO algorithm but it will not have any information of the ACP, so its own power demand variance and its charging cost will be minimized. In this case, impacts on the distribution network may be larger but at least PEV users will continue getting service to charge their PEVs. The application of the proposed algorithm gives economic advantages to PEV users. However, a mechanism to compensate the provision of DSM services has to be considered to encourage wider participation in the DSM services provision.

Regarding to communication system, it is expected that in short-medium term internet will be available for most of the vehicles, as it will provide a lot of services to drivers such as: navigation systems maps, automatic emergency calls, vehicle's firmware updates, remote control using smartphone apps, vehicle's status checking, etc. This type of services on vehicles is called as "connected car" and PEVs are particularly appropriate for it. But, in order to improve security of the communication system, it is recommended to use an end-to-end encryption (aggregator to PEV). This way, the data transmitted across the communication system will be encrypted and only the aggregator and the corresponding PEV will be able to decoding the communication messages.

Finally, a summary of hardware requirements and actions performed by each entity, involved in the proposed methodology, is presented in Table 5.45.

Table 5.45. Hardware requirements and actions performed by each entity

ENTITY	HARDWARE REQUIREMENTS	ACTIONS PERFORMED
DSO	– Communication system	– ACP monitoring – Request DSM services – Provide load forecasting (MOO-WF) – Take further actions if necessary
AGGREGATOR	– Database – Communication system – Processor unit	– Send ACP to new connected PEVs – Send LF to new connected PEVs – Calculate and update ACP – Delete old VCP – Update ACP with DSM petitions and send it to PEVs
PEV	– Voltage meter (MOO-NF only) – Communication system – Processor unit – On-board charger with control of charging rate – User interface – Bi-directional charger for V2G (optional)	– Measure voltage (MOO-NF only) – Receive ACP – Receive electricity prices – Calculate average power and variance (MOO-WF) – Execute MOO algorithm – Send new VCP – Execute DSM petitions – Send interruption petitions – Send updated VCP if user modify some parameter
USER		– Define departure time – Define final SOC required (optional) – Define battery capacity available for V2G (optional)

5.10 Conclusions

In this chapter, a new methodology for integrating PEVs into the distribution network has been proposed, which covers different relevant aspects.

Driving and charging behavior have a great influence on the impacts that the charge of PEVs can have on LV distribution networks. Thus, a new "social" model, obtained from data of 2009 NHTS, is proposed. This model takes into account not only the difference between a workday and a weekend day but also the type of region (rural or urban) and the trimester of the year.

After driving and charging behavior is modelled, charging cost optimization and PEVs power demand variance optimization algorithms have been analyzed. Charging cost optimization algorithm provides a huge reduction on charging cost to PEV users but impacts of distribution network are larger. In contrast, PEVs power demand variance optimization reduces these impacts but it may increase peak power. Moreover, load variance minimization can be done by using load forecasting. This optimization reduces grid impacts but it does not take into account the electricity prices.

Following, two new smart algorithms that combine cost and variance minimization have been presented. The first one, called MOO-NF, does not need load forecasting and uses very little data such as voltage at the connection point, electricity prices and the ACP provided by the aggregator. This entity has an important role, although it does not control directly the charging of the PEVs. But, it provides a mechanism to influence in the charging decision process of each PEV through changing the ACP (DSM services). A fuzzy control has been designed to define the weigh variable, which determines the importance between optimizing the charging cost or the load variance. This optimization runs continuously in each PEV, in order to reduce grid impacts.

The second one, named as MOO-WF, uses load forecasting to improve overall load variance. In this case, the designed fuzzy control takes into account the average and the variance of the sum of the load forecast and the ACP. This way, it is possible to determine how much the distribution network is loaded and if there is high difference between maximum and minimum power demand. Taking into account this data, fuzzy control provides the value of weight which will be used in the optimization process. Results obtained with this algorithm are more predictable than MOO-NF algorithm but error in load forecasting may affect the results. However, it is expected that with the intensive use of smart meters and shorter time horizons in load forecasting, load forecasting errors will be limited to acceptable values.

Also, voltage unbalances have been identified to be one of the biggest issues when a significant number of PEVs are charged through single-phase chargers. In this context, a voltage unbalance reduction improvement has been proposed (VUR). This mechanism helps to the MOO algorithms to coordinate the charging of PEVs along the three phases, reducing voltage unbalances and improving voltage profiles. This method has given very good results in both MOO algorithms and at any PEV-PR.

Additionally, the proposed algorithms are able to use V2G concept and V2G provision can be limited by the user by setting the maximum battery capacity percentage available for V2G. This way, battery degradation could be reduced if a low battery capacity value is selected by the user (around 10-20%). Furthermore, it has been proven that higher battery

capacity reserved to V2G does not provide significant improvements in terms of charging cost and overall load variance. In addition, at medium-high PEV-PRs, V2G does not provide any improvement and could even provide worse overall results.

The proposed methodology also allows the use of DSM services. An entity such as the DSO could modify easily the ACP in order to reduce or increase the PEVs power demand. This way, demand side management could be provided by PEVs. Additionally, the DSO can monitor ACPs which are accumulated charging profiles, so as to decide if there is necessity to take further actions to ensure the distribution network reliability.

As a decentralized methodology, it presents other advantages. For example, PEV user's privacy is not compromised because only charging profile and location of each PEV is sent to the aggregator. Reliability is improved even if the aggregator is offline or not accessible. PEVs will continue executing the MOO algorithm and they will charge as usual, avoiding lack of charging. However, impacts on the LV network will be higher. Additionally, computation time will not depend on the number of PEVs.

From the simulation data obtained, the proposed methodology has proven its adequacy in terms of charging cost, load variance optimization and voltage levels, comparing to uncontrolled charging and the rest of smart charging algorithms presented. Furthermore, the proposed algorithms do not use PEVs power demand forecasting, as some centralized solutions use or dynamic pricing signals that may distort the electricity cost for users.

Finally, the proposed algorithms have demonstrated that they can improve load factor allowing the integration of more renewable energy, reducing energy losses and avoiding or delaying grid reinforcement needs. All these aspects lead to conclude that the proposed algorithms in this thesis improve PEVs integration on LV distribution networks, while simplicity of operation and user's privacy is kept as much as possible.

CHAPTER 6

CONCLUSIONS

6.1 - CONCLUSIONS OF THE THESIS

6.2 - FUTURE WORK

6. CONCLUSIONS

6.1 Conclusions of the thesis

Global warming and air pollution of urban areas are pushing the marketing of new generation of vehicles. Between them, electric vehicles are the most popular. In general, electric mobility is considered as another step towards energy sustainability in modern society. However, there are several challenges to be addressed as those ones related to the battery technology and the deployment and efficient operation of the charging infrastructure. In this context, integration of PEVs in electrical distribution networks should be beneficial to all stakeholders, improving the efficiency of the system both technically and economically. Smart charging concept is the key to achieve this ambitious objective.

The integration of electric vehicles in electric networks will lead an increase of overall energy demand and, as a consequence, higher profits for electric utilities. In addition, if a smart charging algorithm such as the one proposed in this thesis is implemented, the load factor of the network could be higher. This way, more renewable energy sources and/or base load generation could be integrated, reducing operational costs. Others possible benefits to be considered are the ancillary services provision and the incentives related to CO_2 emission credits.

Currently, PEVs are considered as uncontrolled electric loads due to their low market penetration level. However, it is expected that, in the medium-long term, PEVs will have a significant penetration level in the market of light-duty vehicles. The charge of a large amount of PEVs will lead to non-negligible impacts on electric distribution networks, such as increase of energy losses and peak power, overload of lines and transformers, voltage drops, voltage unbalances, reduction of distribution transformer lifetime, reduction of load factor, etc. These impacts depend significantly on the driving and charging behavior of PEV users. Thus, it is necessary to model these aspects prior developing smart charging algorithms. In this regard, a new driving and charging behavior model has been developed within this thesis, which takes into account aspects such as type of day, type of location (rural or urban) and season of the year.

The mentioned driving and charging behavior model has been applied to know what the uncontrolled charging impacts will be in a real distribution network. Results show that uncontrolled charging will increase energy losses, peak power and voltage deviations and unbalances. In this context, two alternatives can be considered to accommodate the increase of load due to the charge of PEVs: increase the network capacity or the implementation of a smart charging control. The first approach can be difficult to carry out due to economic, environmental and technical reasons. In contrast, the second approach could avoid or delay grid reinforcements as well as providing several opportunities to be exploited.

Thus, researchers have proposed smart charging algorithms in order to achieve some certain objectives related to PEVs integration. Most of them are focused on solving partial problems, but neglecting the impact that these solutions will have in other important aspects such as voltage levels, voltage unbalances, energy losses, charging costs or PEV users' privacy. In addition, very few proposed solutions have been simulated in real LV distribution networks with real load demand data.

Considering these aspects, this thesis has proposed a new smart charging algorithm to be applied at LV distribution network level. A real distribution network located in Borup (Denmark) has been used as model to test the effectiveness of the proposed algorithm. The main objectives of this algorithm are to reduce energy losses, voltage drops and unbalances and charging costs, while increasing peak power is avoided. Two different versions of a MOO algorithm have been proposed. The first one is based on using the electricity prices as an indicator of how much loaded the distribution network is, while the second one uses load forecasting directly. Both methods do not cope with voltage unbalances generated by PEVs. Regarding to this problem, an improvement has been proposed to coordinate the charging of multiple PEVs along the three phases. The results obtained in the simulations have proven that this enhancement reduce noticeably the voltage unbalances as well as increase the minimum voltage values. In addition, a sensitivity analysis has been carried out in order to know the influence of load forecasting errors.

Furthermore, the proposed solution has been implemented in a decentralized architecture which provides several advantages. Aspects such as users' privacy, reliability and scalability are improved compared to centralized control architectures.

Finally, it can be highlighted that some of the results obtained during the development of this thesis have been published in the following conferences and journals:

- "Co-simulation with DIgSILENT PowerFactory and Matlab: Optimal integration of plug-in electric vehicles in distribution networks" Book Chapter. Advanced Smart Grid Functionalities based on Power Factory, Springer. (Accepted).
- "Decentralized Multi-objective Optimization Control of Plug-in Electric Vehicles in LV Distribution Networks" (Under review. Applied Energy).
- "Vehicle to home: Integration of micro-RES and EV" (Under review. Journal of Modern Power Systems and Clean Energy).
- "Decentralized Control Techniques for Plug-in Electric Vehicles in MV/LV distribution networks", International Conference of Renewable Energies and Power Quality (ICREPQ'16), Madrid (Spain), 2016.
- "Integración de Generación Distribuida Intermitente y Vehículos Eléctricos Enchufables", XVI Encuentro Regional Iberoamericano de Cigré (ERIAC), Puerto Iguazú (Argentina), 2015.
- "Delivering Energy from PEV batteries: V2G, V2B and V2H approaches", International Conference of Renewable Energies and Power Quality (ICREPQ'15), La Coruña (Spain), 2015.
- "Modelling Social Patterns of Plug-in Electric Vehicles Drivers for Dynamic Simulations", IEEE International Electric Vehicle Conference (IEVC), Firenze (Italy), 2014.
- "Plug-in Electric Vehicles in Electric Distribution Networks: A Review of Smart Charging Approaches", Renewable & Sustainable Energy Reviews, Vol. 38, pp.717-731, 2014.
- "Influence of Social Behaviour in the Future Trend of EVs", Book chapter. Autonomous Hybrid Vehicles: Intelligent Transport Systems and Automotive Technologies, University of Pitesti (Romania), pp. 117-143, 2013, ISBN 978-606-560-327-1.

6.2   Future work

Regarding to the future work that can be developed in this research field, several ideas have arisen:

- Individual control of each phase in three-phased EVSEs. This type of control could reduce the energy demand unbalances between the phases, whenever is possible. This way, voltage unbalances will be reduced as well as energy losses. In addition, the proposed algorithm can be easily adapted to provide this new service.

- Within the previous idea, V2G could provide a balancing path, transferring energy from one phase to another phase. This enhancement should be limited to certain cases to avoid premature battery degradation and energy losses.

- Reactive power control. The proposed algorithm can be extended to control the reactive power in order to improve voltage levels. Two different approaches can be developed: a coordinated droop control, taking advantage of the already control architecture, and an optimized reactive power control, which remains almost unexplored in the current literature.

- Application of a model predictive control in order to reduce load forecasting errors and improve V2G concept implementation at medium/high PEV-PRs.

- Other objective functions which can take into account intermittent distributed generation such as wind generation, in order to improve their grid integration.

REFERENCES

REFERENCES

[1]   DOE/EIA, "Annual Energy Review 2011," *U.S. Energy Information Administration*, 2012. [Online]. Available: http://www.eia.gov/totalenergy/data/annual/pdf/aer.pdf.

[2]   U.S. Deparment of Energy, "Lessons Learned – The EV Project Greenhouse Gas (GHG) Avoidance and Cost Reduction. Final Report," 2012.

[3]   Electric Power Research Institute, "Environmental assessment of plug-in hybrid electric vehicles," vol. 1. pp. 1–56, 2007.

[4]   United Nations Environment Programme (UNEP), "The Emissions Gap Report," 2012.

[5]   The European Parliament and the Council of the European Union, *Regulation (EC) No 715/2007*. 2007.

[6]   B. Berman and J. Gartner, "Plug-in Electric Vehicles Battery Electric and Plug-in Hybrid Electric Vehicles : OEM Strategies , Demand Drivers , Technology Issues, Key Industry Players, and Global Market Forecasts," 2012.

[7]   U.S. Deparment of Energy, "PEV definition [Internet]." [Online]. Available: http://www.afdc.energy.gov/laws/law/NC/9355. [Accessed: 14-Mar-2015].

[8]   A. Kirubakaran, S. Jain, and R. K. Nema, "A review on fuel cell technologies and power electronic interface," *Renew. Sustain. Energy Rev.*, vol. 13, no. 9, pp. 2430–2440, 2009.

[9]   D. Wu and S. S. Williamson, "Status Review of Power Control Strategies for Fuel Cell Based Hybrid Electric Vehicles," *Electr. Power Conf. 2007. EPC 2007. IEEE Canada*, vol. 2, pp. 218–223, 2007.

[10]   M. Melaina and M. Penev, "Hydrogen Station Cost Estimates," 2013.

[11]   EV Everywhere, "Road to Success," 2014. [Online]. Available: http://energy.gov/sites/prod/files/2014/02/f8/eveverywhere_road_to_success.pdf. [Accessed: 14-Jan-2015].

[12]   K. L. Gering, S. V. Sazhin, D. K. Jamison, C. J. Michelbacher, B. Y. Liaw, M. Dubarry, and M. Cugnet, "Investigation of path dependence in commercial lithium-ion cells chosen for plug-in hybrid vehicle duty cycle protocols," *J. Power Sources*, vol. 196, no. 7, pp. 3395–3403, 2011.

[13]   T. M. O'Sullivan, C. M. Bingham, and R. E. Clark, "Zebra battery technologies for all electric smart car," in *International Symposium on Power Electronics, Electrical Drives, Automation and Motion (SPEEDAM)*, 2006, p. 243.

[14]   M.-K. Song, Y. Zhang, and E. J. Cairns, "A long-life, high-rate lithium/sulfur cell: a multifaceted approach to enhancing cell performance.," *Nano Lett.*, vol. 13, no. 12, pp. 5891–9, Jan. 2013.

[15]   X. Feng, M.-K. Song, W. C. Stolte, D. Gardenghi, D. Zhang, X. Sun, J. Zhu, E. J. Cairns, and J. Guo, "Understanding the degradation mechanism of rechargeable lithium/sulfur cells: a comprehensive study of the sulfur-graphene oxide cathode after discharge-charge cycling.," *Phys. Chem. Chem. Phys.*, vol. 16, no. 32, pp. 16931–40, Aug. 2014.

[16]   K. G. Gallagher, S. Goebel, T. Greszler, M. Mathias, W. Oelerich, D. Eroglu, and V. Srinivasan, "Quantifying the promise of lithium–air batteries for electric vehicles," *Energy Environ. Sci.*, vol. 7, no. 5, p. 1555, 2014.

[17]   Evatran,   "Plugless   Power   Tech   Specs."   [Online].   Available: http://www.pluglesspower.com/wp/wp-content/uploads/2014/02/Plugless_Tech_Specs.pdf. [Accessed: 12-May-2015].

[18]   R. W. Carlson and B. Normann, "Test Results of the PLUGLESS™ Inductive Charging System from Evatran Group, Inc.," *SAE Int. J. Altern. Powertrains*, vol. 3, no. 1, pp. 64–71, 2014.

[19]   S. Y. Choi, B. W. Gu, S. Y. Jeong, and C. T. Rim, "Advances in Wireless Power Transfer Systems for Roadway-Powered Electric Vehicles," *IEEE J. Emerg. Sel. Top. Power Electron.*, vol. 3, no. 1, pp. 18–36, 2015.

[20]   Z. Darabi and M. Ferdowsi, "Aggregated Impact of Plug-in Hybrid Electric Vehicles on Electricity Demand Profile," *IEEE Trans. Sustain. Energy*, vol. 2, no. 4, pp. 501–508, Oct. 2011.

[21]   S. Shafiee, M. Fotuhi-Firuzabad, and M. Rastegar, "Investigating the Impacts of Plug-in Hybrid Electric Vehicles on Power Distribution Systems," *IEEE Trans. Smart Grid*, vol. 4, no. 3, pp. 1351–1360, Sep. 2013.

[22]   A. Foley, B. Tyther, P. Calnan, and B. Ó Gallachóir, "Impacts of Electric Vehicle charging under electricity market operations," *Appl. Energy*, vol. 101, pp. 93–102, 2013.

[23]   K. Clement-Nyns, E. Haesen, and J. Driesen, "The Impact of Charging Plug-In Hybrid Electric Vehicles on a Residential Distribution Grid," *IEEE Trans. Power Syst.*, vol. 25, no. 1, pp. 371–380, Feb. 2010.

[24]   C. Farmer, P. Hines, J. Dowds, and S. Blumsack, "Modeling the Impact of Increasing PHEV Loads on the Distribution Infrastructure," in *43rd Hawaii International Conference on System Sciences*, 2010, pp. 1–10.

[25]   A. D. Hilshey, P. D. H. Hines, P. Rezaei, and J. R. Dowds, "Estimating the Impact of Electric Vehicle Smart Charging on Distribution Transformer Aging," *IEEE Trans. Smart Grid*, vol. 4, no. 2, pp. 905–913, Jun. 2013.

[26]   D. M. Said and K. M. Nor, "Effects of harmonics on distribution transformers," in *Australasian Universities Power Engineering Conference*, 2008, pp. 1–5.

[27]   Green   eMotion,   "Green   eMotion: Project   Results,"   2015.   [Online].   Available: http://www.greenemotion-project.eu/upload/pdf/deliverables/Project-Results-online.pdf. [Accessed: 22-May-2015].

[28]   J. Smart and S. Schey, "Battery Electric Vehicle Driving and Charging Behavior Observed Early in The EV Project," *SAE Int. J. Altern. Powertrains*, vol. 1, no. 1, pp. 27–33, Apr. 2012.

[29]   J. Smart and S. Schey, "Extended Range Electric Vehicle and Charging Behaviour Observed Early in the EV Project," *SAE Int. J. Altern. Powertrains*, vol. 1, no. 1, pp. 1–9, Apr. 2012.

[30]   U.S. Department of Transportation, "2009 National Household Travel Survey," 2009.

[31]   D. T. Nguyen and L. B. Le, "Joint Optimization of Electric Vehicle and Home Energy Scheduling Considering User Comfort Preference," *IEEE Trans. Smart Grid*, vol. 5, no. 1, pp. 188–199, Jan. 2014.

[32]   A. D. Hilshey, P. Rezaei, P. D. H. Hines, and J. Frolik, "Electric vehicle charging: Transformer impacts and smart decentralized solutions," in *IEEE Power and Energy Society General Meeting*, 2012, pp. 1–8.

[33] J. Tan and L. Wang, "Integration of plug-in hybrid electric vehicles into residential distribution grid based on two-layer intelligent optimization," *IEEE Trans. Smart Grid*, vol. 5, no. 4, pp. 1774–1784, 2014.

[34] J. Garcia-Villalobos, I. Zamora, P. Eguia, J. I. San Martin, and F. J. Asensio, "Modelling social patterns of plug-in electric vehicles drivers for dynamic simulations," in *IEEE International Electric Vehicle Conference (IEVC)*, 2014, pp. 1–7.

[35] A. P. Robinson, P. T. Blythe, M. C. Bell, Y. Hübner, and G. A. Hill, "Analysis of electric vehicle driver recharging demand profiles and subsequent impacts on the carbon content of electric vehicle trips," *Energy Policy*, vol. 61, pp. 337–348, Oct. 2013.

[36] C. Corchero, S. Gonzalez-Villafranca, and M. Sanmarti, "European electric vehicle fleet: driving and charging data analysis," in *IEEE International Electric Vehicle Conference (IEVC)*, 2014, pp. 1–6.

[37] Green eMotion, "Green eMotion - D9.1: Consumers' preferences and attitudes to, demand for, and use of electric vehicles (EV)," 2015.

[38] Advanced Powertrain Research Facility, "Nissan Leaf Testing and Analysis," 2012. [Online]. Available: http://www.transportation.anl.gov/D3/data/2012_nissan_leaf/AVTALeaftestinganalysis_Maj or summary101212.pdf.

[39] ECOtality North America, "Q2 2012 Report," 2012.

[40] M. Neaimeh, G. Hill, P. Blythe, R. Wardle, Jialiang Yi, and P. Taylor, "Integrating smart meter and electric vehicle charging data to predict distribution network impacts," in *IEEE PES ISGT Europe*, 2013, pp. 1–5.

[41] M. Sanduleac, M. Eremia, L. Toma, and P. Borza, "Integrating the Electrical Vehicles in the Smart Grid through unbundled Smart Metering and multi-objective Virtual Power Plants," in *IEEE PES International Conference and Exhibition on Innovative Smart Grid Technologies*, 2011, pp. 1–8.

[42] A.-H. Mohsenian-Rad, V. W. S. Wong, J. Jatskevich, R. Schober, and A. Leon-Garcia, "Autonomous Demand-Side Management Based on Game-Theoretic Energy Consumption Scheduling for the Future Smart Grid," *IEEE Trans. Smart Grid*, vol. 1, no. 3, pp. 320–331, Dec. 2010.

[43] J. Hu, S. You, M. Lind, and J. Østergaard, "Coordinated charging of electric vehicles for congestion prevention in the distribution grid," *IEEE Trans. Smart Grid*, vol. 5, no. 2, pp. 703–711, 2014.

[44] W. Kempton and J. Tomić, "Vehicle-to-grid power fundamentals: Calculating capacity and net revenue," *J. Power Sources*, vol. 144, no. 1, pp. 268–279, Jun. 2005.

[45] J. A. P. Lopes, P. M. Rocha Almeida, and F. J. Soares, "Using vehicle-to-grid to maximize the integration of intermittent renewable energy resources in islanded electric grids," in *International Conference on Clean Electrical Power*, 2009, pp. 290–295.

[46] C. Yang, "Fuel electricity and plug-in electric vehicles in a low carbon fuel standard," *Energy Policy*, vol. 56, pp. 51–62, 2013.

[47] "BMWi ChargedForward Program." [Online]. Available: http://www.bmwichargeforward.com/. [Accessed: 14-Jan-2015].

[48] The Cleantech Group, "Ancillary Services: A Huge, Under The Radar Storage Market Opportunity," 2010.

[49]   J. R. Pillai and B. Bak-Jensen, "Impacts of electric vehicle loads on power distribution systems," in *IEEE Vehicle Power and Propulsion Conference*, 2010, pp. 1–6.

[50]   G. A. Putrus, P. Suwanapingkarl, D. Johnston, E. C. Bentley, and M. Narayana, "Impact of electric vehicles on power distribution networks," in *IEEE Vehicle Power and Propulsion Conference*, 2009, pp. 827–831.

[51]   G. J. Offer, M. Contestabile, D. A. Howey, R. Clague, and N. P. Brandon, "Techno-economic and behavioural analysis of battery electric, hydrogen fuel cell and hybrid vehicles in a future sustainable road transport system in the UK," *Energy Policy*, vol. 39, no. 4, pp. 1939–1950, Apr. 2011.

[52]   P. Papadopoulos, S. Skarvelis-Kazakos, I. Grau, L. M. Cipcigan, and N. Jenkins, "Predicting Electric Vehicle impacts on residential distribution networks with Distributed Generation," in *IEEE Vehicle Power and Propulsion Conference*, 2010, pp. 1–5.

[53]   R. Villafafila-Robles, P. Lloret-Gallego, D. Heredero-Peris, A. Sumper, I. Cairo, M. Cruz-Zambrano, and N. Vidal, "Electric vehicles in power systems with distributed generation: Vehicle to Microgrid (V2M) project," in *11th International Conference on Electrical Power Quality and Utilisation*, 2011, pp. 1–6.

[54]   S. Schey, D. Scoffield, and J. Smart, "A First Look at the Impact of Electric Vehicle Charging on the Electric Grid in The EV Project," in *International Battery, Hybrid and Fuel Cell Electric Vehicle Symposium (EVS26)*, 2012, pp. 1–12.

[55]   M. O. W. Grond, N. H. Luong, J. Morren, and J. G. Slootweg, "Multi-objective optimization techniques and applications in electric power systems," in *47th International Universities Power Engineering Conference (UPEC)*, 2012, pp. 1–6.

[56]   R. T. Marler and J. S. Arora, "Survey of multi-objective optimization methods for engineering," *Struct. Multidiscip. Optim.*, vol. 26, no. 6, pp. 369–395, Apr. 2004.

[57]   I. Y. Kim and O. de Weck, "Adaptive Weighted Sum Method for Multiobjective Optimization," in *10th AIAA/ISSMO Multidisciplinary Analysis and Optimization Conference*, 2004, no. September, pp. 1–13.

[58]   W. Kempton and J. Tomić, "Vehicle-to-grid power implementation: From stabilizing the grid to supporting large-scale renewable energy," *J. Power Sources*, vol. 144, no. 1, pp. 280–294, Jun. 2005.

[59]   A. Brooks, "Vehicle-to-grid demonstration project: Grid regulation ancillary service with a battery electric vehicle," 2002. [Online]. Available: http://www.udel.edu/V2G/docs/V2G-Demo-Brooks-02-R5.pdf. [Accessed: 21-Jun-2014].

[60]   J. R. Pillai and B. Bak-Jensen, "Vehicle-to-grid systems for frequency regulation in an Islanded Danish distribution network," in *IEEE Vehicle Power and Propulsion Conference*, 2010, pp. 1–6.

[61]   A. Nebel, C. Kruger, and F. Merten, "Vehicle to grid and demand side management - an assessment of different strategies for the integration of electric vehicles," in *IET Conference on Renewable Power Generation (RPG 2011)*, 2011, pp. 143–143.

[62]   J. Druitt and W. G. Früh, "Simulation of demand management and grid balancing with electric vehicles," *J. Power Sources*, vol. 216, pp. 104–116, Oct. 2012.

[63]   S. B. Peterson, J. F. Whitacre, and J. Apt, "The economics of using plug-in hybrid electric vehicle battery packs for grid storage," *J. Power Sources*, vol. 195, pp. 2377–2384, 2010.

[64] R. J. Bessa and M. A. Matos, "Economic and technical management of an aggregation agent for electric vehicles: a literature survey," *Eur. Trans. Electr. Power*, vol. 22, no. 3, pp. 334–350, Apr. 2012.

[65] J. A. P. Lopes, F. J. Soares, and P. M. R. Almeida, "Integration of Electric Vehicles in the Electric Power System," *Proc. IEEE*, vol. 99, no. 1, pp. 168–183, Jan. 2011.

[66] C. Guille and G. Gross, "Design of a Conceptual Framework for the V2G Implementation," in *IEEE Energy 2030 Conference*, 2008, pp. 1–3.

[67] R. J. Bessa and M. A. Matos, "The role of an aggregator agent for EV in the electricity market," in *7th Mediterranean Conference and Exhibition on Power Generation, Transmission, Distribution and Energy Conversion*, 2010, pp. 123–131.

[68] Sekyung Han, Soohee Han, and K. Sezaki, "Development of an Optimal Vehicle-to-Grid Aggregator for Frequency Regulation," *IEEE Trans. Smart Grid*, vol. 1, no. 1, pp. 65–72, Jun. 2010.

[69] M. D. Galus, M. G. Vayá, T. Krause, and G. Andersson, "The role of electric vehicles in smart grids," *Wiley Interdiscip. Rev. Energy Environ.*, vol. 2, no. 4, pp. 384–400, Jul. 2013.

[70] F. J. Soares, P. M. R. Almeida, and J. A. P. Lopes, "Quasi-real-time management of Electric Vehicles charging," *Electr. Power Syst. Res.*, vol. 108, pp. 293–303, Mar. 2014.

[71] A. Zakariazadeh, S. Jadid, and P. Siano, "Multi-objective scheduling of electric vehicles in smart distribution system," *Energy Convers. Manag.*, vol. 79, pp. 43–53, Mar. 2014.

[72] D. Q. Oliveira, A. C. Zambroni de Souza, and L. F. N. Delboni, "Optimal plug-in hybrid electric vehicles recharge in distribution power systems," *Electr. Power Syst. Res.*, vol. 98, pp. 77–85, May 2013.

[73] S. Deilami, A. S. Masoum, P. S. Moses, and M. A. S. Masoum, "Real-Time Coordination of Plug-In Electric Vehicle Charging in Smart Grids to Minimize Power Losses and Improve Voltage Profile," *IEEE Trans. Smart Grid*, vol. 2, no. 3, pp. 456–467, Sep. 2011.

[74] E. Sortomme, M. M. Hindi, S. D. J. MacPherson, and S. S. Venkata, "Coordinated Charging of Plug-In Hybrid Electric Vehicles to Minimize Distribution System Losses," *IEEE Trans. Smart Grid*, vol. 2, no. 1, pp. 198–205, Mar. 2011.

[75] S. Paudyal and S. Dahal, "Impact of plug-in hybrid electric vehicles and their optimal deployment in smart grids," in *Universities Power Engineering Conference (AUPEC)*, 2011, pp. 1 – 6.

[76] L. Jian, Y. Zheng, X. Xiao, and C. C. Chan, "Optimal scheduling for vehicle-to-grid operation with stochastic connection of plug-in electric vehicles to smart grid," *Appl. Energy*, vol. 146, pp. 150–161, 2015.

[77] L. Jian, X. Zhu, Z. Shao, S. Niu, and C. C. Chan, "A scenario of vehicle-to-grid implementation and its double-layer optimal charging strategy for minimizing load variance within regional smart grids," *Energy Convers. Manag.*, vol. 78, pp. 508–517, Feb. 2014.

[78] A. Subramanian, M. Garcia, A. Dominguez-Garcia, D. Callaway, K. Poolla, and P. Varaiya, "Real-time scheduling of deferrable electric loads," in *American Control Conference (ACC)*, 2012, pp. 3643–3650.

[79] J. Kang, S. J. Duncan, and D. N. Mavris, "Real-time Scheduling Techniques for Electric Vehicle Charging in Support of Frequency Regulation," *Procedia Comput. Sci.*, vol. 16, pp. 767–775, Jan. 2013.

[80]   M. Singh, P. Kumar, and I. Kar, "Implementation of Vehicle to Grid Infrastructure Using Fuzzy Logic Controller," *IEEE Trans. Smart Grid*, vol. 3, no. 1, pp. 565–577, Mar. 2012.

[81]   R. J. Bessa, F. J. Soares, J. A. Pecas Lopes, and M. A. Matos, "Models for the EV aggregation agent business," in *IEEE Trondheim PowerTech*, 2011, vol. 0, pp. 1–8.

[82]   D. Wu, D. C. Aliprantis, and L. Ying, "Load Scheduling and Dispatch for Aggregators of Plug-In Electric Vehicles," *IEEE Trans. Smart Grid*, vol. 3, no. 1, pp. 368–376, Mar. 2012.

[83]   A. Di Giorgio, F. Liberati, and S. Canale, "Electric vehicles charging control in a smart grid: A model predictive control approach," *Control Eng. Pract.*, vol. 22, pp. 147–162, Jan. 2014.

[84]   M. Rivier, T. Gómez, R. Cossent, and I. Momber, "MERGE Project - D5.1 - New actors and business models for the integration of EV in power systems," 2011.

[85]   F. Marra, G. Y. Yang, Y. T. Fawzy, C. Traeholt, E. Larsen, R. Garcia-Valle, and M. M. Jensen, "Improvement of Local Voltage in Feeders With Photovoltaic Using Electric Vehicles," *IEEE Trans. Power Syst.*, vol. 28, no. 3, pp. 3515–3516, Aug. 2013.

[86]   M. Tokudome, K. Tanaka, T. Senjyu, A. Yona, T. Funabashi, and C.-H. Kim, "Frequency and voltage control of small power systems by decentralized controllable loads," in *International Conference on Power Electronics and Drive Systems*, 2009, pp. 666–671.

[87]   J. R. Pillai and B. Bak-Jensen, "Vehicle-to-Grid for islanded power system operation in Bornholm," in *IEEE PES General Meeting*, 2010, pp. 1–8.

[88]   K. Knezovic, M. Marinelli, R. J. Moller, P. B. Andersen, C. Traholt, and F. Sossan, "Analysis of voltage support by electric vehicles and photovoltaic in a real Danish low voltage network," in *49th International Universities Power Engineering Conference*, 2014, pp. 1–6.

[89]   F. Geth, N. Leemput, J. Van Roy, J. Buscher, R. Ponnette, and J. Driesen, "Voltage droop charging of electric vehicles in a residential distribution feeder," in *3rd IEEE PES Innovative Smart Grid Technologies Europe*, 2012, pp. 1–8.

[90]   N. Leemput, F. Geth, J. Van Roy, A. Delnooz, J. Buscher, and J. Driesen, "Impact of Electric Vehicle On-Board Single-Phase Charging Strategies on a Flemish Residential Grid," *IEEE Trans. Smart Grid*, vol. 5, no. 4, pp. 1815–1822, 2014.

[91]   H. Liu, Z. Hu, Y. Song, and J. Lin, "Decentralized Vehicle-to-Grid Control for Primary Frequency Regulation Considering Charging Demands," *IEEE Trans. Power Syst.*, vol. 28, no. 3, pp. 3480–3489, Aug. 2013.

[92]   Z. Ma, D. Callaway, and I. Hiskens, "Decentralized charging control for large populations of plug-in electric vehicles," in *49th IEEE Conference on Decision and Control*, 2010, pp. 206–212.

[93]   L. Gan, U. Topcu, and S. H. Low, "Optimal Decentralized Protocol for Electric Vehicle Charging," *IEEE Trans. Power Syst.*, vol. 28, no. 2, pp. 1–12, 2012.

[94]   H. K. Nguyen and J. Bin Song, "Optimal charging and discharging for multiple PHEVs with demand side management in vehicle-to-building," *J. Commun. Networks*, vol. 14, no. 6, pp. 662–671, Dec. 2012.

[95]   A. Sheikhi, S. Bahrami, A. M. Ranjbar, and H. Oraee, "Strategic charging method for plugged in hybrid electric vehicles in smart grids; a game theoretic approach," *Int. J. Electr. Power Energy Syst.*, vol. 53, pp. 499–506, Dec. 2013.

[96]   S. D. J. McArthur, E. M. Davidson, V. M. Catterson, A. L. Dimeas, N. D. Hatziargyriou, F. Ponci, and T. Funabashi, "Multi-Agent Systems for Power Engineering Applications—Part I: Concepts, Approaches, and Technical Challenges," *IEEE Trans. Power Syst.*, vol. 22, no. 4, pp. 1743–1752, Nov. 2007.

[97]   M. Wooldridge and N. R. Jennings, "Intelligent agents: theory and practice," *Knowl. Eng. Rev.*, vol. 10, no. 02, p. 115, Jun. 1995.

[98]   E. L. Karfopoulos and N. D. Hatziargyriou, "A Multi-Agent System for Controlled Charging of a Large Population of Electric Vehicles," *IEEE Trans. Power Syst.*, vol. 28, no. 2, pp. 1–1, 2012.

[99]   J. Hu, A. Saleem, S. You, L. Nordström, M. Lind, and J. Østergaard, "A multi-agent system for distribution grid congestion management with electric vehicles," *Eng. Appl. Artif. Intell.*, vol. 38, pp. 45–58, 2015.

[100]   I. Grau Unda, P. Papadopoulos, S. Skarvelis-Kazakos, L. M. Cipcigan, N. Jenkins, and E. Zabala, "Management of electric vehicle battery charging in distribution networks with multi-agent systems," *Electr. Power Syst. Res.*, vol. 110, pp. 172–179, May 2014.

[101]   Z. Fan, "A Distributed Demand Response Algorithm and Its Application to PHEV Charging in Smart Grids," *IEEE Trans. Smart Grid*, vol. 3, no. 3, pp. 1280–1290, Sep. 2012.

[102]   K. Zhou and L. Cai, "Randomized PHEV Charging Under Distribution Grid Constraints," *IEEE Trans. Smart Grid*, vol. 5, no. 2, pp. 879–887, Mar. 2014.

[103]   E. B. Iversen, J. M. Morales, and H. Madsen, "Optimal charging of an electric vehicle using a Markov decision process," *Appl. Energy*, vol. 123, pp. 1–12, Jun. 2014.

[104]   O. Beaude, Y. He, and M. Hennebel, "Introducing decentralized EV charging coordination for the voltage regulation," in *IEEE PES ISGT Europe*, 2013, pp. 1–5.

[105]   E. L. Karfopoulos, P. Papadopoulos, S. Skarvelis-Kazakos, I. Grau, L. M. Cipcigan, N. Hatziargyriou, and N. Jenkins, "Introducing electric vehicles in the microgrids concept," in *16th International Conference on Intelligent System Applications to Power Systems*, 2011, pp. 1–6.

[106]   P. Richardson, D. Flynn, and A. Keane, "Local Versus Centralized Charging Strategies for Electric Vehicles in Low Voltage Distribution Systems," *IEEE Trans. Smart Grid*, vol. 3, no. 2, pp. 1020–1028, Jun. 2012.

[107]   M. Gonzalez Vaya and G. Andersson, "Centralized and decentralized approaches to smart charging of plug-in vehicles," in *IEEE Power and Energy Society General Meeting*, 2012, pp. 1–8.

[108]   J. A. P. Lopes, N. Hatziargyriou, J. Mutale, P. Djapic, and N. Jenkins, "Integrating distributed generation into electric power systems: A review of drivers, challenges and opportunities," *Electr. Power Syst. Res.*, vol. 77, no. 9, pp. 1189–1203, Jul. 2007.

[109]   European Commission, "Energy 2020: A strategy for competitive, sustainable and secure energy," *COM (2010)*, 2010. [Online]. Available: http://eur-lex.europa.eu/LexUriServ/LexUriServ.do?uri=COM:2010:0639:FIN:EN:PDF. [Accessed: 23-Jun-2013].

[110]   T. L. Vandoorn, B. Zwaenepoel, J. D. M. De Kooning, B. Meersman, and L. Vandevelde, "Smart microgrids and virtual power plants in a hierarchical control structure," in *2nd IEEE PES International Conference and Exhibition on Innovative Smart Grid Technologies*, 2011, pp. 1–7.

[111] T. G. Werner and R. Remberg, "Technical, economical and regulatory aspects of Virtual Power Plants," in *2008 Third International Conference on Electric Utility Deregulation and Restructuring and Power Technologies*, 2008, pp. 2427–2433.

[112] P. Asmus, "Microgrids, Virtual Power Plants and Our Distributed Energy Future," *Electr. J.*, vol. 23, no. 10, pp. 72–82, Dec. 2010.

[113] A. Brooks and T. Gage, "Integration of electric drive vehicles with the electric power grid—a new value stream," in *The International Battery, Hybrid and Fuel Cell Electric Vehicle Symposium (EVS-18)*, 2001, pp. 1 – 15.

[114] A. Y. Saber and G. K. Venayagamoorthy, "Plug-in Vehicles and Renewable Energy Sources for Cost and Emission Reductions," *IEEE Trans. Ind. Electron.*, vol. 58, no. 4, pp. 1229–1238, Apr. 2011.

[115] S. Skarvelis-Kazakos, P. Papadopoulos, I. Grau, A. Gerber, L. M. Cipcigan, N. Jenkins, and L. Carradore, "Carbon optimized virtual power plant with electric vehicles," in *45th International Universities Power Engineering Conference (UPEC)*, 2010, pp. 1 – 6.

[116] A. F. Raab, M. Ferdowsi, E. Karfopoulos, I. G. Unda, S. Skarvelis-Kazakos, P. Papadopoulos, E. Abbasi, L. M. Cipcigan, N. Jenkins, N. Hatziargyriou, and K. Strunz, "Virtual Power Plant Control concepts with Electric Vehicles," in *6th International Conference on Intelligent System Applications to Power Systems*, 2011, pp. 1–6.

[117] B. Jansen, C. Binding, O. Sundstrom, and D. Gantenbein, "Architecture and Communication of an Electric Vehicle Virtual Power Plant," in *First IEEE International Conference on Smart Grid Communications*, 2010, pp. 149–154.

[118] M. Vasirani, R. Kota, R. L. G. Cavalcante, S. Ossowski, and N. R. Jennings, "An Agent-Based Approach to Virtual Power Plants of Wind Power Generators and Electric Vehicles," *IEEE Trans. Smart Grid*, vol. 4, no. 3, pp. 1314–1322, Sep. 2013.

[119] R. Lasseter, "Control of distributed resources," in *Proc. Bulk Power System Dynamics and Control IV - Reestructuring*, 1998.

[120] R. Lasseter, A. Akhil, C. Marnay, and J. Stephens, "Integration of distributed energy resources. The CERTS Microgrid Concept," 2002.

[121] J. A. P. Lopes, A. G. Madureira, and C. C. L. M. Moreira, "A view of microgrids," *Wiley Interdiscip. Rev. Energy Environ.*, vol. 2, no. 1, pp. 86–103, Jan. 2013.

[122] A. Karnama, F. O. Resende, and J. A. P. Lopes, "Optimal management of battery charging of electric vehicles: A new microgrid feature," in *IEEE Trondheim PowerTech*, 2011, pp. 1–8.

[123] J. A. P. Lopes, S. A. Polenz, C. L. Moreira, and R. Cherkaoui, "Identification of control and management strategies for LV unbalanced microgrids with plugged-in electric vehicles," *Electr. Power Syst. Res.*, vol. 80, no. 8, pp. 898–906, Aug. 2010.

[124] B. Ramachandran, S. K. Srivastava, and D. A. Cartes, "Intelligent power management in micro grids with EV penetration," *Expert Syst. Appl.*, vol. 40, no. 16, pp. 6631–6640, Nov. 2013.

[125] M. A. López, S. Martín, J. A. Aguado, and S. de la Torre, "V2G strategies for congestion management in microgrids with high penetration of electric vehicles," *Electr. Power Syst. Res.*, vol. 104, pp. 28–34, Nov. 2013.

[126] P. Summary, "Grid-for-Vehicles About G4V Objectives and key elements of G4V," no. 241295, 2013.

[127] N. Hatziargyriou and J. Lopes, "MERGE Project - Dissemination," 2011.

[128] C. Binding, D. Gantenbein, B. Jansen, O. Sundstrom, P. B. Andersen, F. Marra, B. Poulsen, and C. Traeholt, "Electric vehicle fleet integration in the danish EDISON project - A virtual power plant on the island of Bornholm," in *IEEE PES General Meeting*, 2010, pp. 1–8.

[129] SmartV2G project, "Project objectives," 2012. [Online]. Available: http://www.smartv2g.eu/deliverables.html.

[130] "MOBINCITY- Smart Mobility in Smart City," 2013. [Online]. Available: http://www.mobincity.eu/publications/MOBINCITY_D8.4_Annex_B_HT_MIPRO Presentation.pdf. [Accessed: 20-May-2005].

[131] The EV Project, "Information, dissemination and plan presentation," 2013.

[132] R. Garcia-Valle and J. Peças Lopes, *Electric Vehicle Integration into Modern Power Networks*. New York, NY: Springer New York, 2013.

[133] "Plug-in Market sales." [Online]. Available: http://www.ev-sales.blogspot.ch/2015/04/world-all-time-top-10-updated-to-25th.html. [Accessed: 17-Jul-2015].

[134] Vermont Energy Investment Corporation, "An Assessment of Level 1 and Level 2 Electric Vehicle Charging Efficiency," 2013.

[135] J. Sears, D. Roberts, and K. Glitman, "A comparison of electric vehicle Level 1 and Level 2 charging efficiency," in *2014 IEEE Conference on Technologies for Sustainability (SusTech)*, 2014, pp. 255–258.

[136] J. Smart and S. Schey, "Battery Electric Vehicle Driving and Charging Behavior Observed Early in The EV Project," pp. 1–23, Apr. 2012.

[137] S. Humeau, T. K. Wijaya, M. Vasirani, and K. Aberer, "Electricity load forecasting for residential customers: Exploiting aggregation and correlation between households," in *Sustainable Internet and ICT for Sustainability*, 2013.

[138] A. Garulli, S. Paoletti, and A. Vicino, "Models and Techniques for Electric Load Forecasting in the Presence of Demand Response," *IEEE Trans. Control Syst. Technol.*, vol. 23, no. 3, pp. 1087–1097, May 2015.

[139] M. Ghiafeh Davoudi, A. Bashian, and J. Ebadi, "Effects of unsymmetrical power transmission system on the voltage balance and power flow capacity of the lines," in *11th International Conference on Environment and Electrical Engineering*, 2012, pp. 860–863.

[140] T. Chen, C. Yang, T. Hsieh, and S. Chen, "Case Studies of the Impact of Voltage Imbalance on Power Distribution Systems and Equipment," *Proc. 8th WSEAS Int. Conf. Appl. Comput. Appl. Comput. Sci.*, no. 1, pp. 461–465, 2009.

[141] B. Hayes, J. Gruber, and M. Prodanovic, "Short-Term Load Forecasting at the local level using smart meter data," in *IEEE Eindhoven PowerTech*, 2015, pp. 1–6.

ANNEX

ANNEX A – ADDITIONAL DATA OF PEV-PR CASES

This annex contains additional information of each PEV-PR case regarding to parameters such as: arrive and departure time, initial SOC of PEVs and even where they have been connected. Regarding to this last point, PEVs are connected in two different streets: Hørmarken and Græsmarken. Hørmarken street is composed by 17 houses (H1-H17) while Græsmarken by 26 (G1-G26). Data are presented in form of histograms and have been grouped according to the PEV-PR case. In addition, Table A.1 presents a summary of each PEV-PR case and average values of arrive time, departure time and initial SOC.

Table A.1. Summary data of the different PEV-PR cases

PEV-PR (%)	Number of PEVs	Volt	Leaf	Tesla	Average arrive time	Average departure time	Average initial SOC (%)	Total energy demand (MWh)	Energy demand phase A (kWh)	Energy demand phase B (kWh)	Energy demand phase C (kWh)
10	11	3	5	3	18:30	07:00	66	0.138	37	67	34
30	29	11	14	4	19:05	07:15	60	0.337	109	148	80
50	52	21	25	6	18:55	07:45	59	0.584	250	202	132
70	72	16	43	13	19:05	07:55	65	0.788	204	285	300
90	93	33	48	12	19:20	07:55	61	1.01	356	335	318
100	97	34	50	13	19:20	07:55	59	1.06	397	342	322

From Figure A.1 to Figure A.6, histograms of the different PEV-PR cases are presented. In some cases, a high number of PEVs has an initial SOC of 30-40%. This is due to Chevrolet Volt PEV has its minimum SOC limited to 35% in order to maximize the life of the battery pack.

(a)

(b)

(c)

(d)
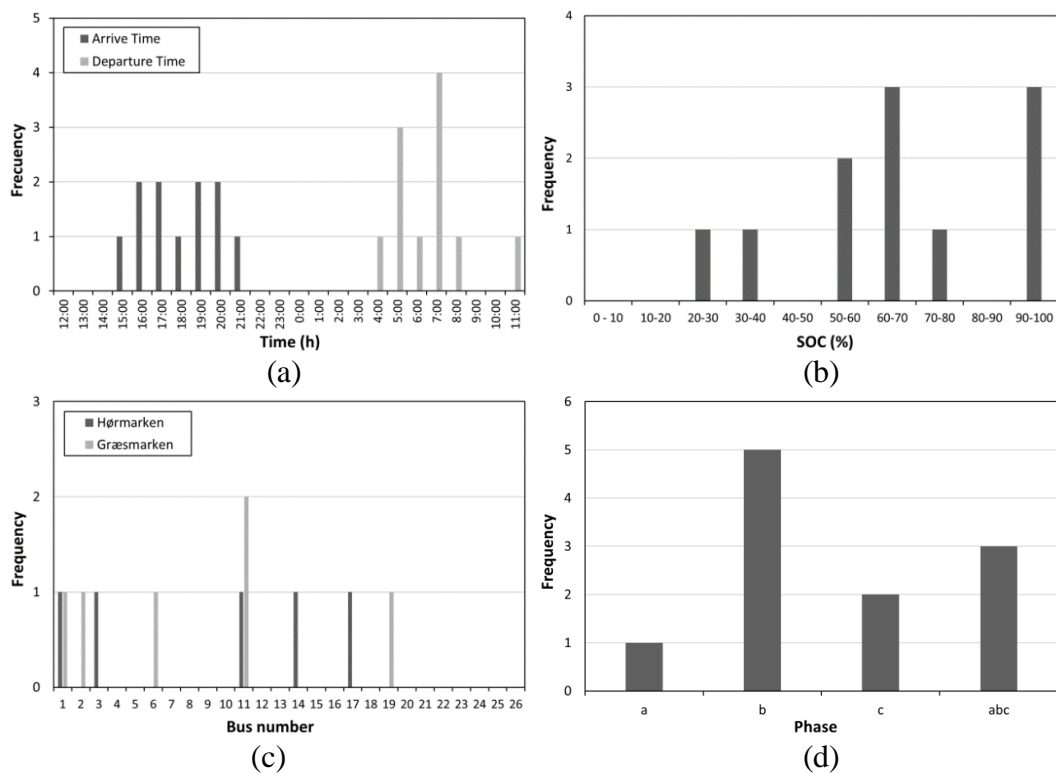
Figure A.1. Histograms of 10% PEV-PR case: (a) departure and arrive time, (b) initial SOC, (c) bus number and (d) connection phase

(a)

(b)

(c)

(d)
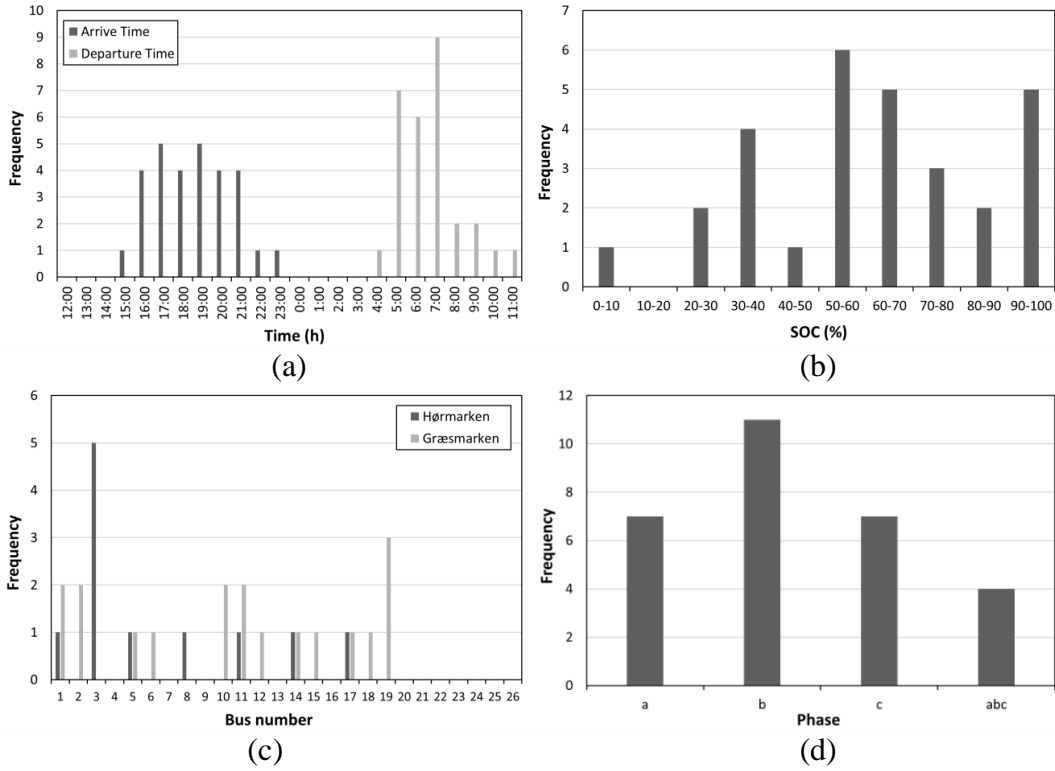
Figure A.2. Histograms of 30% PEV-PR case: (a) departure and arrive time, (b) initial SOC, (c) bus number and (d) connection phase

(a)

(b)

(c)

(d)
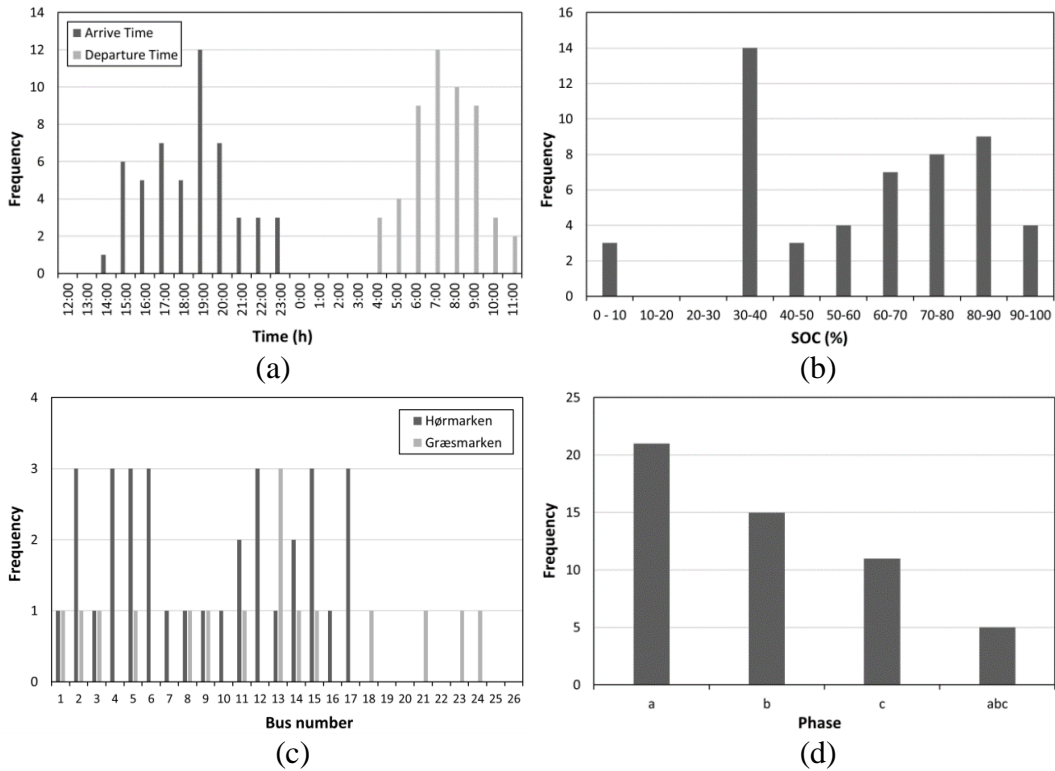
Figure A.3. Histograms of 50% PEV-PR case: (a) departure and arrive time, (b) initial SOC, (c) bus number and (d) connection phase
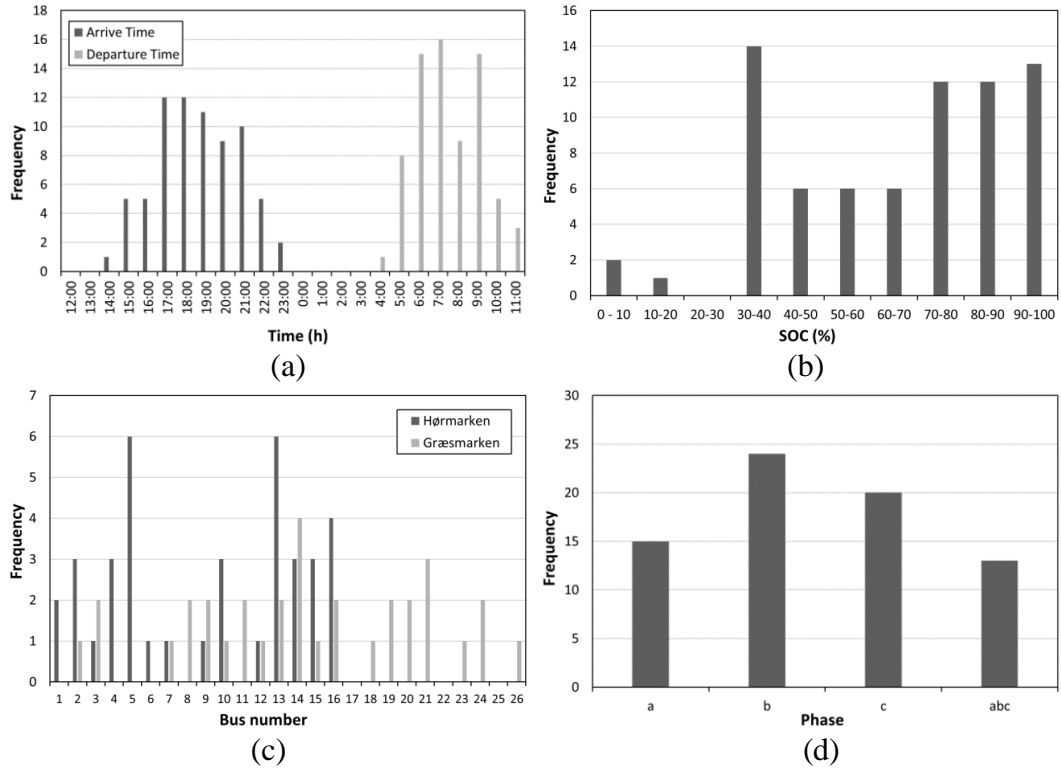
Figure A.4. Histograms of 70% PEV-PR case: (a) departure and arrive time, (b) initial SOC, (c) bus number and (d) connection phase
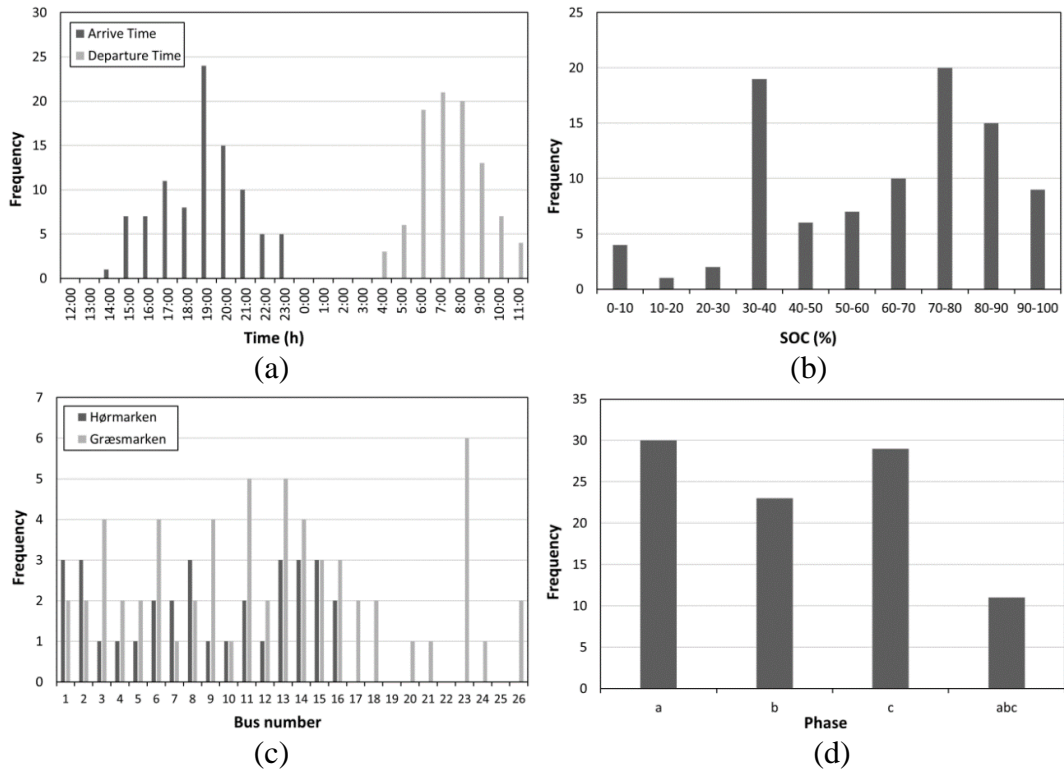
Figure A.5. Histograms of 90% PEV-PR case: (a) departure and arrive time, (b) initial SOC, (c) bus number and (d) connection phase
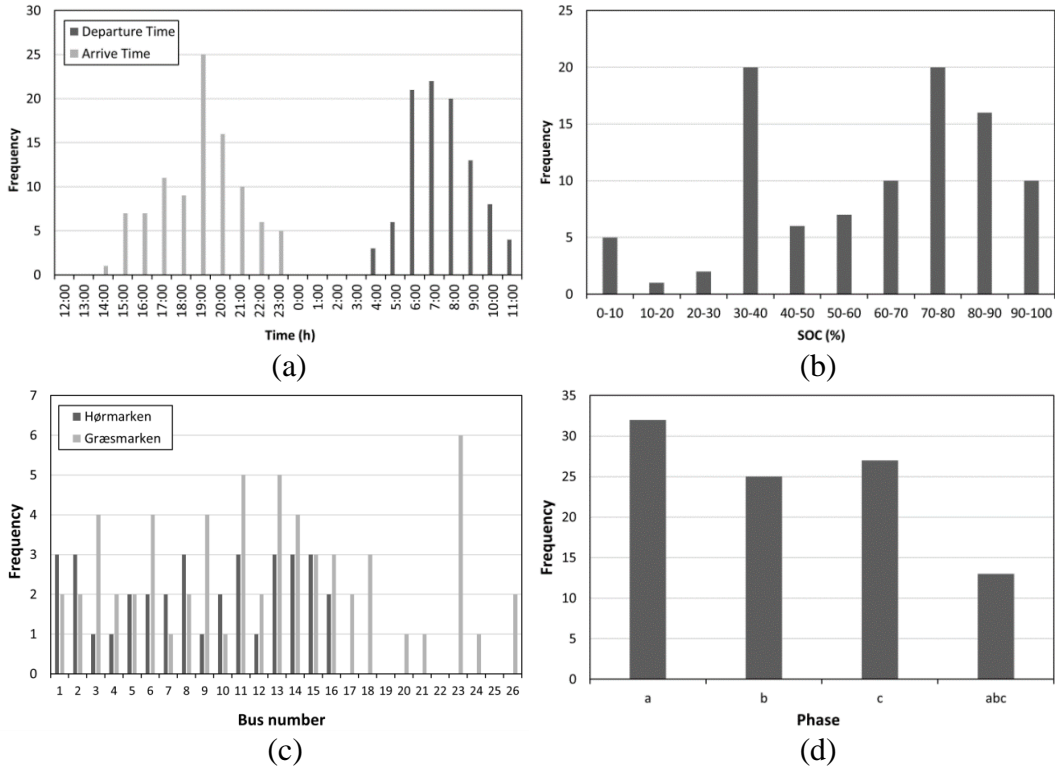
Figure A.6. Histograms of 100% PEV-PR case: (a) departure and arrive time, (b) initial SOC, (c) bus number and (d) connection phase

ANNEX B – FIGURES OF MOO-NF ALGORITHM

Annex B presents the results obtained by applying the MOO-NF algorithm, with VUR, to the different PEV-PR cases. The figures show in detail the evolution of the distribution transformer load, the line-neutral voltages at node 613, the power demand of PEVs for each phase and the overall power demand compared to electricity cost.

In general, the MOO-NF algorithm induces the charge of PEVs at off-peak hours, achieving a valley-filling effect. Line-neutral voltages at node 613 remain above 0.9 p.u. except for very short periods of time in the 70 and 100% PEV-PR cases. In addition, PEVs power demand for the three phases have a similar shape due to the application of VUR enhancement. This way, voltage unbalances generated by the charging of PEVs are reduced while overall voltage level is slightly increased. Furthermore, the MOO-NF algorithm programs the charging of PEVs at hours where electricity prices are the lowest ones, allowing a reduction of charging cost for PEV users.
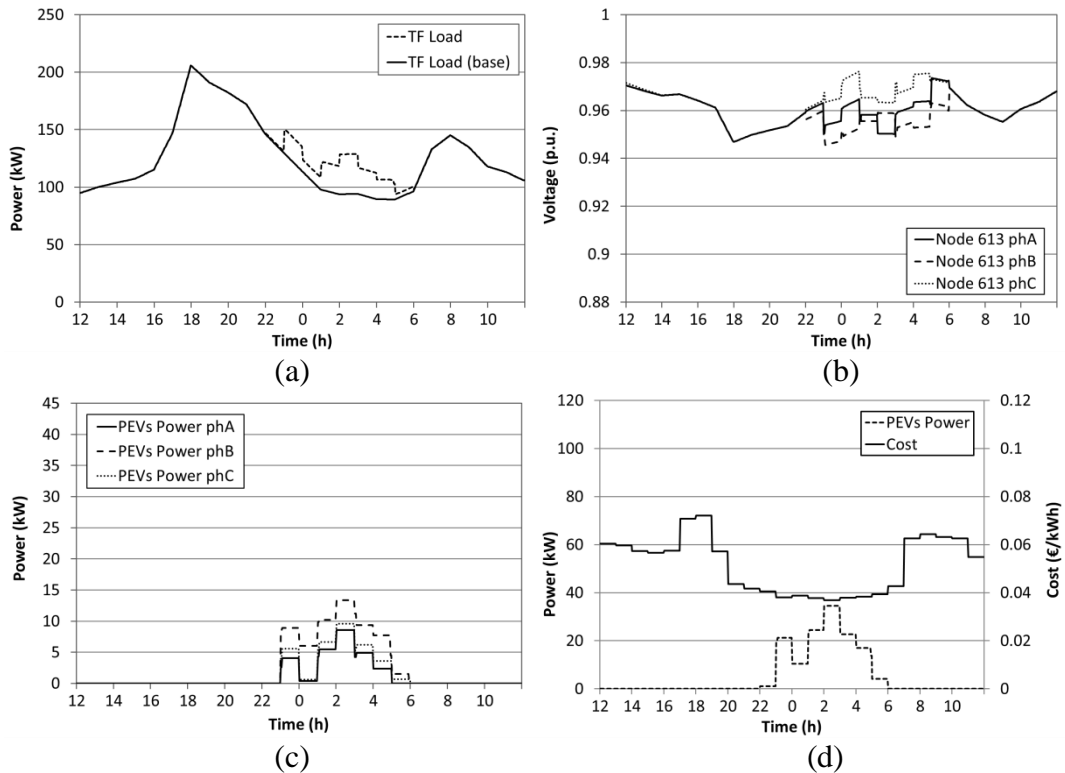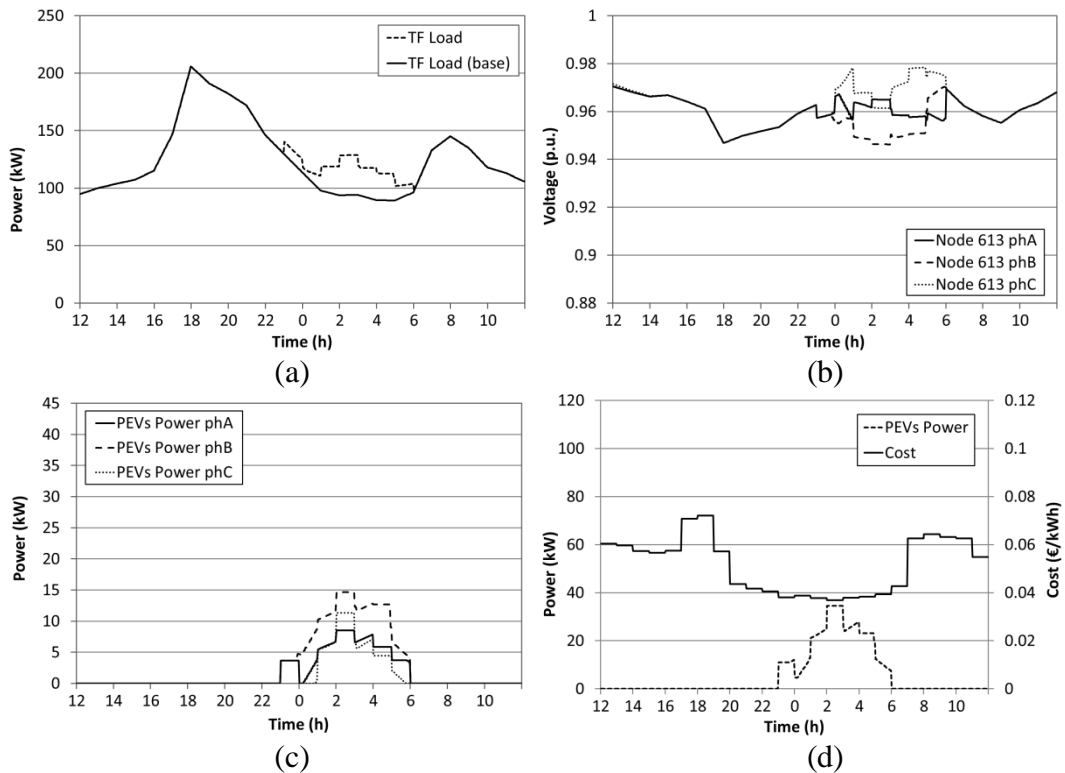

Figure B.1. 10% PEV-PR case: (a) transformer load, (b) line-neutral voltages at node 613, (c) PEVs power demand power phase and (d) PEVs power demand and electricity cost
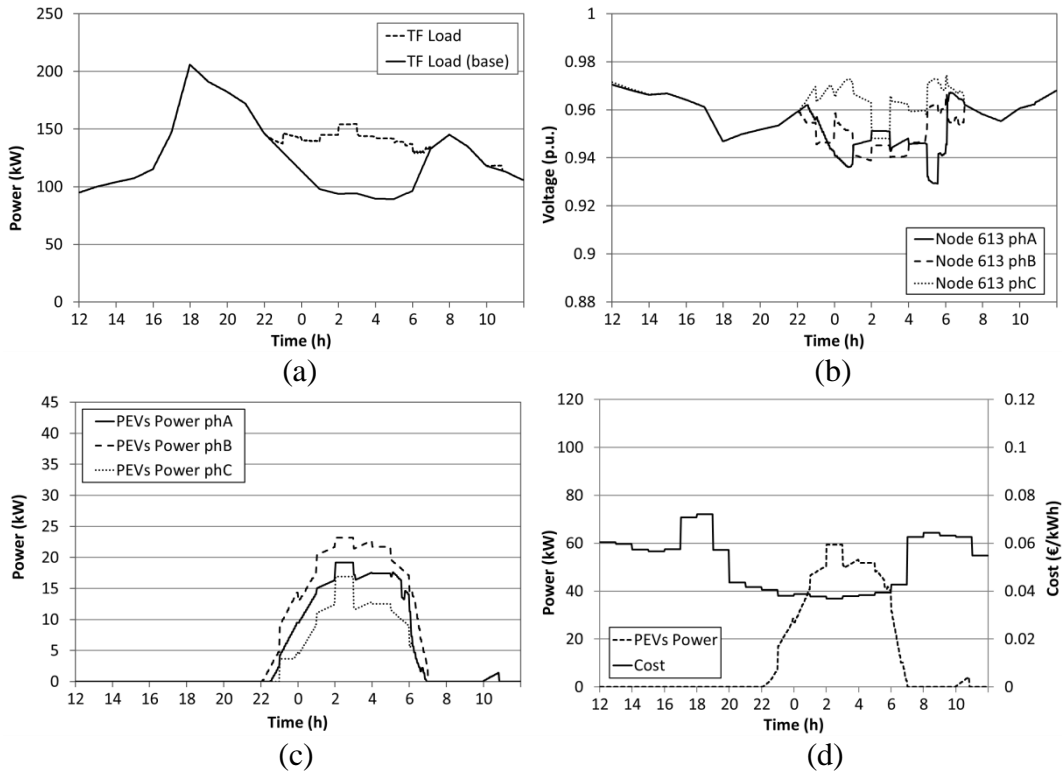
(a)

(b)

(c)

(d)
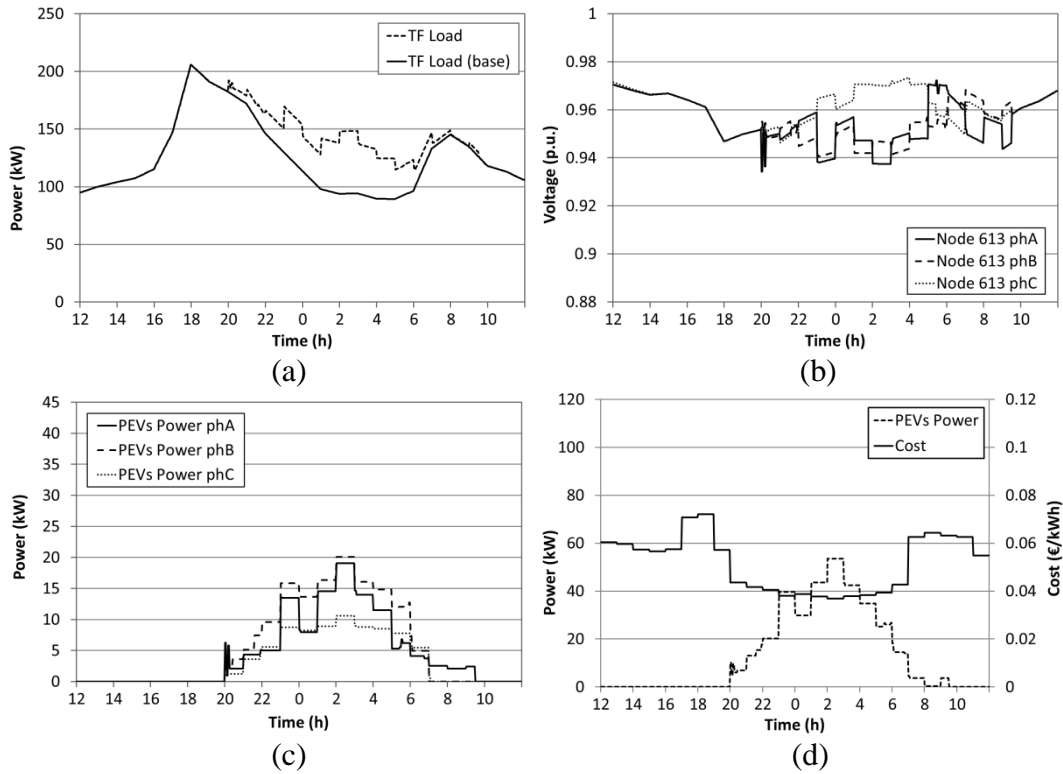
Figure B.2.   30% PEV-PR case: (a) transformer load, (b) line-neutral voltages at node 613, (c) PEVs power demand power phase and (d) PEVs power demand and electricity cost

(a)

(b)

(c)

(d)
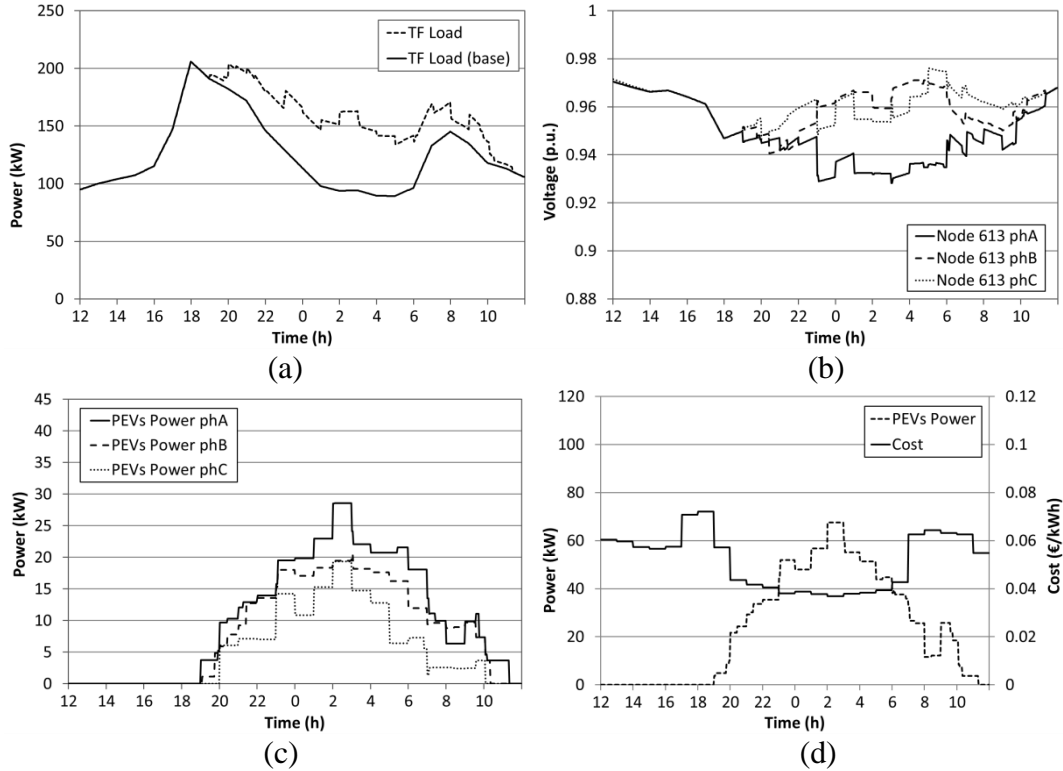
Figure B.3.   50% PEV-PR case: (a) transformer load, (b) line-neutral voltages at node 613, (c) PEVs power demand power phase and (d) PEVs power demand and electricity cost
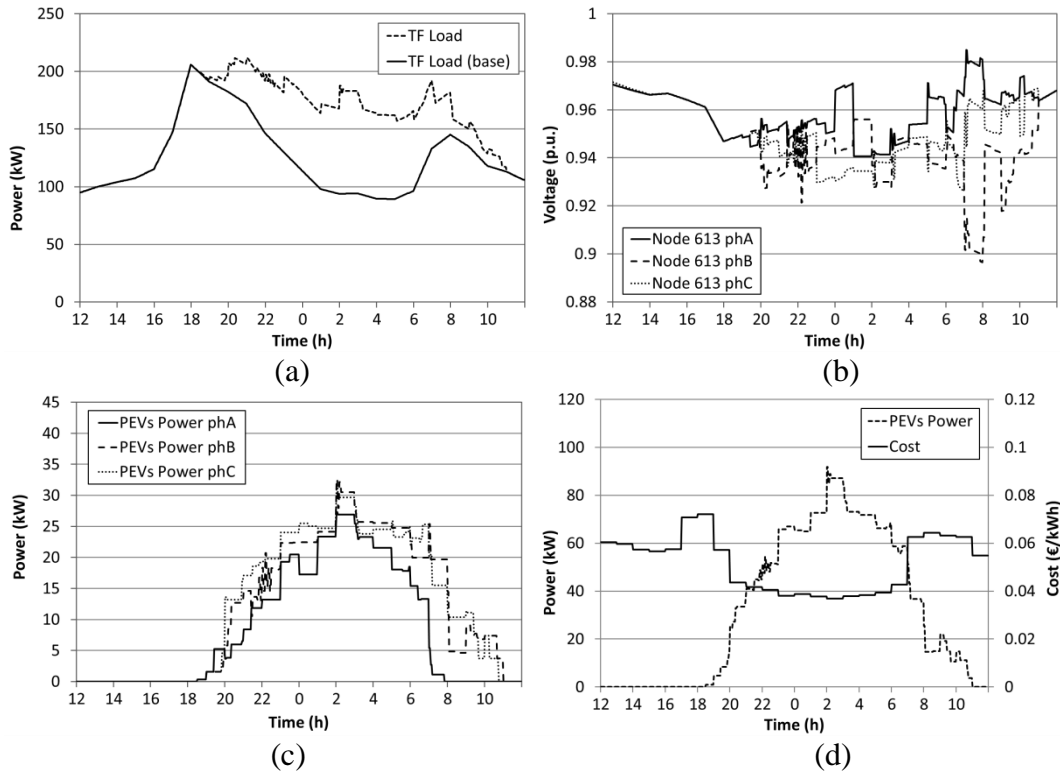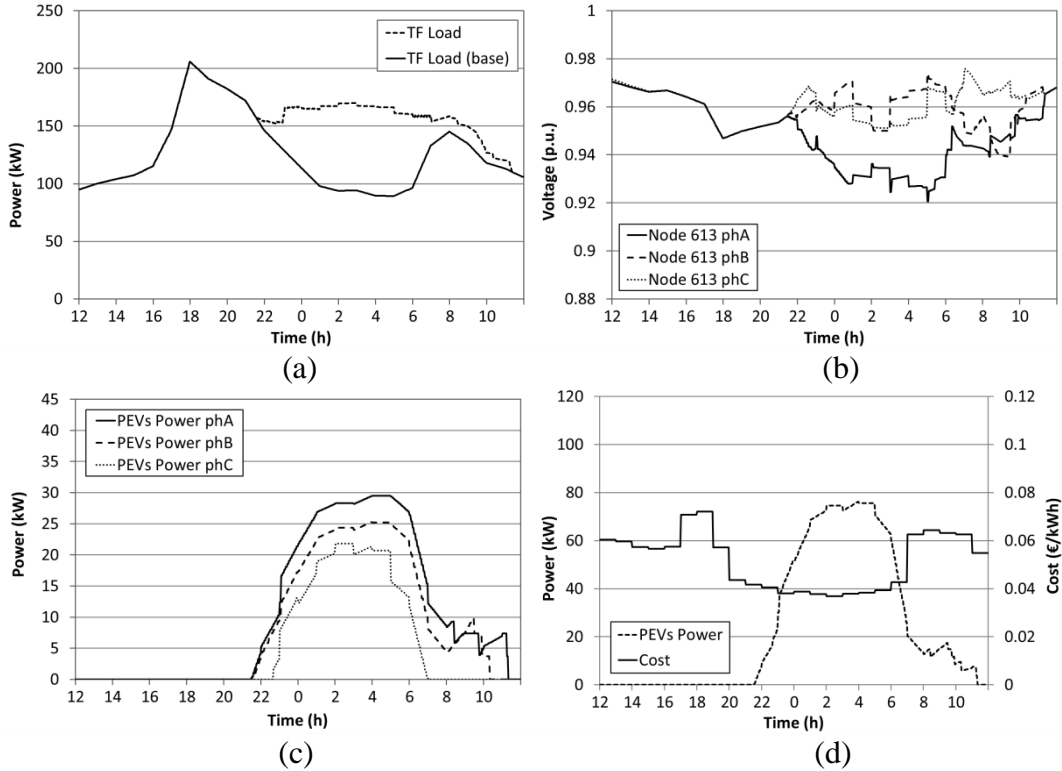
Figure B.4. 70% PEV-PR case: (a) transformer load, (b) line-neutral voltages
at node 613, (c) PEVs power demand power phase and (d) PEVs power demand and
electricity cost
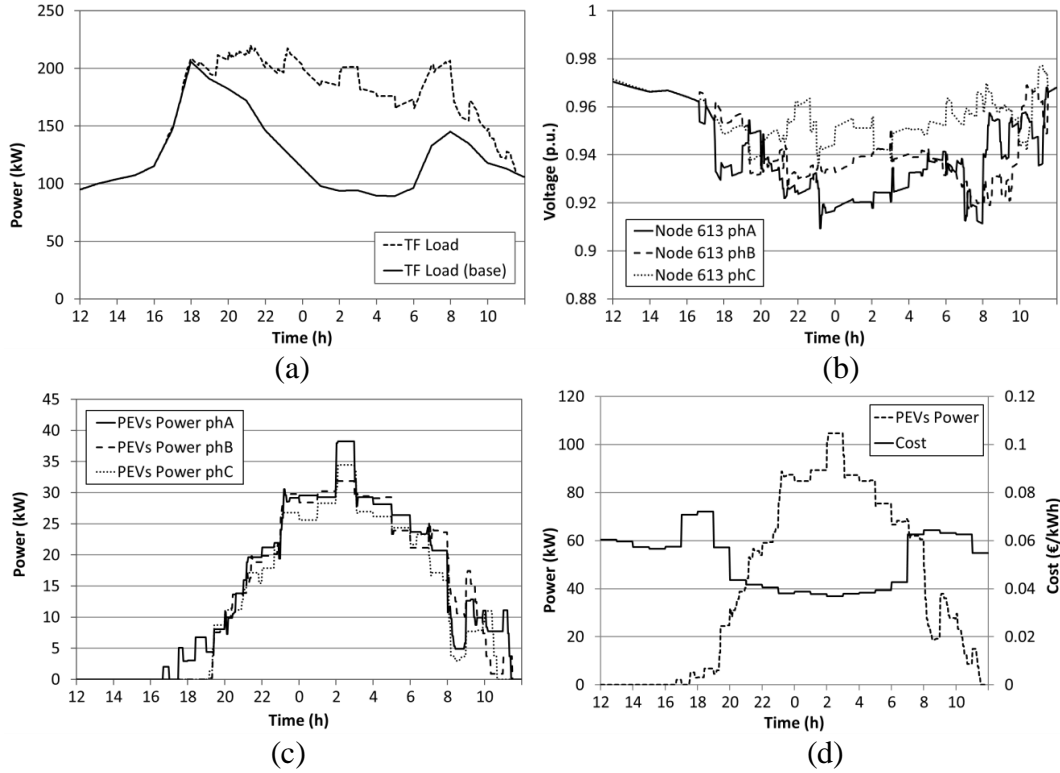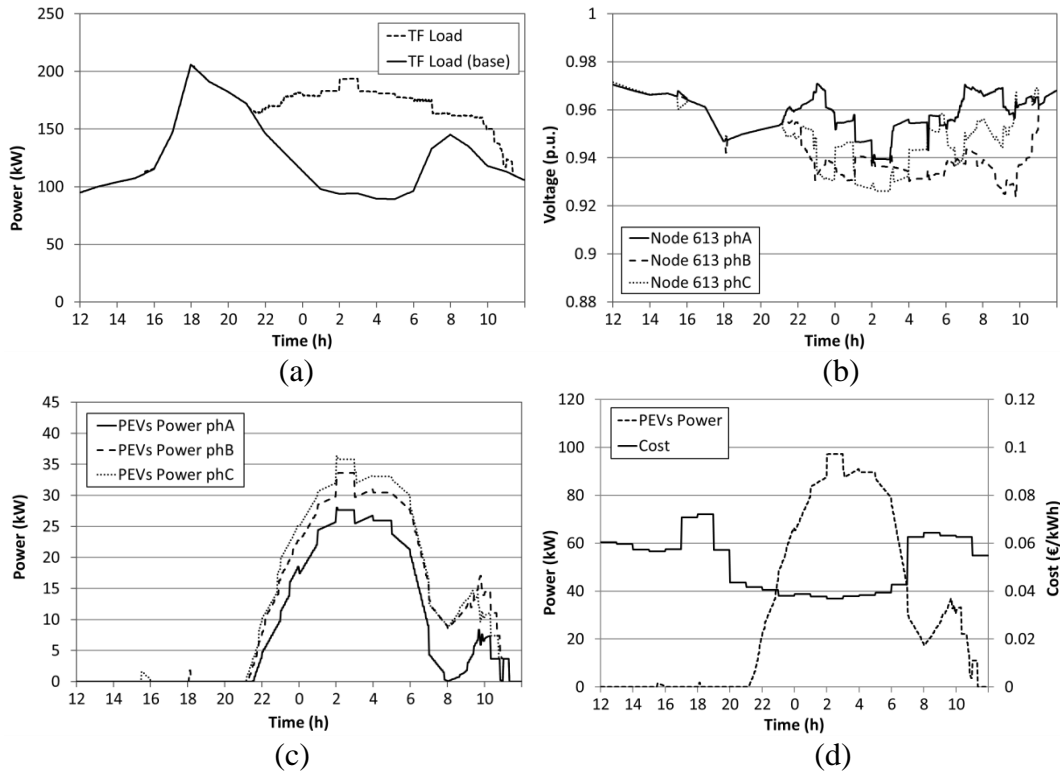

Figure B.5. 90% PEV-PR case: (a) transformer load, (b) line-neutral voltages
at node 613, (c) PEVs power demand power phase and (d) PEVs power demand and
electricity cost
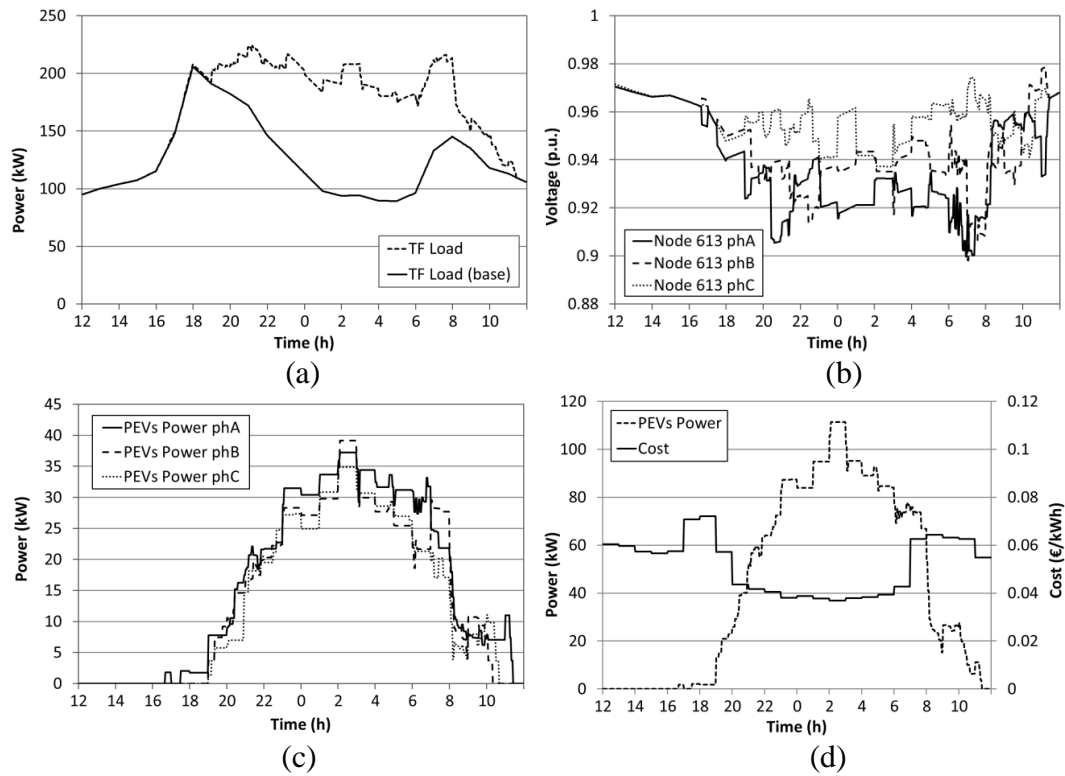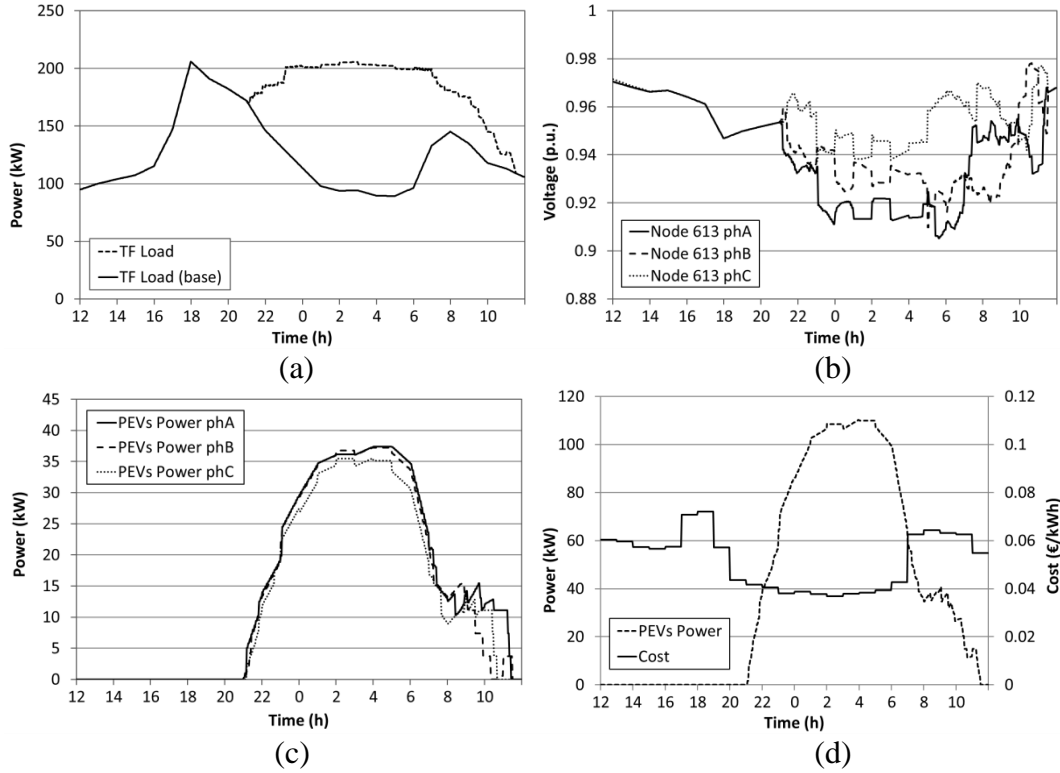
Figure B.6.   100% PEV-PR case: (a) transformer load, (b) line-neutral voltages at node 613, (c) PEVs power demand power phase and (d) PEVs power demand and electricity cost

ANNEX C – FIGURES OF MOO-WF ALGORITHM

This Annex C presents the results obtained by applying the MOO-WF algorithm with VUR, to the different PEV-PR cases. The different figures show in detail the evolution of the distribution transformer load, the line-neutral voltages at node 613, the power demand of PEVs for each phase and the overall power demand compared to electricity cost.

The application of the MOO-WF algorithm causes the charging of PEVs at off-peak hours. In contrast to the MOO-NF algorithm, this algorithm performs a better valley-filling effect. However, it should be taken into account the possible deviations due to load forecasting errors. Regarding to voltages at furthest node, these voltages remain above 0.9 p.u. in all cases. Thanks to the application of VUR enhancement, PEVs power demand per phase shows a similar evolution reducing the voltage unbalances, as it happens in the MOO-NF algorithm. Finally, the MOO-WF algorithm also takes into account the charging cost, programming the charge of PEVs at hours where electricity prices are the lowest ones whenever it is possible.

Figure C.1.   10% PEV-PR case: (a) transformer load, (b) line-neutral voltages at node 613, (c) PEVs power demand power phase and (d) PEVs power demand and electricity cost

(a)

(b)

(c)

(d)

Figure C.2.   30% PEV-PR case: (a) transformer load, (b) line-neutral voltages
at node 613, (c) PEVs power demand power phase and (d) PEVs power demand and
electricity cost

(a)

(b)

(c)

(d)

Figure C.3.   50% PEV-PR case: (a) transformer load, (b) line-neutral voltages
at node 613, (c) PEVs power demand power phase and (d) PEVs power demand and
electricity cost

Figure C.4. 70% PEV-PR case: (a) transformer load, (b) line-neutral voltages at node 613, (c) PEVs power demand power phase and (d) PEVs power demand and electricity cost

Figure C.5. 90% PEV-PR case: (a) transformer load, (b) line-neutral voltages at node 613, (c) PEVs power demand power phase and (d) PEVs power demand and electricity cost
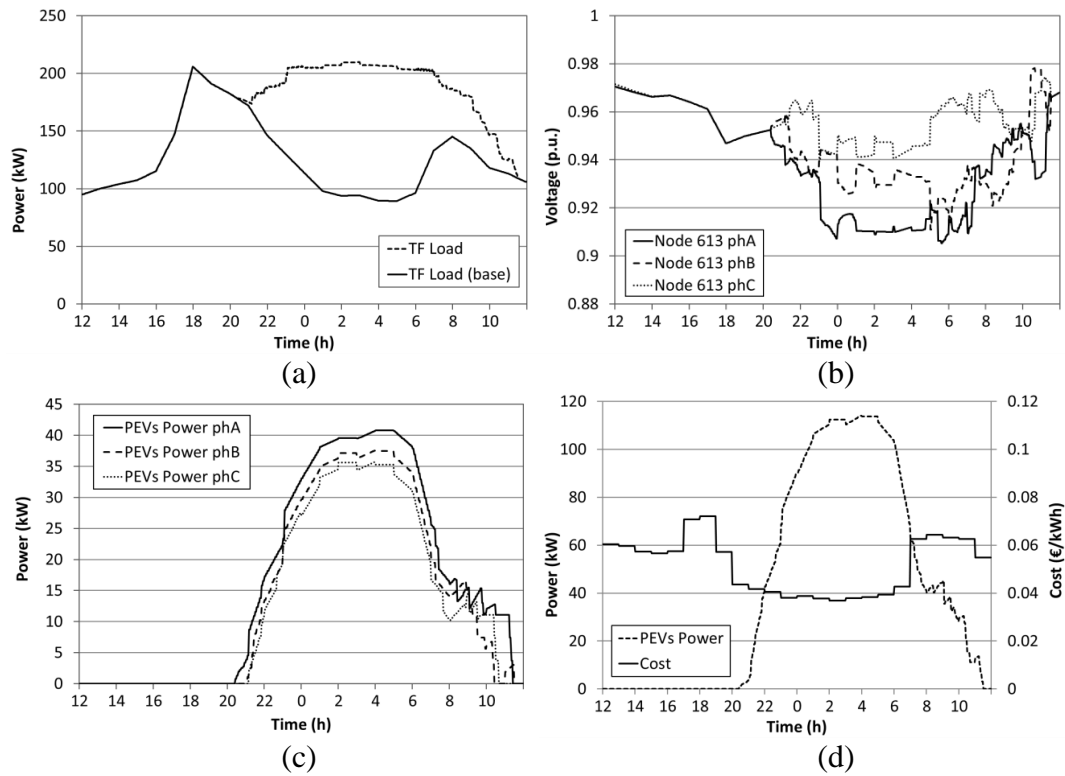
Figure C.6.   100% PEV-PR case: (a) transformer load, (b) line-neutral voltages at node 613, (c) PEVs power demand power phase and (d) PEVs power demand and electricity cost

ANNEX D – FIGURES OF LOAD FORECASTING ERROR

In this Annex D, additional information of the sensitivity analysis carried out in section 5.7.7 can be found. The mentioned sensitivity analysis is composed by 10 different cases, as shown in Table 5.37. As a result of load forecasting errors, peak power at distribution transformer level is increased in all cases. In addition, line-neutral voltages at node 613 are worse than in the optimal case. However, these voltage deviations are within EN50160 standard.
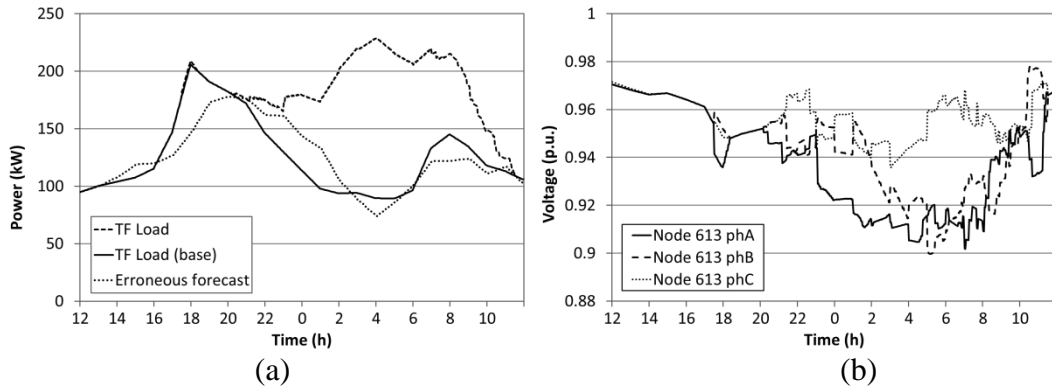
Figure D.1. Case 1: (a) transformer load and (b) line-neutral voltages at node 613
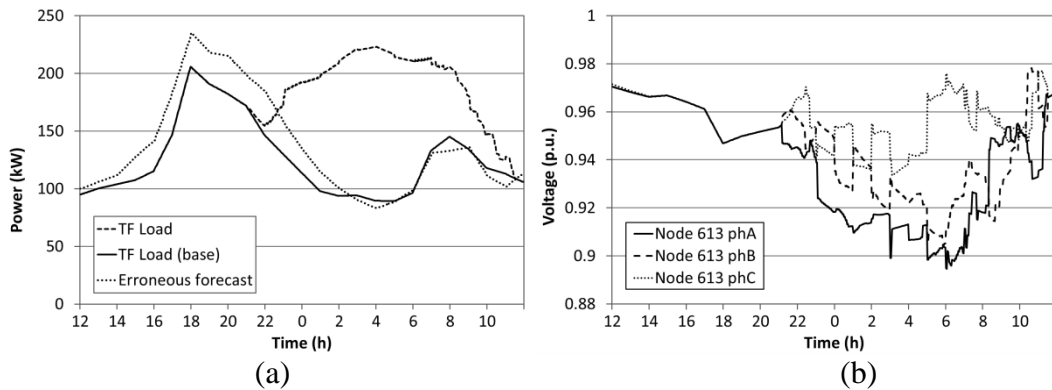
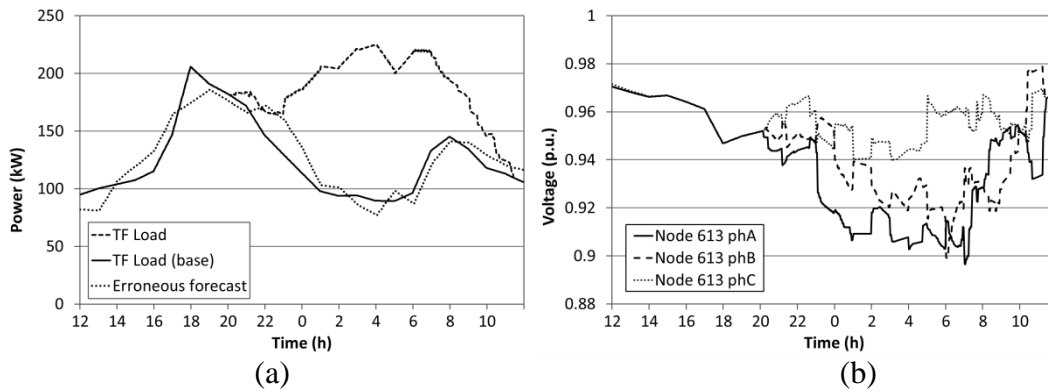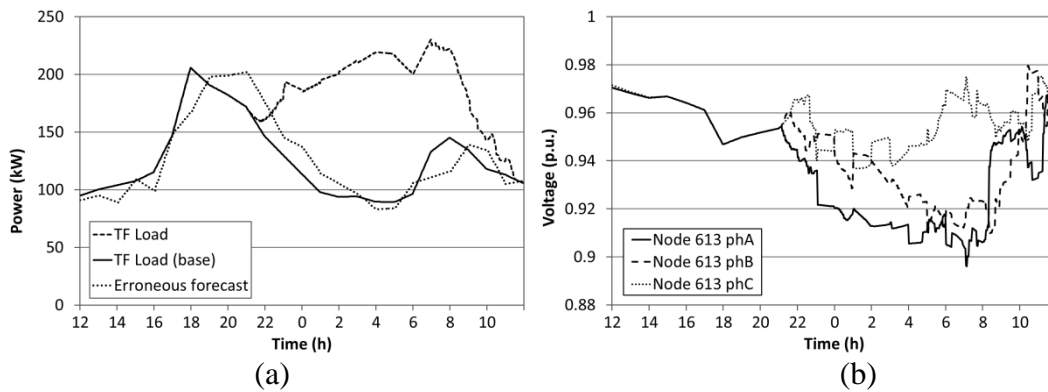Figure D.2. Case 2: (a) transformer load and (b) line-neutral voltages at node 613
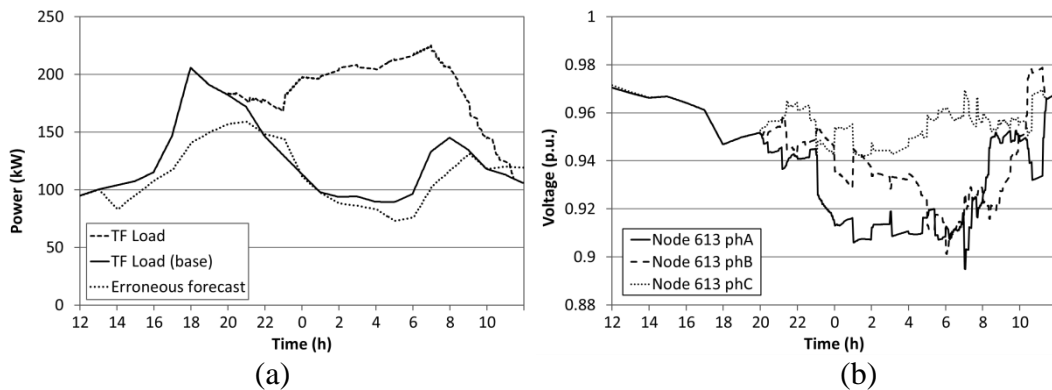
Figure D.3. Case 3: (a) transformer load and (b) line-neutral voltages at node 613
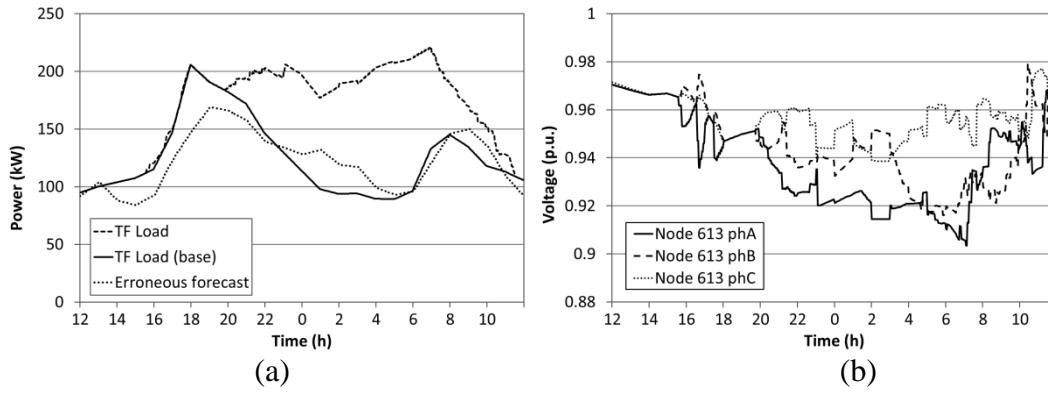
Figure D.4. Case 4: (a) transformer load and (b) line-neutral voltages at node 613
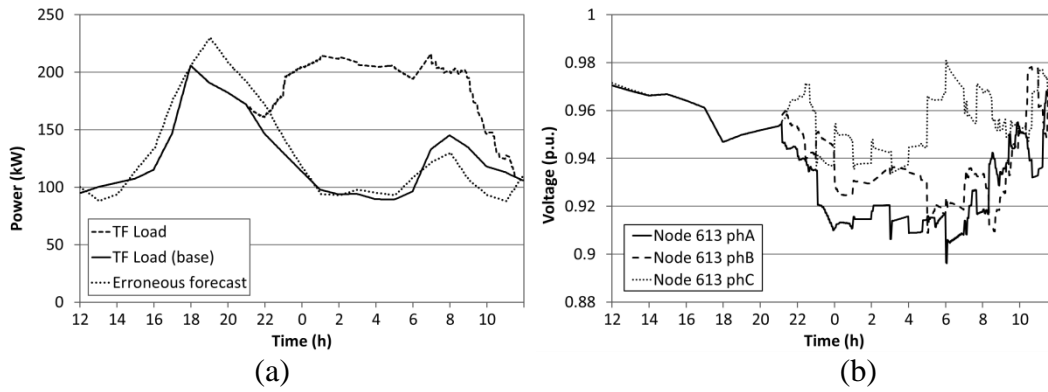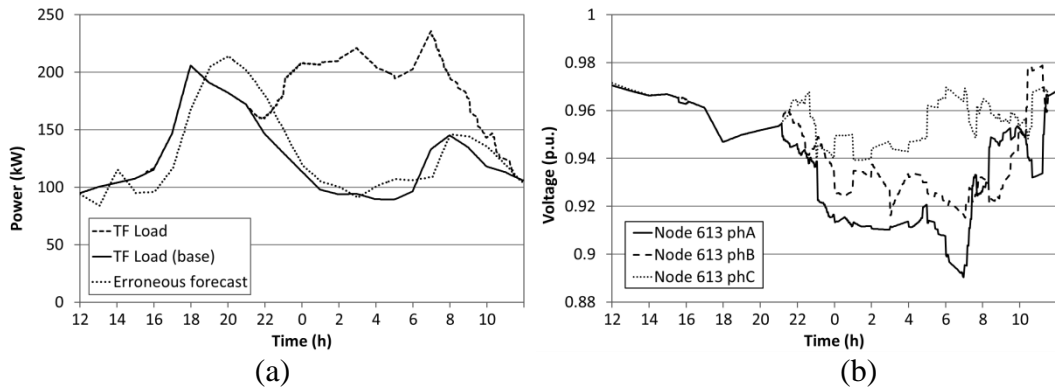

Figure D.5. Case 5: (a) transformer load and (b) line-neutral voltages at node 613

Figure D.6. Case 6: (a) transformer load and (b) line-neutral voltages at node 613

Figure D.7. Case 7: (a) transformer load and (b) line-neutral voltages at node 613

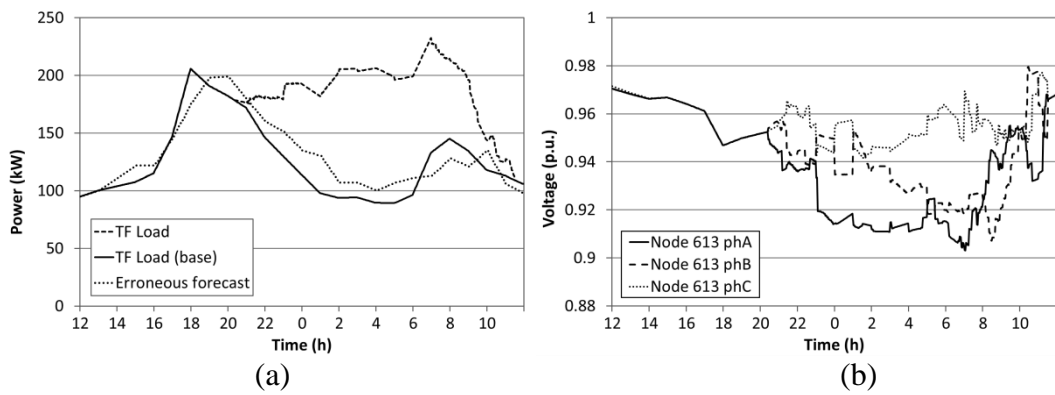Figure D.8. Case 8: (a) transformer load and (b) line-neutral voltages at node 613

Figure D.9. Case 9: (a) transformer load and (b) line-neutral voltages at node 613
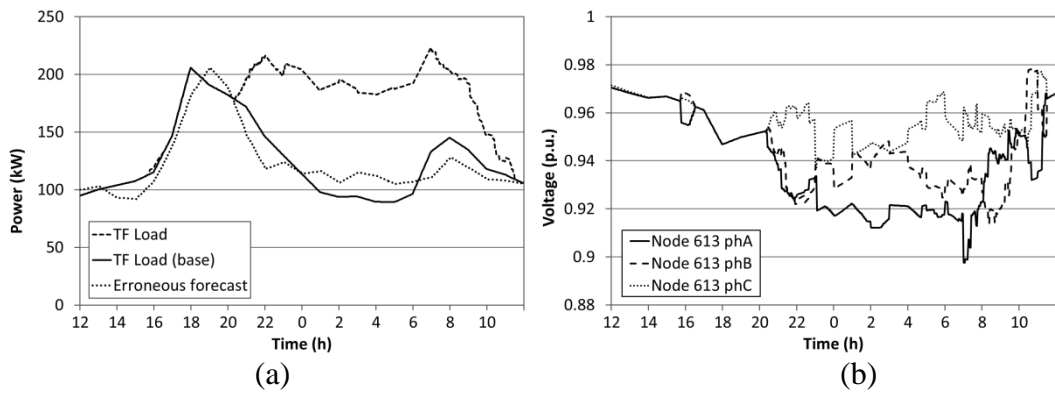

Figure D.10. Case 10: (a) transformer load and (b) line-neutral voltages at node 613